



**HAL**  
open science

# Deformation modes and kinematic implications of hyper-extended rifted margins : the examples of the southern North Atlantic

Michael Nirrengarten

► **To cite this version:**

Michael Nirrengarten. Deformation modes and kinematic implications of hyper-extended rifted margins : the examples of the southern North Atlantic. Geophysics [physics.geo-ph]. Université de Strasbourg, 2016. English. NNT : 2016STRAH014 . tel-01546810

**HAL Id: tel-01546810**

**<https://theses.hal.science/tel-01546810>**

Submitted on 26 Jun 2017

**HAL** is a multi-disciplinary open access archive for the deposit and dissemination of scientific research documents, whether they are published or not. The documents may come from teaching and research institutions in France or abroad, or from public or private research centers.

L'archive ouverte pluridisciplinaire **HAL**, est destinée au dépôt et à la diffusion de documents scientifiques de niveau recherche, publiés ou non, émanant des établissements d'enseignement et de recherche français ou étrangers, des laboratoires publics ou privés.

*École Doctorale des Sciences de la Terre et de l'Environnement (ED 413)*

*Institut de Physique du Globe de Strasbourg (UMR 7516)*

**Thèse** présentée par :

**Michael NIRRENGARTEN**

soutenance prévue le : **1 décembre 2016**

pour obtenir le grade de : **Docteur de l'Université de Strasbourg**

Discipline/ Spécialité : Sciences de la Terre – Géologie - Géophysique

**Modes de déformation et implications cinématiques des marges hyper-étirées: Les exemples du sud de l'Atlantique Nord**

**THÈSE dirigée par :**  
Pr. MANATSCHAL Gianreto

Université de Strasbourg

**RAPPORTEURS :**  
Pr. RESTON Tim  
Pr. JOLIVET Laurent

University of Birmingham  
Université d'Orléans

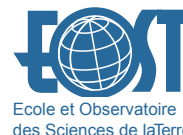
**EXAMINATEURS :**  
Dr. HEINE Christian  
Dr. SAUTER Daniel

Shell international, Den Haag  
Université de Strasbourg





UNIVERSITÉ DE STRASBOURG



UNIVERSITY OF  
LIVERPOOL

**Thèse** présentée par :

**Michael NIRRENGARTEN**

soutenance prévue le : **1 décembre 2016**

pour obtenir le grade de : **Docteur de l'Université de Strasbourg**

Discipline/ Spécialité : Sciences de la Terre – Géologie - Géophysique

**Modes de déformation et implications cinématiques des marges hyper-étirées: Les exemples du sud de l'Atlantique Nord**

**THÈSE dirigée par :**  
Pr. MANATSCHAL Gianreto  
Pr. KUSZNIR Nick J.

Université de Strasbourg  
University of Liverpool

**RAPPORTEURS :**  
Pr. RESTON Tim  
Pr. JOLIVET Laurent

University of Birmingham  
Université d'Orléans

**EXAMINATEURS :**  
Dr. HEINE Christian  
Dr. SAUTER Daniel

Shell international, Den Haag  
Université de Strasbourg

**INVITÉ :**  
Pr. FRIZON DE LAMOTTE Dominique

Université de Cergy-Pontoise



# *AVANT-PROPOS*

Ces travaux de thèse font partie intégrante de la recherche développée depuis de nombreuses années à l'Université de Strasbourg sur l'évolution des systèmes de rift hyper-étirés. Cette étude s'inscrit dans une suite logique de projets de recherche ayant pour but d'observer, de comprendre et de modéliser l'évolution d'un système de rift. Cette thèse a été encadrée par Gianreto Manatschal à l'Université de Strasbourg et par Nick Kuszniir à l'Université de Liverpool. Elle a de plus bénéficié de la collaboration de Julie Tugend et de Daniel Sauter (Univ. Strasb) ainsi que de Xiaoping Yuan (ENS Paris) et Bertrand Maillot (Univ Cergy-Pontoise).

Le soutien financier de ce contrat doctoral a été fourni par le consortium MM4 (Margin Modelling phase 4) qui réunit l'Université de Strasbourg et celle de Liverpool avec des compagnies pétrolières (BP, Conoco Phillips, Statoil, Petrobras, Total, Shell, Hess, BHP-Billiton et BG).



# ***RÉSUMÉ ÉTENDU***

Les marges hyper-étirées sont issues des processus de rifting qui étirent et amincissent la lithosphère continentale jusqu'à la création d'une lithosphère océanique. L'étirement de la lithosphère continentale entraîne des modifications thermo-mécaniques qui induisent une évolution de la déformation extensive dans le temps et dans l'espace. Cette évolution polyphasée du rifting est enregistrée dans l'architecture crustale des marges qui a été classifiée en différents domaines correspondant à des modes de déformation propre. Le sud de l'Atlantique Nord est bordé par plusieurs marges passives et bassins sédimentaires qualifiés «d'hyper-étirés» qui présentent peu d'addition magmatique. Le terme «hyper-étiré» est utilisé pour caractériser l'architecture d'une marge ainsi que son mode de déformation. De ce fait, une marge « hyper-étirée » est définie par la présence d'une croûte continentale très fine (<10 km) qui s'amincit à l'extrême jusqu'à sa disparition et la création d'une nouvelle surface composée de manteau lithosphérique exhumé avant une croûte océanique magmatique.

Ce travail se base sur l'observation de l'architecture des marges hyper-étirées afin de comprendre l'évolution des processus de déformation en deux dimensions avant d'analyser l'évolution des modes de déformation dans le temps et dans l'espace. Cette thématique est vaste et l'étude se focalise sur deux objectifs : le premier est de caractériser physiquement la déformation de la croûte continentale hyper-étirée. Le second vise à analyser l'évolution de la déformation des systèmes de rift hyper-étirés dans le temps et dans l'espace. Cependant ceci nécessite un modèle cinématique préexistant fiable, ce qui n'est pas le cas du sud de l'Atlantique Nord à cause de l'anomalie magnétique J interprétée comme une anomalie océanique isochrone ou liée à un sous plaquage magmatique au moment de la rupture lithosphérique. Ainsi la nature et la pertinence de l'anomalie J dans les reconstructions cinématiques restent à déterminer. Une méthode de reconstruction cinématique se basant sur des données de rift a été développée afin d'analyser la propagation et le partitionnement de la déformation des systèmes hyper-étirés du sud de l'Atlantique Nord.

## ***1. L'apport de la théorie du prisme de Coulomb pour les marges hyper-étirées***

La première partie du travail de thèse se focalise sur le mode de déformation de la croûte continentale hyper-étirée. Ce domaine est imagé sur de nombreux exemples dans le sud de l'Atlantique Nord et est exposé à l'affleurement dans la nappe d'Err (Alpes Suisses). Le but de cette section est de mesurer les angles de la terminaison continentale des marges hyper-étirées et de les comparer avec la théorie du prisme de Coulomb.



La théorie du prisme de Coulomb décrit les limites de stabilité d'un prisme frictionnel glissant sur un décollement basal. Cette théorie est utilisée en géologie compressive pour analyser les prismes d'accrétion et les chaînes d'avant-pays, cependant ces équations sont également valables pour des prismes en extension dont l'angle d'ouverture diminue. L'imagerie sismique et les analogues de terrain ont mis en évidence la forme prismatique de la terminaison continentale d'une marge, la déformation cassante/frictionnelle des roches crustales et mantelliques ainsi que le décollement frictionnel à la base de la croûte. La croûte continentale cassante se brise suivant un « cisaillement simple » qui produit un prisme de plaque supérieure dans le toit de la faille de détachement et un prisme de plaque inférieure situé dans le mur. Cependant la base du prisme inférieur correspond également à un niveau de décollement à faible friction (imagé par le réflecteur S). La direction du cisaillement est opposée entre les deux prismes, vers le continent pour le prisme supérieur et vers l'océan pour le prisme inférieur, ces directions sont respectivement caractéristiques des prismes de Coulomb extensifs et gravitaires. Les mesures des angles de surfaces et basaux de différentes marges hyper-étirées ont été comparées avec les enveloppes de stabilité d'un prisme de Coulomb extensif et d'un prisme gravitaire. Les coefficients de friction ont été déterminés grâce aux roches de domaine hyper-étirés forées sur la marge ibérique (serpentine, phyllosilicates) et les pressions de fluide paramétrées avec la stabilité des prismes gravitaires. Les résultats majeurs sont que : la forme finale des prismes inférieurs correspond toujours à un prisme gravitaire critique alors que les prismes supérieurs peuvent être super-critiques, sub-critiques ou critiques. L'architecture des bassins bordés par des failles contre-régionales et la présence de blocs allochtones sont des observations expliquées par un modèle de séparation continentale utilisant la théorie du prisme de Coulomb. De plus cette théorie physique simple permet de lier des observations partielles de sismique ou de terrain afin d'obtenir une interprétation tectono-sédimentaire cohérente avec les processus physiques.

## ***2. Reconstruction d'un système de rift hyper-étiré***

La seconde partie du travail de thèse analyse le partitionnement de la déformation extensive dans le sud de l'Atlantique Nord. Cette étude illustre l'influence de l'extension pré-océanique dans la cinématique de la plaque ibérique. La démarche idéalisée de ce projet se résume en 4 étapes : 1) restauration océanique grâce aux anomalies marines considérées comme isochrones, 2) suppression des domaines de manteau exhumé, 3) détermination du volume de croûte continentale amincie (sur des profils perpendiculaires à la marge), 4) restauration palinspatique de la croûte continentale. Cependant malgré la grande quantité de données et d'études sur la zone il reste une incertitude majeure concernant l'âge de la première anomalie océanique ce qui entraîne des restaurations problématiques. Ainsi le second chapitre est consacré

à la détermination caractérisation de l'anomalie magnétique J et de son implication dans les modèles cinématiques.

### ***2.1 Nature et implications de l'anomalie magnétique J***

L'anomalie magnétique J est une anomalie plus ou moins continue située dans la transition océan-continent de la marge de Terre-Neuve et d'Ibérie. Ces anomalies conjuguées sont symétriques par rapport à la dorsale océanique. Cependant si on utilise ces anomalies comme des structures isochrones au chron M0 (~125 Ma), la restauration résultante induit un océan Pyrénéen au Crétacé inférieur et une subduction de cet océan avant ~83 Ma, ce qui est incompatible avec les observations de terrain. La seconde interprétation de l'anomalie J correspond à un sous plaquage magmatique initiant la croûte océanique. Cette interprétation peut impliquer une anomalie J synchrone ou diachrone dans le cas où la séparation lithosphérique initiant l'accrétion océanique se propage vers le nord. Une formation synchrone de J mène à des reconstructions contestables car elles induisent une accélération brutale de la vitesse d'extension océanique alors qu'un modèle utilisant la propagation de J est encore à tester. L'interprétation de lignes sismiques recoupant l'anomalie J à différents endroits de la marge met en évidence que l'anomalie n'est pas située sur de la croûte océanique tout le long de la marge, ni à la transition entre la croûte océanique et le manteau exhumé. Ainsi l'anomalie J ne correspond pas à une anomalie océanique classique ni à une limite de domaine. En revanche l'anomalie J correspond à des additions magmatiques qui ont été datées par endroit et qui présentent une grande variabilité d'âge (145 Ma à l'actuel). Ainsi cette anomalie magnétique résulte d'additions magmatiques qui se sont orientées N-S et qui suivent potentiellement des structures mantéliques héritées. En conclusion l'anomalie J n'est pas utilisable pour les reconstructions cinématiques et la position de l'Ibérie n'est contrainte que par des anomalies magnétiques océaniques seulement après la période magnétique calme du Crétacé (~83 Ma).

### ***2.2 Le partitionnement et la propagation de la déformation***

Etudier le partitionnement et la propagation de la déformation revient à synthétiser les informations géologiques majeures de chaque domaine de rift identifié et d'intégrer ces observations dans un modèle cinématique afin d'observer ses implications sur des zones où peu de données sont disponibles. Ce travail se base sur une cartographie précise des domaines de rift effectuée grâce à l'imagerie sismique, à l'inversion gravimétrique et aux méthodes potentielles. Cette carte couplée à des informations stratigraphiques et géochronologiques ponctuelles permet de modéliser l'évolution 3D de la déformation du rift en utilisant le logiciel de restauration de plaques Gplates. La restauration du sud de l'Atlantique Nord met en valeur

l'importante déformation pendant l'hyper-extension et son influence sur la cinématique des plaques. L'orientation de l'extension n'est pas forcément continue tout au long du rifting, ainsi prendre un pôle de rotation à la première anomalie océanique et un second au moment de la reconstruction palinspatique ne permet pas de prendre en compte l'évolution du rifting. De plus, il est nécessaire d'inclure des micro-blocs qui se comportent de manière semi-autonome des plaques majeures et permettent le partitionnement de la déformation entre différents systèmes de rift. De plus, l'individualisation de micro-blocs et la création de pseudo-limites de plaque permet d'introduire des mouvements tectoniques de moins grande importance (<100km) mais qui cumulés sont significatifs dans l'évolution cinématique du système. L'étude met en évidence la relation entre le domaine hyper-étiré d'Ibérie-Terre Neuve et le bassin d'Orphan qui accommode autant d'extension E-O avant la relocalisation de la déformation entre le Banc de Galice et le micro-bloc du Bonnet Flamand. Ainsi la propagation de la déformation extensive continentale est orientée vers le nord cependant elle n'est pas continue et est segmentée par différentes zones de transfert. Par contre l'exhumation du manteau et l'océanisation de ce domaine semblent se propager de manière continue en forme de V. Le mode de propagation en V n'implique pas dans cet exemple de compression à l'avant du propagateur car de l'extension oblique est accommodée en amont du propagateur, dans le Golfe de Gascogne et entre les marges irlandaises et NE de Terre-Neuve. Ainsi ce modèle cinématique fondé sur des données pluridisciplinaires provenant des marges hyper-étirées et de la croûte océanique initie de nouvelles perspectives pour les restaurations de plaque. De plus, il souligne l'évolution complexe, polyphasée et inhomogène d'un système de rift avant l'océanisation.

En conclusion, la déformation qualifiée d'hyper-extension est en 2D principalement dirigée par les propriétés physiques du matériel cassant ainsi que par des lois mécaniques. En revanche l'analyse d'un système de rift hyper-étiré en 3D et dans le temps est plus difficile. Les anomalies magnétiques ne permettent pas à elles seules de déterminer le mouvement relatif des plaques durant le rifting. En effet, il est essentiel de coupler le maximum d'informations pour modéliser l'évolution d'un système de rift et d'analyser ses implications cinématiques. Cette thèse se base sur les exemples du sud de l'Atlantique Nord qui possède une des meilleures collections de données cependant cette méthode peut s'appliquer sur d'autres océans pour déterminer leur cinématique initiale.

# ***EXTENDED ABSTRACT***

Hyper-extended rifted margins are shaped by rifting processes that stretch and thin the continental lithosphere until the formation of an oceanic lithosphere. The stretching of the continental lithosphere creates thermo-mechanical modifications which induce an evolution of the extensional deformation through time and space. This polyphased rift evolution has been recorded in the crustal architecture of rifted margins that can be classified in different domains associated to a specific deformation mode. The southern North Atlantic is surrounded by several hyper-extended margins and basins which do not exhibit many magmatic additions. The word hyper-extended is used to characterize margin architecture as well as its deformation mode. Therefore, a hyper-extended rifted margin is defined by a very thin continental crust (<10km) which extremely thins to 0 and enabling the creation of a new top basement surface composed of exhumed lithospheric mantle prior to a magmatic oceanic crust formation.

This work is based on the observation of the architecture of hyper-extended margin to understand the evolution of deformation processes in 2D and to analyze the evolution of deformation modes through time and space. However this topic is large and the study focuses on two goals: the first one aims at characterizing the physical processes related to the deformation of hyper-extended continental crust. The second one aims analyzes the evolution of the deformation of hyper-extended rift systems through time and space. However, this task needs a reliable kinematic context which is not the case for the southern North Atlantic due to the interpretations of the J magnetic anomaly. Therefore the nature and the pertinence of the J-anomaly for plate restorations needs to be determined. A plate reconstruction method has been developed to analyze the propagation and partitioning of deformation of the hyper-extended rift systems from the southern North Atlantic.

## ***1. The contribution of the critical Coulomb wedge theory to hyper-extended rifted margins***

The first part of this thesis is focused on the deformation mode of the hyper-extended continental crust. This domain has been imaged on many examples in the southern North Atlantic and is outcropping in the Err nape (Swiss Alps). The aim of this section is to measure the angles of the termination of hyper-extended rifted margins and to compare them to the critical Coulomb wedge theory.

The critical Coulomb wedge theory describes the stability limits of a frictional wedge gliding on a basal décollement. This theory is extensively used in convergent tectonic such as

accretionary prism, thrust and fold belts... However the equations are also valid for extensional wedges which aperture angle is decreasing. Seismic sections, boreholes data and field studies highlight the wedge shape of the continental crust termination, the frictional behavior of hyper-extended rocks and the basal décollement below the wedge. The continental crust breaks in a “simple shear” mode producing an upper plate wedge in the hangingwall of the detachment fault and a lower plate wedge in the footwall. However the base of the lower plate wedge is also a low friction décollement level (imaged as the S reflector). The direction of shearing is opposite in the two wedges, toward the continent for the upper plate wedge and toward the ocean for the lower plate wedge, this direction are respectively characteristic of a tectonic extensional Coulomb wedge and a gravitational wedge. Frictional coefficients are determined on hyper-extended rocks drilled on the Iberia margin (serpentinites, phyllosilicates) and fluid pressures are parameterized with the stability of gravitational wedges. Major results are that: the final shape of lower plate wedge always corresponds to a critical gravitational wedge whereas upper plate wedges can be sub-, sup- critic or critic. Basins bounded by continentward oriented faults and the presence of extensional allochthons are explained by a continental breakup model based on the critical Coulomb wedge theory. Moreover this simple physical theory is able to link partial seismic or field observations to integrate them in a tectono-stratigraphic interpretation coherent with physical processes.

## ***2. Reconstruction of a hyper-extended rift system***

The second part of this PhD project analyzes the partitioning and propagation of extensional deformation in the southern North Atlantic. This study illustrates the influence of pre-oceanic extension in the kinematic evolution of the Iberia plate. The idealized workflow is summarized in 4 steps: 1) restoration of the oceanic domain using oceanic magnetic anomalies considered as isochrons, 2) removal of exhumed mantle domains, 3) determination of thinned continental crust volume (on profiles extracted perpendicularly to the margin), 4) palinspatic reconstruction of the continental crust. However, in spite of the numerous data and studies available in this area, there is still a major uncertainty related to the first isochron oceanic magnetic anomaly, leading to problematic plate reconstructions. Therefore the second chapter is dedicated to the determination/characterization of the J-magnetic anomaly and the implications for plate modeling.

## ***2.1 Nature of the J-magnetic anomaly***

The J-magnetic anomaly is a more or less continuous magnetic anomaly located at the continent-ocean transition of the Iberia-Newfoundland conjugate margins. These conjugate anomalies are symmetrical with respect to the mid-Atlantic ridge. The use of the J-anomaly as an isochron at chron M0 (~125 Ma) leads to debated reconstructions in which a Pyrenean ocean which is subducted before ~83 Ma, however there are no observation to support this model. The second interpretation of the J-anomaly corresponds to magmatic underplating and intrusions related to the initiation of an oceanic crust. This interpretation can imply a synchron or diachron formation of the J-anomaly if the lithospheric breakup initiating the oceanic accretion propagates northward. A synchronous formation results in reconstructions with rapid mid Atlantic ridge accretion rate variation whereas a propagation of the J-magnetic-anomaly has still to be tested. Seismic interpretations of sections crosscutting the J anomaly along the entire conjugate margins revealed that the J-anomaly is neither on oceanic crust nor at the oceanic crust- exhumed mantle boundary everywhere. Hence the J-anomaly neither corresponds to a classical oceanic magnetic anomaly, nor to a domain boundary. In contrast the J-anomaly corresponds to several magmatic additions which present highly variable ages (145 Ma to present). Hence this anomaly results from magmatic addition oriented N-S which are potentially following inherited mantle structures. In conclusion the J-anomaly can not be used for plate reconstructions and the position of Iberia can only be constrained by oceanic magnetic anomaly after the Cretaceous normal polarity superchron (~83 Ma).

## ***2.2 Partitioning and propagation of the deformation***

The study of the partitioning and propagation of the deformation is based on the synthesis of major geological data in each rift domain that are integrated in the plate reconstruction model to observe the implications on less constrained area. This work uses seismic interpretations, gravity inversions and potential field methods to perform an accurate mapping of rift domains. This mapping approach coupled to stratigraphic and geochronologic data represent the input to model the 3D evolution of the rift deformation using the plate reconstruction software Gplates. This model highlights the influence of the hyper-extended deformation processes on the kinematic of the southern North Atlantic. The orientation of extension is not necessarily continuous along all the rift system, hence taking a rotation pole at the first oceanic magnetic anomaly and a second at the full-fit cannot take into account the rift evolution. In contrast it is necessary to include micro-blocks which are acting semi-independently from the main plates to partition the deformation in the different rift systems. Moreover the individualization

of micro-blocks and the creation of pseudo plate boundaries introduce smaller scale tectonic motions (<100km) which can be significant if they are cumulated. The study highlights the partitioning between the hyper-extended system of Iberia-Newfoundland and the Orphan basin which accommodated as much E-W extension prior to the re-localization of the deformation as between Galicia-Bank and Flemish Cap. Hence the propagation of the deformation in continental crust is oriented northward and segmented. In contrast the exhumation and oceanization seem to propagate in a V-shape style. The V-shape propagation as discussed in this work does not imply compression at the tip of the propagator because it is compensated by oblique extension in front of the propagation, in the Bay of Biscay and between the Northeastern Newfoundland and Irish margins. Hence this plate model based on pluri disciplinary data coming from hyper-extended margins and oceanic domains initiates new outlooks to perform plate reconstruction. Moreover it highlights the complex, polyphased and inhomogeneous evolution of a hyper-extended rift system prior to oceanic accretion.

To conclude, the so-called hyper-extended deformation is in 2D mostly ruled by physical properties of the brittle material and by mechanical laws. In contrast the 4D analysis of a hyper-extended rift system is more complex. Oceanic magnetic anomalies cannot alone determine the relative plate motion during rifting. Indeed it is crucial to link different kind of data to model an hyper-extended system and to evaluate its implications. This thesis use the southern North Atlantic examples as natural laboratory, however this method can be applied on other oceanic domains to determine the partitioning of the deformation related to their formation.







# **REMERCIEMENTS**

Faire une thèse c'est presque être schizophrène, durant cette expérience scientifique on est à la fois la souris de laboratoire et le chercheur qui l'étudie. Cette période particulière nous en apprend beaucoup sur nous même, mais comme tout bon projet cette expérience a été réalisée en équipe, ainsi j'aimerai dans ces quelques lignes remercier tout les participants.

Mes premiers remerciements vont à la personne la plus impatiente de lire cette section, mon directeur de thèse Gianreto Manatschal. En effet, ton intérêt pour les petites histoires entre collègues n'a d'égal que ta passion pour la géologie des marges hyper-étirées. Merci Gianreto de m'avoir ramené de Norvège, de m'avoir soutenu et de m'avoir fait comprendre que le plus important ce sont les questions. Mon expérience de thèse a été positive en grande partie grâce à toi. Comme on dit dans le Val Müstair « Grazcha Gianreto ! »

Je tiens à remercier mon co-directeur de thèse Nick Kuzsnir qui m'a toujours accueilli avec enthousiasme à l'Université de Liverpool. Son « Agricultural physics » a été d'un grand secours dans la compréhension de la mécanique du prisme de Coulomb et des inversions gravimétriques. Je me souviendrai également des nombreux « Go to meeting » qui m'ont permis d'améliorer le modèle cinématique et de poser toujours plus de nouvelles questions.

Je remercie les membres du jury de thèse, Timothy Reston, Laurent Jolivet, Christian Heine, Daniel Sauter et Dominique Frizon de Lamotte, d'avoir lu mon manuscrit et d'avoir été présents le jour de la soutenance pour y partager leurs questions et leurs idées. Cette journée du 1er décembre 2016 reste pour moi un excellent souvenir et je vous en remercie pour cela.

Mon travail de thèse a été financé par les partenaires industriels du consortium MM3 qui a évolué en MM4. Ainsi j'aimerai adresser mes remerciements à BP, Conoco Phillips, Statoil, Petrobras, Total, Shell, Hess, BHP-Billiton et BG. Je rajouterai à ces remerciements ION GXT qui nous a permis de dessiner et de réfléchir sur certaines de leurs lignes sismiques durant les meetings annuels du consortium. Alan Roberts et Andy Alvey de Badley's Geoscience sont également à remercier pour leurs conseils et le prêt de la licence FlexDecomp.

Je souhaite remercier Laurent Gernigon, ce breton expatrié en Norvège qui m'a, durant mes stages de master, appris les méthodes et la rigueur scientifique, sans toi ma thèse aurait été plus compliquée. Comme je l'ai dit précédemment l'équipe de recherche est indispensable ainsi j'aimerai particulièrement remercier Geoffroy qui m'a mis en relation avec ses collègues de l'Université de Cergy Pontoise et de l'ENS respectivement Bertrand Maillot et Xiaoping Yuan. Merci Xiaoping et Bertrand de m'avoir patiemment expliqué la mécanique du prisme de Coulomb et d'avoir cru en cette application inédite. Julie, tu m'as aidé et accompagné dans

ma recherche depuis mon premier jour à l'institut de géologie pour cela je t'en suis hyper-reconnaisant. Un merci particulier à Daniel qui est toujours là pour pointer les problèmes du modèle. Plus généralement, je remercie toute l'équipe DylBas (bientôt Geols ou un autre acronyme bien senti) votre entrain au travail est communicatif .

Un grand merci à tous ceux qui m'ont aidé administrativement, techniquement ou logistiquement : Ghenima, Dilek, Marc, Betty, Joëlle, David, Didier, Annie.

Je remercie la Liverpool team, j'ai nommé : Leanne ton humour british est exceptionnel, Ludovic merci pour ces repas dignes de chefs étoilés lors de mes visites, Mila avec toi tout est possible, Julia de Catalunya and Caroline from Beuremingham bonne chance à vous tous.

Une triste nouvelle est cependant arrivée, Marco ton énergie, tes connaissances et ta motivation nous manque à tous, tu resteras pour moi l'exemple du géologue par excellence.

Voilà la partie qui concerne le premier étage et les quelques expatriés au deuxième ou plus loin. Le réaménagement des bureaux de l'équipe a été effectué durant mes premiers mois de thèse, ainsi les chercheurs « expérimentés » ont migrés vers le deuxième étage alors que les « novices » se sont regroupés au premier. Ce qui confirme le dicton quand le chat n'est pas là les souris dansent. De ce trou de souris se sont échappés quelques bons éléments, Victor do Brasil, mon co-bureau à l'accent chantant, Isa sport forever, Alexis fait la job, Pierre j'espère qu'Attila ne t'a pas mangé, Alesandro et Emilien le vosgien. Cependant il reste encore des hyper-souris : la sans-dent Marie-Eva (c'était pour la petite souris), Benoit plus suisse qu'un suisse, Rodolphe avec ses chemises bien repassées, Morgane avec le petit Jacky, Pauline ma bienveillante co-bureau, la légende de l'aéroport Francis, Bruno dans sa chrysalide, Médéric à l'odorat subtile, la fille du grand sud Charlotte, les Jeanne<sup>2</sup>, Paul en mission top secret, Sonia et son huile d'olive, Coralie qui déborde d'énergie, Quentin qui ma fait découvrir la spiruline et enfin le dernier de la portée Simon.

Merci à tous mes amis accumulés au cours des années vous avez tous des hyper-projets, je vous souhaite à tous qu'ils se réalisent.

Je remercie très chaleureusement ma famille, plus particulièrement mes parents qui m'ont tout appris, ma sœur pour toutes ses qualités (notamment sa cuisine) ainsi qu'Arnaud.

Finalement, la souris de laboratoire se sent beaucoup mieux aux cotés d'une autre souris. Ainsi je remercie infiniment la petite souris qui partage ma vie.





---

# ***SOMMAIRE***

---

# **SOMMAIRE**

|  |     |
|--|-----|
| AVANT-PROPOS   | 5   |
| RÉSUMÉ ÉTENDU  | 7   |
| EXTENDED ABSTRACT  | 11  |
| REMERCIEMENTS  | 17  |
| SOMMAIRE   | 21  |
| INTRODUCTION   | 25  |
| <b>1. Structures et processus de déformation des marges hyper-étirées</b>  | 27  |
| <b>2. Les restaurations cinématiques</b>   | 36  |
| <b>3. L'exemple des domaines hyper-étirés du sud de l'Atlantique Nord</b>  | 40  |
| <b>4. Grandes questions, démarche scientifique et plan de la thèse</b>   | 49  |
| CHAPITRE I   | 57  |
| <b>Abstract</b>  | 59  |
| <b>1. Introduction</b>   | 60  |
| <b>2. The Critical Coulomb Wedge Theory (CCWT)</b>   | 61  |
| <b>3. Hyper-Extended Continental Wedges (HECW): characterisation, terminology and definitions</b>  | 63  |
| <b>4. Results</b>  | 73  |
| <b>5. Discussion</b>   | 74  |
| <b>6. Conclusions</b>  | 79  |
| <b>Acknowledgments</b>   | 80  |
| <b>Outlooks: Crustal and associated sedimentary architecture of hyper-extended continental wedges in sediment- and magma- starved rifted margins</b> | 81  |
| <b>Supplementary material</b>  | 89  |
| CHAPITRE II  | 91  |
| <b>Abstract</b>  | 93  |
| <b>1. Introduction</b>   | 93  |
| <b>2. The J-magnetic anomaly: definition and interpretations</b>   | 94  |
| <b>3. Nature of the J-anomaly</b>  | 97  |
| <b>4. Implications for plate reconstructions and conclusion</b>  | 101 |
| <b>Acknowledgements</b>  | 103 |
| <b>Supplementary material</b>  | 104 |
| CHAPITRE III   | 107 |

|  |     |
|--|-----|
| <b>Abstract</b>  | 109 |
| <b>1. Introduction</b>   | 110 |
| <b>2. The North Atlantic Ocean: geography, inheritance and kinematic framework</b> | 112 |
| <b>3. Hyper-extended rifted margins: a kinematic description</b>                   | 114 |
| <b>4. Hyper-extended rifted margins and basins</b>                                 | 121 |
| <b>5. Tectonic evolution of the southern North Atlantic rift domains</b>           | 127 |
| <b>6. Discussion</b>   | 135 |
| <b>7. Conclusion</b>   | 146 |
| <b>Acknowledgements</b>  | 147 |
| <b>Supplementary material</b>  | 148 |
| CHAPITRE IV  | 151 |
| DISCUSSION GÉNÉRALE  | 152 |
| CONCLUSION   | 165 |
| PERSPECTIVES   | 171 |
| RÉFÉRENCES   | 177 |
| ANNEXES  | 197 |
| <b>A.1 Les données de méthodes potentielles</b>                                    | 199 |
| <b>A.2 Les données de sismique réfraction</b>                                      | 201 |
| <b>A.3 Les forages profonds DSDP, OPD, IODP</b>                                    | 207 |
| <b>A.4 Inversion Gravimétrique</b>   | 208 |
| <b>A.5 Flexural Backstripping</b>  | 211 |
| <b>A.6 Modèle Cinématique</b>  | 213 |
| <b>A.7 Annexe électronique</b>   | 219 |





---

# ***INTRODUCTION***

---



D'après la théorie de la dérive des continents (Wegener, 1915) et ensuite la tectonique des plaques (Vine and Matthews, 1963; Morgan, 1968; Bullard, 1965; Le Pichon, 1968) une lithosphère continentale est amenée à se fragmenter en plusieurs plaques, s'éloignant les unes des autres par l'accrétion d'une nouvelle lithosphère océanique au niveau des dorsales médio-océaniques. Les lithosphères continentales et océaniques sont, une fois formées, des systèmes stables, respectivement inerte et en accretion. Cependant l'étape de transition entre ces deux états stationnaires implique de nombreux processus tectonophysiques qui sont encore mal connus. Cette étape nommée rifting est enregistrée dans les marges passives et correspond à l'étirement et à l'amincissement de la lithosphère continentale précédant la mise en place l'installation d'une limite de plaque divergente stable. Alors que l'architecture crustale des marges, et particulièrement celle des marges « hyper-étirées » est assez bien définie grâce aux données sismiques, les modes de déformation d'un système de rift restent peu contraints. Dans ce travail, nous nous intéresserons spécifiquement aux processus physiques contrôlant l'architecture de la terminaison de la croûte continentale ainsi qu'à l'évolution dans le temps et dans l'espace des différents modes de déformation. De plus, nous mettrons en valeur l'importance des modes de propagation d'un système de rift pour l'évolution cinématique d'un océan en formation.

L'introduction de cette étude apporte une description générale des différents domaines d'une marge hyper-étirée pauvre en magma reprenant ainsi les grands concepts sur leur mode de formation. Elle présente aussi les méthodes de reconstructions cinématiques avant d'introduire les marges du sud de l'Atlantique Nord et d'aborder les problématiques majeures ainsi que la démarche suivie dans ce manuscrit de thèse.

## **1. STRUCTURES ET PROCESSUS DE DÉFORMATION DES MARGES HYPER-ÉTIRÉES**

### **1.1 Définitions générales**

Le terme de marge est utilisé en tectonique pour décrire la zone de transition entre une lithosphère océanique et une lithosphère continentale. Cependant ces zones de transition ne sont pas toujours des limites de plaques. En effet, il existe deux types de marges continentales, celles dites «actives» présentent une forte sismicité due à la subduction de la lithosphère océanique sont des limites de plaques actuelles, alors que les marges dites «passives» ne présentent pas cette activité et ne sont plus des limites à l'heure actuelle.

Une marge passive résulte de l'amincissement extrême d'une lithosphère continentale qui se brise pour créer deux plaques continentales séparées par une nouvelle lithosphère océanique. Deux modes d'amincissement lithosphérique ont été proposés en « cisaillement

pur» (McKenzie, 1978) et en « cisaillement simple » (Wernicke, 1985) (Fig. 1). Le premier implique un amincissement uniforme de la lithosphère, ainsi le facteur d'amincissement de la croûte est égale à celui du manteau lithosphérique. Ce modèle implique une symétrie des marges conjuguées et produit des bassins de rifts bordés par des failles normales caractéristiques de nombreux systèmes de rift. Le cisaillement simple est un modèle proposé pour expliquer l'asymétrie des marges conjuguées, dans ce cas l'amincissement et l'extension lithosphérique sont contrôlés par une faille de détachement à faible pendage. Pourtant l'observation de la déformation crustale montre qu'aucune des deux propositions n'est applicable à l'ensemble de l'évolution du rift. Ainsi nous allons décrire la structure des marges riftées et discuter de l'évolution de leurs modes de déformations.

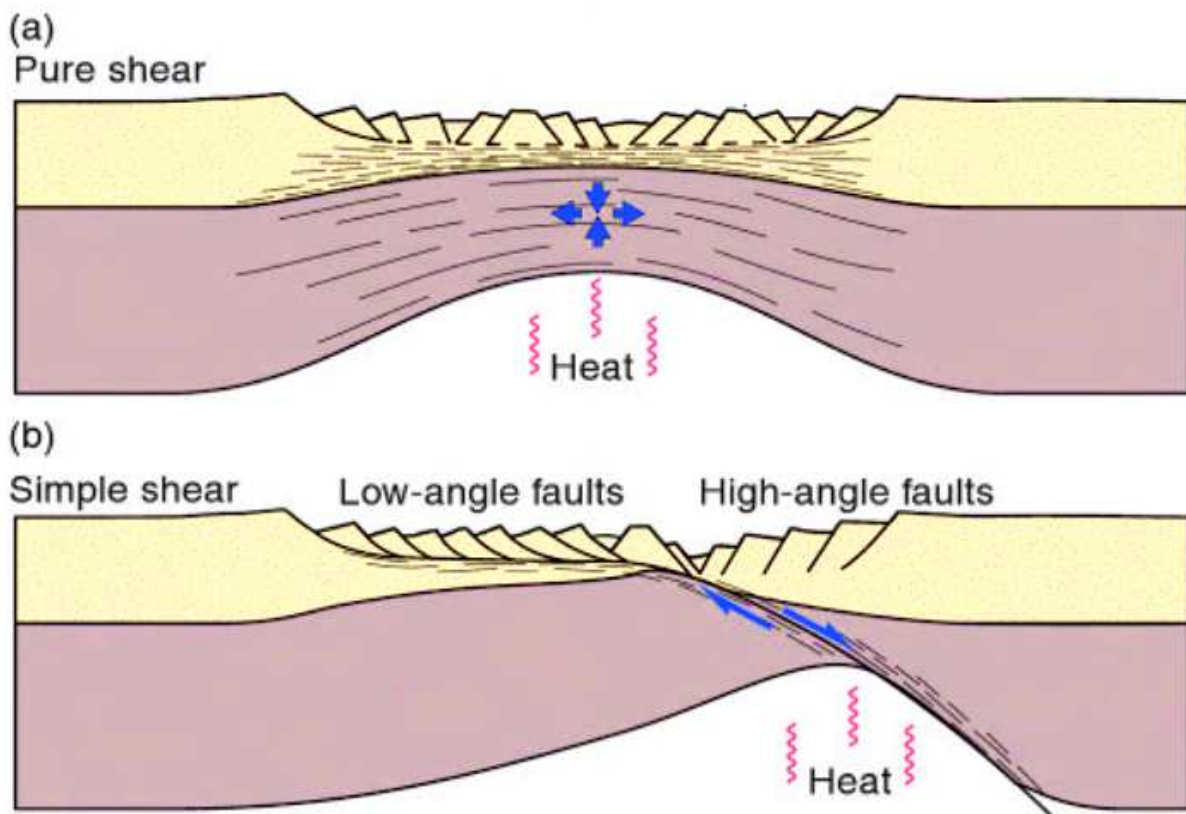


**Fig. 1:** Mode d'extension de la lithosphère continentale. a) Le mode de cisaillement pur correspond à une extension uniforme (McKenzie, 1978). b) Le mode de cisaillement simple implique une faille de détachement à faible angle séparant la lithosphère en une plaque supérieure et une plaque inférieure (Wernicke, 1985) (Fossen, 2010)

**Fig. 1:** Continental lithosphere extension mode. a) Pure shear mode corresponds to a uniform extension (McKenzie, 1978). b) Simple shear mode imply a low angle detachment fault separating the lithosphere in an upper and lower plates (Wernicke, 1985) (Fossen, 2010).

## 1.2 Structure d'une marge hyper-étirée

Il existe trois grands types de marges passives, les marges pauvres en magma, celles riches en magma et les marges transformantes (Reston, 2009) (Fig. 2). Cette caractérisation semble bien définie, pourtant ces trois types sont des extrêmes et de nombreux exemples ne correspondent pas uniquement à une catégorie. Cette étude se focalise sur les marges à faible budget magmatique, présentant une ouverture orthogonale car les structures sont mieux imagées et plus simples à intégrer dans un contexte géodynamique. Le terme de marge hyper-étirée est assez vague et est soit lié à une croûte très fine et à l'exhumation du manteau (Sutra et al., 2013; Unternehr et al., 2010) soit au type de déformation crustale (Tugend et al., 2015b). Dans les deux cas, le terme de marge hyper-étirées peut être utilisé lorsqu'une marge présente une épaisseur crustale fine (<10 km) et que les failles recoupent l'ensemble de la croûte continentale. Cependant et malgré les fortes variations morphologiques, sédimentaires et magmatiques des marges hyper-étirées, leurs architectures à grande échelle présentent des similitudes permettant de déterminer des domaines structuraux. Pourtant chaque étude redéfinit ces domaines en fonction de l'objectif scientifique. Ainsi la terminologie utilisée ci-dessous est définie pour ce projet et n'est pas nécessairement celle utilisée par d'autres auteurs (e.g. (Chenin et al., 2015; Peron-Pinvidic and Osmundsen, 2016; Sutra et al., 2013; Tugend et al., 2015b) (Fig. 3)

**Le domaine proximal** (gris-brun Fig. 4) possède une croûte continentale peu ou pas amincie (généralement  $30 \pm 5$  km d'épaisseur) et est caractérisé par la présence de nombreux hemi-grabben bordés par des failles normales listriques s'enracinant dans la croûte moyenne. Cette déformation extensive permet de créer des structures de croissance sédimentaire en éventail cependant elle ne permet pas un amincissement significatif de la lithosphère ou de la croûte continentale. Ce domaine peut être vaste et s'étendre sur plusieurs centaines de kilomètres (e.g. les Grands Bancs >300km). Parmi les exemples les plus caractéristiques des bassins proximaux, on retrouve le bassin de Jeanne d'Arc sur les Grands Bancs canadien (Tankard et al., 1989) et le bassin de Generoso dans les Alpes italiennes et suisses (Manatschal, 2004).

**Le domaine de croûte continentale amincie** (orange Fig. 4) est limité du côté continental par la ligne de necking (NL) (étranglement) qui correspond au début de l'amincissement crustal et du côté océan par la pointe de la croûte continentale (Edge of the Continental Crust ECC) qui indique la disparition de la croûte continentale. Cette définition est utilisée dans le troisième chapitre de ce manuscrit car elle permet de simplifier la méthode de restauration. En revanche, on peut distinguer le domaine de necking et le domaine de croûte continentale hyper-étirée à l'intérieur du domaine la croûte amincie.

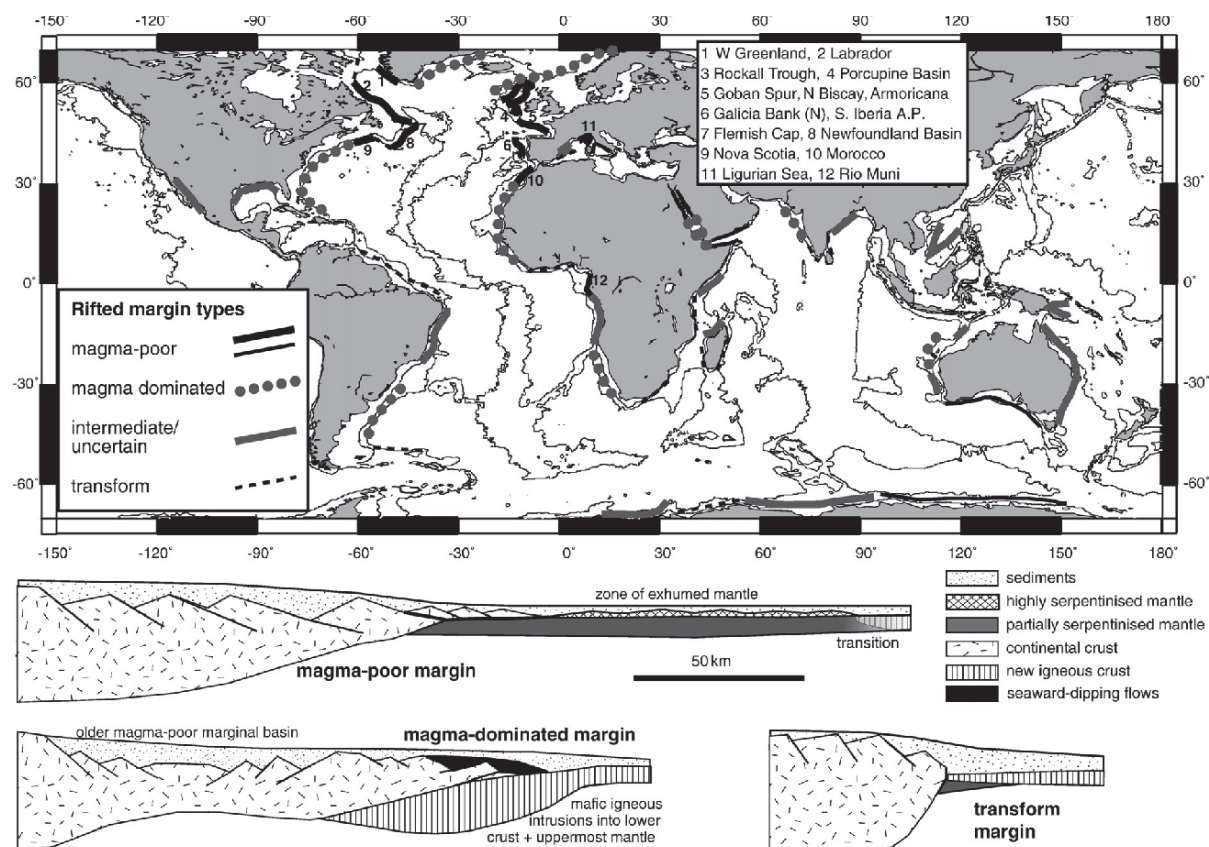


**Fig. 2:** Carte présentant la localisation des marges passives riftées, accompagnée de représentations classiques de différents types de marges : pauvre en magma, magmatique et transformante (Reston, 2009)

**Fig. 2:** Worldwide distribution of different passive rifted margin types. Classical representations of the different margin types: magma poor, magma rich and transform margins (Reston, 2009)

**Le domaine de necking** (jaune Fig. 4) est caractérisé par une réduction brutale de l'épaisseur crustale de plus de 30 km à moins de 10 km d'épaisseur sur des distances relativement faibles souvent inférieures à 100 km (Mohn et al., 2012). Cette diminution de l'épaisseur crustale est observée le long de profils de sismique réfraction (Funck et al., 2003; Van Avendonk et al., 2006) et est facilement interpolée avec des données gravimétriques car la zone de necking induit la remontée de matériel mantellique dense. Les bassins de la zone de necking sont bordés par des failles normales mais présentent généralement un remplissage sédimentaire plus important que les bassins du domaine proximal. Ainsi cette zone est marquée par une forte augmentation de l'espace d'accommodation. Ainsi le toit du socle et le Moho semblent converger dans cette zone (Osmundsen and Redfield, 2011).

**Le domaine de croûte continentale hyper-étirée** (violet Fig. 4) constitue la terminaison continentale d'une marge passive. La transition avec la zone de necking est marquée par une rupture de pente du Moho et par une modification de l'architecture des bassins sédimentaires. Ce domaine contrairement au necking présente souvent une asymétrie de marges conjuguées. Ainsi une marge peut présenter une terrasse caractérisée par un toit du socle et

un Moho parallèle ainsi que des failles ne recoupant pas la totalité de la croûte et formant des petits bassins sédimentaires (Hauptert et al., 2016). La terminaison océanique de cette terrasse est formée par une ou plusieurs grandes failles s'enracinant au niveau du Moho et délimitant avec la pointe continentale un prisme de croûte continentale très déformée. La marge conjuguée présente une alternance de blocs basculés et de bassins. Les failles s'enracinent sur le Moho qui réduit progressivement sa profondeur, alors que le toit du socle s'approfondit ce qui forme un prisme.

**Le domaine de manteau exhumé** (vert Fig. 4) marque un changement de composition du socle. Du manteau serpentinisé a été pour la première fois dragué puis foré sur la marge ibérique dans les années 80 (Boillot et al., 1987, 1980). Depuis ce domaine a été étudié grâce aux forages ODP (Sawyer, 1994; Tucholke and Sibuet, 2006; Whitmarsh et al., 1998), aux études de terrain ainsi qu'à différentes méthodes géophysiques. L'extension maximale de ce domaine n'est pas connue mais il possède une largeur de plus de 200 km sur la marge Antarctique et est composé d'une alternance de hauts et de bas topographiques (Gillard et al., 2016a). La profondeur moyenne du socle est en général plus grande que celle de la croûte continentale et océanique ce qui induit un fort espace d'accommodation. De plus ce domaine est marqué par une absence de Moho sismique (Dean et al., 2000) mais présente un gradient de vitesse correspondant à un gradient de serpentinsation (Hopper et al., 2007).

**Le domaine de croûte océanique** (bleu Fig. 4) correspond à une structure conventionnelle de la croûte océanique définie comme de type « Penrose » (e.g. Penrose conference 1972). Cette croûte conventionnelle a une épaisseur de 5 à 7 km et est composée principalement d'une couche basaltique composée de pillow lava et de filons et d'une couche gabbroïque recouvrant le manteau asthénosphérique. Ainsi le Moho pétrologique est bien défini et correspond au Moho sismique plat caractérisant le domaine de croûte océanique. De plus les roches de la croûte océanique sont moins denses que celles du domaine de manteau exhumé ce qui induit un toit du socle moins profond. Cependant cette structure de croûte océanique ne représente que les systèmes à fort budget magmatique dont la vitesse d'extension est élevée (>60 mm/a d'extension total) (Dick et al., 2003). Dans les systèmes peu magmatiques qui possèdent des vitesses lentes (<60 mm/a) à ultra-lentes (<20 mm/a) les couches volcaniques ne sont pas continues, la croûte océanique est alors composée d'intrusions magmatiques incluses dans du manteau serpentinisé (Cannat, 1996) et est similaire au domaine de manteau exhumé.

### 1.3 Evolution et phases de déformation des rifts hyper-étirés

Les différents domaines structuraux définis précédemment présentent des morphologies distinctes qui enregistrent l'évolution des modes de déformations différents. Ainsi chaque



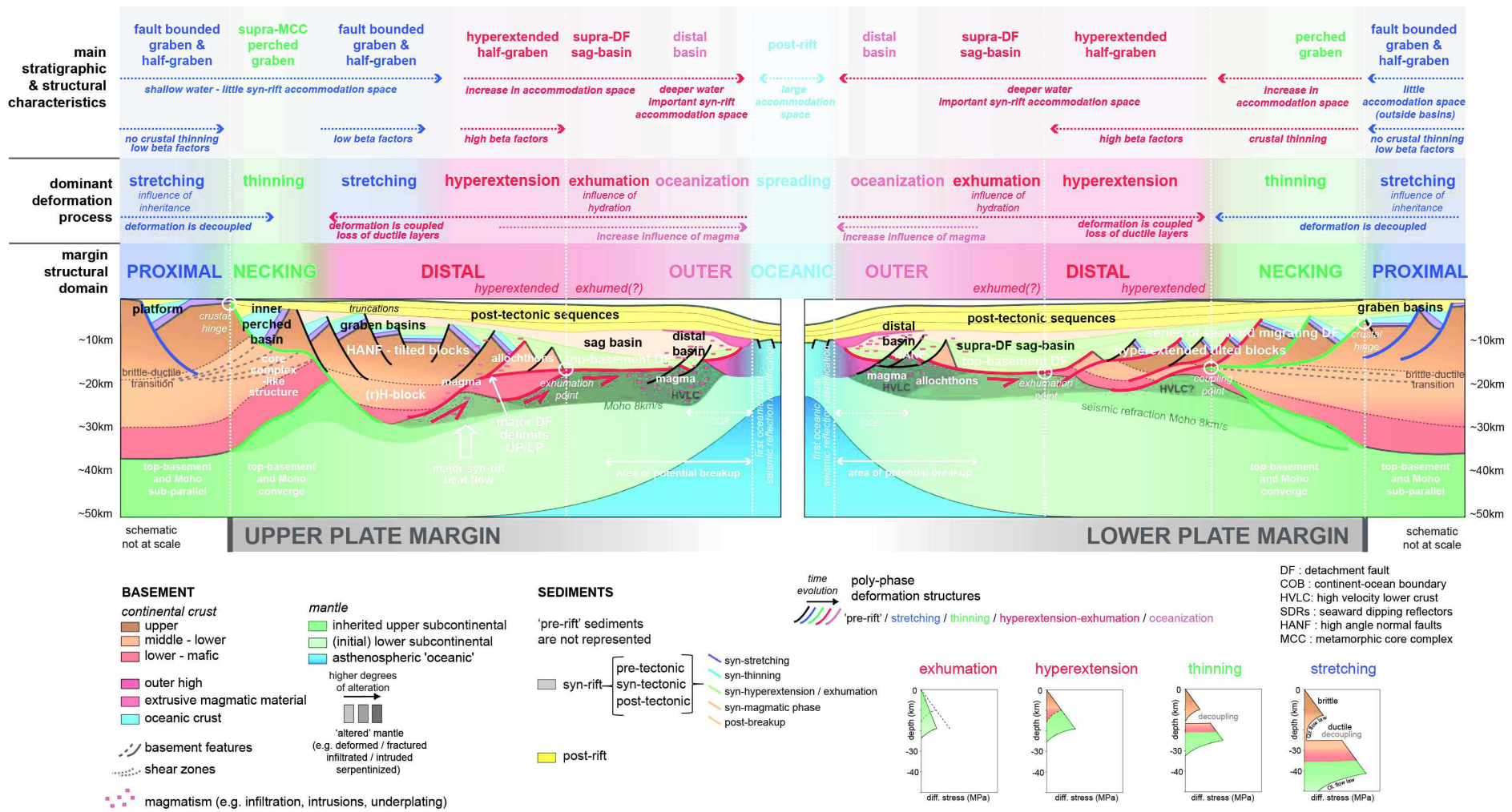
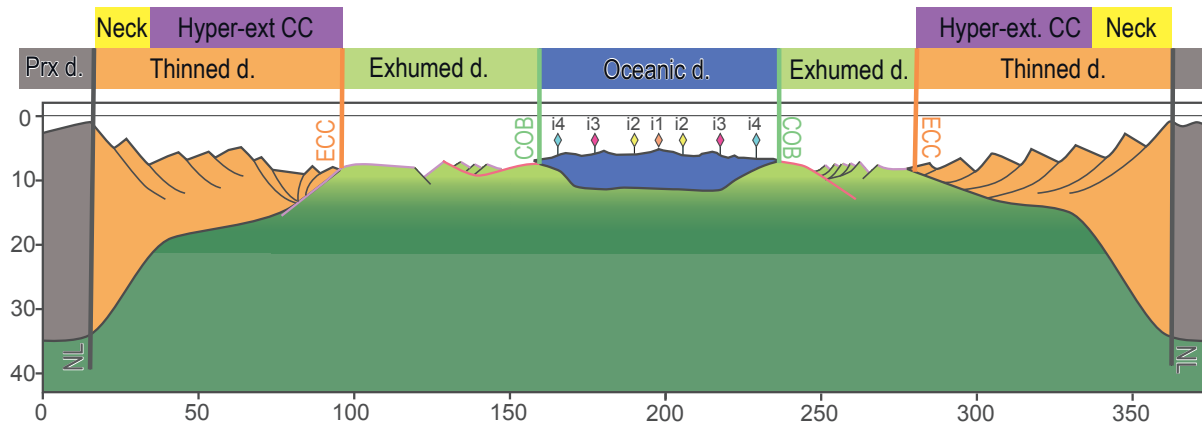


Fig. 3: Schéma représentant la structure de marges conjuguées. Cette figure résume les caractéristiques structurales et stratigraphiques, les processus ainsi que les domaines d'un système de rift hyper-étiré. (Peron-Pinvidic and Osmundsen, 2016)

Fig. 3: Schematic representation of conjugate margins structure. This figure summarize stratigraphic characteristic, tectonic processes as well as structural domains of a hyper-extended rift systems (Peron-Pinvidic and Osmundsen, 2016)



**Fig. 4:** Schéma illustrant un système de marge conjugué avec la terminologie utilisée tout au long du manuscrit (Prx, proximal domain ; Neck, necking domain ; Hyper-ext CC, hyper-extended continental crust ; NL, necking line ; ECC edge of the continental crust ; COB, continent ocean boundary)

**Fig. 4:** Cartoon of a conjugate margin system with the terminology used all along the manuscript (Prx, proximal domain ; Neck, necking domain ; Hyper-ext CC, hyper-extended continental crust ; NL, necking line ; ECC edge of the continental crust ; COB, continent ocean boundary)

domaine est principalement déformé par un mode propre (Fig. 5) dû à l'évolution des propriétés rhéologiques et à la focalisation de la déformation. Ces phases de déformation ont été décrites principalement en deux dimensions sur des observations sismiques (Gillard et al., 2015; Péron-Pinvidic and Manatschal, 2009; Sutra and Manatschal, 2012), sur des analogues de terrain (Beltrando et al., 2015; Manatschal, 2004; Masini et al., 2013; Mohn et al., 2012) et par des modèles numériques (Brune et al., 2014; Huisman and Beaumont, 2014; Lavier and Manatschal, 2006)

**La phase d'étirement** (stretching) est la mieux préservée dans les bassins du domaine proximal. Elle correspond au « wide rift » défini par Buck, 1991 et est caractérisée par une déformation de la croûte supérieure cassante décollée du reste de la déformation lithosphérique par une croûte moyenne ductile (cf. profils rhéologique Fig. 3) . Cependant la structure initiale de la croûte est liée à l'héritage post-orogénique (Petri, 2014) ainsi son profil rhéologique peut être différent de celui défini pour une lithosphère varisque et ainsi peut modifier le mode de déformation.

**La phase de necking** (thinning) provoque une forte réduction de l'épaisseur crustale, généralement de plus de 30 km à moins de 10 km d'épaisseur. Cette phase localise la déformation sur un domaine réduit et isole un bloc aminci (Bloc H, Lavier and Manatschal, 2006) entre les domaines proximaux conjugués. Cependant les processus de l'amincissement ne sont pas bien compris. En effet la déformation cassante de la croûte continentale est insuffisante pour accommoder à elle seule l'amincissement (Kusznir et al., 2004; Sibuet, 1992). Cette différence entre l'extension observée de la partie cassante et l'amincissement total a été expliqué par une extension différentielle des différentes couches crustales (e.g. depth dependent

thinning; Huismans and Beaumont, 2011; Kuszniir et al., 2004) ou par le fait qu'une partie non négligeable de la déformation cassante n'est pas visible sur les lignes sismiques (McDermott and Reston, 2015; Reston, 2007). Les analogues de terrains exposés dans les Alpes montrent des évidences de l'excision de la croûte moyenne ductile durant cette phase (Mohn et al., 2012). Ainsi la rhéologie initiale semble prédominante dans le mode de déformation et l'architecture du necking.

**L'hyper-extension** est la phase de déformation qui amincit la croûte continentale jusqu'à sa disparition. Cette phase correspond à la déformation du bloc H par des systèmes de failles de détachement (Péron-Pinvidic and Manatschal, 2009). Le refroidissement et l'hydratation de ce bloc aminci entraînent un changement de la rhéologie initiale et une déformation cassante couplant la croûte et le toit du manteau (Pérez-Gussinyé and Reston, 2001; Sutra and Manatschal, 2012). Cette modification permet l'installation d'une faille de détachement majeure impliquant une extension en cisaillement simple (Wernicke, 1985) expliquant l'asymétrie du domaine hyper-étiré. La position de cette faille de détachement n'est pas fixe et sa migration vers son toit entraînant un fluage de la croûte inférieure vers la surface (Brune et al., 2014; Ranero and Pérez-Gussinyé, 2010) permet d'expliquer la forte asymétrie observée par exemple sur les marges conjuguées de Campos et d'Angola en Atlantique Sud (Unternehr et al., 2010). Ce domaine a cependant été interprété de manière différente: 1) comme résultant de l'extrusion de la croûte inférieure (Driscoll and Karner, 1998; Jolivet et al., 2015), 2) provenant de l'effondrement crustal au centre du bassin (Brun and Beslier, 1996; Nagel and Buck, 2004), 3) ou par un système de deux failles de détachement conjuguées et symétriques (Direen et al., 2013)

**L'exhumation** permet d'accommoder des centaines de kilomètres d'extension sans l'installation d'une dorsale médio-océanique où déformation et système magmatique sont localisés et restent localisés. Cependant ce domaine ne correspond pas simplement à une faille de détachement exhument le manteau (Manatschal et al., 2011), mais est constitué de plusieurs failles de détachement se distribuant en et hors séquence (Gillard et al., 2016a, 2015; Reston and McDermott; 2011, Sibuet et al., 2007a). Ces structures tectoniques sont accompagnées et interdépendantes de systèmes magmatiques et hydrothermaux qui modifient la structure du manteau exhumé (Gillard et al., 2016b; Pinto et al., 2015). Ces processus ne semblent pas directement influencés par l'héritage et la rhéologie est uniquement influencée par l'hydratation et le magmatisme syn-tectonique.

**L'accrétion océanique** correspond à l'expansion symétrique d'une croûte océanique mafique au niveau d'une dorsale médio-océanique stable. Cependant cette définition n'est valable que dans le cas des dorsales rapides qui ont des vitesses supérieures

à 60 mm/a (Dick et al., 2003), pour les dorsales lentes et surtout ultra-lentes (<20 mm/a) le mode d'extension n'est pas uniquement basé sur la création de matériel magmatique. En effet la dorsale Est-Indienne présente des segments où l'extension s'est faite par l'exhumation du manteau (Cannat et al., 2006). Ainsi même si la composition du plancher océanique peut être similaire au domaine exhumé, l'extension tectonique reste localisée à l'aplomb de la remontée asthénosphérique grâce à des failles en flip-flop (Sauter et al., 2013). Dans les contextes pauvres en magma la rupture lithosphérique correspondant à la localisation de la déformation est ainsi complexe à déterminer et des domaines de croûte océanique embryonique peuvent être définis (Gillard et al., 2015).

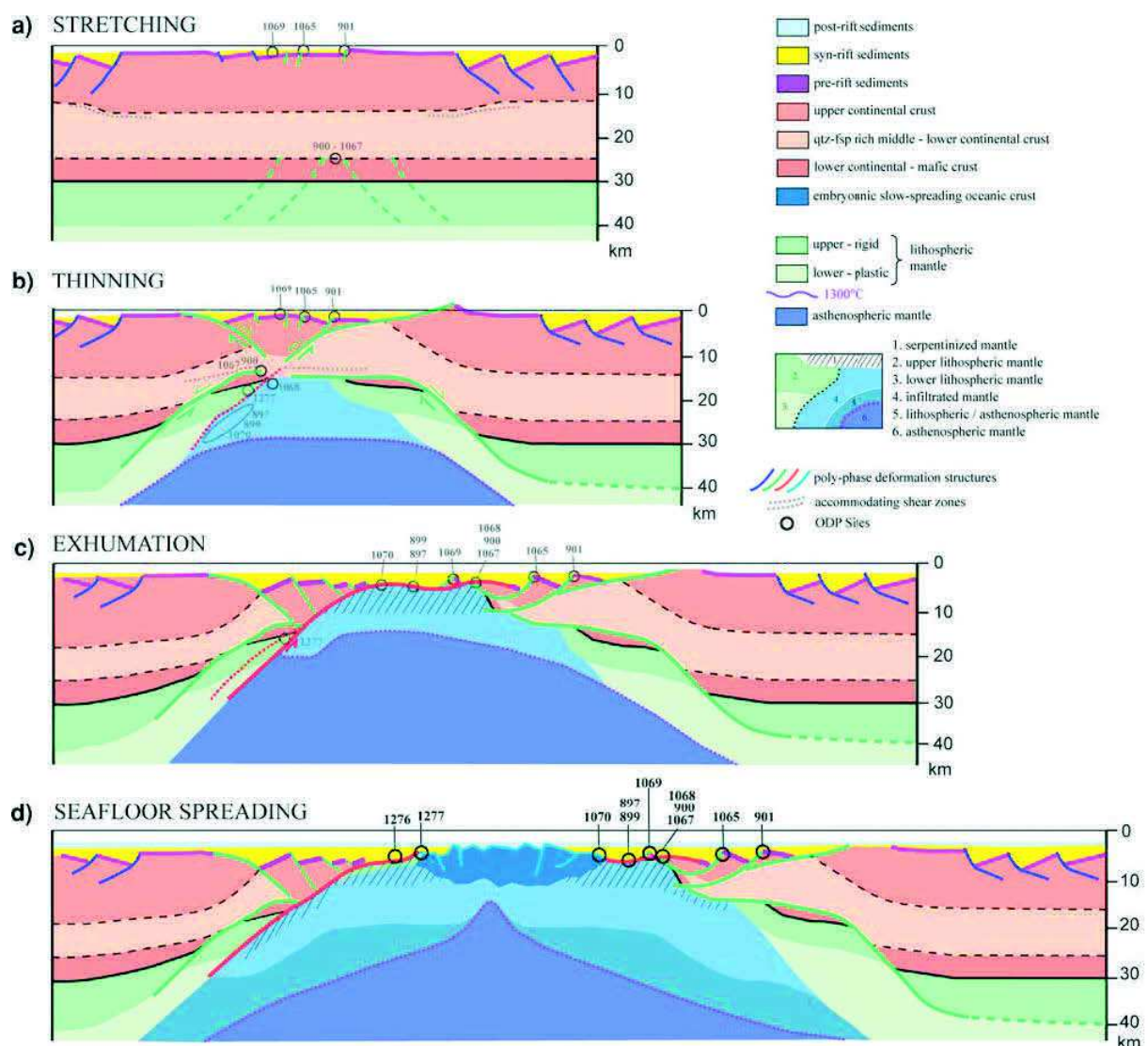


**Fig. 5:** Modèle conceptuel de l'évolution polyphasée d'un système de rift hyper-étiré peu magmatique : a) La phase d'étirement; b) la phase d'amincissement; c) la phase d'exhumation; d) la phase d'accrétion océanique. (Péron-Pinvidic and Manatschal, 2009)

**Fig. 5:** Conceptual model of the polyphased evolution of magma poor hyper-extended rift system: a) stretching; b) thinning; c) exhumation; d) oceanic accretion. (Péron-Pinvidic and Manatschal, 2009)

## 2. LES RESTAURATIONS CINÉMATIQUES

### 2.1 Définitions générales

La cinématique des plaques est l'étude du mouvement des plaques tectoniques aux cours du temps. Les premiers travaux cinématiques ont été effectués par Wegener (1915) (Fig. 7) qui propose une première reconstruction de l'Atlantique basée sur la géométrie des côtes américaines et africaines ainsi que sur des critères paléontologiques. Cependant une solution présentant moins de trous et de superpositions est trouvée en utilisant l'isobathe 500m (Bullard et al., 1965) correspondant approximativement à ce que nous qualifierions de ligne de necking. Ces restaurations ne représentent pas les mouvements mais seulement deux instants dans l'évolution d'un système océanique. La cinématique des plaques est basée sur la définition par le mouvement d'une plaque par rapport à une autre plaque fixe ou par rapport à un référentiel défini. Tout mouvement sur une sphère est défini par une rotation autour d'un axe passant par le centre de la sphère, l'intersection entre l'axe et la surface de la sphère sont les pôles de rotations eulériens (Fig. 6). Ainsi le mouvement d'une plaque est déterminé par les coordonnées de son pôle de rotation et son angle de rotation.

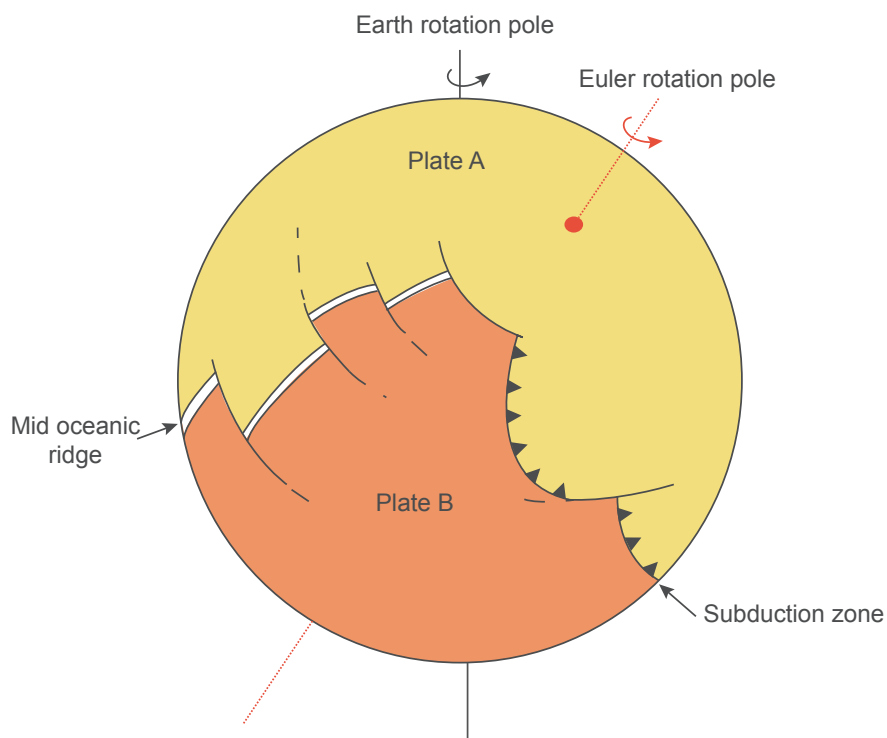


**Fig. 6:** Schéma illustrant le mouvement relatif de deux plaques suivant un pôle de rotation eulérien, la plaque A est considérée fixe.

**Fig. 6:** Relative motion of two plates following an Euler rotation pole, plate A is considered fixed.

Trois principales méthodes sont utilisées pour proposer des reconstructions cinématiques: 1) les reconstructions basées sur les anomalies magnétiques marines, 2) les reconstructions basées sur le paléomagnétisme et 3) les reconstructions géologiques qualitatives. Evidemment certaines études compilent deux voire trois types d'informations (Torsvik et al., 2008; Vissers and Meijer, 2012a). En revanche toutes ces méthodes ont des limites ainsi les anomalies magnétiques marines ne permettent de faire des restaurations que pour les derniers 220 Ma si le domaine étudié est en partie océanique (Müller et al., 1997). Le paléomagnétisme donne la paléo-latitude et l'angle de rotation d'un bloc, sa résolution spatiale est plus faible mais son emprise temporelle est plus grande ( $> 2\text{Ga}$  Evans and Pisarevsky, 2008). Alors que les données géologiques ne permettent pas des reconstructions contraintes spatialement mais donne une bonne notion de l'évolution d'un système et sont le plus souvent proposées dans des systèmes compressifs (Handy et al., 2010; Stampfli and Hochard, 2009).

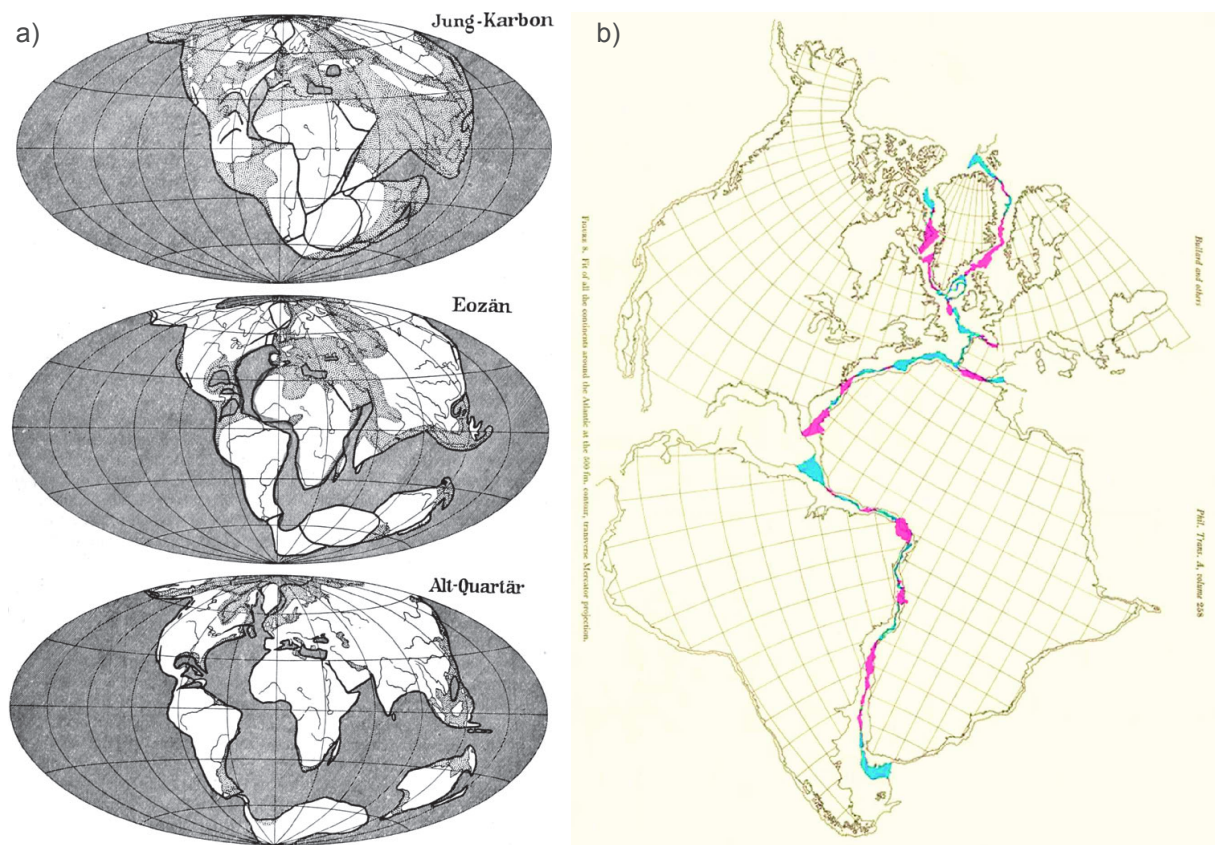


**Fig. 7:** Premières tentatives de restauration paléogéographique : a) Restauration de la Pangée (Wegener, 1915) b) Fermeture palinspatique de l'Océan Atlantique (Bullard et al., 1965)

**Fig. 7:** First attempts of paleogeographic reconstructions: a) Pangea reconstruction (Wegener, 1915) b) Palinspatic closure of the Atlantic Ocean (Bullard et al., 1965)

## **2.2 Les anomalies magnétiques océaniques et leur utilisations**

Les anomalies magnétiques océaniques sont des anomalies magnétiques linéaires présentes au niveau de la croûte océanique. Leur origine est due au comportement ferromagnétique des roches de la croûte océanique (Bullard and Masson, 1963). Ainsi le magma asthénosphérique refroidit au niveau de la dorsale, se solidifie, enregistre le champ magnétique régional de cette époque et est déplacé latéralement du fait de l'expansion du plancher océanique. Les changements successifs de polarité du champ magnétique terrestre sont alors enregistrés au cours du temps et définissent des blocs d'aimantation normale et inverse. L'expansion symétrique de la croûte océanique se poursuit et forme ainsi des anomalies linéaires parallèles à l'axe de la dorsale. Ces anomalies ont le même âge sur toute leur longueur et sont appelées isochrones (Vine and Matthews, 1963), cet âge est déterminé grâce à des inversions du signal géomagnétique (Heirtzler et al., 1968). Ainsi l'identification de ces isochrones (Fig. 8) permet de déterminer l'âge de la lithosphère océanique (Müller et al., 1997). Cependant pour effectuer une reconstruction cinématique il faut l'âge et la direction du mouvement. Les mouvements sont enregistrés grâce aux fractures transformantes océaniques (Müller and Roest, 1992) qui séparent deux segments de dorsale. Ainsi les mouvements des plaques sont déterminés très précisément les uns par rapport aux autres. La définition d'un référentiel terrestre basé sur la stabilité des points chaud du Pacifique (Wessel and Kroenke, 2008) permet même une restauration absolue. Cependant la majorité de la croûte océanique est Crétacé ou plus récente ce qui permet de modéliser moins de 4% de l'évolution de la Terre. De plus durant la période Jurassique calme (>154 Ma) et durant le super isochrone à polarité normale du Crétacé (120.6-83.5 Ma) le champ magnétique n'a pas été favorable à la création d'isochrone, ce qui rend les restaurations incertaines. Il faut également noter que les anomalies magnétiques dans les transitions océan-continent (Russell and Whitmarsh, 2003; Sibuet et al., 2007; Nirrengarten et al. 2016b) sont contestées car la mise en place de ces domaines ne se sont pas faits par des processus symétriques (Gillard et al., 2016b) et que les processus magmatiques de la rupture lithosphérique créant également des anomalies magnétiques ne sont pas bien compris (Bronner et al., 2011).

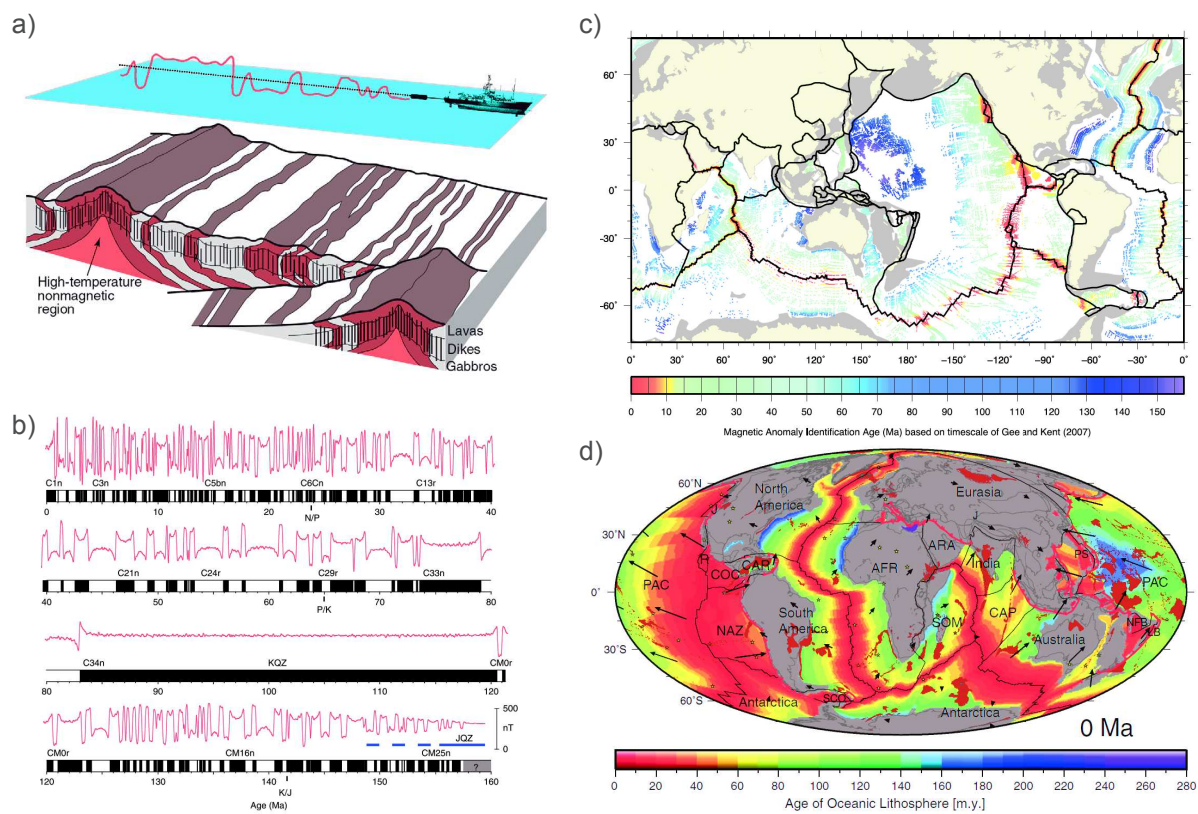


**Fig. 8:** a) Schéma tridimensionnel montrant la formation d'une croûte océanique et l'enregistrement des inversions de la polarité du champ magnétique au cours du temps. Les bandes sombres correspondent à des zones accrétées dans une période normale et les blanches durant des périodes inverses (Gee and Kent, 2007). b) Echelle des inversions géomagnétiques au cours du temps et signal magnétique synthétique associé (Gee and Kent, 2007). c) Carte représentant une compilation pointée des isochrones magnétiques (Seton et al., 2014). d) Carte de l'âge de la croûte océanique déduit des anomalies magnétiques (Seton et al., 2012)

**Fig. 8:** a) Three dimensional cartoon presenting the formation of an oceanic crust and the record of geomagnetic field reversals through time. Dark bands correspond to areas accreted during normal polarity periods and white bands during reverse periods (Gee and Kent, 2007). b) Geomagnetic polarity timescale and the associated synthetic magnetic signal (Gee and Kent, 2007) c) Global compilation of magnetic anomaly identification (Seton et al., 2014) d) Age of the oceanic crust determined with magnetic anomalies (Seton et al., 2012)

### 2.3 Intégration des données de rift

La plupart des modèles cinématiques utilise des plaques rigides indéformables, certains travaux (Srivastava and Tapscott, 1986; Unternehr et al., 1988) ont mis en évidence l'impossibilité de réaliser des reconstructions palinspatiques sans subdiviser les plaques majeures. De plus les bassins sédimentaires, le volcanisme et les failles de transfert intracontinentaux montrent que les plaques évoluent également en leur centre. La déformation intra-plaque majeure est cependant liée aux marges hyper-étirées qui peuvent avoir accommodées des centaines de kilomètres d'extension. Ce problème a déjà été soulevé (Aslanian and Moulin, 2012; Heine et al., 2013; Williams et al., 2011). Ainsi ces études essaient de restaurer des polygones continentaux avant la déformation de rift et ajoutent un pôle de rotation correspondant à la fermeture totale du domaine. Cependant l'utilisation de seulement deux pôles de rotation, un à la fermeture totale



et un à la première anomalie magnétique, implique un développement continu et identique du système de rift. De plus il apparait que de nombreux systèmes de rift ne peuvent se résumer à une extension localisée entre deux plaques continentales majeures (Tugend et al., 2015a; Welford et al., 2010a,b). L'intégration des données géologiques des rifts hyper-étirés, couplées à un modèle cinématique basé sur des anomalies magnétiques semble être un moyen de contraindre spatialement et de représenter l'évolution d'un système de rift jusqu'à la première anomalie océanique.

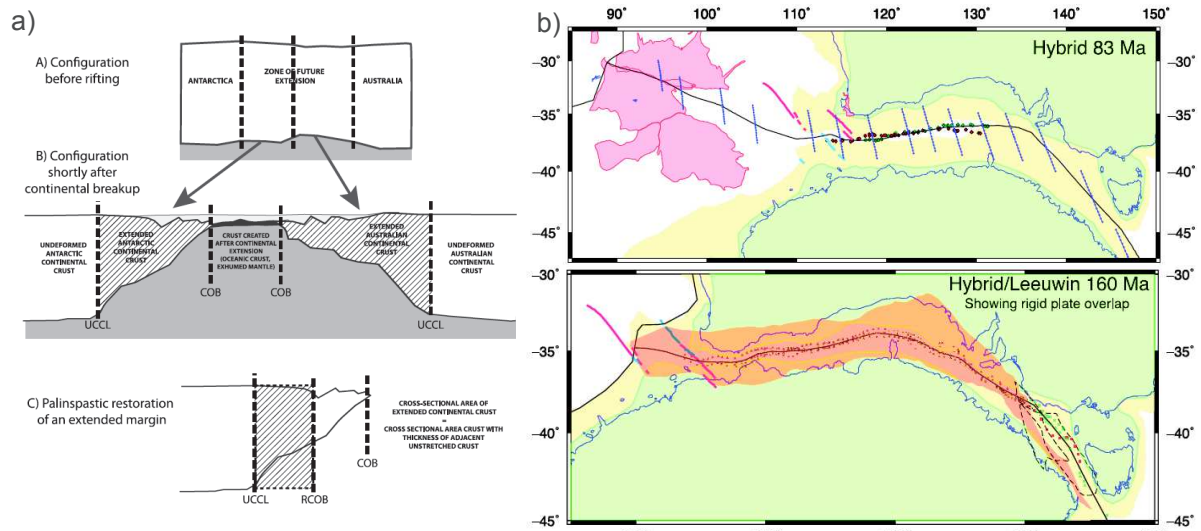


**Fig. 9:** a) Schéma d'un système de rift montrant la méthode permettant de prendre en compte la déformation crustale dans un modèle cinématique à plaques rigides. b) Restauration totale de la marge Australo-Antarctique et à la première anomalie océanique montrant la superposition des plaques (représentée en orange, Williams et al., 2011)

**Fig. 9:** a) Cartoon of a rift system showing the areal balancing method to take into account the crustal deformation in a rigid plate modeling. b) Full fit reconstruction of the Australia-Antarctica rifted margin and reconstruction at the first oceanic magnetic anomaly. The plate overlap is colored in orange (Williams et al., 2011)

### 3. L'EXEMPLE DES DOMAINES HYPER-ÉTIRÉS DU SUD DE L'ATLANTIQUE NORD

Le choix de la zone de travail est basé sur plusieurs critères : 1) La présence de marges hyper-étirées pauvres en magma, 2) la connaissance structurale et stratigraphique de la zone, 3) l'accessibilité, la variabilité et la qualité des données, et 4) la présence de problèmes cinématiques de premier ordre. Ainsi le segment océanique du sud de l'Atlantique Nord, ses marges et ses bassins hyper-étirés ont été choisis pour mener cette étude. De plus ces exemples comportent les marges conjuguées d'Ibérie et de Terre-Neuve (Tucholke and Sibuet, 2006) qui sont les seules marges pénétrées par des forages profonds ainsi que le système Golfe de Gascogne-Pyrénées partiellement exposé à terre (Jammes et al., 2009; Tugend et al., 2014).

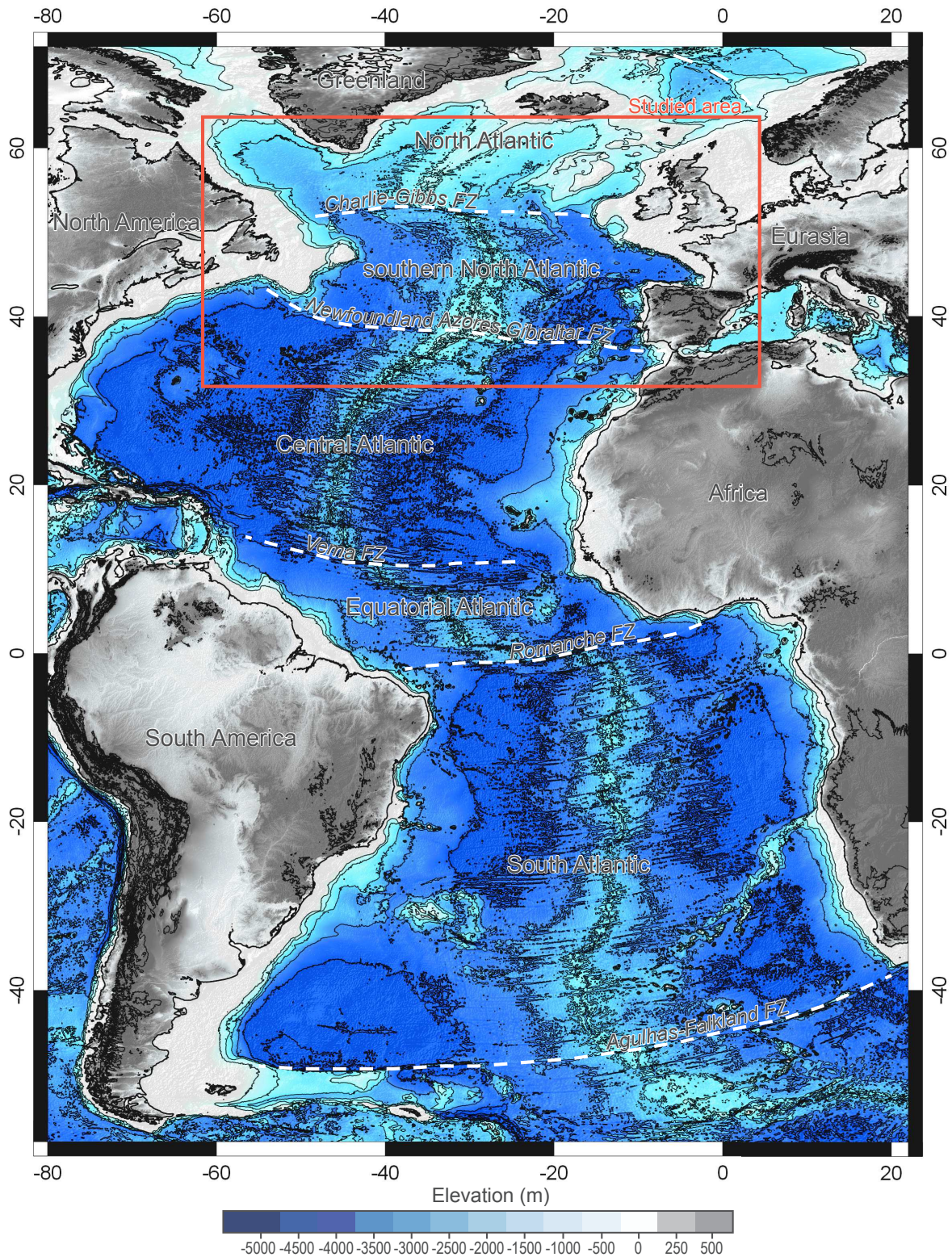


**Fig. 10:** Carte bathymétrique de l'Océan Atlantique avec la localisation de la zone d'étude (ETOPO1 Amante and Eakins, 2009)

**Fig. 10:** Bathymetric map of the Atlantic Ocean (Amante and Eakins, 2009), the red rectangle delimits the study area

### **3.1 L’océan Atlantique et son ouverture**

L’Océan Atlantique se situe entre les continents africain, sud et nord-américain et eurasiatique, il s’étend sur une superficie de 92 400 000 km<sup>2</sup> entre l’Océan Arctique au nord et l’Océan Antarctique au sud. Il résulte de la séparation de la Pangée au Mésozoïque (Stampfli et al., 2013; Wegener, 1929) suivi de l’accrétion océanique au niveau de la dorsale médio-Atlantique (Fig. 8). De grandes zones de failles transformantes séparent l’Atlantique en quatre segments, le sud, l’équatorial, le central et le nord. Ces segments se sont ouverts de manière diachrone. Le rifting de l’Atlantique central débute au Trias (Kneller et al., 2012; Sahabi et al., 2004) avec des bassins sédimentaires caractéristiques des systèmes de « wide rift » (Leleu et al., 2016). Cette période est suivie de l’ouverture océanique au Jurassique Inférieur (Labails et al., 2010; Schettino and Turco, 2009). L’Atlantique Sud s’ouvre de manière diachrone du sud vers le nord à partir du Berriasien (140 Ma) et se finit dans l’Atlantique Equatorial à l’Albien (104 Ma) (Heine et al., 2013). Des bassins de rifts se développent du Permien au Jurassique Inférieur dans l’ensemble de l’Atlantique Nord (Rasmussen et al., 1998; Shannon, 2009) et enregistrent la première phase extensive. La seconde phase de rift est datée du Jurassique Supérieur au Crétacé Inférieur, celle-ci est considérée comme la phase d’hyper-extension du sud de l’Atlantique Nord mais aussi le long des marges norvégiennes (Peron-Pinvidic et al., 2013). Cependant seulement le domaine au sud de la zone de fracture de Charlie Gibbs atteint l’océanisation durant cette période (Tucholke et al., 2007). L’accrétion océanique entre le Groenland et l’Eurasie ne débute qu’à 55 Ma (Eldholm et al., 1989) après une troisième phase d’extension Crétacé Supérieur-Paléocène. De plus, une croûte océanique se forme dans la mer du Labrador et la Baie de Baffin entre l’Amérique du Nord et le Groenland de 63 Ma à 34 Ma (Oakey and Chalmers, 2012).

### **3.2 Structure du sud de l’Atlantique Nord, de ses marges et des bassins hyper-étirés**

Le sud de l’Atlantique Nord est un segment océanique séparé du reste de l’Atlantique par la zone de fracture de Terre-Neuve-Açores-Gibraltar au sud et par la zone de fracture de Charlie Gibbs au nord. La dorsale active à l’heure actuelle est la dorsale médio-atlantique qui provoque l’écartement de l’Eurasie et de l’Amérique du Nord à une vitesse d’environ 2 cm/an. Cette zone inclut le domaine océanique avorté du Golfe de Gascogne qui forme un V entre l’Europe de l’Ouest et l’Ibérie.

Le sud de l’Atlantique Nord est bordé de marges et de bassins hyper-étirés du sud vers le nord on retrouve : les marges conjuguées d’Ibérie et de Terre Neuve, la marge Nord Ibérique ou Cantabre conjuguées aux marges Armoricaïne et des Entrées de la Manche qui

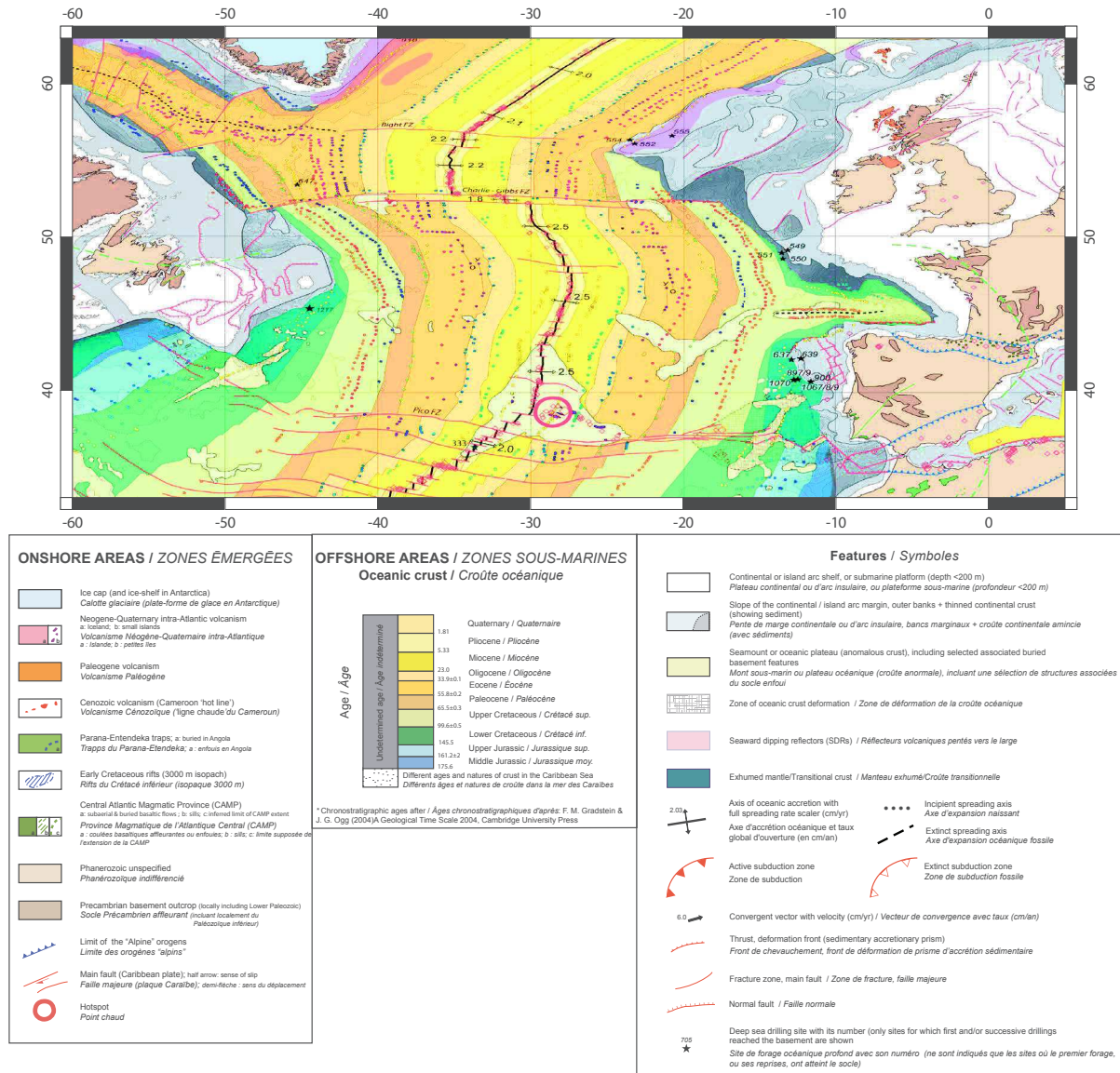


Fig. 11: Carte structurale du sud de l'Atlantique Nord (Miles et al., 2012)

Fig. 11: Structural map of the southern North Atlantic Ocean (Miles et al., 2012)

se terminent dans le bassin de Parentis à l'est, le système Pyrénéen, les deux sous bassins Est et Ouest Orphan, les marges conjuguées du Bonet Flamand et de Goban Spur, le bassin de Porcupine et le bassin de Rockall. Ces marges et bassins hyper-étirés sont marqués par une forte augmentation de la bathymétrie, généralement de moins de 500 m à plus de 2000 m. La structure de ces marges le long d'un profil est similaire à la description faite dans la section 1, cependant l'architecture est la taille des domaines de rift sont variables le long d'un même système (Welford et al., 2010c, 2012). Il n'y a pas d'orientation préférentielle des marges, même si certaines sont pseudo-parallèles à la dorsale médio-océanique. Les Pyrénées sont un système de rift fossile repris en compression lors de la remontée de l'Afrique vers le nord (Rosenbaum et al., 2002), ce mouvement a également entraîné la formation d'un prisme d'accrétion le long

de la marge Nord Ibérique (Roca et al., 2011) ainsi que des chevauchements le long de la zone de fracture d'Açores Gibraltar (e.g. Banc de Gorringer, Sallarès et al., 2013).

### **3.3 L'héritage et cinématique pré-rift**

L'Atlantique Nord ne s'ouvre pas à travers une lithosphère homogène. Celle-ci est composée de différents blocs amalgamés durant des événements orogéniques pour former la Pangée (Fig. 7) (Wegener, 1915). La première phase orogénique est caractérisée par la fermeture de l'océan Tornquist à l'Ordovicien Supérieur (Torsvik and Rehnström, 2003) liant ainsi les blocs continentaux de Baltica et Avalonia (Fig. 12a). Cette suture est suivie de la fermeture de l'océan Iapetus qui forme le méga-continent Laurussia et la chaîne des Calédonides (van Staal et al., 2012). La fermeture de l'océan Rheic et l'amalgamation de fragments continentaux dérivés du Gondwana au Carbonifère forment la chaîne Varisque et la Pangée (Matte, 1986) (Fig.13).

Cette phase orogénique est suivie d'une évolution tectonique caractérisée par la mise en place de grandes failles de décrochement de la fin du Carbonifère jusqu'au début du Permien (e.g. Failles de Toulouse, des Cévènes...) (Fig. 12b). Ces zones de failles ont plus ou moins participé à la formation de l'oroclinal Cantabre (Martínez Catalán, 2011; Pastor-Galan et al., 2015). De plus, on ne connaît pas exactement la quantité de mouvement relatif sur ces grandes structures décrochantes (Arthaud and Matte, 1977). L'évolution permienne est caractérisée par la formation de bassins sédimentaires transtensionnels associés à un volcanisme intense, cette évolution entraîne le rééquilibrage de la croûte continentale (Petri, 2014). De nombreux bassins de rifts intracontinentaux se forment durant le Trias (e.g. Mer Celte, Jeanne d'Arc, Lusitanien, Carson, Rockall...). Ces bassins se répartissent sur tout le domaine et sont liés à l'extension E-O induite par le rifting de l'Atlantique Central (Leleu et al., 2016).

### **3.4 La cinématique sud de l'Atlantique Nord**

Même si de l'extension triasique est enregistrée dans de nombreux bassins sédimentaires nous considérons généralement que le système Nord-Atlantique est complètement fermé au Jurassique Inférieur (Barnett-Moore et al., 2016b; Schettino and Turco, 2011; Vissers and Meijer, 2012a). La position des continents à 200 Ma n'est que faiblement contrainte par des données paléo-magnétiques (Torsvik et al., 2008), celle-ci entraîne des superpositions continentales de plus de 100km. Barnett-Moore et al., (2016b) présentent une restauration de l'ensemble de l'Atlantique Nord basée sur une limite de continent pré-déformé calculée grâce à l'inversion gravimétrique (Chappell and Kusznir, 2008). Cette proposition est en accord avec toutes les reconstructions qui ne proposaient pas un « full-fit » contraint par une méthode géophysique.

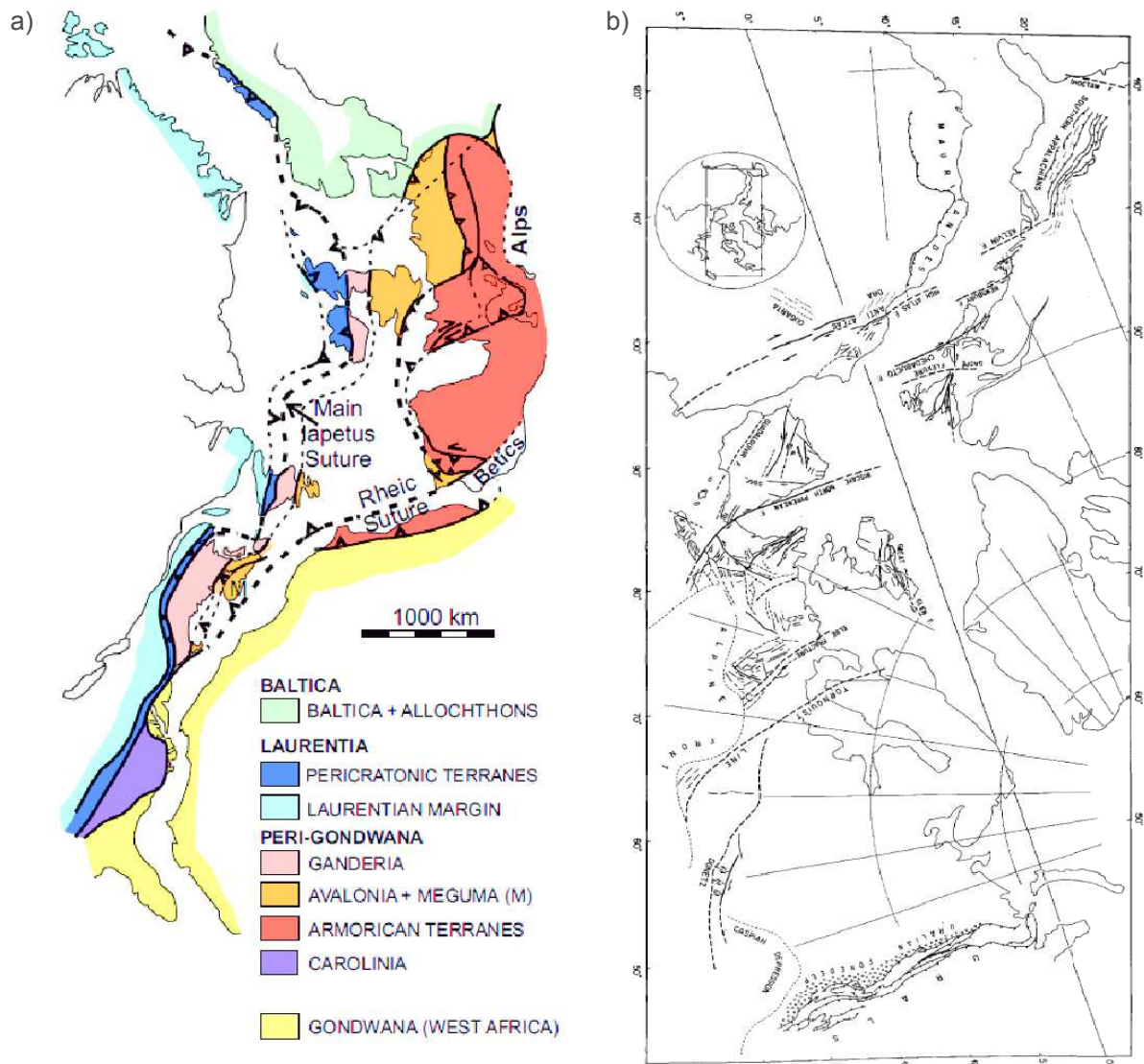


**Fig. 12:** a) Carte paléogéographique de l'Atlantique Nord au Trias présentant les différentes unités tectoniques et les sutures liées aux orogènes Varisque et Callédonien (van Staal et al., 2012). b) Carte reconstruite au Permien présentant les structures tardi-varisques (Arthaud and Matte, 1977)

**Fig. 12:** a) Paleogeographic map of the North Atlantic at Trias showing the different Tectonic units and sutures linked to the Variscan and Caledonian orogenies (van Staal et al., 2012). b) Reconstructed map at Permian time presenting the late Variscan structures (Arthaud and Matte, 1977)

L'évolution des différents systèmes de rift du sud de l'Atlantique Nord n'est pas synchrone, en effet même si les déformations majeures sont au Jurassique Supérieur et au Crétacé Inférieur chaque segment de rift a sa propre évolution (Alves et al., 2009; Mohn et al., 2015; Tugend et al., 2014). Ces systèmes de rift provoquent l'extension puis la rupture continentale menant à l'exhumation du manteau (Boillot et al., 1987) et à l'installation d'une croûte océanique. Cependant ces phases représentant plusieurs millions d'années et des dizaines de kilomètres d'extension ne sont jamais représentées dans des modèles cinématiques. En règle générale la seconde étape d'une restauration correspond à la première anomalie magnétique marine. De ce fait aucune restauration du sud de l'Atlantique Nord ne prend en compte l'évolution complexe des systèmes de rift hyper-étirés.

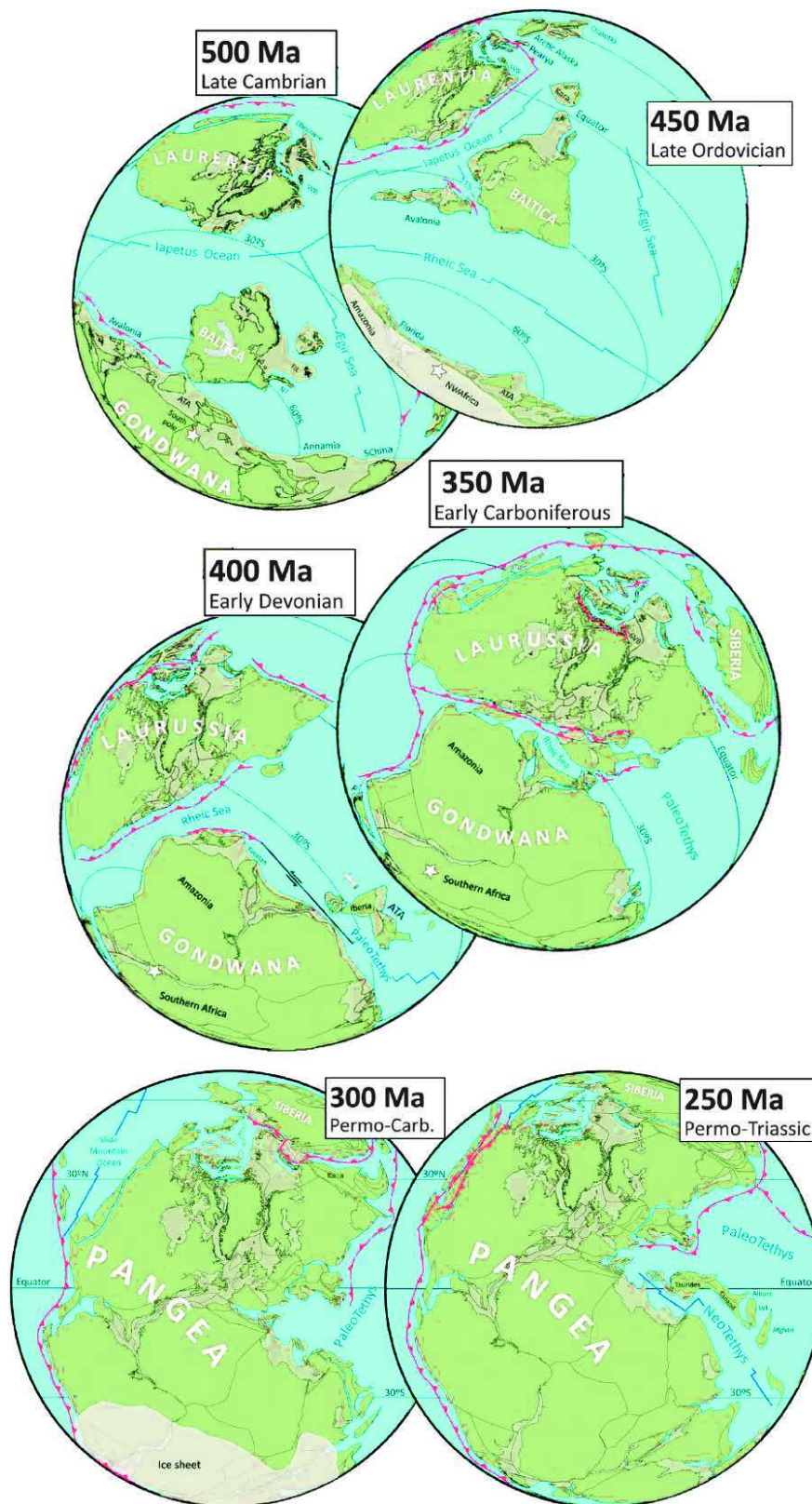


**Fig. 13:** Reconstruction cinématique globale du Cambrien au Trias (Torsvik et al., 2012) (TS : Tornquist Seaway)

**Fig. 13:** Global plate reconstruction from Cambrian to Trias (Torsvik et al., 2012) (TS: Tornquist Seaway)

Pourtant dans le cas du sud de l'Atlantique Nord l'identification de la première anomalie magnétique est sujette à débat et induit plusieurs restaurations contrastées (Bronner et al., 2011; Tucholke and Sibuet, 2012). Les anomalies magnétiques localisées avant le super-chron à polarité normale du Crétacé entre Ibérie et Terre-Neuve interprétées comme des isochrones océaniques (Srivastava et al., 2000) sont localisées sur des domaines de manteau exhumé. Ainsi leurs origines, la méthode de mise en place du matériel créant l'anomalie (Bronner et al., 2011; Gillard et al., 2015; Russell and Whitmarsh, 2003; Sibuet et al., 2007) et leur utilité dans les restaurations cinématiques doivent être investiguées. De plus le signal magnétique sur ces deux marges conjuguées enregistre une anomalie de forte amplitude appelée J, qui est interprétée comme l'isochrone M0 (Sibuet et al., 2004) (Fig. 14) ou comme enregistrant un sous-plaquage magmatique dû à la rupture lithosphérique (Bronner et al., 2011). Certains modèles utilisent l'anomalie M0 (Klitgord and Schouten, 1986; Sibuet et al., 2004; Vissers and Meijer, 2012a) et proposent ainsi une ouverture en ciseau de l'Aptien au Santonien du Golfe de Gascogne concomitante avec une subduction au niveau des Pyrénées. Des images tomographiques montrent une zone froide sous l'actuel Algérie interprétée comme la lithosphère océanique subductée sous les Pyrénées puis détachée à la fin de l'Aptien (Vissers et al., 2016). Cependant d'autres données tomographiques ne montrent pas cette zone (Barnett-Moore et al., 2016a) et il n'y a pas d'évidence de terrain pour étayer l'hypothèse d'une subduction dans les Pyrénées au cours de l'Aptien. Un second type de modèle suggère un mouvement décrochant ou transtensif sénestre de l'Ibérie par rapport à l'Eurasie (Choukroune et al., 1973; Le Pichon et al., 1970; Olivet, 1996), mais ce modèle n'explique pas l'hyper-extension à l'Albien dans les Pyrénées (Lagabrielle and Bodinier, 2008; Jammes et al., 2009; Masini et al., 2014). Le dernier modèle proposé se base sur les observations des Pyrénées et suggère une ouverture orthogonale du rift pyrénéen à l'Albien (Jammes et al., 2009) cependant celui-ci implique un arrêt de l'extension entre Ibérie et Terre-Neuve qui n'est pas observé. En plus de ces reconstructions contestées à environ 125-120 Ma il n'y a pas d'anomalie magnétique utilisable jusqu'à C34 (83.5Ma) du fait du super-isochrone à polarité normale du Crétacé. Ainsi et même si beaucoup d'efforts ont été faits sur la compréhension du partitionnement de la déformation (Tugend et al., 2015a) et sur la compréhension des anomalies magnétiques dans les transitions océan-continent (Bronner et al.,



2011), aucun modèle cinématique ne satisfait les données géologiques et géophysiques du sud de l'Atlantique Nord (Barnett-Moore et al., 2016a).

En revanche l'évolution cinématique est bien contrainte grâce aux anomalies magnétiques océaniques après l'isochrone C34 (83.5 Ma) (Roest and Srivastava, 1991; Rosenbaum et al., 2002; Vissers and Meijer, 2012b). Ainsi la remontée de l'Afrique entraîne la fermeture du domaine pyrénéen.

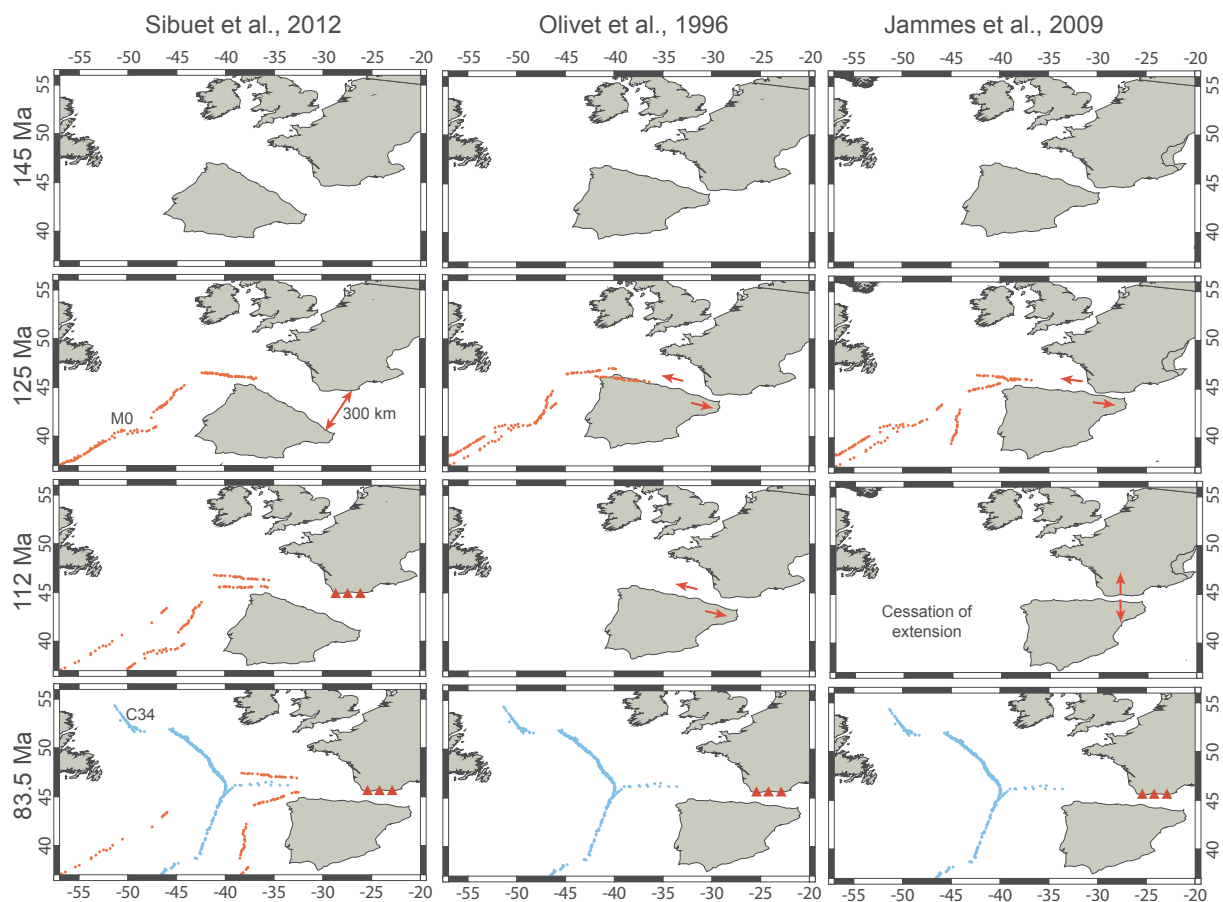


**Fig. 14:** Trois propositions de restauration de la plaque ibérique avec les principaux problèmes cinématiques (Jammes et al., 2009; Olivet, 1996; Sibuet et al., 2012)

**Fig. 14:** Three plate reconstructions of the Iberia plate with the major kinematic problems (Jammes et al., 2009; Olivet, 1996; Sibuet et al., 2012)

## 4. GRANDES QUESTIONS, DÉMARCHE SCIENTIFIQUE ET PLAN DE LA THÈSE

### 4.1 Les problématiques abordées

L'observation et l'analyse des marges hyper-étirées nous renseignent sur l'évolution des processus de déformation d'un système de rift hyper-étiré. Cependant les modes de déformations des systèmes de rift sont sujets à de nombreux débats car leurs analyses demande une compréhension géologique et physique des objets observés. De plus l'évolution de la déformation d'un rift hyper-étiré est dans la plupart des études simplement représentée en 2D alors que les observations montrent une grande variabilité latérale. Le but de cette thèse est double, il vise à exprimer de manière physique la déformation d'une croûte continentale hyper-étirée et aussi à modéliser en 3D l'évolution d'un système de rift en utilisant les exemples des marges et des bassins du sud de l'Atlantique Nord.

La caractérisation physique de l'évolution d'un système de rift est effectuée grâce à des modèles numériques (Brune et al., 2014; Huismans and Beaumont, 2008; Lavier and Manatschal, 2006; Nagel and Buck, 2004) ou par des modèles analogiques (Autin et al., 2010a; Brun and Beslier, 1996), cependant ces modèles sont paramétrés pour reproduire l'évolution d'un seul système de rift. Les observations et les mesures présentent une grande variabilité de la zone de necking cependant les domaines hyper-étirés semblent posséder des formes plus similaires. Ainsi Sutra et Manatschal, (2012) ont montré que la terminaison continentale de la marge ibérique avait une ouverture constante d'environ  $11^\circ$  (Fig. 15). Cette observation implique des processus de déformation similaire et constitue le point de départ de la caractérisation physique du mode de déformation de la terminaison continentale. Ainsi la question relative à la déformation de la terminaison de la croûte continentale est:

*1) Quelle est la relation entre l'architecture de la terminaison continentale et son mode de déformation ? (Chap. I)*

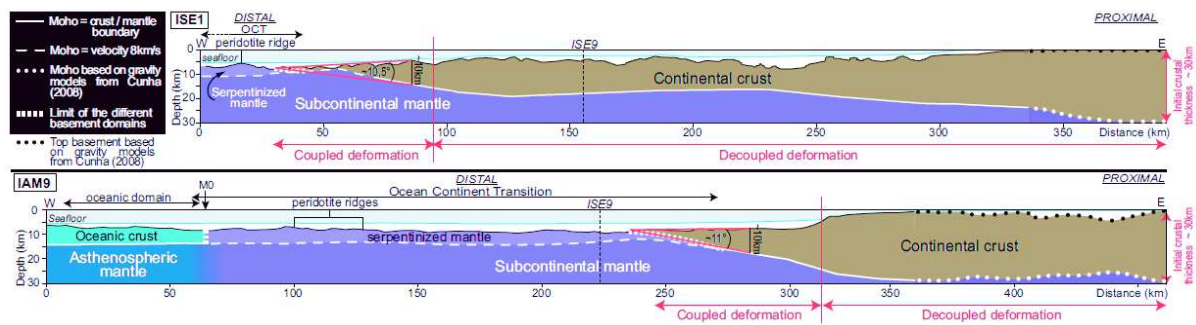


**Fig. 15:** Coupes crustales de la marge ibérique présentant la forme prismatique similaire de terminaison continentale (Sutra and Manatschal, 2012)

**Fig. 15:** Crustal cross section of the Iberia margin presenting the similar wedge shape of the continental termination (Sutra and Manatschal, 2012)

La deuxième problématique de ce travail de thèse est de comprendre comment dans le temps et dans l'espace évolue un système de rift. Cette étude se base sur les différents systèmes de rift hyper-étirés du sud de l'Atlantique Nord et demande ainsi un cadre géodynamique fiable. Cependant l'évolution cinématique du sud de l'Atlantique Nord avant l'anomalie magnétique C34 est très disputée (Barnett-Moore et al., 2016a; Bronner et al., 2011; Neres et al., 2013; Olivet, 1996; Sibuet et al., 2004; Tucholke and Sibuet, 2012; Vissers and Meijer, 2012a) du fait de l'interprétation de l'anomalie magnétique J comme l'isochrone M0. La détermination de la nature de l'anomalie magnétique J a dû être investiguée avant d'analyser l'évolution 3D d'un système de rift. Les questions relatives à ce sujet sont :

2) *Quelle est la nature de l'anomalie magnétique J ? Est-elle utilisable pour des restaurations cinématiques ? (Chap. II)*

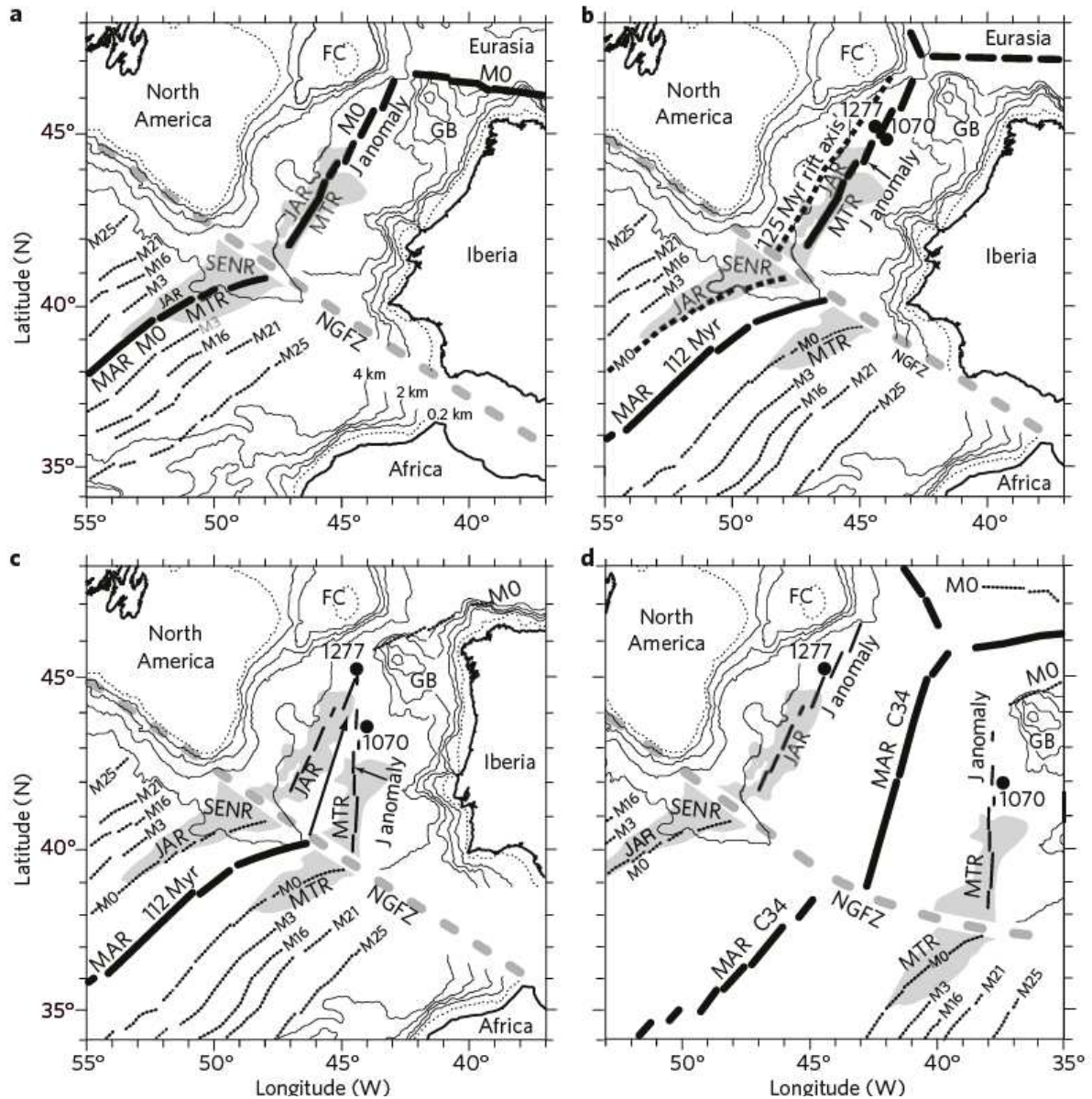


**Fig. 16:** Différentes propositions pour l'évolution Crétacé du sud de l'Atlantique Nord. a) Reconstruction à M0 (125 Ma) (Srivastava et al., 2000), l'anomalie J s'est formée de manière isochrone. b) Reconstruction à 112 Ma, l'anomalie J s'est formée de manière isochrone et correspond à un sous-plaquage magmatique au moment de la rupture lithosphérique. c) Reconstruction à 112 Ma, J est liée à la rupture lithosphérique qui se propage vers le Nord, J n'est dans ce cas pas un isochrone. d) Reconstruction basée sur l'anomalie C34 à 83 Ma (Srivastava et al., 1990) (Tucholke and Sibuet, 2012)

**Fig. 16:** Various propositions for the Cretaceous evolution of the southern North Atlantic. a) Reconstruction at M0 (125 Ma) (Srivastava et al., 2000), the J-anomaly is an isochrons. b) Reconstruction at 112 Ma, the J-anomaly is formed synchronously and corresponds to magmatic underplating at lithospheric breakup time. c) Reconstruction at 112 Ma, the J-anomaly is link to the lithospheric breakup which propagates northward, the J-anomaly is not an isochrons. d) Reconstruction based on the C34 magnetic anomaly at 83 Ma (Srivastava et al., 1990) (Tucholke and Sibuet, 2012)

La déformation des systèmes de rift commence à être plutôt bien comprise en 2D cependant l'évolution 3D de ces phases de déformation reste sujette à de nombreuses questions. Ainsi l'objectif est d'analyser les différences dans le mode de propagation de chaque phase de rift et de déterminer l'impact de la déformation des rifts hyper-étirés sur la cinématique du sud de l'Atlantique Nord. Les questions guidant ce travail sont :

3) *Comment se propage et se partitionne la déformation dans un système de rift hyper-étiré ? (Chap. III)*

4) *Quelles sont les implications des rifts hyper-étirés sur l'évolution du sud de l'Atlantique Nord ? (Chap. III)*

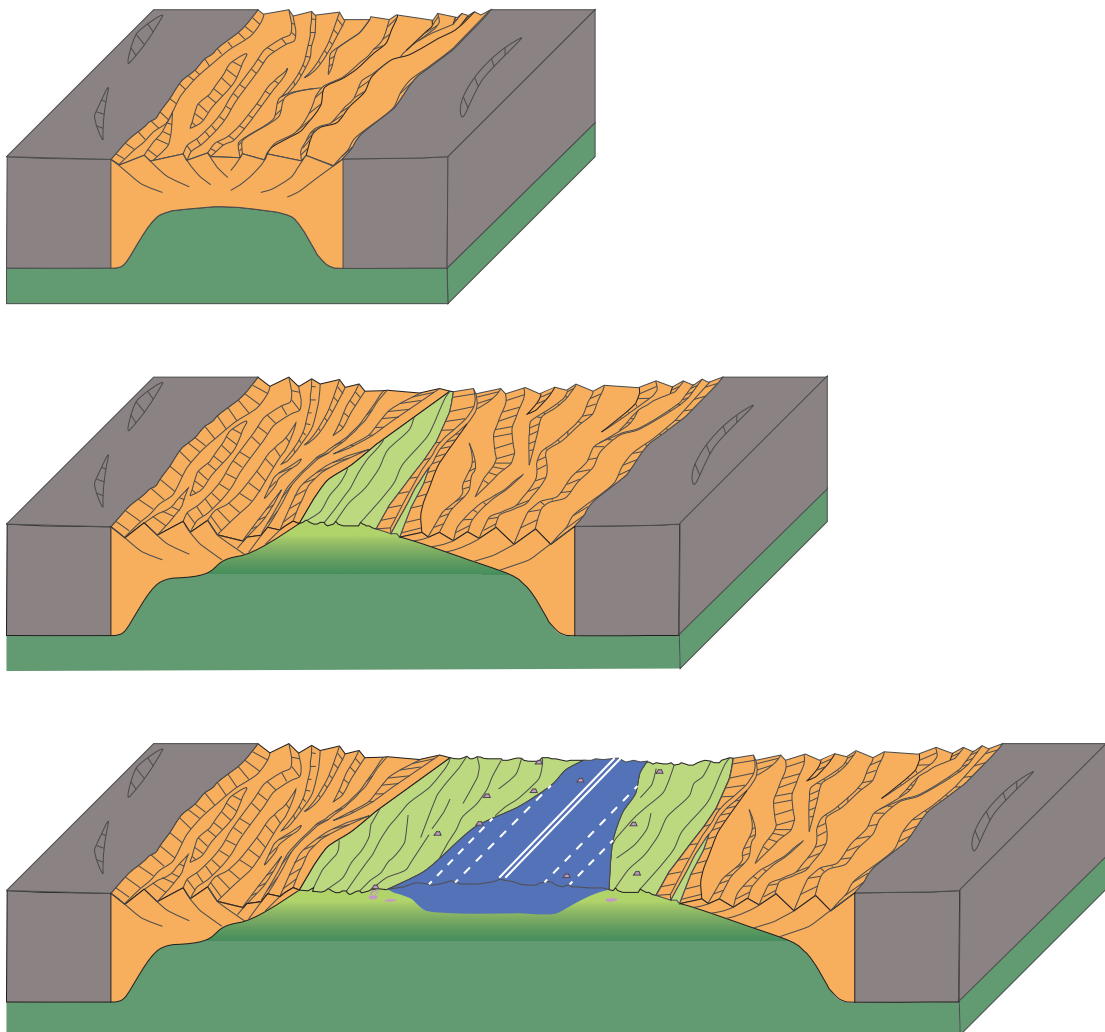


**Fig. 17:** *Modèle évolutif d'un système de rift hyper-étiré pauvre en magma et de propagation de la croûte océanique*

**Fig. 17:** *Evolutionary model of a hyper-extended magma poor rift system and of oceanic crust*

## **4.2 La démarche scientifique et les méthodes utilisées**

Cette thèse aborde trois problématiques distinctes, ainsi une approche pluridisciplinaire est nécessaire pour apporter des éléments de réponse à ces questions. La compilation et l'observation de données géologiques et géophysiques sont la base de ce travail. Ces observations ont été couplées à des modèles d'inversion gravimétrique 3D afin d'obtenir l'épaisseur crustale de toute la zone d'étude. Un objectif est de mesurer les angles du toit du socle et du Moho au moment du rifting du domaine hyper-étiré, nous avons dû pour cela effectuer un « flexural-backstripping » (processus retirant les couches sédimentaires ; leur influence isostatique et l'effet de la subsidence thermique) des profils sismiques afin d'obtenir la géométrie de la marge au moment de la rupture continentale. Ces géométries ont ensuite été comparées à celles modélisées par la théorie du prisme critique de Coulomb. Les trois dernières questions traitent de la déformation des systèmes de rift en 3D ainsi la compilation de données a été confrontée à des modèles cinématiques. Ce travail a été effectué grâce au logiciel de modélisation cinématique Gplates (Boyden et al., 2011) afin de contraindre spatio-temporellement l'évolution d'un système de rift.

## **4.3 Le déroulement du manuscrit de thèse**

L'introduction de ce manuscrit fait un état de l'art sur la connaissance des processus de déformation des marges hyper-étirées, explique brièvement la cinématique des plaques et ses méthodes associées et présente l'objet d'étude. Les trois problématiques font l'objet de trois chapitres de thèse écrits sous forme d'articles scientifiques publiés et en préparation. Les résultats majeurs sont repris et intégrés dans une discussion générale.

Le premier chapitre traite du mode de déformation de la croûte hyper-étirée. Il présente une comparaison entre la forme finale de la terminaison continentale et la théorie du prisme critique de Coulomb. Ce chapitre est constitué de l'article publié dans la revue *Earth and Planetary Science Letters* en mai 2016 est intitulé : “Application of the critical Coulomb wedge theory to hyper-extended, magma-poor rifted margins”.

Le second chapitre présente les problèmes cinématiques liés à l'interprétation de l'anomalie magnétique J. De plus, grâce à des interprétations sismiques et à une synthèse

géochronologique il réévalue la nature de cette anomalie et son utilité pour la cinématique du sud de l'Atlantique Nord. Cette investigation a été valorisée par un article accepté dans la revue *Terra Nova* sous le titre de « Nature and origin of the J-magnetic anomaly offshore Iberia-Newfoundland: implications for plate reconstructions ».

Le troisième chapitre propose une reconstruction du sud de l'Atlantique Nord intégrant la déformation des marges et bassins de rifts hyper-étirés. L'objectif n'est cependant pas de faire une nouvelle reconstruction cinématique mais d'utiliser les méthodes de la cinématique des plaques pour comprendre les modes de propagation d'un système hyper-étiré. Ce travail aborde trois aspects : 1) il propose une nouvelle méthode de restauration basée sur des informations géologiques locales couplées à des contraintes spatiales; 2) il implique de nouvelles interprétations sur l'évolution de l'Atlantique Nord et surtout; 3) il met en évidence les différents modes de propagation d'un système de rifts. Ce chapitre constitue un article en préparation pour le journal *Tectonics*.







---

# *CHAPITRE I*

---

Le premier chapitre a pour but de caractériser physiquement la déformation des marges hyper-étirées. Le point de départ de cette étude est la similarité de l'angle d'ouverture de la terminaison continentale des marges hyper-étirées (Sutra and Manatschal, 2012). De plus de précédentes études ont montré que la terminaison crustale a une forme prismatique, sa base est un niveau de décollement et la dernière phase de déformation est dans le domaine cassant (Pérez-Gussinyé and Reston, 2001). Ces trois observations étant les pré-requis pour l'application de la théorie de Coulomb ont permis l'initiation de cette étude. La démarche suivit dans ce chapitre s'organise ainsi:

- Explication de la théorie du prisme critique de Coulomb
- Sélection des marges et des critères pour définir le prisme continental hyper-étiré
- Mesure des angles de surface et basal de ces prismes avec et sans correction de subsidence
- Paramétrisation des enveloppes de stabilité des prismes de Coulomb avec des frictions typiques des roches de domaines-étirés. Ces test ont été effectués en collaboration avec Xiaoping Yuan et Bertrand Maillot à l'Université de Cergy-Pontoise

Enfin les mesures sont confrontées aux graphiques théoriques de stabilité du prisme de Coulomb pour proposer un modèle évolutif de la rupture continentale qui explique les architectures observées. De plus une dernière partie utilise des exemples de sismique et de terrain montrant l'intérêt de l'application de la théorie du prisme critique de Coulomb pour l'interprétation tectono-stratigraphique des domaines hyper-étirés.

Ce chapitre est constitué d'un article scientifique faisant la comparaison entre l'architecture des marges hyper-étirées et le prisme critique de Coulomb ainsi qu'une extension de cet article présentant des exemples de prismes continentaux hyper-étirés. L'article s'intitule « Application of the critical Coulomb wedge theory to hyper-extended, magma-poor rifted margin » et a été publié en mai 2016 dans la revue *Earth and Planetary Science Letters*.

# ***APPLICATION OF THE CRITICAL COULOMB WEDGE THEORY TO HYPER-EXTENDED, MAGMA-POOR RIFTED MARGINS***

M. Nirrengarten<sup>1</sup>, G. Manatschal<sup>1</sup>, X. Yuan<sup>2</sup>, N.J. Kusznir<sup>3</sup>, B. Maillot<sup>4</sup>

*1 Institut de Physique du Globe de Strasbourg, UMR 7516, Université de Strasbourg/EOST, CNRS; 1 rue Blessig, F-67084 Strasbourg Cedex*

*2 Laboratoire de Géologie, UMR 8538, École Normale Supérieure, CNRS; Paris, France*

*3 Department of Earth and Ocean Sciences, University of Liverpool; Liverpool, UK*

*4 Laboratoire GEC, Université de Cergy-Pontoise; Cergy-Pontoise, France*

## **ABSTRACT**

The Critical Coulomb Wedge Theory (CCWT) has been extensively used in compressional tectonics to resolve the shape of orogenic or accretionary prisms, while it is less applied to extensional and gravitational wedges despite the fact that it can be described by the same equation. In particular, the hyper-extended domain at magma-poor rifted margins, forming the oceanward termination of extended continental crust, satisfies the three main requirements of the CCWT: 1) it presents a wedge shape, 2) the rocks forming the wedge are completely brittle (frictional), and 3) the base of the wedge corresponds to a low friction décollement. However hyper-extended margins present a fully frictional behaviour only for a very thin crust; therefore this study is limited to the termination of hyper-extended continental crust which deforms in the latest stage of continental rifting. In this paper we define a method to measure the surface slope and the basal deep of this wedge that we apply to 17 hyper-extended, magma-poor rifted margins in order to compare the results to the values predicted by the CCWT. Because conjugate pairs of hyper-extended, magma-poor rifted margins are commonly asymmetric, due to detachment faulting, the wedges in the upper and lower plate margins corresponding respectively to the hanging wall and footwall of the detachment system are different. While the stress field in the upper plate wedge corresponds to a tectonic extensional wedge, the one in the lower plate matches that of a gravity extensional wedge. Using typical frictional properties of phyllosilicates (e.g. clays and serpentine), the shape of the hyper-extended wedges can be resolved by the CCWT using consistent fluid overpressures. Our results show that all lower plate margins are gravitationally stable and therefore have a close to critical shape whereas the tectonic extensional wedges at upper plate margins are critical, sub or sup critical due to

the detachment initial angle and the duration of the tectonic activity. In this paper we discuss the geometry and structural evolution of the most distal parts of hyper-extended continental margins and the formation of extensional allochthons during hyper-extension using the CCWT theory.

## **1. INTRODUCTION**

High resolution long-offset seismic reflection images are able to resolve the wedge shape termination of the hyper-extended continental crust at magma-poor rifted margins. Deformation in hyper-extended margins has been investigated and discussed using numerical modelling (Brune et al., 2014; Huisman and Beaumont, 2011), seismic interpretations (Reston and McDermott, 2011; Sutra and Manatschal, 2012), kinematic reconstructions and field observations (Manatschal, 2004). Although the mode of deformation, structural evolution, physical properties and rheology of hyper-extended crust is controversial, it is commonly accepted that the final deformation of this domain is intimately linked to fluids and hydration reactions that occur in the brittle/frictional field (Pérez-Gussinyé and Reston, 2001). Indeed, these reactions lead to serpentinisation of the uppermost mantle and to the alteration of the continental crust, which is associated to a decrease of rocks frictional properties. Observations on field analogues in the Alps (Florineth and Froitzheim, 1994; Manatschal et al., 2006) and seismic interpretations (Reston et al., 1996) demonstrate that the contact between the continental basement and the underlying serpentinised mantle is a décollement surface. After more than thirty years of intense research at hyper-extended magma-poor rifted margins, it appears that the termination of hyper-extended margins can be described as a brittle (frictional), wedge-shaped body, whose base is a décollement corresponding to the crust-mantle boundary (Pérez-Gussinyé and Reston, 2001). Accordingly, hyper-extended margins fulfil the fundamental requirements of the Critical Coulomb Wedge Theory (CCWT), which describes the stability limits of a frictional wedge on a décollement.

The CCWT has been applied to many compressive systems such as thrust and fold belts or accretionary prisms (Davis et al., 1983), as well as in active extensional setting (Xiao et al., 1991). The tapering geometry of thinned continental crust at rifted continental margins has previously been recognised and quantitatively described by Davis and Kusznir (2002) and Osmundsen and Redfield (2011). However CCWT has not been applied to hyper-extended rifted margins. Testing the CCWT on the hyper-extended part of magma-poor rifted margins is new and may help to understand deformation processes involved in hyper-extended magma-poor rifted margins. Therefore we aim to set up a methodology to recognise and measure the basal dip and the surface slope of the wedge in hyper-extended margins, referred to as the

Hyper-Extended Continental Wedge (HECW). The HECW measurements are then plotted and compared with the CCWT using physical properties of rocks from hyper-extended domains to highlight the control by CCWT on the final shape of the continental crust termination.

## 2. THE CRITICAL COULOMB WEDGE THEORY (CCWT)

A series of papers were published in the 1980s about the mechanics of fold-and-thrust belts and accretionary wedges, comparing those geological features with a pile of sand in front of a moving bulldozer (Dahlen, 1984; Davis et al., 1983). The main results of these studies on cohesionless materials are that active accretionary wedges deform until reaching a critical shape, which corresponds to an internal state of stress on the verge of Coulomb failure everywhere (Dahlen, 1984). Once this critical stress state has been reached, sliding occurs along the décollement without any deformation within the wedge (Fig. I-1). The critical angles of the taper depend on the internal angle of friction of the material, the friction along the décollement and the pore fluid pressure. The thrusting wedge was defined with a basal shear sense oriented toward the thinner part of the wedge (Fig. I-1A).

If a frictional wedge becomes unstable due to a change of physical parameter, without any tectonic compressive or extensional forces involved, it can collapse seawards (towards the thinnest part of the wedge), until it returns to a stable state. The stable state for this gravitational wedge corresponds to the upper limit (Fig. I-1B) of the CCWT envelope in Dahlen (1984) (see also Mourgues et al., 2014 for a more developed version). The shear stress at the base is oriented towards the thinnest part of the wedge (Fig. I-1B). This setting is characteristic of gravitational spreading in orogenic wedges and gravitational gliding along passive margins, as exemplified by submarine landslides. Xiao et al. (1991) extended the CCWT to the context of active extensional wedges, where the taper angle decreases with the retreat of the wall until it reaches the critical taper-shape (Fig. I-1C). In this “extensional wedge”, the basal shear stress is oriented toward the inner part of the wedge (Fig. I-1C).

The stability envelopes of tectonic extensional, compressional and gravitational critical wedges are given by the same equation as those described by Dahlen (1984) and later corrected for large taper angle by Wang et al. (2006), Mourgues et al. (2014) and by Yuan et al. (2015).  $\psi_D$  is the angle between  $\sigma_1$  and the décollement and  $\psi_o$  the angle between  $\sigma_1$  and the surface slope, dipping at  $\alpha$ . Therefore, the stability of a frictional wedge depends on the décollement and internal friction coefficients ( $\phi_B, \phi_D$ ) and on the fluid pressure ( $\lambda_B, \lambda_D$ ) in the décollement and within the wedge, as shown by Yuan et al. (2015). Indeed:

$$\alpha + \beta = \psi_D - \psi_0 \quad (1)$$

$$\psi_D = \frac{1}{2} \arcsin \left[ \left( \frac{1-\lambda_D}{1-\lambda_B} \right) \frac{\sin(\varphi_D)}{\sin(\varphi_B)} + \left( \frac{\lambda_D-\lambda_B}{1-\lambda_B} \right) \sin(\varphi_D) \cos(2\psi_0) \right] - \frac{1}{2} \varphi_D \quad (2)$$

$$\psi_0 = \frac{1}{2} \arcsin \left( \frac{\sin(\alpha')}{\sin(\varphi_B)} \right) - \frac{1}{2} \alpha' \quad (3)$$

$$\alpha' = \arctan \left[ \left( \frac{1-\frac{\rho_f}{\rho}}{1-\lambda_B} \right) \tan \alpha \right] \quad (4)$$

where  $\varphi_D$  and  $\varphi_B$  correspond respectively to the friction angles of décollement and the wedge materials.  $\rho_f$  and  $\rho$  are the density of fluid and saturated rocks, respectively.  $\lambda_D$  and  $\lambda_B$  are the fluid pressure ratio in the décollement and within the wedge, respectively.  $\lambda$  ranges between  $\rho_f/\rho$  and 1 corresponding to hydrostatic and lithostatic pressure, respectively. These equations determine the critical condition for a stable wedge without deformation or distributed fault. However, in reality (field examples or sandbox experiments), when the wedge is outside of the stability envelopes of CCWT, it will collapse and the fault will be localised because of the fault softening which is not captured in the CCWT, as observed from sandbox experiments of Xiao et al. (1991).

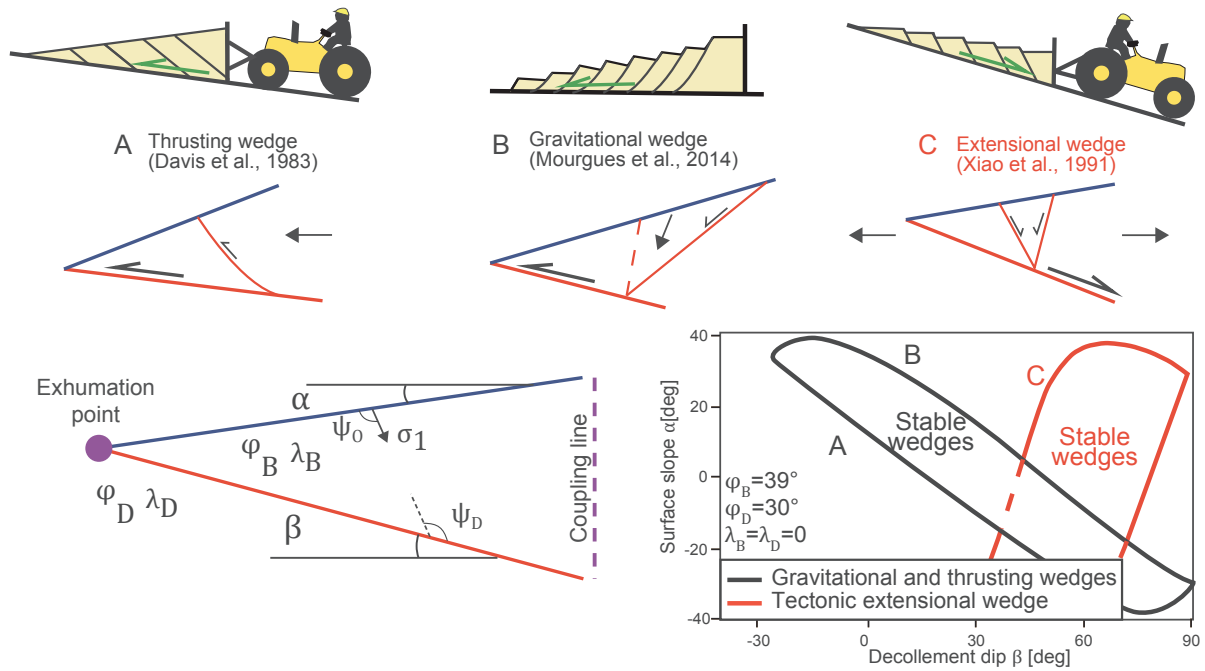


**Fig. I-1:** Visual representation of the three different types of wedges. Schematic cross section of a wedge with geometrical attributes and physical parameters used in the CCWT (see section 2). Stability envelopes for critical Coulomb wedge made of dry sand wedge in compression and extension.

### **3. HYPER-EXTENDED CONTINENTAL WEDGES (HECW): CHARACTERISATION, TERMINOLOGY AND DEFINITIONS**

#### **3.1 Domains, processes and deformation modes at magma-poor rifted margins**

Most magma-poor rifted margins display a similar architecture, comprised of: 1) a necking domain in which the continental crust thins drastically over a few tens of kilometres (Mohn et al., 2012); 2) a so-called hyper-extended domain made of highly thinned continental crust with faults crosscutting the whole crust; 3) an exhumation domain, where serpentinised mantle is directly exposed at the seafloor (Boillot et al., 1987); and 4) a transition into an oceanic crust. The different rift domains are commonly interpreted to be the result of different major tectonic processes: 1) necking which accommodates most of the thinning of the continental crust by excision of its ductile material; 2) hyper-extension which imply an embrittlement of the thinned residual continental crust (Pérez-Gussinyé and Reston, 2001; Sutra and Manatschal, 2012) undergoing sequential faulting (Brune et al., 2014; Ranero and Pérez-Gussinyé, 2010); 3) exhumation of the mantle with in-sequence or out-of-sequence detachment faults (Gillard et al., 2015; Reston and McDermott, 2011) accompanied by variable amounts of magmatism, and 4) steady-state seafloor spreading responsible for the formation of Penrose type oceanic crust.

Brittle and ductile behaviour are two modes of the deformation, ductility is the ability of a solid material to deform without fault while brittleness characterises a material which breaks in function of its frictional properties without significant deformation.

#### **3.2 Definition of the HECW**

Our study is focused only on the final evolution of rifting and comprises only the most distal part of the continental wedge in magma-poor rifted margins (Fig. I-2). Although the material may have experienced a long rift history, including ductile deformation during the thinning phase, here we focus on the hyper-extension deformation phase which starts in an already thinned crust ( $\pm 10$  km thick). As shown by previous studies (Pérez-Gussinyé and Reston, 2001), extension in the most distal crustal wedge appears to be controlled by hydrated material that is largely neo-formed and can be described by in sequence faulting (Ranero and Pérez-Gussinyé, 2010).

The HECW is defined as a wedge, bounded on the proximal side by the oceanward termination of the necking zone defined as the coupling line (for more discussion on the coupling point see Sutra et al. (2013)) (Fig. I-2). This proximal limit coincides with the location where the ductile middle crust is thinned to such an extent that faults can connect and mechanically



couple deformation between the fully brittle thinned crust and the underlying mantle (Pérez-Gussinyé and Reston, 2001). This is illustrated on seismic sections by brittle faults cross cutting the residual, thinned crust and penetrating into mantle (e.g. L reflection at the Iberia margin, Manatschal et al., 2001). Thus, the coupling line corresponds to the continentward termination of the HECW and separates the part of the margin where deformation in the crust and upper mantle is decoupled from the part where it is coupled and brittle. The location of the coupling line (corresponding to the dashed purple line Fig. I-2) is defined by: 1) the two major inflection points of top basement and Moho (the latter only on depth migrated lines), 2) the occurrence of a larger fault block followed by a sequence of blocks decreasing in size oceanwards (Sutra and Manatschal, 2012), and 3) the first fault that cross-cuts the crust and penetrates the underlying mantle. The coupling line is approximately located where crustal thickness is about 10 km. 3D gravity inversion providing constraints on crustal thickness is therefore a useful tool to determine the coupling line and map the HECW through a larger domain.

The oceanward limit of the HECW corresponds to the termination of the continuous, autochthonous continental crust and to the first occurrence of exhumed mantle. It is important to note that it does not necessarily correspond to the last block of continental crust, since extensional allochthons may exist in a more distal part. In this study we use the definition of the exhumation point as proposed by Sutra et al. (2013). The location of the exhumation point (purple dot in Fig. I-2) corresponds to: 1) a change of the nature of the crust marked by a change from reflective to transparent seismic basement, 2) the location where a strong reflector interpreted as the top of serpentinised mantle and referred to in the literature as the “S” reflection (or as “H” or “P” reflection in Reston et al. (2007, 2004, 1996)) intersects the top of the basement. The HECW is floored by a décollement with a dip angle  $\beta$  (red line Fig. I-2) and a top basement envelope with an angle  $\alpha$  (blue line Fig. I-2). The top basement envelope and the basal décollement correspond respectively to lines/surfaces that cross at the exhumation point/line and enclose the top and base of the hyper-extended brittle crust from the coupling line to the exhumation point. The basal décollement follows the strong reflector “S”, interpreted as the contact between continental crust and serpentinised mantle (e.g. base of the CCWT). The upper limit of the CCWT connects roughly the breakaway of each rotated fault block with the exhumation point.

Even if pre and syn rift sedimentation could have an influence on the crustal deformation mode in particular if salt is present, the pre-and syn-tectonic sediments are not taken into account for measuring  $\alpha$ . Our purpose in this first study is to analyse the large scale crustal deformation. Moreover, the determination of the wedge surface slope ( $\alpha$ ) in natural extensional systems is often difficult due to the occurrence of escarpments, whereas in compressional systems this

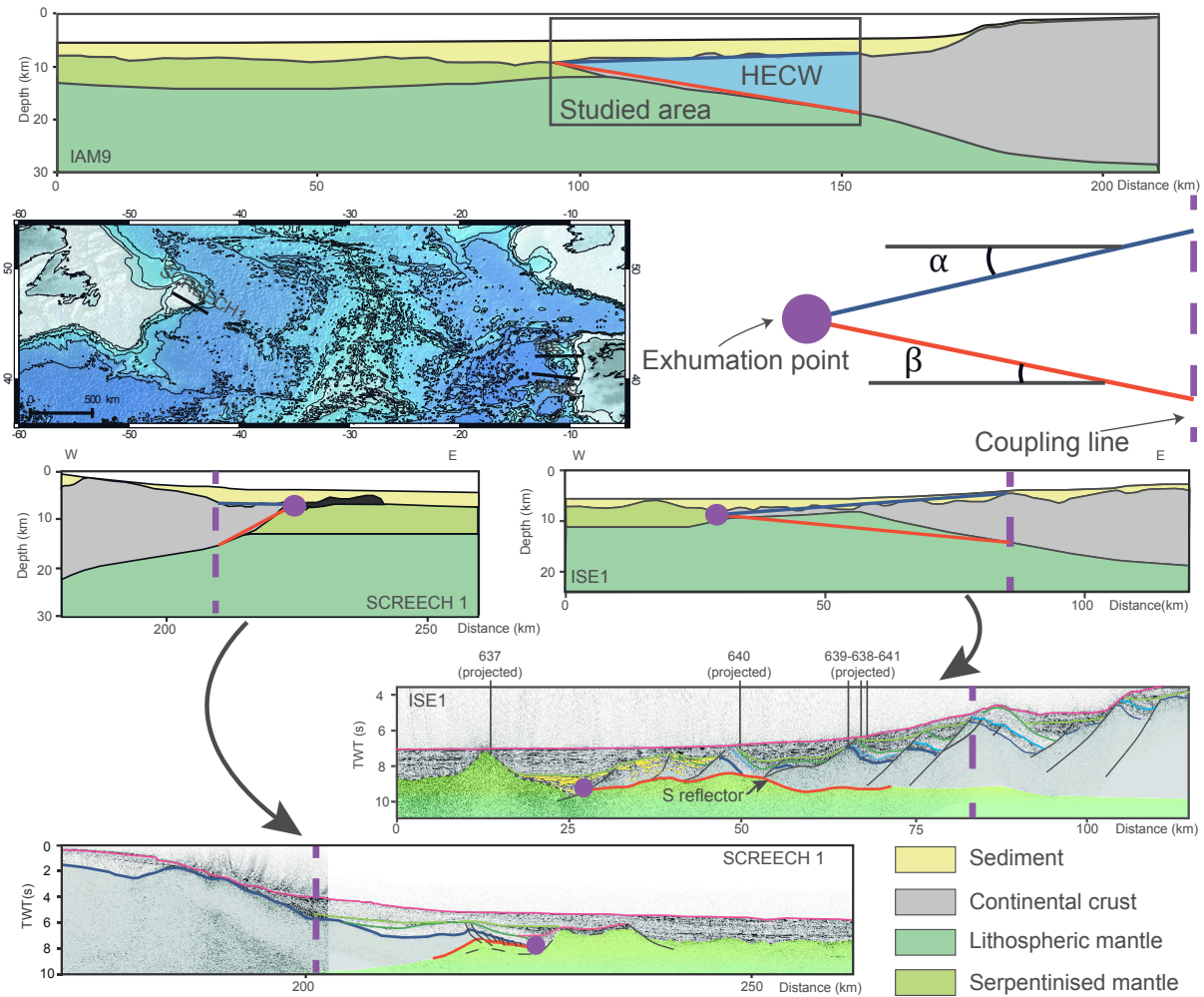


**Fig. I-2:** : Examples of determination of HECW based on the reflection and refraction conjugate lines from the Iberia and conjugate Newfoundland margins, IAM9, ISE 1 and SCREECH1. (Dean et al., 2000; Funck, 2003; Henning et al., 2004; Hopper et al., 2004; Zelt et al., 2003) and location of ODP drill holes (Boillot et al., 1987).

surface is generally smoother. In accordance with the classic CCWT (Davis et al., 1983) a downward oriented  $\beta$  is measured positively whereas an upward oriented  $\alpha$  is positive. Measuring accurately the angles requires to have access to high quality depth converted reflection seismic sections that are imaged parallel to the kinematic transport direction, and where top basement is not masked by magmatic additions, extensional allochthons and/or salt, or refraction lines which fulfil these requirements.

Although post-breakup deformation is commonly limited, thermal subsidence and sediment loading may significantly modify the angles  $\alpha$  and  $\beta$ . Therefore a correction for post-rift flexure is needed to restore the observed angles  $\alpha$  and  $\beta$  to their values during active slip, immediately at the time of continental separation. This correction was made using flexural backstripping and decompaction to remove the effects of post-breakup sediment loading, as well as flexural reverse post-breakup thermal subsidence modelling. However the distinction between syn and post-rift sediments is often complex on our data and we decided to remove

both in our flexural backstripping. These corrections were made using the FlexDecomp 2D software; the methodology and its assumptions are described in detail in Roberts et al. (1998). In the absence of detailed lithological information, post-rift sediments were given shaly-density and compaction parameters and were removed as a single unit. An effective elastic thickness of 5 km was used for lithosphere flexural strength. The lithosphere beta factor used to drive the reverse thermal subsidence modelling was derived from seismically observed crustal basement thinning (and assumes depth uniform lithosphere stretching and thinning). Fig. I-3B,C shows an example of conjugate margin cross-sections corrected for post-rift sediment loading and thermal subsidence using a Late Jurassic syn-rift age for a line across the Porcupine hyper-extended basin. The section highlights an uplift of the hyper-extended continental crust, which steepens the Moho slope ( $\beta$ ) (see P-reflection (Reston et al., 2004)) and flattens top basement ( $\alpha$ ). It is important to note that neither the shape of the wedge nor the total angle of aperture changes.

### **3.3 Upper vs. Lower plate margins**

The asymmetry of conjugate pairs of magma-poor rifted margins is often limited to the hyper-extended domain oceanward of the coupling line, where the remaining crust is fully brittle (Pérez-Gussinyé and Reston, 2001; Fig. I-3A). Many conjugate hyper-extended margins, present on one side a wide thinned continental crustal zone structured by oceanward dipping faults whereas on its conjugate margin it is narrower and structurally more complex, showing ocean and continent dipping faults. This crustal asymmetry of rifted margins was classically explained by the occurrence of a large scale detachment fault (Lister et al., 1986) implying an upper plate margin corresponding to the hanging wall and a lower plate margin corresponding to the footwall of the major lithosphere scale fault. More recent studies show, however, that such lithospheric-scale detachment faults do not exist and that faults soling in the mantle only occur once the crust is thinned to less than 10km (Lavie and Manatschal, 2006). The Porcupine basin in the Irish Sea is one of the best examples showing upper and lower plate margin architectures. Indeed, because the rift did not evolve into seafloor spreading, the conjugate margins are preserved and imaged on the same seismic line. The upper plate margin is sharp and narrow, while the lower plate is smoother and wider (Fig. I-3B). Recent studies highlighted that the hyper-extended crust is related to sequential faulting (Ranero and Pérez-Gussinyé, 2010) in which faults break away and migrate from the lower plate towards the upper plate. Extensional detachment faults, responsible for the exhumation of the footwall underneath the upper plate margin and delaminating the latter, are observed in the field (e.g. Tasna: Florineth and Froitzheim, 1994, Manatschal et al. 2006) and on seismic sections of

Iberia/Newfoundland calibrated with drilling (Whitmarsh et al., 2001). These exhumation faults show a top-to-the-continent sense of shear on the upper plate. This sense of shear implies that the upper plate HECW act like a tectonic extensional Coulomb wedge (Fig. I-3A). While on the lower plate margin, Reston et al. (2007) determined that the sense of shear along the “S” reflector (Fig. I-2 corresponds to the basal dip of the HECW) at the Galicia deep margin is oriented towards the thinnest part of the wedge, i.e. oceanwards (Fig. I-3A) and therefore can be defined as a gravitational Coulomb wedge. However the first stage of hyper-extension, when the two conjugate wedges are not separated, is not related to gravitational reorganisation but to a pseudo rolling hinge deformation (Reston et al., 2007).

### 3.4 Physical properties and parameters of the HECW

In order to calculate and use the CCWT in hyper-extended rifted margins, the frictional parameters and fluid pressures of the HECW have to be determined. Pérez-Gussinyé and Reston (2001) modelled the rheological evolution of hyper-extensional systems. The main result is that

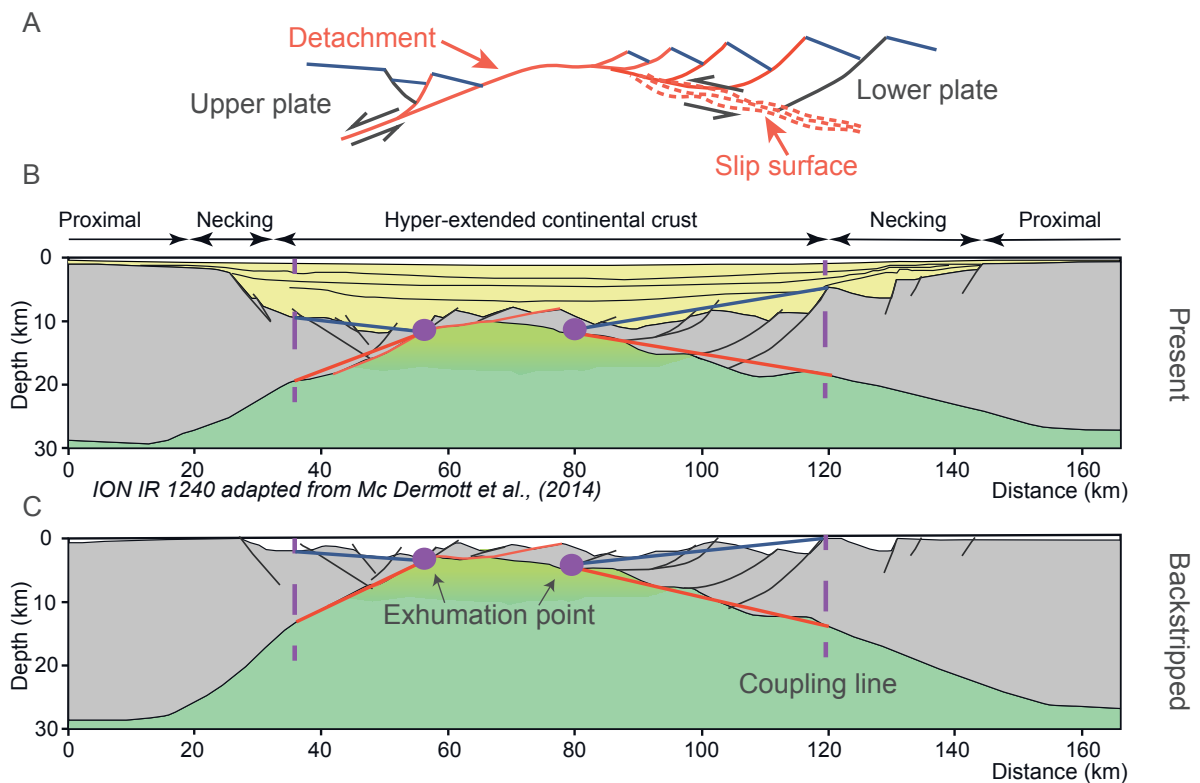


**Fig. I-3:** A) Simplified schematic diagram showing conjugate hyper-extended margins. B) Line drawing of IRI 1240 cross-section crossing the conjugate margins of the Porcupine basin (adapted from McDermott et al., 2014). C) The same cross-section corrected for post-rift sediment loading and thermal subsidence.

the thinning implies a thermal cooling, which makes the continental crust brittle for stretching factors between 3 and 5, depending on the initial rheology of the lower continental crust, the thermal gradient and the strain rate. This crustal embrittlement induces fluid circulation, which leads to fluid-assisted deformation that weakens the crust and the underlying mantle (e.g. serpentinisation).

Because hyper-extended domains are typically at deep water and covered by thick sediments, access to basement rocks of these domains is in most cases impossible. However, a few ODP drill holes reached continental and serpentinised mantle basement along the Iberia-Newfoundland margins (ODP Legs 103, 149, 173, and 210 Boillot et al., 1987; Sawyer, 1994; Tucholke and Sibuet, 2007; Whitmarsh et al., 1998), which enabled investigation of the nature of the rocks forming hyper-extended domains. In the Iberia Abyssal Plain, rocks with a continental affinity were drilled on the Hobby High at ODP Site 900 and 1067, (Fig. I-4) (Manatschal, 2004) and correspond to metagabbros, amphibolites and meta-anorthosites. These rocks present evidence of tectono-sedimentary breccias, cataclasites, fault gouges, veins and pseudo-tachylites formed under greenschist facies conditions. Hydrated minerals such as chlorite and clay minerals are common (Manatschal et al., 2001) indicating the importance of hydration reactions in hyper-extended continental crust (Pinto et al., 2015). Moreover ODP Sites 897, 899, 1068 and 1070 (Fig. I-4) drilled serpentinised peridotites. Beslier et al., (1996) observed at ODP Sites 897 and 899 different stages of deformation with several high temperature deformation phases followed by hydration and brittle deformation under greenschist facies to seafloor conditions. In contrast, ODP Sites 1068 and 1070 lack high temperature deformation and only record a greenschist to seafloor hydration and deformation history (Manatschal et al., 2001).

Ocean-continent transitions have also been recognised in mountain belts like the Alps. Key outcrops are the Tasna OCT exposed over 6km in the Eastern Swiss Alps (Florineth and Froitzheim, 1994) or the Pic de Garalda section exposed in the Basque massifs in the Western Pyrenees (Jammes et al., 2009). The tectono-metamorphic evolution of the Tasna OCT has been extensively studied by Manatschal et al. (2006) (Fig. I-4). The first-order observations are that the continental basement wedges out to zero thickness, bounded by two detachments, the Lower Tasna Detachment (LTD), which separates the continental basement from the serpentinised mantle and the Upper Tasna Detachment (UTD) that forms the top of the basement (Fig. I-4). Serpentinised mantle rocks below the LTD present a complex deformation history including cataclasites, foliated cataclasites and fault gouges, all made of serpentine minerals forming in the footwall of the LTD. The basement rocks are former Variscan or post Variscan meta-gabbros and amphibolites derived from pre-rift mid- to lower crustal levels. They are intensively

faulted and hydrated under greenschist facies to seafloor conditions and show neo-formed clay minerals in the fractures and a general penetrative retrograde hydration including chloritisation and sausrutisation of crustal rocks (Manatschal, 1999). The Tasna example illustrates that deformation in the hyper-extended domain is controlled by an elasto-frictional behaviour within the brittle field (Sibson, 1977). In none of the examples have mylonitic shear zones been found forming simultaneously with the deformation in the hyper-extended domain, supporting the idea that deformation during hyper-extension occurred in a completely embrittled, hyper-extended crust.

Most of the deformation in hyper-extended continental crust and exhumed mantle is accommodated by large normal faults, also sometimes referred to as extensional detachment faults, which are now present at low angle of dip. Colletini, (2011) reviewed the mechanics of observed low angle normal faults and identified two distinct end members: 1) a thick mylonitic shear zone over-printed by cataclastic processes in some locations; and 2) in other places a

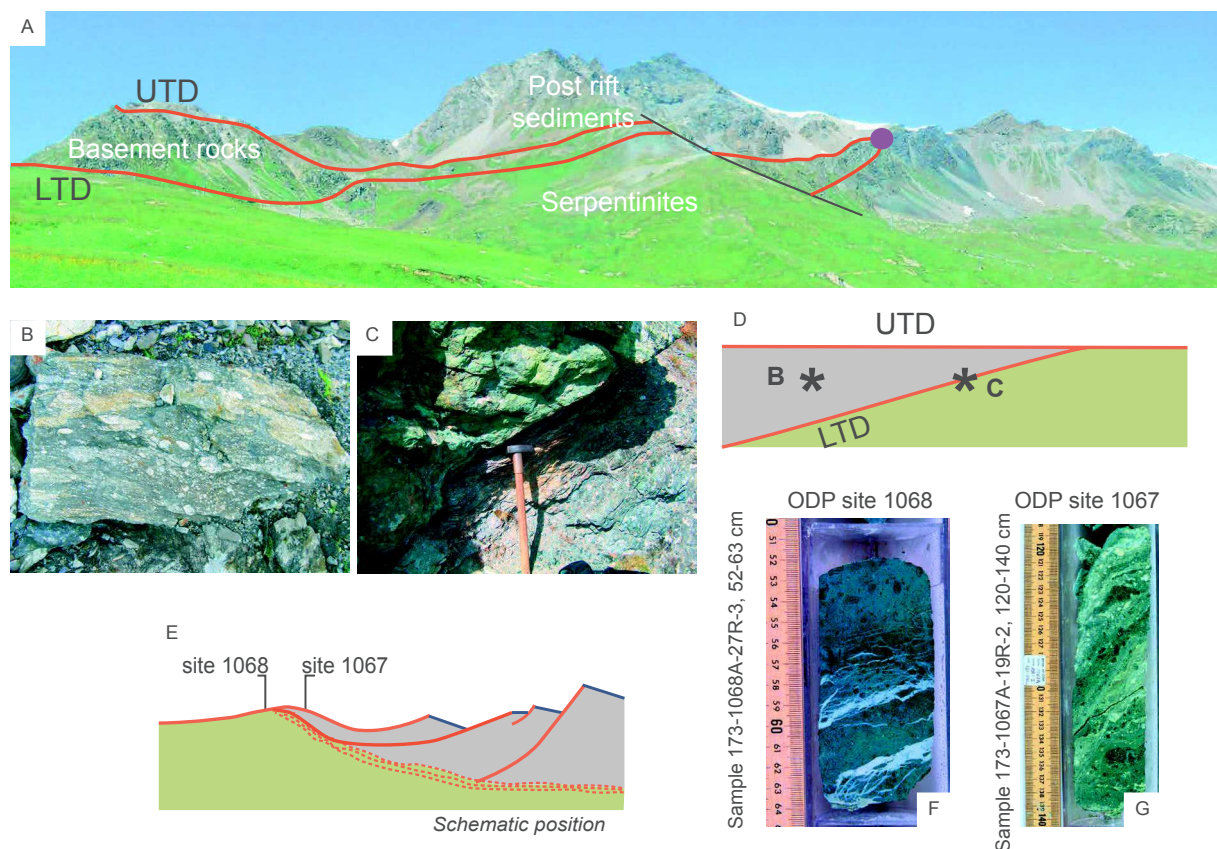


**Fig. I-4:** A) Panoramic view of the fossil ocean continent transition exposed in Tasna (SE Switzerland). B) Field examples of hydrated and foliated continental rocks that formed in the brittle field as gouges or foliated cataclasites. C) The contact between crustal rocks and the serpentinitised mantle representing a décollement horizon. D) Cartoon showing the schematic geometry of the Tasna OCT and the location of the samples shown in B and C. E) Schematic localisation of ODP boreholes drilled over Hobby High in the western Iberia abyssal plain. F) An example of a foliated serpentinite gouge drilled at ODP Site 1068. G) A foliated cataclisite/gouge drilled in the continental crust at ODP Site 1067 made of hydrated continental rocks (for more discussion see Manatschal et al., 2001).

discrete fault core separating hangingwall and footwall blocks affected by brittle processes. As no mylonitic shear zones have been described in hyper-extended continental crust and as low friction coefficient of phyllosilicate can explain movement on extensional detachment faults, we conclude that in accordance with observations the basal surface of the HECW was active as a frictional décollement.

Some seismic interpretations (Jolivet et al., 2015) and numerical modelling (Brune et al., 2014) suggest a ductile lower crustal flow in hyper-extended domains. Indeed, in some numerical models, the deformation in the hyper-extended crust is modelled using a viscous rheology and on the assumption of continuity of the displacement field (no faults). These models calculate an equivalent viscosity to mimic the frictional behaviour, and consider thin shear zones as a proxy to faults (Huisman, 2003). A similar, reverse, approach can be made by calculating an equivalent cohesion from the viscosity with the goal to derive the necessary friction parameters that will produce the same shear stress at the base of the HECW as would be produced by a viscous layer. We consider a viscous layer of thickness  $e$ , viscosity  $\eta$ , separating a fixed base from the cover sliding at the velocity  $V$ . Shear stress at the base of the cover is then  $\tau = \eta \cdot V / e$  if we assume a Couette (i.e. laminar) flow in the viscous layer. Shear stress resulting from a frictional behaviour ( $\phi_D, C_D$ ) of the sliding surface is  $\tau = \tan(\phi_D) \sigma_n + C_D$ . Equating the two shear stresses yields  $\phi_D = 0$  and  $C_D = \eta \cdot V / e$ . Using the latter two equations in the CCWT allows us to account for HECW with a viscous base.  $V$  and  $e$  should be estimated from the interpretation of geophysical or field data. For a HECW with a viscous bulk material, the concept of a critical wedge remains to be defined, for example along the lines of Medvedev, (2002) who analysed viscous wedges in compression.

In our calculations we use the frictional coefficients of phyllosilicates, e.g. clay and serpentine minerals as the weakest mineral phase, based on the observations made in drilled and exposed HECW. Experimental studies showed that smectite clays have low friction angle  $\phi = \sim 5^\circ - 17^\circ$  and illite clays are frictionally stronger, with friction angle  $\phi = \sim 19^\circ - 26^\circ$  (Saffer and Marone, 2003 and references therein). The frictional properties of serpentine minerals are dependent on the temperature and the slip velocity, which can cause strain hardening or weakening. But at room temperature the lizardite shows low friction angles ( $\phi = \sim 8^\circ - 19^\circ$ ), antigorite show higher friction angles  $\phi = \sim 26^\circ - 40^\circ$  (Reinen et al., 1994) and chrysotile has the minimal frictional angle ( $\phi = \sim 5^\circ$ ) at  $100^\circ\text{C}$  (Moore et al., 2004). Serpentinite from the Galicia deep margins are principally composed of chrysotile or mixtures of chrysotile and lizardite, which form at low temperature (Evans and Baltuck, 1988). As there are no direct frictional data from hyper-extended margins, we decided to take arbitrary frictional values of  $\phi_B = 20^\circ$  and  $\phi_D = 10^\circ$ , which are respectively in the range of clay minerals and low temperature serpentines.

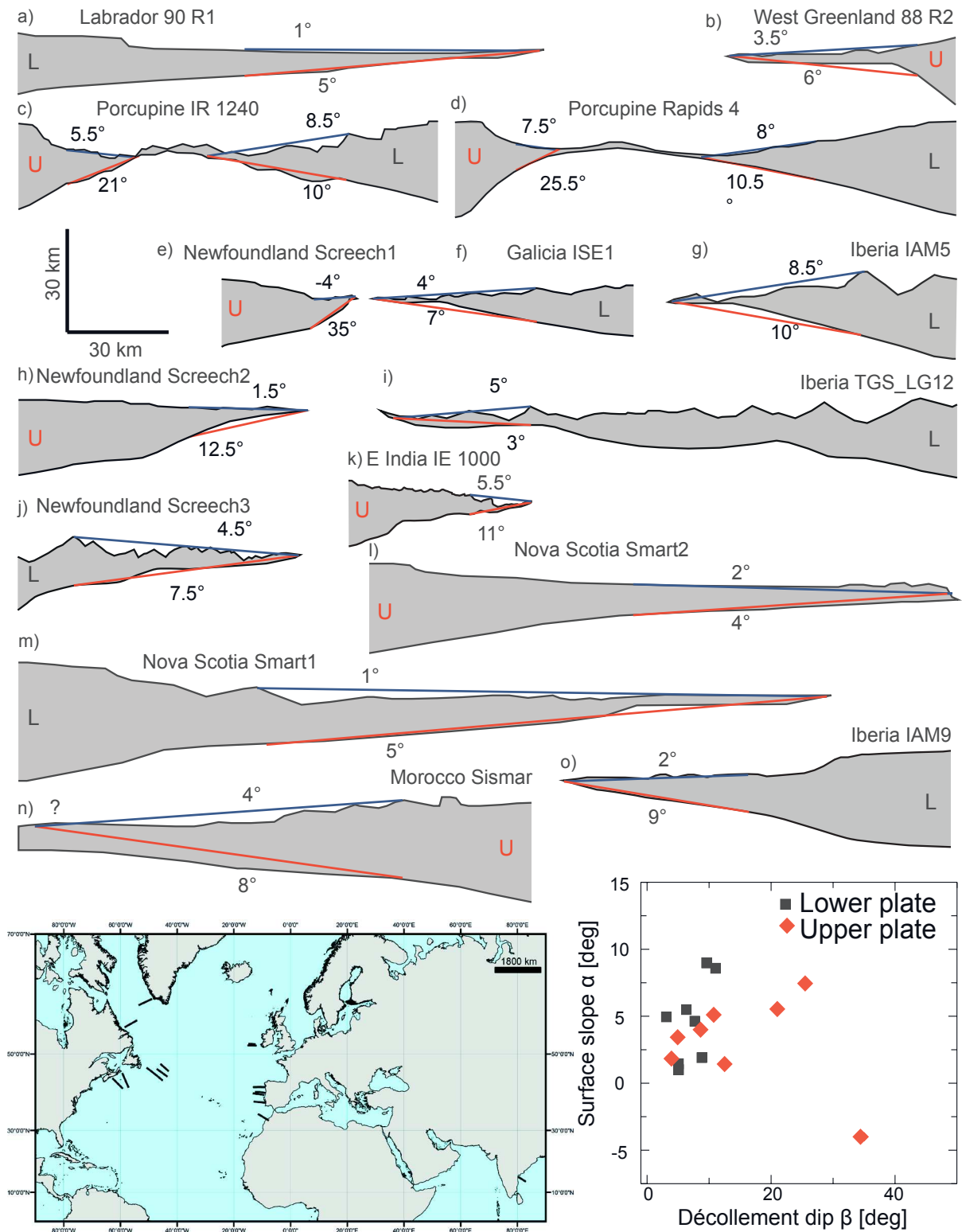


**Fig. I-5:** Measured HECW, L indicates a lower plate margin and U an upper plate margin. Plot of alpha versus beta, note that all measurements have different level of confidence indicated in Table I-1 (Wide angle refraction data that were used for measurements are provided in Table I-2).



There is clear evidence for fluid circulation and re-crystallisation in fault zones, which highlights the path of mantle and marine fluids during the rifting and their relation with the tectonic structures. Moreover mechanical experiments on sediments of ODP Site 1070A and 897D (Ask, 2001; Karig, 1996) highlighted the existence of a very high pore-fluid pressure, interpreted as fluid overpressure, which creates a fluid flow towards the sediments. However the fluid pressure was not quantitatively determined. Because basal and internal fluid pressures are part of the equation of the CCWT and used to determine the stability envelopes of the critical wedge, we consider the fluid overpressure as a variable parameter. Following the CCWT assumptions, the cohesion is ignored in this preliminary work, as it deals with large-scale structures.

### 3.5 Selection of seismic lines

We selected a number of published lines imaging lower and upper plate magma-poor rifted margins, with the aim of defining and measuring the HECW (Fig. I-5). We limited our selection to lines where the shape of the HECW could be defined and measured. The first criteria was to use depth converted lines, where the coupling line, the exhumation point and the

| line          | Measurements |         | Corrected measurements |          | Type        | Location     | Confidence |
|---------------|--------------|---------|------------------------|----------|-------------|--------------|------------|
|               | $\alpha$     | $\beta$ | $\alpha'$              | $\beta'$ |             |              |            |
| ISE1          | 4            | 7       | 3                      | 7.5      | lower       | Iberia       | good       |
| IR1 1240 East | 8.5          | 10      | 5                      | 15       | lower       | Porcupine    | good       |
| Rapids4 East  | 8            | 10.5    | 4                      | 14.5     | lower       | Porcupine    | good       |
| IAM5          | 8.5          | 10      | 6.5                    | 11.5     | $\pm$ lower | Iberia       | medium     |
| IAM9          | 2            | 9       | 1.5                    | 9.5      | lower       | Iberia       | good       |
| Screech3      | 4.5          | 7.5     | 4                      | 8        | lower       | Newfoundland | good       |
| TGS_LG12      | 5            | 3       | 3.5                    | 4        | lower       | Iberia       | medium     |
| Smart1        | 1            | 5       | 2                      | 4        | lower       | Nova Scotia  | medium     |
| 90 R1         | 1            | 5       | 2                      | 3.5      | $\pm$ lower | Labrador     | medium     |
| Smart2        | 2            | 4       | 2                      | 4        | $\pm$ upper | Nova Scotia  | poor       |
| Screech1      | -4           | 35      | -2.5                   | 38       | upper       | Newfoundland | good       |
| IR1 1240 West | 5.5          | 21      | -1.5                   | 27.5     | upper       | Porcupine    | good       |
| Rapids 4 West | 7.5          | 25.5    | 3.5                    | 29       | upper       | Porcupine    | good       |
| Screech2      | 1.5          | 12.5    | 0.5                    | 13.5     | upper       | Newfoundland | medium     |
| IE 1000       | 5.5          | 11      | 3                      | 13.5     | upper       | E India      | poor       |
| SISMAR        | 4            | 8       | 1                      | 11       | upper       | Morocco      | poor       |
| 88R2          | 3.5          | 6       | 1.5                    | 6.5      | $\pm$ upper | E Greenland  | poor       |

**Table I-1:** Measurements of  $\alpha$  and  $\beta$  angle of HECW with the results of the flexural backstripping correction, the type and the location of the measured margin

basal dip can be defined, in order to measure the angles. Therefore, most of our measurements were done on wide angle seismic lines. Time migrated seismic lines are helpful to determine the geometry and location of the coupling line and the exhumation point but need to be converted in depth using a velocity model to define the angles. The selected lines also need to be dip lines, i.e. parallel to the main kinematic transport direction. Moreover, we chose lines where the hyper-extended domain is not masked by magmatic additions and where lower and upper plate margins, the coupling line and the exhumation point can be defined with confidence.

## 4. RESULTS

### 4.1 Measurements of $\alpha$ and $\beta$ values of HECW

Based on the study of two lines from the Iberia hyper-extended margin, Sutra and Manatschal (2012) highlighted that the angle of aperture of the HECW for both lines was about  $11^\circ$ , despite the fact that the lines show different amounts of ductile deformation in the necking zone. In this study we selected 15 lines from the Atlantic and East Indian margins and measured the  $\alpha$  and  $\beta$  values of HECW, following the workflow described in the previous section. The plot of  $\alpha$  versus  $\beta$  (Fig. I-5, Table I-1) shows a clear difference between lower and upper plate margins. For lower plate margins the measured angles are clustered between  $1^\circ$  to  $8^\circ$  for  $\alpha$  and between  $4^\circ$  to  $10.5^\circ$  for  $\beta$ . Moreover,  $\alpha$  and  $\beta$  show some correlation. For the upper plate margins the measured angles are more variable, with  $\alpha$  ranging from  $-4^\circ$  to  $7.5^\circ$  and  $\beta$  from  $4^\circ$  to  $35^\circ$ . These results are very encouraging since they show clear trends. Moreover flexural backstripping modifies these trends only slightly, increasing the values of  $\beta$  by  $1-3^\circ$  and decreasing the values of  $\alpha$  by about the same amount. Note that, in the following sections, we use only angle measurements corrected by flexural backstripping.

### 4.2 Testing the stability of the HECW using the CCWT

A simple trial method has been applied to constrain the critical envelopes of the tectonic extensional and the gravitational wedge using the previously developed equations. The frictional angles were fixed on average values for clay and serpentine minerals, corresponding respectively to  $20^\circ$  and  $10^\circ$ . The hydrostatic pressure ratio  $\lambda_{\text{hydro}}$  is  $\rho_f/\rho = 0.38$  used in this study is assumed to be constant. Sensitivity tests are performed on the fluid pressure in the wedge  $\lambda_b$  and on the décollement pressure  $\lambda_d$ . As passive rifted margins do not present major seismic activity, they are expected to be gravitationally stable and therefore in the stability field of the gravitational extensional CCWT. Thus the parameterisation is performed on the gravitational

stability envelop of the CCWT. Moreover lower plate margins decrease their  $\alpha$  and  $\beta$  to reach the stability, which implies that some time after the cessation of the rifting, they are located on the upper limit of CCWT envelope. Therefore the objective of the parameterisation is to fit the lower plate margin measurements with the upper boundary of the CCWT envelope. An increase in  $\lambda_B$  and  $\lambda_D$  decreases the envelope area and lowers the maximum  $\alpha$  value (Fig. I-6). The best fit is found for  $\lambda_B=0.68$  and  $\lambda_D=0.9$ , which are close to the values determined by Xiao et al., (1991) ( $\lambda_B=0.65-0.7$   $\lambda_D=0.8-0.9$ ) for two sedimentary tectonic extensional wedges in the Gulf of Mexico.

## 5. DISCUSSION

The CCWT is a well-known theory extensively used in compressional tectonic, but has not previously been applied to rifted continental margins. However the three fundamental requirements of CCWT are valid for hyper-extended continental crust in the most distal parts of

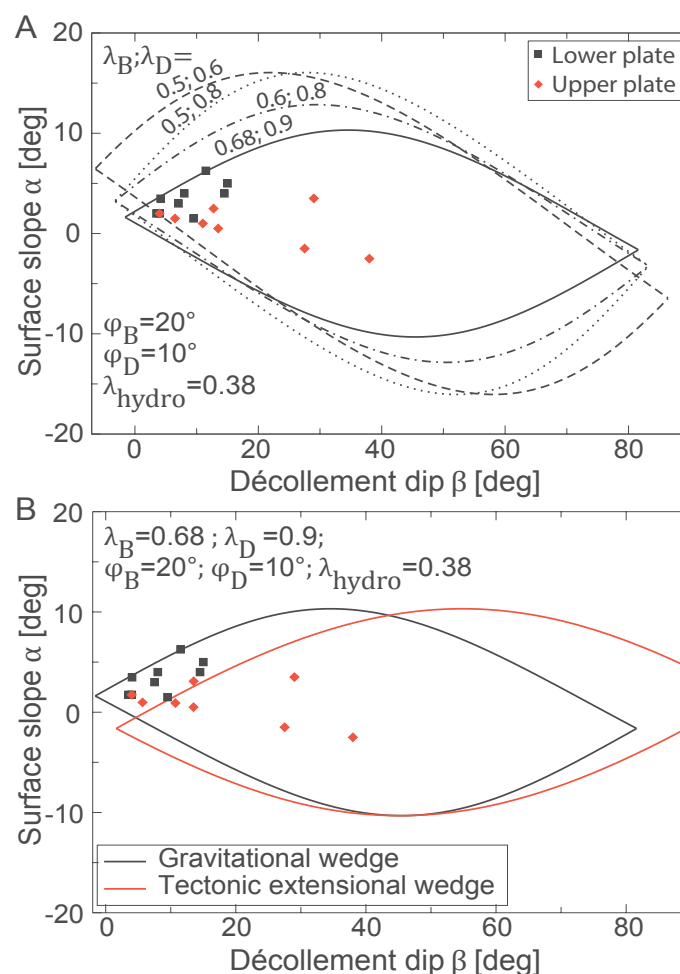


**Fig. I-6:** Stability diagrams for critical Coulomb wedges. Dots represent the corrected measurements of HECW. A) Parameterisation of the gravity extensional critical Coulomb wedge stability envelope by varying  $\lambda_B$  and  $\lambda_D$ . B) Gravity and tectonic extensional critical Coulomb wedge stability envelopes for the fitted  $\lambda_B$  and  $\lambda_D$ .

magma-poor rifted margins. The purpose of this study is to measure the crustal wedge aperture angles ( $\alpha+\beta$ ) at a set of hyper-extended continental margins, to test the applicability of CCWT and to determine whether CCWT can resolve the final geometries of crustal wedges at hyper-extended continental margins. It is important to note that this theory is only applicable for the last deformation continental phase and affects only the frictional hyper-extended crust, prior ductile and brittle deformation are out of the scope of this study.

### **5.1 Lower plate margins: Gravity extensional wedges**

The lower plate margin is the footwall of the extensional detachment fault cross-cutting the thinned continental crust and penetrating mantle (in red Fig. I-7). Note that this normal faults system doesn't correspond to the basal décollement of the lower plate margin, which is a low friction serpentinite layer. The main active fault is located over the lower plate wedge (Fig. I-7). The direction of the basal shear is crucial in determining the type of CCW. In the case of a lower plate margin the basal décollement (corresponding to the "S reflector") of the HECW presents a top to the ocean sense of shear (Reston et al., 2007). A shear direction toward the thin part of the wedge is characteristic of gravitational extensional collapse wedges, where neither compressive nor extensional forces are applied (Mourgues et al., 2014). Sawyer et al. (2005) and Clark et al. (2007) proposed large mass wasting and gravitational landslides over the "S reflector" in the deep Galica Bank, an idea that was discussed by Reston et al. (2007), who finally interpreted the "S reflector" as a rooted extensional detachment fault.

Lower plate measurements present a clear clustering of the measurements indicating a similar geometry of wedges. The measurements of the HECW were fitted with the stability envelope of gravitational extensional collapse with reasonable fluid overpressure. All the measurements (black dots Fig. I-6) are under but close to the upper limit of the envelope. After the end of active extension, the hyper-extended margin had to be gravitationally stable, which is in accordance with our results that show a trend following roughly the upper limit of the CCWT envelope. Therefore, new faults need to be created, or most likely older faults have to be reorganised to reach the gravitational stability in a post tectonic deformation phase. Lower plate hyper-extended rifted margins are typically formed by rotated blocks bounded by faults that dip oceanwards and sole out along a serpentinised layer (décollement level) with blocks showing a decrease in size oceanwards. These observations are characteristic and predicted by the theoretical gravitational extensional collapse, however no compressive deformation is observed at the toe of the wedge. This observation can be explained either by the fact that they do not exist, or that they exist but are not recorded in seismic images due to the low sedimentation rate. The major difference with gravitational landslides is that in rifted margins,

space is created while the slope is unstable, leading to the creation of a free surface, which inhibits compressional structures to form. Although the final shape of the HECW is governed by the CCWT and gravitational reorganisation, prior tectonic deformation due to sequential faulting (Ranero and Pérez-Gussinyé, 2010) seems to have accommodated most extension and pre-structured the hyper-extended margin. Quantitatively partitioning the amount of extension between tectonic extension and gravitational readjustment of the continental crust is an interesting question but it is difficult to evaluate the influence of each of the processes.

## **5.2 Upper plate margin: Tectonic extensional wedge**

The extensional wedge at the tip of the upper plate margin is in the hanging wall of the major extensional detachment fault (Fig. I-7). It experiences a top to the continent sense of shear, characteristic of a tectonic extensional wedge. Measurements of the aperture angles ( $\alpha+\beta$ ) of upper plate margin wedges are more variable than for lower plate margins. Relative to the tectonic extensional stability envelope, some values are above the upper limit, some are close to the limit and some are inside the envelop. It is important to note that all values are in the gravitational collapse stability envelop. Because upper and lower plate margins are connected during the rifting stage, one can assume that the two share the same fluid and frictional properties. This means that upper plate HECW can be critical, sub-critical or super-critical. Critical shapes are explained by internal faulting until stability, sub critical wedges imply that the wedge is already stable at continental separation time. Super-critical shapes could be due to the stopping of faulting on one detachment due to re-localisation of deformation on a new detachment (Gillard et al., 2015) (Fig. I-7) before reaching the wedge stability. The SCREECH 1 (Fig. I-2) line in Newfoundland is an example of a sub critical tectonic extensional wedge. In this line, no major fault is observed in the thinner part of the wedge. Only the termination of the wedge seems to collapse, very similarly to gravitational spreading. Therefore the wedge was probably stable at the time of continental separation, but when activity along the detachment stopped, the edge of the wedge was gravitationally unstable and then equilibrated by gravitational collapse.

Xiao et al., (1991) determined that synthetic faulting in tectonic extensional wedges is oriented toward the thicker part of the wedge and that antithetic faulting is oriented towards the thinner part of the wedge. Antithetic faulting is inhibited because of its geometrical incapability to accommodate finite extension. Observations on upper plate margins show that there are oceanward and continentward dipping faults (e.g. West Porcupine Basin Fig. I-3). In contrast lower plate margins present, with some exceptions, show only oceanward dipping faults. The existence of oceanward dipping faults in upper plate margins is therefore not in accordance

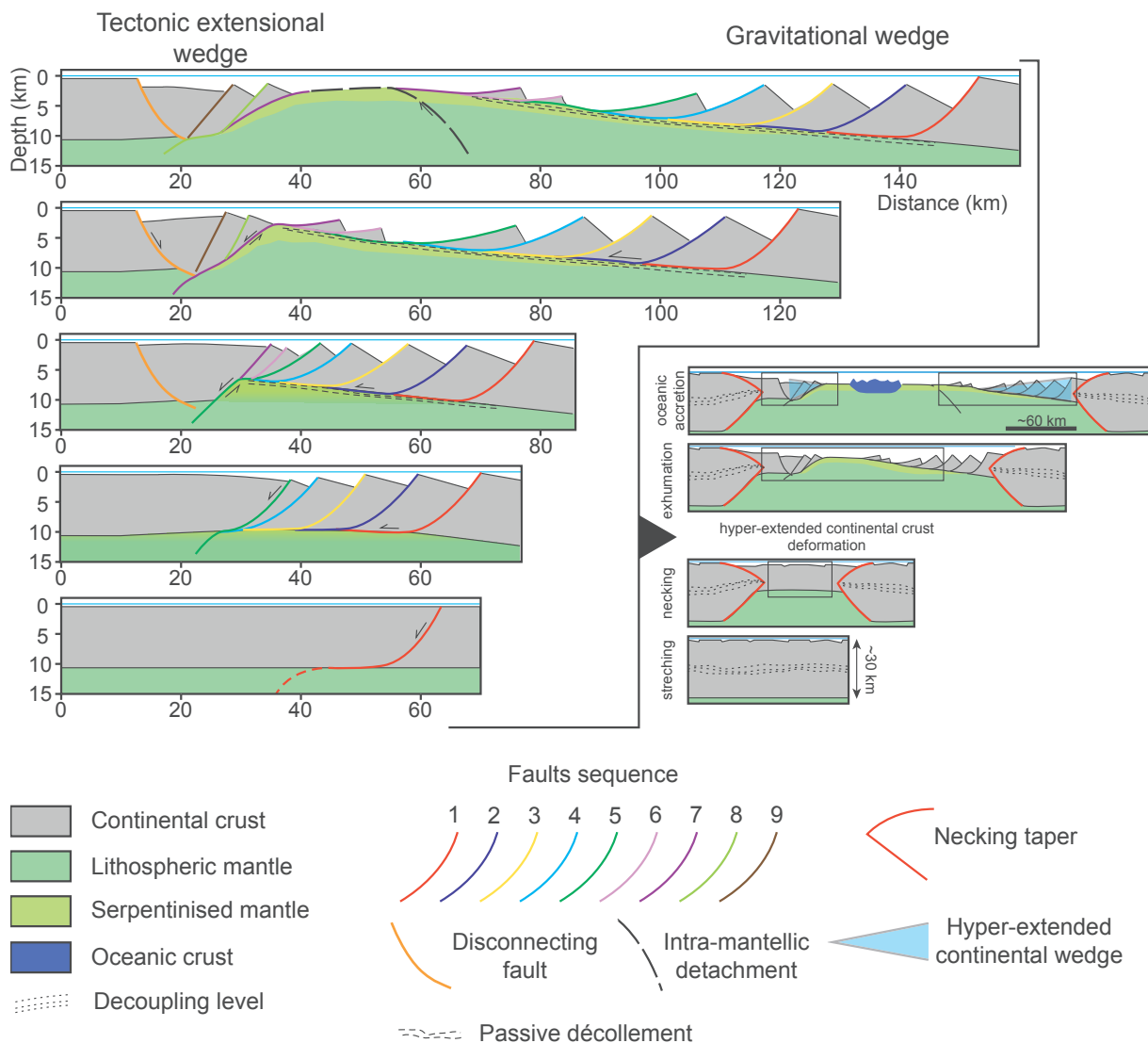


**Fig. I-7:** Conceptual evolution of the most distal part of a hyper-extended, magma-poor rift system. Focus is put on the brittle deformation of the hyper-extended continental crust, which is asymmetric and controlled by in-sequence extensional detachment faults. This system initiates with a pseudo rolling hinge model where the active fault migrates in the hanging wall of the previous inactive fault. A fault will exhume the mantle and will separate the two wedges in an upper and a lower plate margin. The lower plate margin will become tectonically inactive and the final taper shape is due to gravitational readjustment. Whereas in the upper plate the tectonic extensional wedge continues to be active producing extensional allochthons. The upper plate HECW is floored by an active detachment whereas the continentalward hyper-extended upper plate crust is disconnected by an oceanward fault (in orange)

with the CCWT, however prior to the onset of the detachment fault, the deformation was more distributed in the upper crust and associated with the formation of half and full graben basins (e.g. pure shear extension of McKenzie, (1978); stretching mode of Lavier and Manatschal, (2006)). Thus, some of these faults could be inherited from older rift phases. It is also important to note that parts of the upper plate margin are not floored by an active detachment and are not part of a Coulomb wedge. Oceanward dipping faults in this domain (see F2 of Hauptert et al. (2016) or disconnecting fault in orange Fig. I-7) can disconnect the autochthonous terraces

(T2 of Hauptert et al. (2016) from the allochthonous upper plate HECW. Therefore oceanward faulting on the hyper-extended upper plate crust could represent relics of the stretching phase or be related to extension which is not located over the detachment.

### **5.3 Evolution of hyper-extended rifted margins and formation of extensional allochthons**

The evolution of the rheology, the frictional properties, fluid pressures and extension rates in rift systems is accompanied by changes in the mode of deformation. The HECW deformation is in time and space limited, it starts when the continental crust became coupled and stops when deformation is relocalised in the exhumed or oceanic domain, moreover it only influences the most distal few tens of kilometres of a continental margin. We propose a model using the CCWT to explain the final shape of the hyper-extended continental crust; however parts of this model are beyond the scope of our study and need further investigations.

The first fault crosscutting the thinned continental crust and penetrating the mantle determines what will be the upper and the lower plate respectively. At this stage, there is no wedge and only a small amount of extension can be accommodated by a single high angle fault. Faulting migrates sequentially toward the upper plate side (Ranero and Pérez-Gussinyé, 2010) similar to that predicted by a pseudo rolling hinge model (Buck, 1988; Reston et al., 2007), most of the deformation is localised along one or two major normal faults that dip towards the upper plate. Older faults in the lower plate may start to rotate over the serpentinite basal décollement. The rotation of these continental blocks might be accommodated by brittle deformation at their base. After the separation of continental crust, a fault (green fault Fig. I-7) is able to exhume and create a wide domain of exhumed mantle separating the two wedges. On the upper plate a disconnecting fault may cut the hanging wall (in orange fault in Fig. I-7 and R2/T2 relationship discussed in Hauptert et al. (2016)) isolating the HECW floored by an active extensional detachment fault from the hyper-extended terrace. The detachment fault is still active beneath the upper plate HECW, therefore the pink and violet faults are activated to reach the stability field of a critical tectonic extensional Coulomb wedge. The exhumed footwall of the detachment fault will flatten when it reaches the seafloor and will result in the exhumation of the mantle. If the tip of the upper plate tectonic wedge is partly over a flat zone of the detachment system, oceanward of the detachment inflexion point, this part is not anymore in the upper HECW because the active detachment is at the boundary between this bloc and the HECW and not at its base. This process called tectonic regressive wedge creates extensional allochthonous blocks which are locked on the flat surface. Allochthonous blocks are relatively small (<10 km wide) and observed in many deep margins (e.g. Iberia margin; Manatschal,

2004; Reston et al., 1996), South China Sea (Savva et al., 2014), in the fossil Alpine Tethys margins (Manatschal 2004). These blocks originated from the upper plate but can either be on the lower or upper plate side, depending on the subsequent localisation of the major active detachment system in the exhumed mantle (e.g. in sequence vs. out of sequence extension; Gillard et al. (2015)) (black dashed line Fig. I-7) or cutting the upper plate terrace. Moreover the shape of the detachment and its re-localisation are highly dependent to structural and thermal evolution. Therefore the architecture of the upper plate margin is very complex and comparing it to a simple tectonic extensional wedge may be an oversimplification. However the structural evolution of the lower plate, margin seems to be simpler as deformation moves oceanward and the older inactive parts may equilibrate gravitationally. This is also shown by the measured data. Indeed, after the continental separation, deformation will continue in the upper plate margin and exhumed mantle domain, while the lower plate margin decreases its taper angle by internal readjustments to reach the gravitational stability.

## **6. CONCLUSIONS**

This work aims to measure the wedge shape of magma poor hyper-extended margins and to compare it to the Critical Coulomb Wedge Theory (CCWT), well-known in compressive system. The main conclusions of this pioneering study are:

- The large scale crustal architecture of the hyper-extended parts of magma poor rifted margin has been analysed using the CCWT
- The upper plate margin is shown to correspond to a tectonic extensional wedge, whereas the lower plate margin follows the shape of a gravitational wedge.
- The frictional parameters and the fluid pressure control the final shape of lower plate HECW. Faults created during previous extension phases are rearranged to reach the stability of a gravitational CCW
- The migration of the extensional deformation toward the upper plate and the evolution of the basal décollement make the HECW of upper plate margins less predictable than that of the lower plate. Nevertheless, CCWT explain the formation of continent-ward dipping faults and the creation of extensional allochthons.



## **ACKNOWLEDGMENTS**

This project is financially supported by the MM4 consortium (BP, Conoco Phillips, Statoil, Petrobras, Total, Shell, BHP-Billiton, and BG). And Xiaoping Yuan benefited from the support of the China Scholarship Council. We acknowledge our colleagues from Strasbourg University and Cergy-Pontoise University for valuable discussion and comments. We thank also Laurent Jolivet and the editor An Yin reviewer for their constructive comments on the manuscript

## **OUTLOOKS: CRUSTAL AND ASSOCIATED SEDIMENTARY ARCHITECTURE OF HYPER-EXTENDED CONTINENTAL WEDGES IN SEDIMENT- AND MAGMA-STARVED RIFTED MARGINS**

### **Foreword**

This section illustrates and discusses, using seismic and field examples, the importance of the CCW theory in the interpretation of hyper-extended continental crust. The purpose is to test if the conclusions made in the previous section by measuring only the surface and basal dip of hyper-extended continental wedges are in accordance with the deformation/fault geometries inside the wedge. This outlooks section discusses examples and implications of the application of the CCW theory to hyper-extended continental wedges in sediment- and magma- starved rifted margins. The following is an ongoing study which have to be improved before submsion to a journal

### **Introduction**

The stretching and thinning of the continental crust in hyper-extended magma-and sediment-starved rift systems is poly-phased and associated with the creation of several rift domains (Sutra and Manatschal, 2012). In this section we focus on the hyper-extension phase, defined as the phase that thins progressively the previously thinned and embrittled continental crust from <10 to 0 km. This phase post-dates the necking and pre-dates the mantle exhumation phases. The hyper-extended domain typically forms a continental wedges (HECW) that can be observed in seismic sections. This wedge has been structurally defined, measured and successfully compared to the Critical Coulomb Wedge (CCW) theory (Nirrengarten et al., 2016). However the measurements made in this study are based mostly on refraction and reflection seismic lines measuring only the surface and basal dip of the HECW. This study did, however, not discuss yet the crustal and sedimentary architecture of the HECW.

Seismic observations of crustal structures at hyper-extended domains are often masked by thick post-rift sedimentary layers, salt or igneous rocks (Unternehrr et al., 2010; Shillington et al., 2006; Nirrengarten et al., 2014; Stica et al., 2014). The seismic architecture of these domains is therefore often complex and difficult to interpret due to imaging problems and/or the non-unique interpretation of geophysical data (Peron-Pinvidic et al., 2016). Hence, interpretation of these domains are often based on conceptual models (Bond et al., 2012). In the case of field examples, the up-scaling of outcrop-scale observations and their integration at a seismic scale model is often hampered and based on models too (Mohn et al., 2010, Epin et al., *subm*).

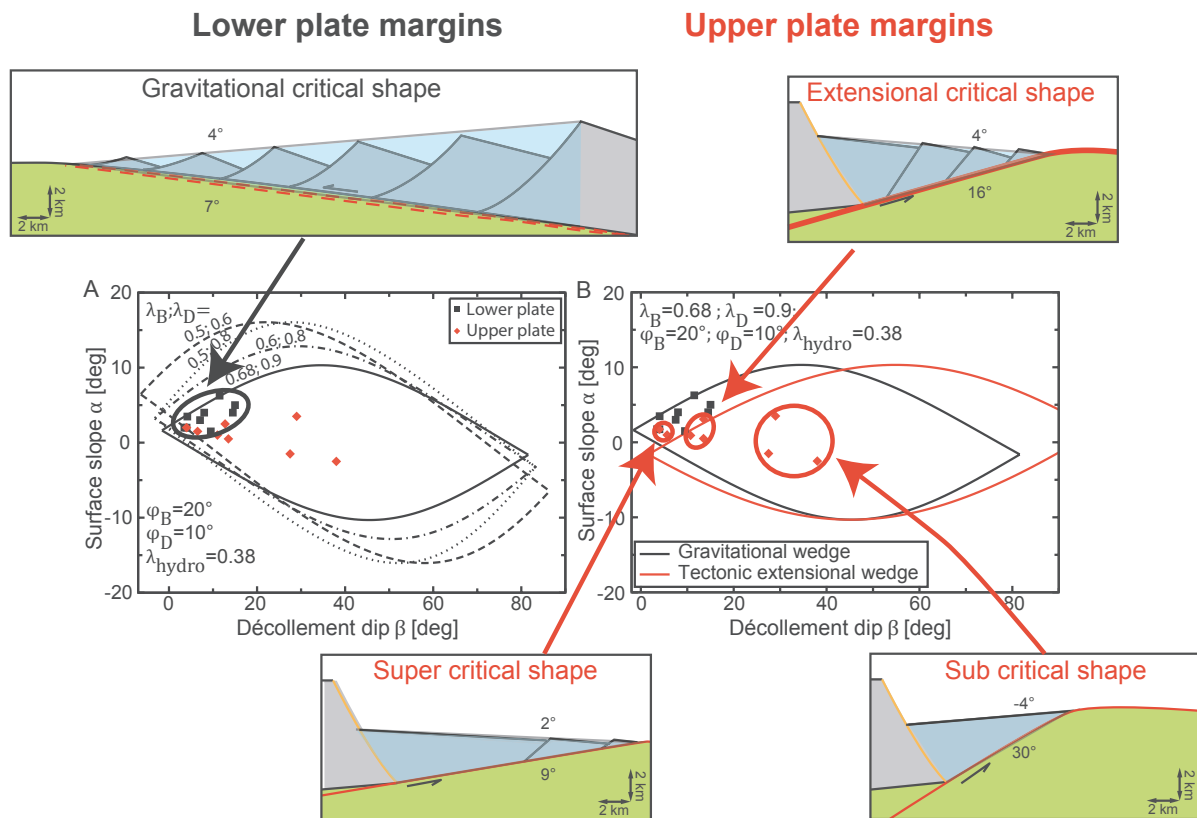


**Fig. I-8:** Stability envelope of a critical gravitational and tectonic extensional wedge with the associated schematic representation of hyper-extended continental wedge

### Definitions and aims

The HECW has been defined in this study as the domain limited continentward by the coupling line which mark the embrittlement of the continental crust (Sutra and Manatschal, 2012; Pérez-Gussinyé and Reston, 2001) and oceanward by the exhumation point, which is the first exhumation of subcontinental mantle at the seafloor. The comparison of a set of HECW with the CCWT results in the existence of 4 different wedge geometries (Nirrengarten et al., 2016a). Lower plate wedges exhibit only the characteristic shape of a gravitational critical shape because all the measurements are close of the critical envelope (Fig. I-8), whereas, upper-plate HECW have sub-, sup- or critical shapes (Fig. I-8). However the deformation inside of the HECW can be predicted by the CCWT but was not compared to the structures observed in seismic sections and field outcrops. Therefore this section focus on the architecture of lower and upper plates HECW by using seismic sections from the Deep Galicia Margin and the East Indian Margin as well as on field outcrops in the Tasna and Err units in the Alps in southeastern Switzerland, where fossil ocean-continent-transitions are exposed (Florineth and Froitzheim, 1994; Manatschal et al., 2006; Manatschal and Nievergelt, 1997).

### **Lower plate HECW:**

Lower plate margin HECW structures have been extensively studied. One of the type examples is the deep Galicia margin (Davy et al., 2016; Dean et al., 2015; Reston et al., 1996; Boillot et al., 1988; Zelt et al., 2003). Along this margin it was possible to highlight the sequence of faulting leading to the formation of a HECW (Ranero and Pérez-Gussinyé, 2010; Reston and McDermott, 2011; Reston et al., 2007). The lower plate HECW present a series of fault bounded rotated crustal blocks presenting a wedge shape. The basal and the oceanward boundaries of these crustal blocks are fault surfaces whereas the continentward boundary is a primary contact with pre-tectonic sediments. On the WE 1 line, pre-tectonic sediments (violet, Fig. I-9) have an almost constant thickness and are parallel to the continentward dipping top basement. The fault offset and the rotation of the crustal blocks create accommodation space filled by syn- and post-tectonic sediments. Because the Iberia margin is sediment starved, the classical syn-tectonic fan architecture is not well develop due to the lack of sediments. However the light purple line (Fig. I-9) could correspond to the top of syn-tectonic sequence. A sequence of reflectors topped by the dark blue line is complexly organized on the oceanward dipping faults. This sequence may correspond to sediments associated to the fault growth and erosion of the exhumed footwall. The sequence topped by the light blue line typically presents a passive infill with sedimentary layers of constant thickness onlapping on the borders of the basin.

The Iberia lower plate margin was often used as an analogue of the fossil Alpine Tethys margins exposed in the Err nappe (Masini et al., 2011; Manatschal and Bernoulli, 1999) the study of the Samedan basin provides strong observational evidence for the sedimentary architecture of hyper-extended domains. In the case of the Err system (Samedan basin) two syn-tectonic sequences are defined by two fans thickening toward the center of the basin (Fig. I-9) and overlain by post-tectonic sediments (Masini et al., 2011). The first fan thickens towards the fault and the sediments are deposited on the pre-tectonic strata (e.g. Bardella system), whereas the second fan, which is interbedded with the first one, is deposited on the exhumed footwall of the detachment fault (e.g. Saluver system) (e.g. Masini et al. 2011). In the example of the seismic line shown in Fig. I-9, the light purple fan is clearly related to the sequential faulting of the hyper-extended crust (Ranero and Pérez-Gussinyé, 2010) the syn-tectonic dark blue fan is only developed if the footwall of the fault is exhumed and imply an active motion during the deposition of sediments. The deformation of the HECW, which follows a gravitational critical Coulomb wedge, only occur after the separation of the two continental wedges, the gravitational re-equilibration is much slower and the associated sediments can be considered as post-tectonic. Therefore it appears that for lower plate margin the influence of the CCW

is quite minor compared to the previous sequential faulting extension phase. However the re-equilibration phase could be recorded if the sedimentation rate were higher.

### Upper plate margins:

Contrarily to lower plate margins the detachment below the HECW is tectonically active during extension in an upper plate margin. In the following two examples are discussed.

#### East India margin

The depth migrated seismic section ION-1000 crosses the East India magma-poor margin (Nemcok et al., 2012; Hauptert et al., 2016) and images the transition from an un-thinned continental crust to unequivocal oceanic crust (Fig. I-10). The crustal architecture has been interpreted by three terraces presenting (T1, T2, T3) an almost flat top basement separated by two escarpment where top basement is dipping oceanwards (R1, R2). This staircase architecture has been described as characteristic of upper-plate margins (Hauptert et al., 2016). On T2 the faults do not crosscut the continental crust, which means that the deformation is not coupled

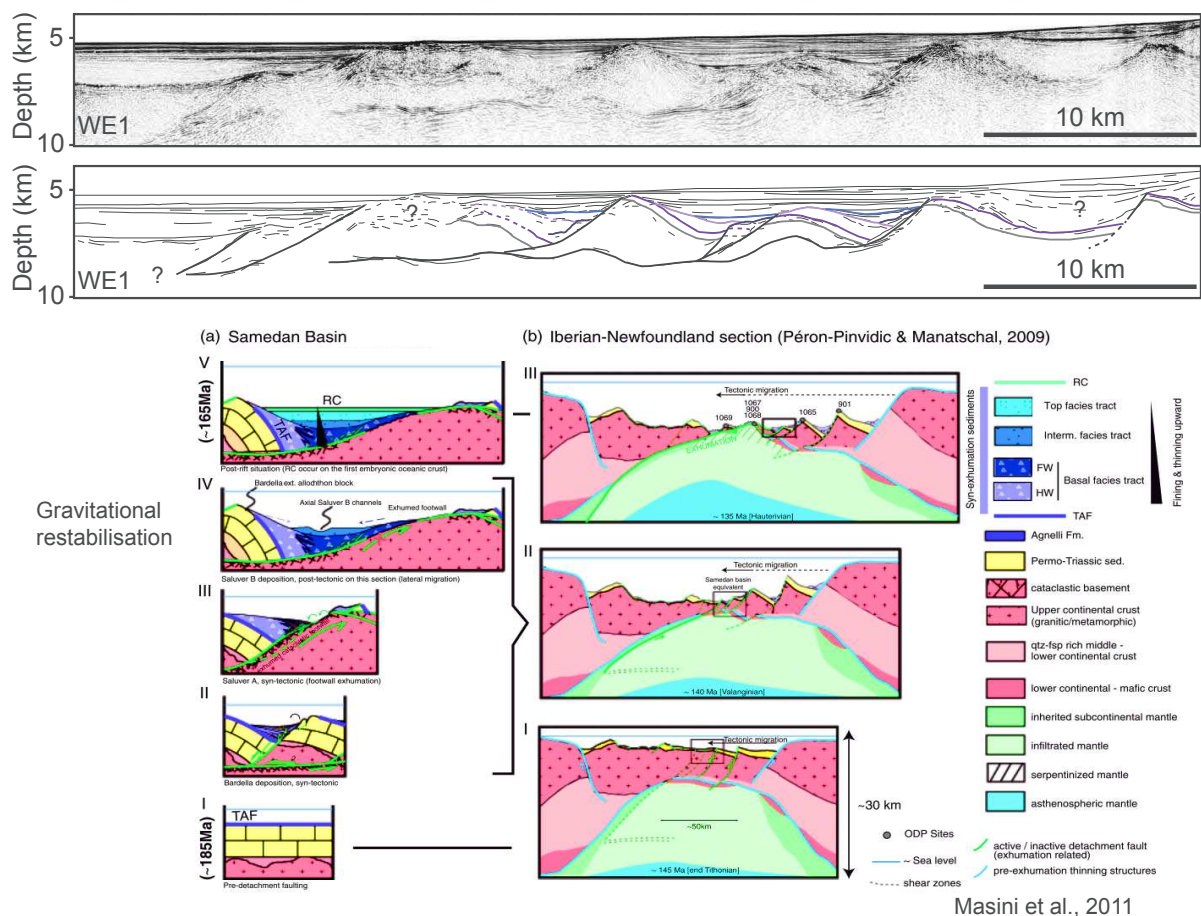
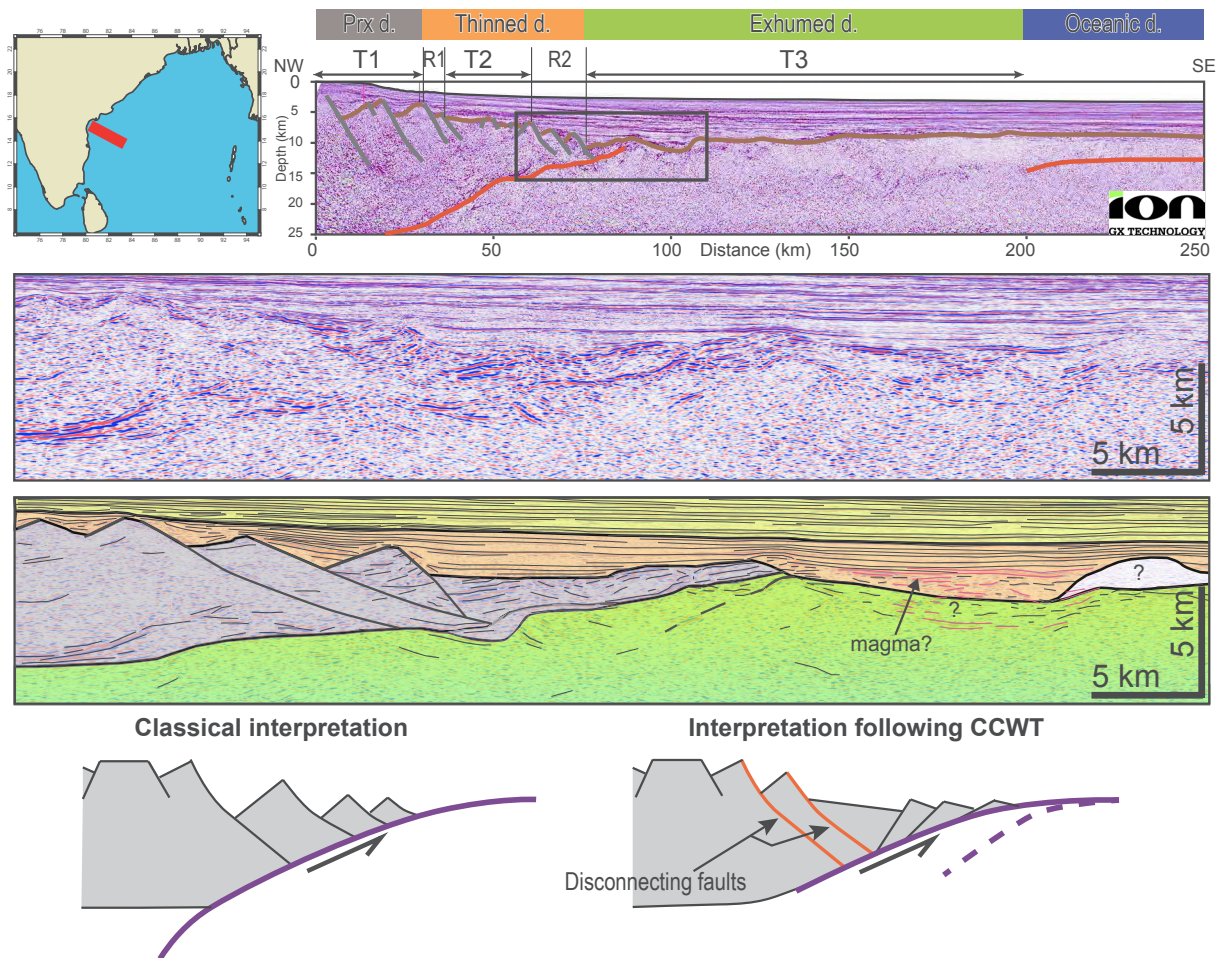


Fig. I-9: Depth converted seismic line WE 1 (Dean et al., 2015) crossing the Deep Galicia margin. Stratigraphic interpretation of a hyper-extended rift basin, the Samedan Basin (Swiss Alps)

(Sutra and Manatschal, 2012) and that the CCWT cannot be used on this terrace. However, the R2 escarpments and the continentward part of T3 present some characteristics of an HECW. Indeed in 35 km the continental crust is thinned from 7km thick to 0. In the R2 escarpment from continent to ocean two major oceanward dipping faults are interpreted followed by a highly reflective zone which terminates oceanward on a basement high. The termination of the zone is interpreted as exhumed mantle with magmatic sills. The interpreted Moho reflection is discontinuous but shallows gently toward the basement high, a small slope break is observed at the continentward limit of R2. The interpretation of the reflective zone, which corresponds to the continental crust termination potentially intruded by magmatic additions is complex, some reflectors are flat other are tilted. In the seismic image it is hard to determine a structure between the Moho and the flat lying post tectonic sediments. Hence two (or more) interpretation can be made: 1) the classical interpretation which proposes that the escarpment is made of decreasing size tilted blocks bounded by oceanward dipping faults located over a margin scale detachment, or 2) part of the R2 escarpment and the continentward part of T3 are an upper-plate HECW and can be consider as a tectonic extensional wedge. In the second case the two large oceanward dipping faults correspond to the disconnecting fault (Nirrengarten et al., 2016a), which separates the terrace from the wedge. The high reflectivity zone constitutes the wedge with continentward dipping faults, which explains why the termination of the continental crust is higher than the continentward part of the HECW. However with the seismic quality or the too low sedimentation rates it is hard to see these faults. The basal detachment is shallow and stops near the intersection with the disconnecting faults, otherwise in accordance with the CCWT more continentward dipping faults have to be observed. Seismic interpretation suggests a second detachment fault located 1 km oceanward of the continental termination, which indicates that the deformation migrates oceanwards. Although the direction of the basal shear and the orientation of the crustal faults are in the classical interpretation incompatible regarding to the CCWT, there are not enough observations to discriminate between the two possible interpretations.



**Fig. I-10:** Seismic line ION IR 1000 (Nemcock et al., 2012) crossing the East India margin and interpretation of the HECW. R, Escarpment; T, Terrace.

### *Tasna outcrop (fossil Alpine Tethys margin)*

The Tasna outcrop (Fig. I-11) constitutes, apart from Zabargad Island (Red Sea, Bonatti and Seyler, 1987), the best example of the transition between continental crust and exhumed mantle. It is exposed in the Engadine window in southeastern Switzerland. It is a relic of the Alpine Tethys margin (Florineth and Froitzheim, 1994), which is undisturbed by later Alpine deformation. Field observations (Florineth and Froitzheim, 1994; Manatschal et al., 2006; Froitzheim and Rubatto, 1998) can be summarized as follows: 1) the continental crust is wedging; 2) the continental crust is made of migmatites and meta-gabbros from pre-rift lower crustal levels; 3) the top and the base of the continental crust are characterized by damage zones and correspond to the upper and lower Tasna detachment (LTD); 4) the top of the exhumed mantle is also formed by a damage zone and is interpreted as the continuation of the upper Tasna detachment (UTD); 5) the sediments above the upper Tasna detachment are flat lying post-rift sediments, and 6) the post-rift stratigraphy has European affinity. The Tasna outcrop was interpreted as an extensional allochthon located on the lower plate (Manatschal et al., 2006)

similar to the continental crust drilled on a basement high at ODP Site 1069 (Whitmarsh and Wallace, 2001). This former interpretation proposes that the LTD is intersected by the UTD. The presented interpretation also proposes that the UTD is cut and therefore younger than the LTD, however the extensional allochthon is located close to the upper plate margin, which is more coherent with the European stratigraphic affinity.

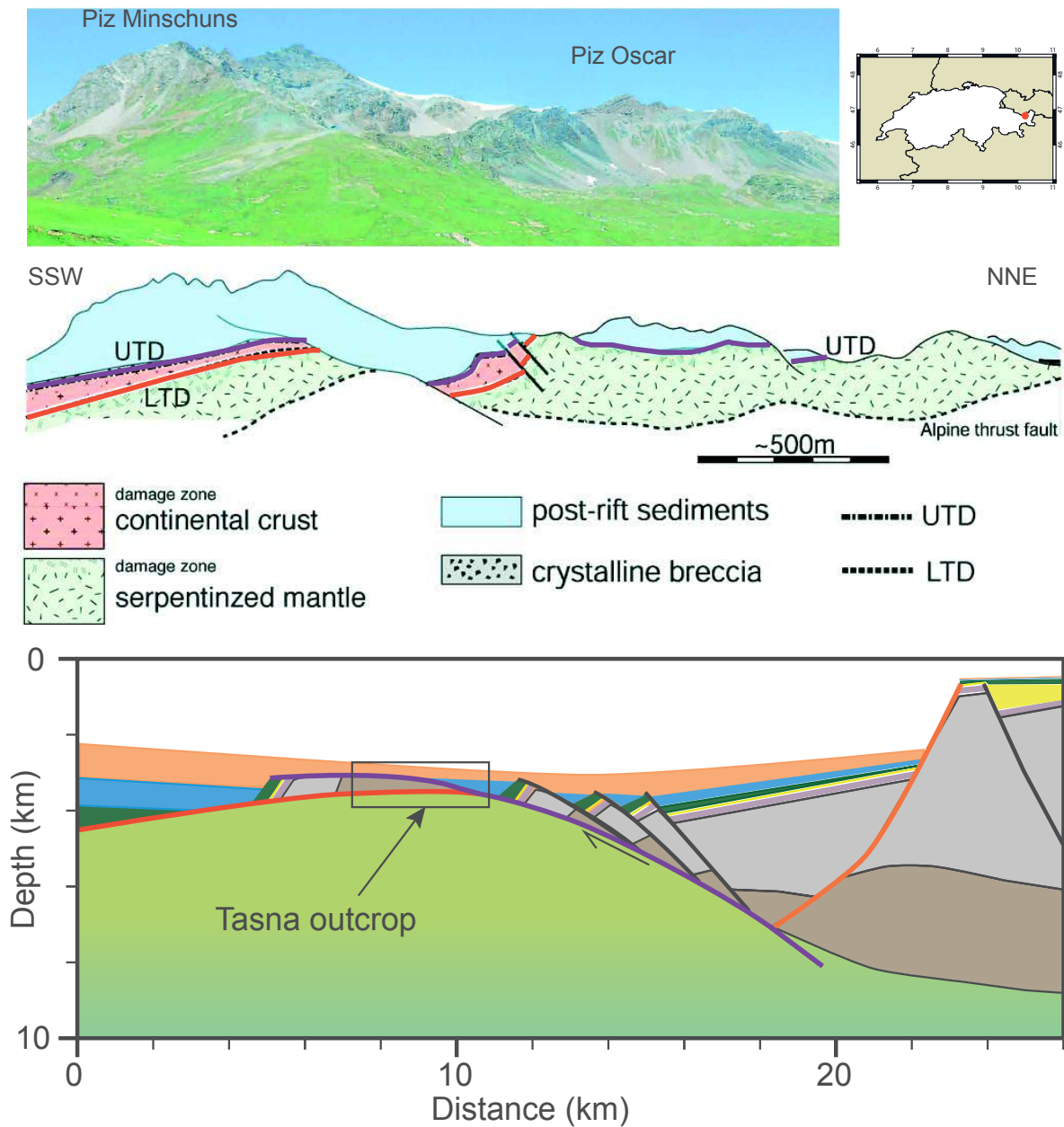


**Fig. I-11:** Panoramic picture of the Tasna outcrop in the eastern Swiss Alps. Geological sketch of the Tasna outcrop highlighting the Upper and Lower Tasna detachment (Manatschal et al., 2006). New interpretation of the Tasna outcrop using the HECW



## **Discussion**

These preliminary observations and models need to be further investigated in particular for the upper plate HECW. The structural and sedimentary architecture have to be analyzed in detail by field studies to determine the evolution of these basins (in particular also taking into account sediment-rich systems). The disconnecting faults seem to have a particular importance for the tectonic evolution. This fault (or fault system) might have migrated toward the continent during the HECW deformation, providing new material to create new extensional allochthons at the expense of the upper plate. The evolution of upper HECW is embedded to the activity of the basal detachment. However, it is not clear whether the detachment is controlled by deep process or by shallow rheological and magmatic modification (as discussed for the exhumed mantle by Gillard et al., 2016b). The tectonic deformation over a detachment in extensional context is therefore a key process, which has to be further studied. The upper plate HECW fault system implies fluid circulations like on the lower plate margin (Pinto et al., 2015), however the geothermal gradient is probably higher (Brune et al., 2014) and could induce strong geothermal activity (e.g. Pyrenean example).

The next step of this study is to include sediment- and magma-rich rift systems. Indeed a larger amount of syn-rift sediments may influence the mode of deformation as they may represent a significant part of the HECW. The magma-rich margins typically presents continentward dipping faults on both conjugate margin (Geoffroy, 2005). The active upwelling of the mantle cause a high geothermal gradient and a lower crust which is potentially ductile (Clerc et al., 2015). This decoupling level is a décollement surface between the lithospheric mantle, which is going up and the brittle upper crust which extend, hence both upper crust conjugate margins experience a top toward the continent basal shear, which make them comparable to the tectonic extensional wedges from the CCWT. However as the rheological behavior and the thickness of the décollement are not conventional for the CCWT, further investigation on magma rich margin are needed.

To conclude, the CCWT application to rifted margins provides new possible interpretations on deep margins. However it is not the only process which thins and deforms the continental crust. The initial rheological behavior and the evolution of the rheological behavior during the lithospheric extension are key parameters to understand the architecture and evolution of rifted margins. The hyper-extended deformation is one deformation mode related to fully frictional material. Other deformation modes may lead to the rupture of a continental crust however they are not following a simple physical law and imply magmatic additions.

## SUPPLEMENTARY MATERIAL

| Profile label in Fig. I-5 | Source                        |
|---------------------------|-------------------------------|
| a                         | Chian et al., 2001            |
| b                         | Chian et al., 2001            |
| c                         | McDermott et al., 2014        |
| d                         | O'Reilly et al., 2006         |
| e                         | Funck, 2003                   |
| f                         | Zelt et al., 2003             |
| g                         | Afilhado et al., 2008         |
| h                         | Van Avendonk et al., 2006     |
| i                         | Sutra and Manatschal, 2012    |
| j                         | Lau et al., 2006              |
| k                         | Hauptert et al., <i>subm.</i> |
| l                         | Wu et al., 2006               |
| m                         | Funck, 2004                   |
| n                         | Contrucci et al., 2004        |
| o                         | Dean et al., 2000             |

**Table I-2:** *References of the sections presented in Fig. I-5*



---

## *CHAPITRE II*

---

Le premier chapitre analyse les architectures et les modes de déformation des marges hyper-étirées en deux dimensions, l'objectif des chapitres suivants est d'analyser l'évolution de la déformation de rift en quatre dimensions. Ceci nécessite un modèle cinématique fiable au moment de la première anomalie magnétique océanique isochrone afin de modéliser l'évolution cinématique du rift de manière consistante. Le sud de l'Atlantique Nord possède les marges hyper-étirées les mieux documentées cependant l'évolution cinématique de la plaque Ibérique est très contestée du fait de l'interprétation de l'anomalie magnétique J comme un isochrone daté au chron M0 (~125 Ma) (Vissers and Meijer, 2012b; Sibuet et al., 2004; Srivastava et al., 2000) ou comme une limite de domaine (Bronner et al., 2011). Ainsi le second chapitre de ce manuscrit décrit des données pluri-disciplinaires afin de déterminer la nature et les implications cinématiques de l'anomalie magnétique J entre Ibérie et Terre-Neuve. Ce chapitre s'organise de la manière suivante:

-Il débute par une revue bibliographique des différents modèles cinématiques proposés expliquant pour chacun, le type de données prises en compte dans ces études et les problèmes de chacune de ces propositions.

-L'interprétation de lignes sismiques recoupant l'anomalie magnétique J ainsi que la compilation de données géochronologiques fournissant les principaux arguments de la discussion.

-La discussion de ce chapitre traite de la nature polygénique et polyphasée de l'anomalie magnétique J, analyse son utilité dans les reconstructions cinématiques et ouvre le débat sur les anomalies magnétiques linéaires en pied de marges.

Ce chapitre fait l'objet d'un article scientifique intitulé « Nature and origin of the J-magnetic anomaly offshore Iberia-Newfoundland: implications for plate reconstructions » qui a été accepté dans la revue *Terra Nova*.

# ***NATURE AND ORIGIN OF THE J-MAGNETIC ANOMALY OFFSHORE IBERIA-NEWFOUNDLAND: IMPLICATIONS FOR PLATE RECONSTRUCTIONS***

M. Nirrengarten<sup>1</sup>, G. Manatschal<sup>1</sup>, J. Tugend<sup>1</sup>, N.J. Kuszniir<sup>2</sup>, D.Sauter<sup>1</sup>

*1 Institut de Physique du Globe de Strasbourg, UMR 7516, Université de Strasbourg/EOST, CNRS; 1 rue Blessig, F-67084 Strasbourg Cedex*

*2 Department of Earth and Ocean Sciences, University of Liverpool; Liverpool, UK*

## **ABSTRACT**

The nature and origin of the J-magnetic anomaly along the Iberia-Newfoundland margins are controversial and its validity for plate kinematic reconstructions questioned. At present, it is interpreted as either an oceanic isochron or as an edge effect of oceanic crust corresponding to lithosphere breakup. Both interpretations result in restorations that are in conflict with the current knowledge from Pyrenean and North Atlantic geology. We combine seismic interpretations and dating of magmatic additions with magnetic data to examine the nature and formation process of this anomaly to discuss its value for plate restorations. We show that the J-anomaly is the result of polygenic and multiple magmatic events occurring during and after the formation of the first oceanic crust. Therefore, we conclude that the J-anomaly cannot be used for plate kinematic studies and, more generally, we question the validity of using ill-defined magnetic anomalies outside unequivocal oceanic domains for plate reconstructions.

## **1. INTRODUCTION**

Plate kinematic reconstructions using oceanic isochrons determined from magnetic anomalies are the most accurate method to determine the relative motion of plates for the last 200Ma (Müller et al., 2008; Seton et al., 2012). Implicit in the use of this technique is that these magnetic anomalies can be considered as isochrons formed at steady state spreading ridges recording the reversals of the geo-magnetic field during cooling of oceanic crust (Heirtzler et al., 1968).

At the Iberia-Newfoundland conjugate rifted margins linear magnetic anomalies have been described over non oceanic domains formed of exhumed mantle or hyper-extended continental crust (Russell and Whitmarsh, 2003; Whitmarsh and Miles, 1995; Funck et al.,

2003). Recently Bronner et al. (2011) questioned the nature and origin of these anomalies, suggesting that they were not produced by geomagnetic field reversals. The most prominent magnetic feature along the Iberia-Newfoundland conjugate rifted margins is the linear J-magnetic anomaly, identified on both sides of the Atlantic Ocean. At present various interpretations of the J-magnetic anomaly exist and result in different contrasting restorations implying for the Pyrenean domain either subduction, transtension and/or hyperextension during Aptian-Albian time (Sibuet, 2004; Olivet, 1996; Jammes et al., 2009). In order to address this plate kinematic problem, we have examined seismic cross-sections, analysed magnetic data and reviewed the age of magmatic rocks to evaluate the nature and origin of the J-magnetic anomaly.

## **2. THE J-MAGNETIC ANOMALY: DEFINITION AND INTERPRETATIONS**

### **2.1 South of the Newfoundland Azores Gibraltar fracture zone (NAGFZ)**

South of the NAGFZ the positive part of the J-magnetic anomaly is a high amplitude linear magnetic anomaly observed on both sides of the Central Atlantic continentward of the Cretaceous Normal Superchron (Pitman and Talwani, 1972) (Fig. II-1). This anomaly extends on the American side from the New England seamounts up to the NAGFZ and on the conjugate European-African side it is associated to the Tore-Madeira rise. Here the J-anomaly is assumed to correspond to the M0 isochron (Rabinowitz et al., 1979; Klitgord and Schouten, 1986) and occurs partly over a basement ridge. The high amplitude of the anomaly (>800 nT) is interpreted to result from either an anomalous high magnetisation or anomalous thicker magnetic-layer within oceanic crust (Tucholke and Ludwig, 1982). The J magnetic anomaly south of the NAGFZ is continuous all along the northern Central Atlantic and is used in most plate restorations (Labails et al., 2010; Klitgord and Schouten, 1986).

### **2.2 North of the NAGFZ**

The J-magnetic anomaly is laterally offset by the NAGFZ, segmented and made of several patches which are generally aligned and oriented N-S to NNE-SSW (Fig. II-1). The amplitude decreases northwards and fades out east of Flemish Cap and west of Galicia Bank. E-W oriented magnetic anomalies, corresponding to the Estremadura Spur and Newfoundland Seamounts interfere with the J-anomaly.

For the domain north of the NAGFZ two main interpretations exist: 1) J is an oceanic magnetic anomaly either corresponding to chron M4, M3 or M0 (Whitmarsh and Miles, 1995) (Fig.2A), or 2) J is the transition from an exhumed mantle domain to a more magmatic oceanic

crust (Bronner et al., 2011). In the second assumption there are two possibilities. Either this transition occurred over very short time and can be considered as an isochron (Fig. II-2B) or it resulted from a northward propagation of the lithospheric breakup as suggested by Bronner et al. (2011) (Fig. II-2C) and is diachronous.

Sibuet et al. (2004) assumed that the J-anomaly north of the NAGFZ corresponds to the chron M0 and mapped it further north into the Bay of Biscay (Fig. II-2 A). Their reconstruction leads to 1) a V-shape ocean of Aptian age in the Pyrenean domain that is 300km wide at its western part which was followed 2) by the a subduction of this oceanic domain related to a counter clockwise rotation of the Iberia plate by about 35° before anomaly C34 (83.5 Ma). More recently, Vissers et al. (2016) suggested, mainly based on paleomagnetic data (Van der Voo, 1969; Gong et al., 2008) that this subduction occurred during Aptian time. However those data have been questioned due to the lack of reliable paleomagnetic poles with satisfactory statistical criteria and age (Neres et al., 2012). Moreover, Neres et al. (2013) show that the position of

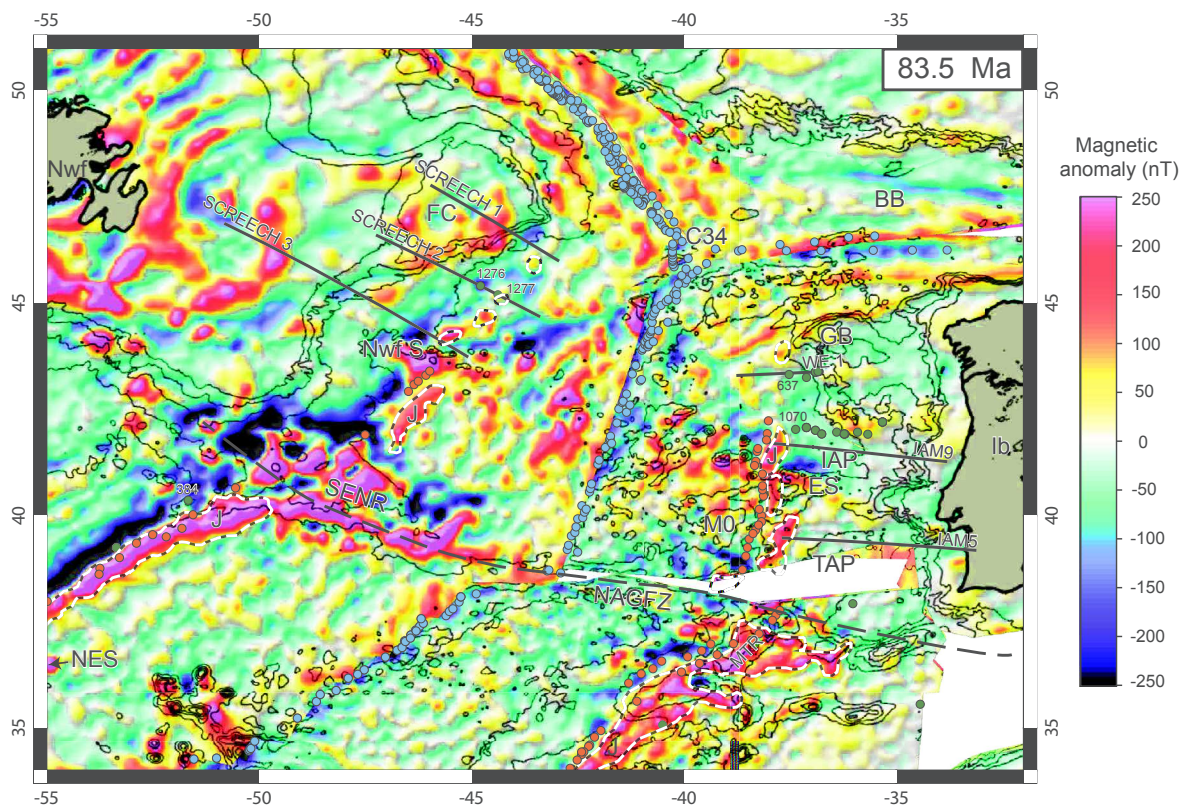


**Fig. II-1:** Reconstructed magnetic map *Emag2v3* (Meyer et al., 2016) at chron C34 (using the rotation pole of Srivastava et al. (1990)). Zones surrounded by black and white dashed line are the positive part of the J-magnetic anomaly. Green circles indicate ODP and DSDP sites. Orange and light blue circles are respectively the picking of the M0 and C34 isochron (Klitgord and Schouten, 1986; Seton et al., 2014). Black lines are the seismic lines used in Fig. 3-4. BB, Bay of Biscay; ES, Estremadura Spur; FC, Flemish Cap; GB Galicia Bank; Ib, Iberia; MTR, Madeira-Tore Rise, NAGFZ, Newfoundland Acores Gibraltar fracture zone, NES New-England Seamounts; NwF, Newfoundland; NwF S Newfoundland Seamounts; SENR Southeast Newfoundland ridge; TAP Tagus Abyssal Plain,



Iberia using the M0 isochron is not compatible with the Global Apparent Polar Wander Path. Geological observations across the Pyrenean domain suggest a NNE-SSW extension during Albo-Cenomanian time, associated with mantle exhumation and the creation of thick turbidite sequences both of which are compatible with hyperextension (Tugend et al., 2014; Clerc and Lagabrielle, 2014; Vacherat et al., 2016; Jammes et al., 2009). Onset of convergence in the Pyrenean domain is marked by a major unconformity of late Santonian age (Capote et al., 2002). Finally, tomographic data show no evidence for a subducted slab beneath the Pyrenean orogeny (Chevrot et al., 2014) or North Africa (Barnett-Moore et al., 2016)

An alternative interpretation is that the J-anomaly corresponds to an edge effect resulting from the juxtaposition of an exhumed mantle domain and a magmatic oceanic domain. In the case of a synchronous breakup at Aptian-Albian time (~113Ma) (Tucholke et al., 2007), the J-anomaly would correspond to an isochron, but would be younger than M0 as commonly suggested. To reconcile this with the commonly accepted position of Iberia at C34, seafloor spreading rates should have been ~1.5 faster north of the NAGFZ than on its southern side before 83.5Ma and then should have slowed down after C34 (Fig. II-2B, Tucholke and Sibuet, 2012). In the case of a northward propagation of breakup, as suggested by (Reston and Morgan, 2004; Bronner et al., 2011, 2012), the J-anomaly would get younger northward and would not correspond to an isochronal oceanic anomaly (Fig. II-2C). Moreover, since the oldest rocks drilled at ODP Site 1277 have been dated at 128 Ma (gabbros intruded in mantle rocks; Jagoutz et al., 2007), this would also imply that breakup propagated into an already exhumed mantle domain. Thus, the J-anomaly would have been associated with magmatic additions emplaced into existing basement. For Tucholke and Sibuet, (2012) this hypothesis implies a melt anomaly track in a nearly opposite direction to the absolute plate motion determined by hotspots (Müller et al., 1993). However, even if this interpretation has to be further tested, the resulting plate modelling (Fig. II-2C) suggest a relatively narrow opening of the Pyrenean realm as indicated by geological studies (Roca et al., 2011; Tugend et al., 2015)

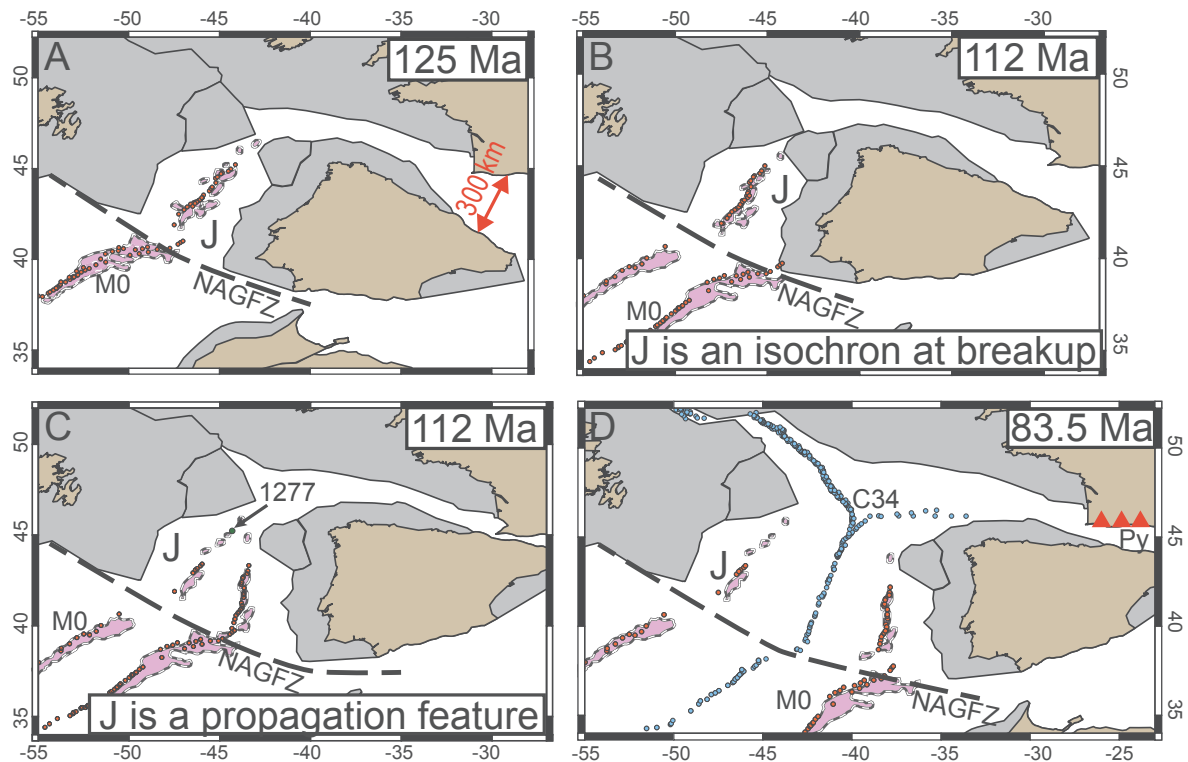


**Fig. II-2:** Southern North Atlantic plate reconstruction. A) Reconstruction at ~125 Ma using the J anomaly as recording the geomagnetic reversal of chron M0 (Sibuet et al., 2012) B) Plate reconstruction at 112 Ma assuming that J record the magmatic event at breakup time which is nearly isochronal along the margin. C) Plate reconstruction at 112 Ma supposing that J is related to the lithospheric breakup which propagates from ~125Ma to 112 Ma near ODP site 1277. D) Chron C34 reconstruction (Srivastava et al., 1990). Pink areas surrounded by black and white dashed line correspond to the positive part of the J anomaly. Py, Pyrenees; For other abbreviations and labels see Fig II-1. See supplementary material Table II-1 for rotation poles.

### 3. NATURE OF THE J-ANOMALY

#### 3.1 Nature of basement underlying the J-anomaly

In the Tagus Abyssal plain the J-anomaly occurs over a basement showing a seismic velocity structure characteristic of oceanic crust (Afilhado et al., 2008) that is thickened at the magmatic Tore-Madeira rise (western termination of IAM5 line Fig.II-3). In contrast on the Iberia Abyssal Plain (IAM9 line Fig. II-3), the J-anomaly is located at the boundary between exhumed mantle and oceanic crust as indicated by a change in the seismic velocity structure at the J-anomaly (Dean et al., 2000; Minshull et al., 2014). ODP Site 1070 located 40km northward of the IAM9 line and close to the J-anomaly, sampled a serpentinized peridotites ridge intruded by gabbroic bodies. The crystallization ages from the gabbros range between ~127 Ma and ~101 Ma (Beard et al., 2002; Jagoutz et al., 2007). The basement at ODP Site 1070 is therefore assumed to be emplaced before 127 Ma. In the deep Galicia margin the pick of M0 (Srivastava et al., 2000) is located 30 km to the west of the peridotite ridge drilled at ODP Site 637. This

domain has been imaged by seismic reflection (Fig. II-3 WE1) (Dean et al., 2015; Davy et al., 2016) and interpreted as serpentinized mantle with magmatic additions on the top potentially corresponding to an extremely thin oceanic crust (0.5-1.5km).

On the Newfoundland margin south of the Newfoundland seamounts, the J-anomaly is close to discontinuous basement ridges, which crop out at the seafloor (see supplementary material Fig II-6). These ridges are at the boundary between the oceanic crust and a landward basement of unknown composition overlain by the U-reflector (Tucholke et al., 1989). The seaward end of the Screech 3 line (Fig. II-4) is just a few kilometres north of the Newfoundland Seamounts. There, the J-anomaly is over oceanic crust (Lau et al., 2006b) overprinted by post breakup magmatism ~97.7 Ma. The J-anomaly on the Screech 2 line is interpreted as the transition from exhumed mantle to oceanic crust with a basement high drilled at ODP Site 1277 (Tucholke and Sibuet, 2006). Drilling penetrated thin basalts interleaved with sediments and overlying serpentinized mantle intruded by dykes (Tucholke and Sibuet, 2006). The oldest magmatic rocks found at ODP Site 1277 are alkaline magmatic rocks dated at  $\sim 128 \pm 3$  Ma and emplaced in an already formed basement (Jagoutz et al., 2007). An Aptian/Albian age ( $\sim 113.2 \pm 2.1$  Ma Jagoutz et al., 2007), which corresponds to the age of lithospheric breakup proposed by Tucholke et al. (2007), was obtained by dating alkaline magmatic veins intruding the exhumed mantle rocks at ODP Site 1277. Seismic interpretation and drill hole data highlight that the formation of this high had to occur before early Albian, since Albian sediments passively onlap the basement high (Robertson, 2007). Oceanward of this ridge, basement highs are wider and on average higher than top basement toward the continent suggesting ultra-slow seafloor spreading. However, detachment faults which affect the overlying sediments, indicate that this domain did not form at a steady state oceanic spreading centre (Gillard et al., 2016). East of Flemish Cap, the J-anomaly is less well marked. It does not correspond to a basement high but lies within an exhumed mantle domain, about 25 km landward of the oceanic crust (Welford et al., 2010).

### **3.2 Evidence for post- breakup magmatism**

In the southern North Atlantic many occurrences of post-breakup alkaline magmatism are observed (Merle et al., 2009). Among them, the Tore-Madeira Rise follows the trend of the J-anomaly in the Tagus Abyssal Plain (Fig. II-5). It consists of magmatic rocks dated at 103 Ma to recent (Merle et al., 2009 and reference there). On the conjugate margin, the Newfoundland seamounts that cross the J-anomaly have been dated at ~97 Ma (Sullivan and Keen, 1977) and the two sills coinciding with the U reflector and drilled at ODP Site 1276 are dated at ~106 and ~95 Ma respectively (Hart and Blusztajn, 2006). Moreover volcanic edifices dated as Early to

mid Cretaceous occur farther north in the Porcupine Basin, Rockall Basin and close to Orphan Knoll (Calvès et al., 2012; Kimbell et al., 2010; Pe-Piper et al., 2013) as well as in large areas of the Newfoundland Basin (Peron-Pinvidic et al., 2010). Thus, magmatic activity is widespread and is found to be both syn- and post breakup in age.

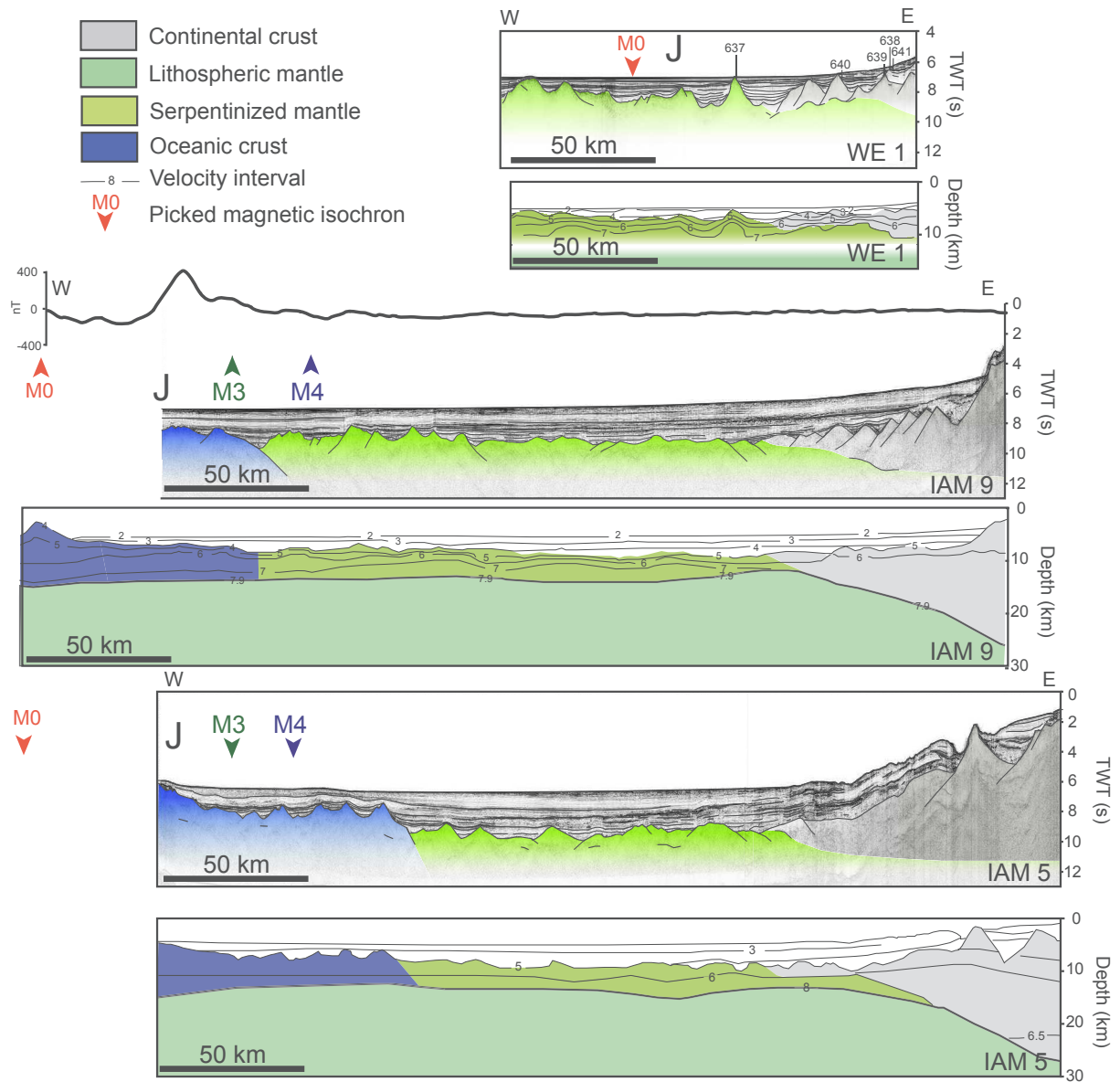


**Fig. II-3:** Reflection and refraction seismic lines from the Iberia margin with the location of the picked magnetic isochrons (Srivastava et al., 2000), the J-anomaly corresponds to the interval between M4-M0 (Tucholke and Ludwig, 1982). See location of the line on Fig. II-1. Line WE 1 (Dean et al., 2015, Davy et al., 2016). Line IAM 9, (Dean et al., 2000) IAM 5 (Afilhado et al., 2008). Magnetic data were record during RRS Discovery cruise 215 (1995). Projected ODP sites from Leg 103 (Boillot et al., 1988).

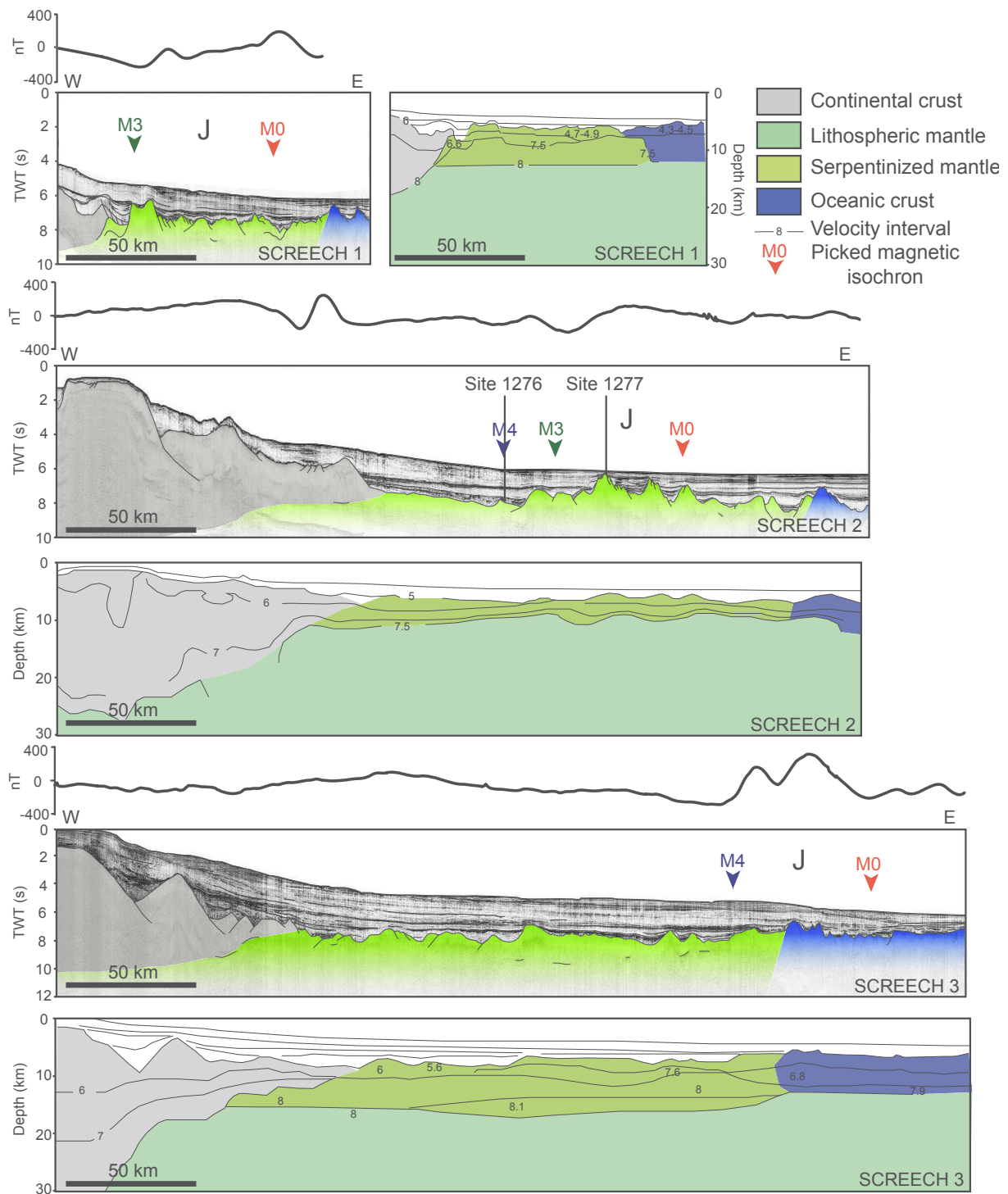


**Fig. II-4:** Reflection and refraction seismic lines from the Newfoundland margin with the location of the picked magnetic isochrons (Srivastava et al., 2000), the J-anomaly corresponds to the interval between M4-M0 (Tucholke and Ludwig, 1982). See location of the line on Fig. 1. reflection lines SCREECH 1 (Hopper et al., 2004), SCREECH 2 (Shillington et al., 2006), SCREECH 3 (Lau et al., 2006a) and refraction lines SCREECH 1 (Funck et al., 2003), SCREECH 2 (Van Avendonk et al., 2006), SCREECH 3 (Lau et al., 2006b). Magnetic data were recorded during R/V Maurice Ewing cruise EW-007 (2000). ODP sites from Leg 210 (Tucholke and Sibuet, 2006)

### **3.3 Polygenic nature of the J-anomaly and the role of magmatism**

It is clear then that the J-anomaly does not lay over the same type of basement all along the margin. To the south it is located on oceanic crust or close to its continentward boundary, whereas in the north it lies over exhumed mantle (Fig. II-3, II-4 and II-5). Thus, the J-anomaly cannot be interpreted over all its length as the result of an edge effect between oceanic crust and exhumed mantle. Moreover, magmatic additions, which greatly impact the magnetic anomalies, are widespread in the southern North Atlantic and show scattered ages (Fig. II-5, supplementary material Table II-2). The fact that magmatic additions of various ages were emplaced on existing basement also discards the hypothesis of a classical oceanic magnetic anomaly produced at an oceanic spreading ridge. Therefore we believe that the J magnetic anomaly is not the result of a unique process but is rather the result of the superposition of several magmatic events including syn- and post-breakup magmatism of different ages.

The symmetrical pattern of the J-anomaly at both conjugate margins in the southern North Atlantic is nevertheless intriguing. In the north, where the anomaly has lower amplitude, it may correspond to syn-tectonic magmatism that was emplaced during mantle exhumation (e.g. Gillard et al, 2016). In the central domain the J-anomaly seems to be related to an uplifted basement resulting from magmatic intrusions and underplating of an exhumed mantle domain during breakup (Bronner et al., 2011). In the southern segment the post breakup alkaline magmatism is more present on the European-African side, (Merle et al., 2009) and most likely related to an hotspot. The symmetric pattern of these syn- to post-break-up magmatic additions cannot be explained by a single event that is occurring at the spreading ridge, because magmatic additions are not genetically linked with the underlying basement. The symmetrical pattern of the J-anomaly may partially be explained by the existence of inherited (pre-rift or rift-related) structures that preferentially channelized syn to post break-up magmatic additions or to variations of mantle fertility. This remains however to be further investigated.

## **4. IMPLICATIONS FOR PLATE RECONSTRUCTIONS AND CONCLUSION**

Even though the J-anomaly looks symmetric all along the two conjugate margins, it does not appear to record a unique monogenic event. Therefore, the J-anomaly does not fulfil the requirement of an isochronous oceanic magnetic anomaly. Neither does the J-anomaly define a crustal type domain boundary (Fig. II-5); the transition to the first oceanic crust seems rather gradual and occurs over a wide zone similar to what has been reported for the southern Australia margin (Gillard et al., 2015). Therefore, we suggest that plate restorations using the J-anomaly are not appropriate. The integration of the well documented geological record of the Pyrenees



## **ACKNOWLEDGEMENTS**

We acknowledge funding from the MM4 consortium (BP, Conoco Phillips, Statoil, Petrobras, Total, Shell, BHP-Billiton, and BG). We thank Tim Minshull, an anonymous reviewer and the editor Jason Phipps Morgan for their valuable comments.



SUPPLEMENTARY MATERIAL

| Fig. II-2:                          | Chron   | Age (Ma) | Lat   | Lon    | Angle  | Source                                  |
|-------------------------------------|---------|----------|-------|--------|--------|---|
| Africa relative to fixed N America  |         |          |       |        |        |   |
| A                                   | M0      | 125      | 65.95 | -20.46 | -54.56 | Labails et al., 2010                    |
| B                                   | Apt/Alb | 112      | 68.09 | -20.49 | -46.62 | modified from Tucholke and Sibuet, 2012 |
| C                                   | Apt/Alb | 112      | 68.09 | -20.49 | -46.62 | modified from Tucholke and Sibuet, 2012 |
| D                                   | C34     | 83.5     | 76.55 | -20.73 | -29.6  | Klitgord and Schouten, 1986             |
| Iberia relative to fixed N America  |         |          |       |        |        |   |
| A                                   | M0      | 125      | 64.71 | -18.94 | -58.11 | Srivastava et al., 2000                 |
| B                                   | Apt/Alb | 112      | 70.8  | -14.36 | -48.25 | modified from Tucholke and Sibuet, 2012 |
| C                                   | Apt/Alb | 112      | 83.76 | 13.28  | -32.6  | modified from Tucholke and Sibuet, 2012 |
| D                                   | C34     | 83.5     | 87.18 | 57.43  | -24.67 | Srivastava et al., 1990                 |
| Eurasia relative to fixed N America |         |          |       |        |        |   |
| A                                   | M0      | 125      | 69.67 | 154.26 | -23.17 | Srivastava and Verhoef, 1992            |
| B                                   | Apt/Alb | 112      | 68.22 | 152.88 | -21.9  | modified from Tucholke and Sibuet, 2012 |
| C                                   | Apt/Alb | 112      | 68.22 | 152.88 | -21.9  | modified from Tucholke and Sibuet, 2012 |
| D                                   | C34     | 83.5     | 64.35 | 149.97 | -19.21 | Srivastava et al., 1988                 |

Table II-1: Poles of rotation used in Fig. II-2

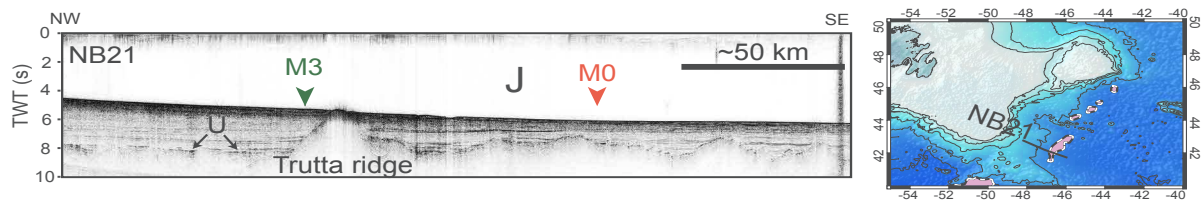


Fig. II-6: Seismic line NB21 from the Seismic Project Information RC2510 (Tucholke et al., 1989)

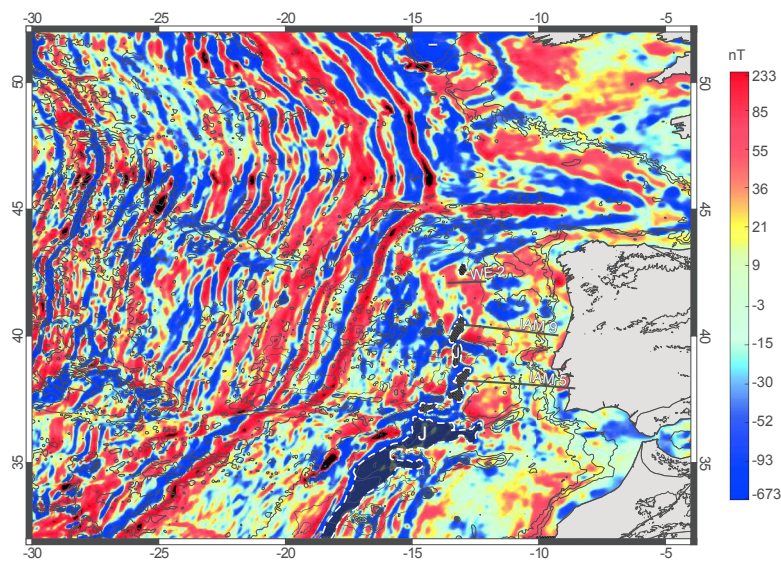


Fig. II-7: Magnetic anomaly map reduced to the pole, with the drawing of the positive part of J on raw magnetic map Emag 2v3 (see Fig. II-1) with the seismic lines presented on Fig. II-3

| Name                               | Age   | Appro | Sample                          | Method                | Long   | Lat   | Source                             |
|------------------------------------|-------|-------|---------------------------------|-----------------------|--------|-------|------------------------------------|
| <b>Gorringe</b>                    | 145   | 1     | Gabbro                          | 40AR/39AR Hornblende  | -11.26 | 36.68 | Feraud et al., 1986                |
| <b>Gorringe</b>                    | 143   | 1     | Gabbro                          | 40AR/39AR Hornblende  | -11.26 | 36.68 | Feraud et al., 1986                |
| <b>Gorringe<br/>GOR-07-05</b>      | 137.5 | 0.8   | Gabbro                          | Zircon                | -11.19 | 36.74 | Schärer et al., 2000               |
| <b>Gorringe<br/>GOR-07-02</b>      | 137.5 | 0.5   | Leucogabbro                     | Zircon                | -11.19 | 36.74 | Schärer et al., 2000               |
| <b>Brant P-87</b>                  | 135   | 6     | Basalts sills                   | K/Ar                  | -55.39 | 43.89 | Jansa, Pe pipper 1986              |
| <b>leg 210 site<br/>1277</b>       | 128   | 3     | Alkaline gabbro                 | 40AR/39AR Phlogopite  | -44.39 | 45.19 | Jagoutz et al., 2007               |
| <b>leg 173 site<br/>1070</b>       | 127   | 4     | Gabbro                          | Zircon                | -12.72 | 40.80 | Beardet al., 2002                  |
| <b>leg 173 site<br/>1070</b>       | 124.2 | 0.7   | Gabbro                          | 40AR/39AR Hornblende  | -12.73 | 40.80 | Jagoutz et al., 2007               |
| <b>leg 173 site<br/>1070</b>       | 123.9 | 1.2   | E-MORB<br>gabbroic<br>pegmatite | 40AR/39AR Hornblende  | -12.73 | 40.80 | Jagoutz et al., 2007               |
| <b>Gal-86-10-09</b>                | 122   | 0.6   | diorite                         | 40AR/39AR Amphiboles  | -12.63 | 42.95 | Schäer et al., 1995                |
| <b>leg 210 site<br/>1277</b>       | 113.2 | 2.1   | Gabbro                          | Zircon                | -44.38 | 45.20 | Jagoutz et al., 2007               |
| <b>leg 173 site<br/>1070</b>       | 111   | 0.3   | Gabbro                          | 40AR/39AR Plagioclase | -12.73 | 40.81 | Jagoutz et al., 2007               |
| <b>DSDP 384</b>                    | 106   | 4     | Basalt                          | K/Ar                  | -51.67 | 40.36 | Houghton et al., 1979              |
| <b>Leg 210 site<br/>1276</b>       | 105.9 | 1.8   | Alkaline<br>diabase             | 40AR/39AR Whole rock  | -44.78 | 45.41 | Hart and Blusztajn 2006            |
| <b>Sponge Bob</b>                  | 102.8 | 0.7   |                                 |                       | -12.97 | 38.43 | Merle et al., 2009                 |
| <b>Newfoundlan<br/>d seamounts</b> | 97.7  | 1.5   | Trachyte                        | 40AR/39AR Plagioclase | -45.58 | 43.75 | Sullivan and Keen 1977             |
| <b>Ashton</b>                      | 97.4  | 1.2   |                                 |                       | -13.40 | 37.97 | Merle et al., 2009                 |
| <b>leg 210 site<br/>1276</b>       | 95.9  | 2     | Alkaline<br>diabase             | 40AR/39AR Whole rock  | -44.79 | 45.40 | Jagoutz et al., 2007               |
| <b>Gago<br/>Couthino</b>           | 95    |       | Alkaline rocks                  | U/Pb                  | -13.94 | 37.50 | Merle et al., 2009 and ref inthere |
| <b>Bikini Bottom</b>               | 90    |       | Alkaline rocks                  | 40AR/39AR mineral     | -14.45 | 40.09 | Merle et al., 2009 and ref inthere |
| <b>Tore N</b>                      | 88.3  | 3.8   | Alkaline rocks                  | U/Pb                  | -12.54 | 39.74 | Merle et al., 2009 and ref inthere |
| <b>Jo Sister</b>                   | 86-89 | 3.7   | Alkaline rocks                  | U/Pb                  | -14.54 | 36.29 | Merle et al., 2009 and ref inthere |
| <b>Tore NW</b>                     | 80.5  | 0.9   | Alkaline rocks                  | U/Pb                  | -13.68 | 39.68 | Merle et al., 2009 and ref inthere |
| <b>Lion</b>                        | 80    |       | Alkaline rocks                  | U/Pb                  | -15.59 | 35.29 | Merle et al., 2009 and ref inthere |
| <b>Godzilla</b>                    | 67.7  | 0.2   | Alkaline rocks                  | 40AR/39AR mineral     | -15.59 | 34.46 | Merle et al., 2009 and ref inthere |
| <b>Ormonde</b>                     | 68-58 |       | Alkaline rocks                  | 40AR/39AR Plagioclase | -11.56 | 36.53 | Feraud et al., 1986                |
| <b>Torillon</b>                    | 60    |       | Alkaline rocks                  | 40AR/39AR mineral     | -14.96 | 38.97 | Merle et al., 2009 and ref inthere |
| <b>Ampere</b>                      | 31.7  | 0.2   | Alkaline rocks                  | 40AR/39AR Whole rock  | -12.96 | 35.07 | Merle et al., 2009 and ref inthere |
| <b>Unicorn</b>                     | 27.8  | 2.4   | Alkaline rocks                  | 40AR/39AR Whole rock  | -14.51 | 34.72 | Merle et al., 2009 and ref inthere |
| <b>Seine</b>                       | 24.4  | 0.4   | Alkaline rocks                  | 40AR/39AR mineral     | -14.35 | 33.78 | Merle et al., 2009 and ref inthere |
| <b>Josephine</b>                   | 16    | 8     | Alkaline rocks                  | 40AR/39AR Whole rock  | -14.29 | 36.82 | Merle et al., 2009 and ref inthere |
| <b>Josephine N</b>                 | 7.5   | 0.5   | Alkaline rocks                  | 40AR/39AR Whole rock  | -13.90 | 36.99 | Merle et al., 2009 and ref inthere |
| <b>Dragon</b>                      | 1     | 4     | Alkaline rocks                  | 40AR/39AR Whole rock  | -16.47 | 34.86 | Merle et al., 2009 and ref inthere |

Table II-2: Recorded magmatic activity in the southern North Atlantic



---

## *CHAPITRE III*

---

Le troisième chapitre vise à relier la déformation des systèmes de rift hyper-étirés et l'évolution cinématique des plaques. Ainsi la plupart des reconstructions cinématiques propose une reconstruction complète et une reconstruction à la première anomalie océanique cependant la distance entre ces deux positions peut être de plusieurs centaines de kilomètres et représenter une extension de plusieurs dizaines de millions d'années. De plus ce travail permet d'amorcer une réflexion sur le mode de propagation et le partitionnement de la déformation des systèmes de rift hyper-étirés. Cette étude se base sur les marges et bassins hyper-étirés du sud de l'Atlantique Nord qui ont été investigués à de nombreuses reprises par des méthodes pluridisciplinaires. Ce chapitre s'organise de la manière suivante :

- Présentation du contexte cinématique générale et des problèmes majeurs
- Définition de la terminologie et présentation de la méthode de reconstruction
- Détermination des données utilisées en entrée du modèle cinématique, réalisé avec le logiciel Gplates (Boyden et al., 2011)
- Résultat de la modélisation étape par étape
- Discussion du modèle cinématique axée sur trois thématiques : les limites de la méthode utilisée, les implications géodynamiques pour le sud de l'Atlantique Nord et le mode de propagation d'un système hyper-étiré.

Ce chapitre fait l'objet d'un article scientifique intitulé « Kinematics of the southern North Atlantic: implications for the formation of hyper-extended rift systems » en préparation pour la revue *Tectonics*.

# ***KINEMATICS OF THE SOUTHERN NORTH ATLANTIC: IMPLICATIONS FOR THE FORMATION OF HYPER-EXTENDED RIFT SYSTEMS***

M. Nirrengarten<sup>1</sup>, G. Manatschal<sup>1</sup>, J. Tugend<sup>1</sup>, N.J. Kusznir<sup>2</sup>

*1 Institut de Physique du Globe de Strasbourg, UMR 7516, Université de Strasbourg/EOST, CNRS; 1 rue Blessig, F-67084 Strasbourg Cedex*

*2 Department of Earth and Ocean Sciences, University of Liverpool; Liverpool, UK*

## **ABSTRACT**

Modes of deformation of hyper-extended rift systems are generally investigated by 2D studies. In this contribution we propose to link the rift deformation with plate kinematic modelling to highlight the partitioning and the propagation of deformation in a hyper-extended rift system using the examples of the southern North Atlantic rifted margins. The kinematic evolution of this area is well determined after the Cretaceous normal polarity superchron (~120-83 Ma) by well-defined oceanic magnetic anomalies. However the rift and early seafloor spreading evolution are highly disputed due to the conflicting interpretation of the J magnetic anomaly as the chron M0 and the existence of hyper-extension in the Pyrenean domain. Recent studies highlight that the J-anomaly is polygenic, polyphased and unlikely corresponds to an isochron. Therefore we propose a new palinspastic restoration based on 3D gravity inversion, which does not take into account the J-magnetic anomaly but which integrates the rift deformation using structural, stratigraphic and geochronological data. Although we present here a new restoration for the southern North Atlantic, the restoration by itself is not the aim of the study, but a tool to understand the 3D evolution of a hyper-extended rift system. Based on the results of the restoration, we discuss local and regional aspects of the formation of a hyper-extended magma-poor rift system. The addition of continental micro-blocks in the plate reconstructions allows the inclusion of observed post Aptian extension in the Pyrenees suggests that the Aptian “breakup unconformity” in the southern North Atlantic is potentially related to the initiation of a triple ridge junction. Deformation of the continental crust is shown to be partitioned in different segments which are linked by transfer zones. This partitioning of the rift deformation results from the competition between lithospheric inheritance, tectonic stresses and initial plate organisation. The localisation of these transfer faults can be correlated to inherited structures or

sutures from the previous orogenic phase. In contrast, V-shape propagators are limited to newly created top basements (exhumed mantle and oceanic crust) and are accompanied by secondary oblique rift systems to compensate the compression at the tip of the propagator due to rotation of the two rigid plates.

## **1. INTRODUCTION**

Since Wegener (1915) and the initiation of plate tectonics, many models have been proposed to restore the Atlantic Ocean by analysing relative motions between Africa, America and Eurasia (Bullard et al., 1965; Klitgord and Schouten, 1986; Le Pichon et al., 1977; Pitman and Talwani, 1972; Rowley and Lottes, 1988). This task greatly improved by the understanding of the emplacement process of oceanic magnetic anomalies (Heirtzler et al., 1968) and by the identification of oceanic fracture zones, representing important kinematic indicators (Müller and Roest, 1992). These tools enabled the creation of accurate global plate kinematic models (Müller et al., 2016; Seton et al., 2012). At present, all current models for the Central and southern North–Atlantic agree respectively on the post Jurassic Quiet Zone (JQZ) (older than ~154 Ma) and on the post Cretaceous Normal Polarity Superchron (CNPS) (~120-83 Ma) tectonic evolution. However, rift domains formed prior to seafloor spreading or during long magnetic quiet zones cannot be restored using classical methods of plate reconstruction and their restorations are in most cases uncertain and still debated.

Hyper-extended rifted margins can accommodate significant extension prior to lithospheric breakup but their kinematic evolution is little constrained. Hyper-extended rifted margins and aborted rift basins represent structural domains that can accommodate large extensional deformation and characterized by thin continental crust (often <10km) (Sutra et al., 2013) and in some examples also by exhumed mantle domains and variable volumes of magmatic additions. The understanding of hyper-extended rift systems improved thanks to numerous studies based on seismic interpretations (e.g. Autin et al., 2010; Franke et al., 2014; Péron-Pinvidic et al., 2007; Ranero and Pérez-Gussinyé, 2010; Reston and McDermott, 2011), field observations (e.g. Jammes et al., 2009; Manatschal, 2004; Mohn et al., 2012), numerical and analogue modelling (e.g. Brun and Beslier, 1996; Brune et al., 2014; Huisman and Beaumont, 2014; Lavier and Manatschal, 2006). Nevertheless, the integration of the 3D rift evolution in plate modeling remains complex and yet unresolved. Some studies proposed palinspastic restorations (e.g. Heine et al., 2013; Hosseinpour et al., 2013; Williams et al., 2011), however they only use two rotation poles, one at full-fit and the second at the first magnetic anomaly or an intermediate one for rift phase interrupted by tectonic quiescence (Barnett-Moore et al., 2016b). This approach limits the visualization and comprehension of propagating rift systems

and on the partitioning of deformation.

In order to develop a plate restoration methodology, we have targeted the hyper-extended rift systems of southern North Atlantic (Fig.III-1; north of the Newfoundland Azores Gibraltar fracture zone NAGFZ and south of the Charlie Gibbs fracture zone). This region includes the Iberia-Newfoundland rift system, the only place where scientific deep water drilling penetrated hyper-extended continental crust and exhumed mantle (Boillot et al., 1987; Sawyer, 1994; Tucholke and Sibuet, 2006; Whitmarsh and Wallace, 2001). Numerous seismic reflection and refraction data from these domains are also available (e.g. Afilhado et al., 2008; Dean et al., 2000). It can be considered as one of the best documented hyper-extended rift system. The case study also includes the Pyrenean domain, which records a well-studied Albian to Cenomanian hyper-extension phase (Clerc and Lagabrielle, 2014; Masini et al., 2014; Tugend et al., 2014; Vacherat et al., 2016), the Bay of Biscay, which is created by seafloor spreading from Albian to Santonian (Montadert et al., 1979; Thinon et al., 2003) as well as the hyper-extended rift basins on the Newfoundland and Irish margins (Welford et al., 2012). The first order kinematics of the southern North Atlantic is related to the eastward motion of the Iberia/Eurasian plates relative to the North-America plate from Trias to present. However, the Iberia plate motion, before and during the Cretaceous normal polarity superchron, has been often questioned (Barnett-Moore et al., 2016a; Le Pichon and Sibuet, 1971; Olivet, 1996; Rosenbaum et al., 2002; Sibuet, 2004; Vissers and Meijer, 2012a). These controversies are mostly related to different interpretations and restorations of the J-magnetic anomaly offshore the Iberia and Newfoundland margins that are incompatible with geological observations (Bronner et al., 2011; Tucholke and Sibuet, 2012). The compilation of seismic and geochronological data (Nirrengarten et al., 2016) showed that the J-anomaly does not correspond to an oceanic anomaly and therefore cannot be used as such for kinematic restorations.

These uncertainties motivated the development of a new methodology to propose an alternative restoration of hyper-extended rifted margins and early seafloor spreading stages in the southern North Atlantic. The novelty of our approach is to perform a palinspastic restoration of the southern North Atlantic that integrates the deformation of each hyper-extended rift system by introducing continental micro-blocks (continental ribbons; e.g. Lister et al., 1986; Peron-Pinvidic and Manatschal, 2010), the direction of the transfer zones and key geological time constraints. A major input of this work is provided by an accurate mapping of the rift system based on reflection and refraction seismic interpretations and gravity inversion coupled with key stratigraphic and geochronological data (Alves et al., 2009; Jagoutz et al., 2007). Areal balancing of gravity-inversion crustal cross-sections was performed to determine the pre-deformation shape of continental polygons that are used for plate modelling. Well constrained areas are



considered as inputs of the model, whereas the implications on less well known domain are outputs. However, although we propose a new plate restoration of the southern North Atlantic, it is important to note that the model itself is not the goal of this study but a tool to describe and discuss the partitioning of the deformation in hyper-extended rift systems. The model presented in this paper is one solution that can fit the sparse available datasets but the existence of other solutions that do not violent existing geological knowledge cannot be excluded. Results from our model suggest that the rift evolution is complex and includes propagators, transfer zones, localization, migration and stepping of rift systems producing a strongly segmented array of basins and continental ribbons prior to lithospheric breakup.

## **2. THE NORTH ATLANTIC OCEAN: GEOGRAPHY, INHERITANCE AND KINEMATIC FRAMEWORK**

The Atlantic Ocean is surrounded by passive continental margins and is only locally invaded by subduction zones (Duarte et al., 2013), providing an uninterrupted record from continental rifting to current oceanic accretion. The Atlantic Ocean is composed of several segments separated by transform faults. Our study is limited segment of the North Atlantic that is called the southern North Atlantic between the NAGFZ to the south and the Charlie-Gibbs fracture zone to the north (Fig. III-1). However to integrate this study in the global kinematic network, we also need to have a look at the neighbouring segments, the Central Atlantic south of the NAGFZ and the North Atlantic north of the Charlie Gibbs fracture zones.

The Atlantic resulted from the breakup of the super continent Pangea (Frizon de Lamotte et al., 2015), which was created by the progressive amalgamation of mainly continental blocks during the Carboniferous (Stampfli et al., 2013). Some but not all of the sutures of this super-continent were reactivated in extension during Mesozoic time to form the Atlantic Ocean (Buitter and Torsvik, 2014; Chenin et al., 2015; Wilson, 1966).

The Central Atlantic opening initiated in Trias and Early Jurassic by the divergence of North America and Africa. There are questions related to the early stages of extension, principally concerning the identification of magnetic anomalies and the initiation of rifting (Kneller et al., 2012; Labails et al., 2010; Schettino and Turco, 2009), however the kinematics of the Central Atlantic is relatively well defined by oceanic magnetic anomalies and fracture zones after the Jurassic Quiet Zone JQZ (>154 Ma). The left lateral movement of northwest Africa relative to Eurasia was at the origin of rifting and formation of the Alpine Tethys domain east of Iberia, and the formation of several hyper-extended/exhumed/oceanic domains east west of Adria (Meliata-Vardar, Piemonte-Liguria-Valais) (Handy et al., 2010; Schettino and Turco, 2011). The Central Atlantic and the Alpine Tethys are connected by the Gibraltar transform

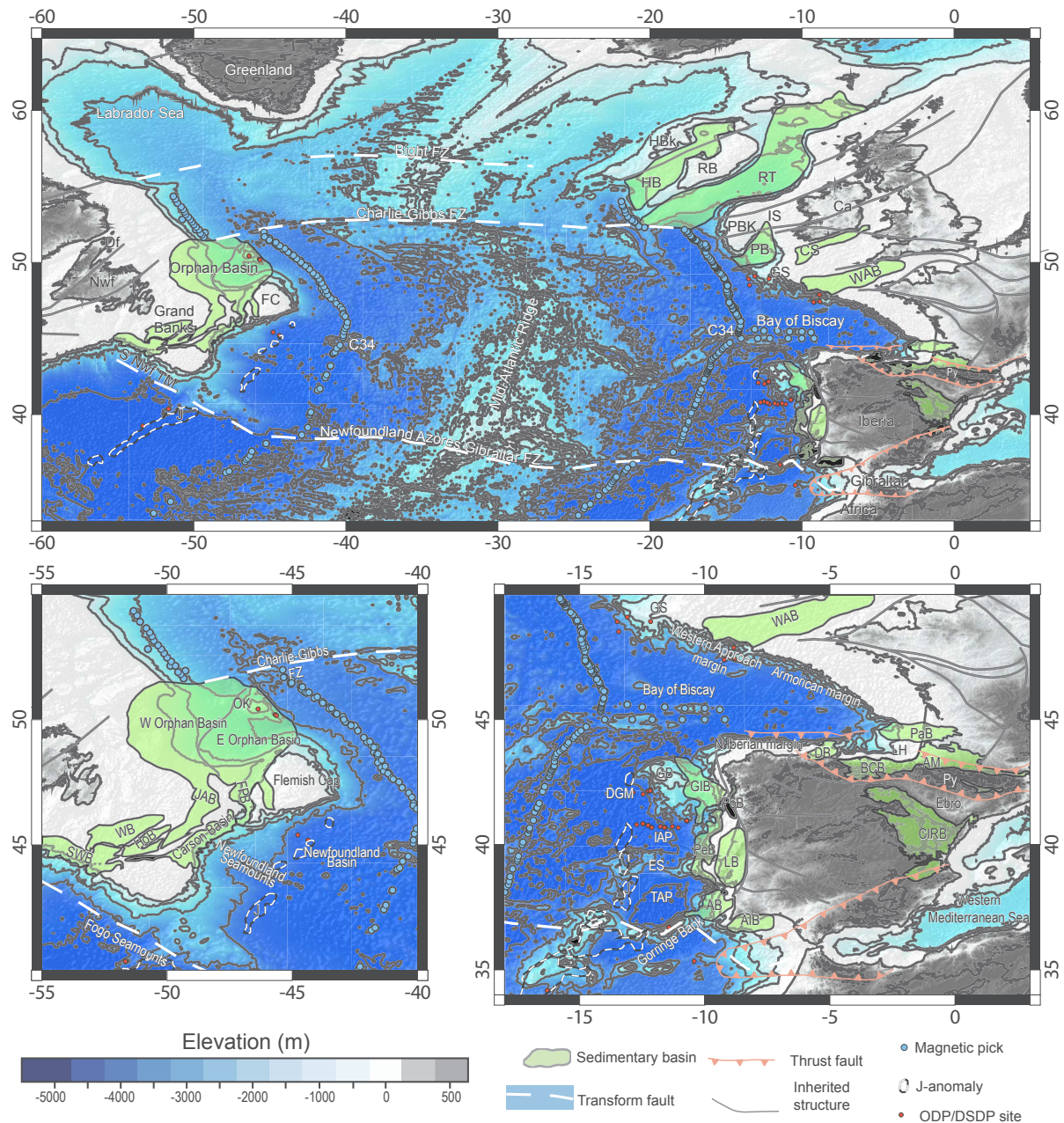


**Fig. III-1:** Bathymetric maps of the southern North Atlantic and zoom on the Newfoundland margins and west-European margins. AB, Alentejo Basin; AlB, Algarve Basin; AM, Arzacq Mauléon Basins; BCB Basque Cantabrian Basin; CIRB, Central Iberian rift basins; Ca, Caledonian suture; CS, Celtic Sea; DB, Le Danois Basin; Df, Dover fault; DGM, Deep Galicia Margin; ES, Estremadura Spur; FC, Flemish Cap; FPB, Flemish Pass Basin; GB, Galicia Bank; GS, Goban Spur; HB, Hatton Basin; HBk, Hatton Bank; HoB, Horseshoe Basin; IAP, Iberia Abyssal Plain; IS, Irish shelf; JAB, Jeanne d'Arc Basin; LB, Lusitanian Basin; LH, Landes High; Nwf, Newfoundland; OK, Orphan Knoll; PaB, Parentis Basin; PB, Porcupine Basin; PBK, Porcupine Bank; PeB, Peniche Basin; PoB, Porto Basin; Py, Pyrenees; RB, Rockall Bank; RT, Rockall Trough; S Nwf TM, South Newfoundland Transform Margin; SWB, South Whale Basin; TAP, Tagus Abyssal Plain; WAB, Western Approach Basin; WB, Whale Basin;

zone, which probably experienced oblique rifting and highly segmented seafloor spreading during Late Jurassic (Frizon de Lamotte et al., 2011; Sallarès et al., 2011). However, the tectonic evolution east and south of the Iberia plate is not quantitatively constrained because of the Late Cretaceous and Cenozoic Alpine reactivation and subduction of parts of the system.

North of the Charlie Gibbs fracture zone, the opening of the North Atlantic resulted in a magma-rich breakup between Greenland and Eurasia at about 55 Ma (Eldholm et al., 1989). However, the rift history of this region is older and starts at Permo-Trias time with a renewed event during Late Jurassic–Early Cretaceous forming a highly thinned crust, thick sedimentary basins and a crustal extension of 50-70 km (Skogseid et al., 2000). The motion of Greenland is determined after chron C27n (~62 Ma) by the marine magnetic anomalies of the Labrador Sea and Baffin Bay (Oakey and Chalmers, 2012) and the Eurasia motion is well constrained after chron C33n present in the southern North Atlantic and north east of Eurasia (Gaina et al., 2002).

The study focuses on the tectonic and kinematic evolution of the southern North Atlantic segment between the end of the Trias (200 Ma) and magnetic chron C34 (83 Ma). This period corresponds to the full-fit of Iberia, North-America and Eurasia and to the first oceanic isochron magnetic anomaly present from the NAGFZ to the Charlie Gibbs fracture zones. We hence model the plate motion during rifting and early stages of seafloor spreading.

### **3. HYPER-EXTENDED RIFTED MARGINS: A KINEMATIC DESCRIPTION**

#### **3.1 Rift domains and domain boundaries**

Despite some variations on the crustal, sedimentary and magmatic evolution, Atlantic magma-poor rifted margins share comparable first order architectures (Peron-Pinvidic et al., 2013; Reston, 2009). This architecture is characterized from continent to ocean by a proximal domain, a thinned domain, an exhumed domain and an oceanic domain (e.g. Sutra et al., 2013; Tugend et al., 2015b) (Fig. III-2). The thinned domain includes the necking domain and the hyper-extended continental crust. In kinematic studies the boundaries of each domain are of particular importance as they can be spatio-temporal markers. In this study, we defined and mapped the necking line (NL), the oceanward edge of the continental crust (ECC) and the continentward limit of first oceanic crust, referred as the Continent Ocean Boundary (COB).

The mapping methodology (Sutra et al., 2013; Tugend et al., 2015b) is designed to determine variation of basement architecture and nature in 2D sections, which can be extrapolated laterally using potential field methods (Stanton et al., 2016; Tugend et al., 2014). Hence we use seismic reflection and refraction (Dean et al., 2000; Funck et al., 2003; Gerlings et al., 2012; Hopper et al., 2004; Shillington et al., 2006; Watremez et al., 2015), borehole data (Tucholke

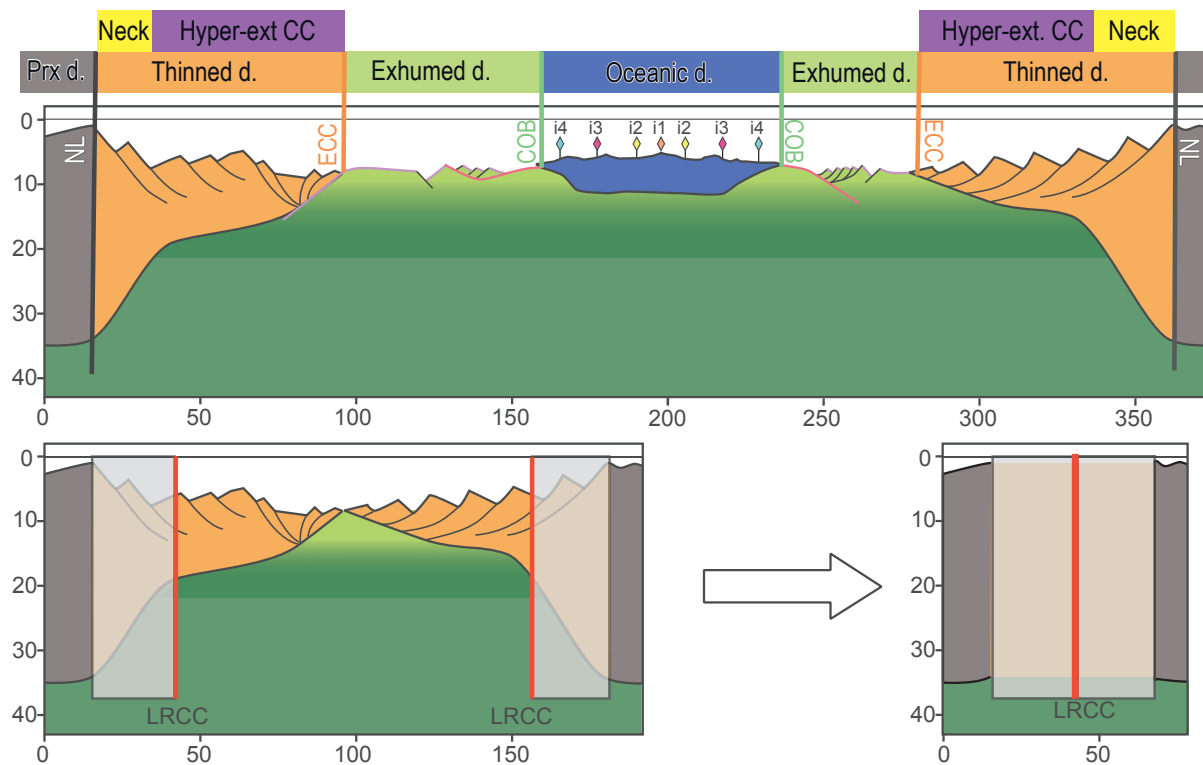


**Fig. III-2:** Schematic restoration of conjugate margins with the associated rift domains. COB, continent-ocean boundary; ECC, edge of the continental crust; NL, necking line; I, isochrons.

and Sibuet, 2006), gravity (Sandwell and Smith, 2009) and magnetic maps (Maus et al., 2007), published rift domain maps (Peron-Pinvidic et al., 2013; Tugend et al., 2014; Welford et al., 2010a, 2010b) as well as new crustal thickness maps. The crustal thickness maps shown in Fig. III-3 were determined by 3D spectral-domain gravity inversion; the detailed methodology is described in Chappell and Kusznir, (2008) and include a correction for the lithosphere thermal gravity anomaly and a parameterization of decompression melting to predict magmatic addition. The input data of the gravity inversion are public domain data (e.g. free-air gravity anomaly; Sandwell and Smith, 2009, bathymetry; Smith and Sandwell, 1997, sediment thickness map; NOAA Divins, 2003, and oceanic isochrons; Müller et al., 2008).

The thermal re-equilibration (cooling) time of oceanic lithosphere is given by ocean isochron ages; the cooling time of continental margin lithosphere is given by the margin breakup age. Gravity inversion results (Moho depth, crustal basement thickness and continental lithosphere thinning) are used to calibrate four parameters used in the gravity inversion. These parameters are: 1) the reference Moho depth, which is related to the long wavelength component of the Earth's gravity field arising from deep mantle structure and processes (and current dynamic topography); 2) the magnitude of magmatic addition from decompression melting corresponding to the thickness of the first oceanic crust; 3) the critical lithosphere thinning factor at which decompression melting commences; and 4) the continental breakup age which

gives the thermal equilibration time of continental margin lithosphere (Chappell and Kusznir, 2008). Four different different gravity inversions were carried out (Fig. III-3) because of the different parameter values for the Iberia margin, Newfoundland margin, Eurasian margin and Greenland-Hatton). Parameters values are given in the supplementary material.

The characteristic of the proximal domains (brownish in Fig. III-2) is that there is thinning of the continental crust/lithosphere outside the fault bounded half-graben basins. The necking line (NL Fig. III-2) corresponds to the continentward boundary of the thinned continental crust (Orange in Fig. III-2). This line marks the transition from a weakly -to a substantially thinned continental crust, where Moho switches from horizontal to steeply shallowing and top basement dips oceanwards (Fig. III-2). The oceanward edge of the continental crust (ECC Fig. III-2) marks a change in material composition from continental crust to oceanic crust or exhumed mantle (in green Fig. III-2). This boundary is best estimated by the location where a strong reflector (S-reflection; Reston et al., 2007) intersects with top basement (for details see Sutra et al. 2013). In magma-poor margins, the seismic facies often change from reflective (thinned continental crust) to transparent (serpentinized mantle) across the ECC. The COB marks the limit to first oceanic crust, which typically coincides with the continentward termination of indisputable oceanic crust, characterized by parallel top-basement and Moho reflections. Moreover, top basement is typically found around 8 sec (TWT) and characterized by a sedimentary passive infill. The COB is often marked by a ramp of top basement from 9 to 10 seconds (top of exhumed mantle with a low magmatic budget) compared with the typically 8s of thermally equilibrated normal Penrose oceanic crust (for more details and definitions of rift domains see Tugend et al., 2015b).

The resulting domain map (Fig. III-4) displays some aspects that are important for the study of the evolution of rifting along the whole system, which are: 1) the width of the thinned domain (measured in the extension direction) is highly variable and ranges from ~50 km to more than 300 km, 2) on the same margin the limits between the domains are not parallel and 3) the distance between the first oceanic magnetic anomaly (C34) and the COB decreases northward.

### **3.2 Restoration methodology**

First, without any time constraints the restoration of an ideal 2 D cross section (Fig. III-2) can be done by removing the oceanic and exhumed mantle domains as both domains comprise new materials defining new surfaces (new real estate). The remaining cross section hence is formed by the two thinned conjugate continental margins. The extension of this deformed continental crust has to be taken into account for palinspastic restorations (e.g. Aslanian and Moulin, 2012; Heine et al., 2013; Williams et al., 2011). As magma-poor margins do not have

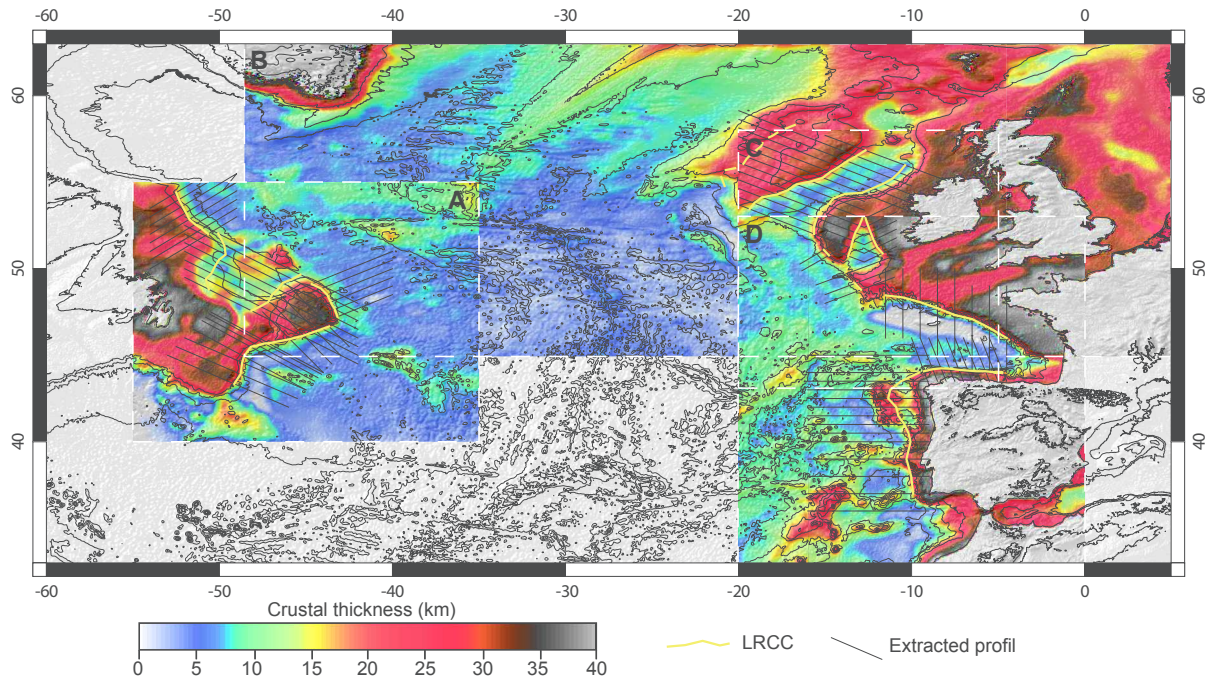


**Fig. III-3:** Crustal thickness maps resulting from gravity inversion. Parameters used for the gravity inversion are in supplementary material.

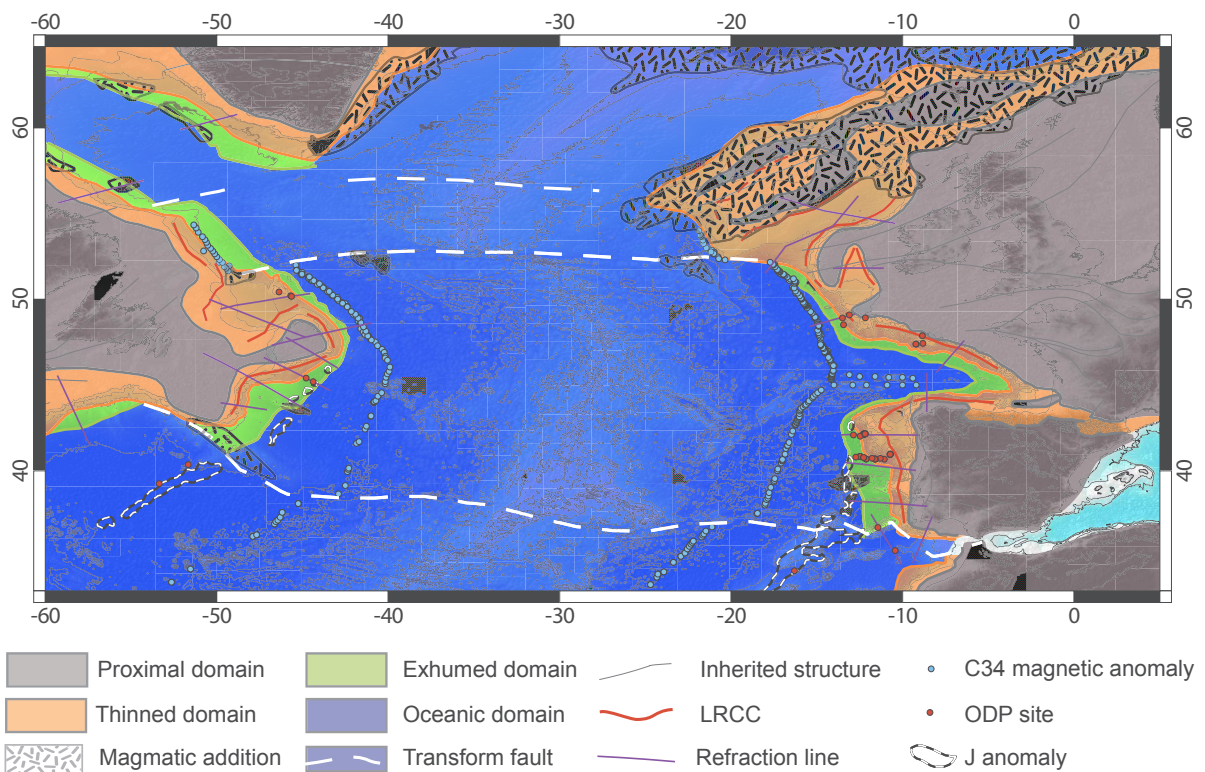


**Fig. III-4:** Map of the rift domains of the southern North Atlantic based on seismic interpretation, crustal thickness Fig III-3 and local mapping by Peron Pinvidic et al. (2013), Tugend et al. (2014) and Welford et al. (2010a,b). Magmatic additions after Chenin et al. (2015), inherited structures are from the compilation of Pollock et al. (2012) and from Ballèvre et al. (2014), magnetic pick are from the repository for magnetic anomaly (Seton et al., 2014).

a large amounts of magmatic additions, we can assume quite confidently that the volume of thinned continental crust is equal to the initial crustal volume (no gain or loss of continental crust). We assume that the material does not laterally flow along strike and that the restored section is a dip line parallel to extension (Fig. III-3). The volume of thinned continental crust, between the mapped necking line (NL) and the edge of the continental crust (ECC) is extracted from the crustal thickness maps determined by gravity inversion. This volume is then divided by the initial crustal thickness to determine the limit of reconstructed continental crust (LRCC) (RCOB from Williams et al., 2011). The initial crustal thickness may differ depending on the pre-rift inheritance of each continental block. In this study we choose 37.5 km as the initial crustal thickness for all the system, which corresponds to the maximum crustal thickness modelled by refraction data (Lau et al., 2006). This method is, however, not valid for magma rich margins (e.g Hatton Bank margin) since these margins present consequent magmatic additions, which lead to the formation of new crust (with a gain in crustal volume). In magma rich margins restorations can only be done if the volume of the magmatic additions can be estimated to determine a pseudo LRCC (Barnett-Moore et al., 2016b).

Time constraints are important for plate modelling. The most classical and accurate time constraints are given by oceanic magnetic anomalies. They record reversals of the geomagnetic field and their ages can be constrained by magnetic modelling. Hence each isochron can be compared to its conjugate on the other side of the oceanic ridge. Magnetic anomalies also exist on exhumed mantle domains (Russell and Whitmarsh, 2003; Sibuet et al., 2007a). However, since the emplacement process of exhumed mantle surfaces is not necessarily symmetric, these anomalies record reversals that do not necessarily have a conjugate anomaly nor a precise age (Gillard et al., 2015). The COB can be dated by the first sedimentary sequence (reflector) downlapping onto first oceanic crust. This method does not work for exhumed mantle. In thinned domains, deformation has been shown to migrate oceanward through time (Masini et al., 2013; Péron-Pinvidic and Manatschal, 2009), hence the first post-tectonic sediments on thinned domains correspond to the initiation of mantle exhumation. This stratigraphical process is also observed continentwards, the end of syn-tectonic deposition in the proximal basins corresponds to the localization of the deformation between the two necking lines. Therefore, in theory, each mode of deformation can be dated and restored on a 2D section. However these sedimentary markers are ill defined and need to be dated accurately in order to calibrate the age of each domain deformation and domain boundary. Along present-day deep water rifted margins, this has only been done so far along the Iberia margin (Sutra et al., 2013).

To determine the LRCC on a map and to perform a full fit restoration, profiles spaced at 1° to 0.5° intervals were extracted from the crustal thickness grid along all rifted margins

and basins (Fig. III-3). Williams et al. (2011) showed that the orientation of the profiles does not change much the position of the LRCC hence we choose to extract them perpendicularly to the necking and parallel to transfer faults in the continent, which correspond to the supposed main extension direction (flowlines). The LRCC is used to determine the shape of each polygon defined in the plate modelling software Gplates (Boyden et al., 2011). It is important to note that the LRCC defines the smallest possible polygon because the initial crustal thickness is 37.5 km, which is the maximum thickness of this area, hence the aim is to reduce the overlap even if it creates gaps elsewhere. The polygons (Fig. III-5) can be subdivided into: 1) major tectonic plates, which are still at present tectonic plates defined by active plate boundaries, 2) secondary tectonic plates, which are large continental units separated from the major plates by transient plate boundaries, and 3) micro-blocks, which are smaller and not separated from the major tectonic plates by active, well determined plate boundaries (continental ribbons following the definition of Peron-Pinvidic and Manatschal, 2010). We define 3 kinds of plate boundaries: convergent (subduction zones), divergent (mid oceanic ridges) and strike-slip (active transform zones connecting two major plate boundaries).

The directions of extension, which correspond to the flow-lines, constrain the plate motions. In oceanic domains, large fracture zones are oriented parallel to the extension and can be considered as flow-lines (Müller and Roest, 1992). Transfer zones in the exhumed domain and thinned continental crust could approximate flow-lines. However transfer faults affecting only the continental crust can often be related to inherited structures and the deformation can be oriented obliquely to the main extension (Bellahsen et al., 2013), which makes them inappropriate for plate restoration. Indeed transfer faults are only good markers of the direction of extension if they penetrate newly created surfaces such as exhumed mantle domains. But the full rift motion cannot be determined with transfer zones only. The full-fit position is determined by the LRCC fit on the conjugate side of the Atlantic and laterally helped by the presence of pin points such as inherited sutures (e.g. Caledonian; Variscan domain boundaries) which separate crustal units of different origins. However, such pin points are based on onshore mapping which require substantial further extrapolation offshore.

### **3.3 Kinematic significance of domain boundaries, kinematic markers and model inputs**

Mapped and restored boundaries have not the same meaning in space and time, the identification of their significance is crucial for plate reconstruction. It is impossible to superpose two conjugates NL because the deformed continental crust in between has to be integrated and therefore the LRCC has been introduced (Williams et al., 2011). However there is no general



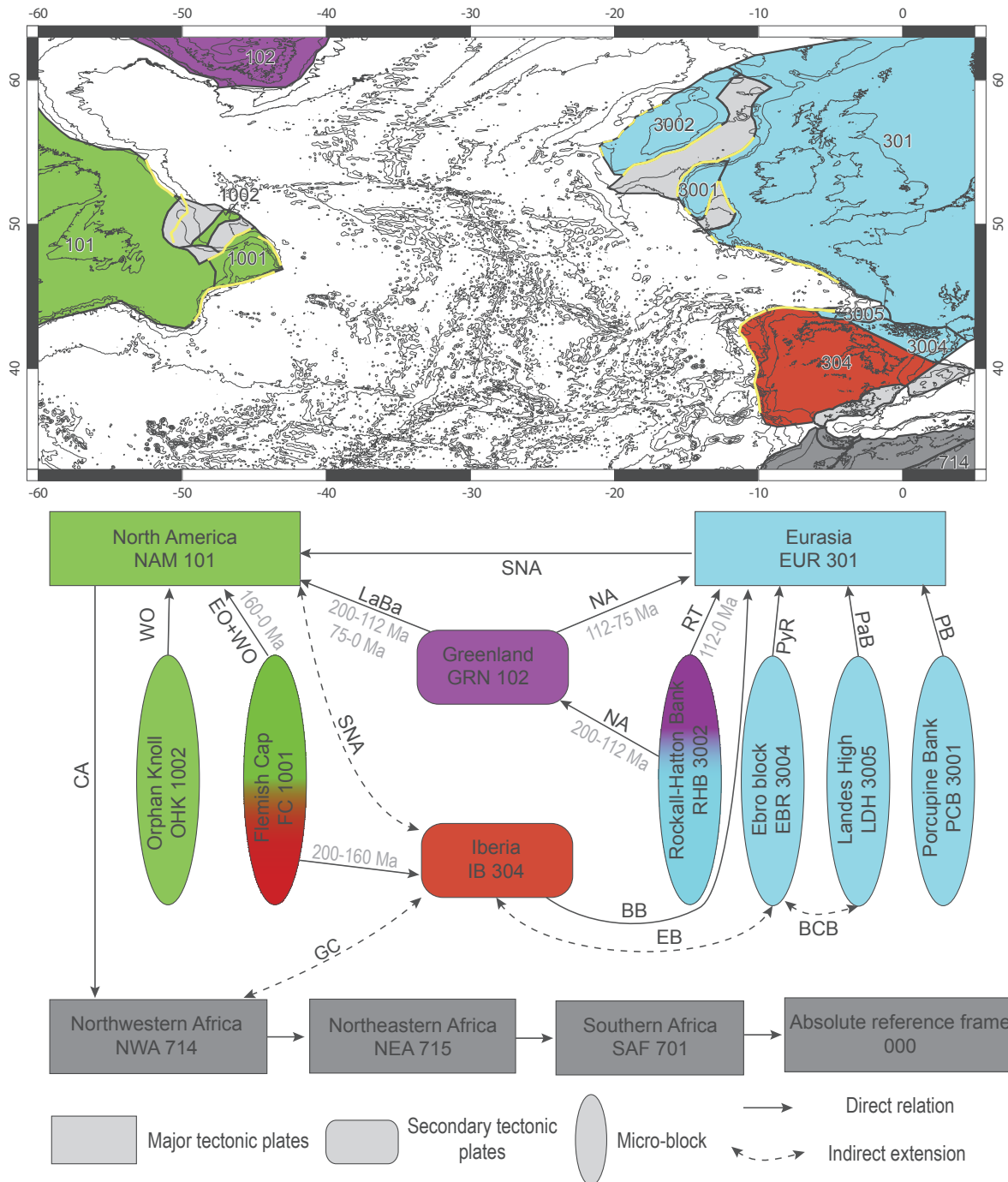


**Fig. III-5:** Polygons and plate circuit used in the modeling associated with their geographical positions. Abbreviations and the associated number are used in the Gplates rotation file provided in electronic supplementary material.

observation to determine whether the necking starts simultaneously along the entire margin, along one segment or if it propagates. The ECC and the COB are not necessarily synchronous along the entire margin and may be the result of a propagation, especially if marine magnetic anomalies are not parallel to this boundary (e.g. South China Sea, Gulf of Aden Barckhausen et al., 2014; Fournier et al., 2010). Hence the COB and ECC independently of the quality of the mapping, cannot be used as a marker for plate kinematics because COB on both sides of the oceanic domain can never be superposed (Eagles et al., 2015). Transfer faults cutting the thinned domain and exhumed domain provide the direction of motion during a stage of deformation; however they do not provide time indications. The extensive knowledge on the evolution of part of the Iberia-Newfoundland and Bay of Biscay-Pyrenean rift systems are used as the primary input of the model. The visual fitting of polygons follows these data and observations. The major output is therefore the evolution of the surrounding rift systems.

#### **4. HYPER-EXTENDED RIFTED MARGINS AND BASINS**

The southern North Atlantic system comprises three tectonic plates, Africa, North-America and Eurasia, two secondary plates, Greenland and Iberia, and six micro-blocks (Fig. III-5). In the next section we review timing, motion and deformation mode of each rift system.

##### **4.1 Iberia-Newfoundland**

The Iberia–Newfoundland conjugate margins result from the divergence between Iberia and North-America. A first extension phase occurred from Triassic to Middle Jurassic forming several sedimentary rift basins located over the Newfoundland Grand Banks and the Iberian Peninsula (e.g. Lusitanian, Jeanne d'Arc, Porto, Horseshoe and Whale Basins, Fig. III-1) (Rasmussen et al., 1998; Tankard et al., 1989). These sedimentary basins are typically asymmetric half grabens, filled by Triassic evaporates and Jurassic carbonates (Murillas et al., 1990; Pereira and Alves, 2011). A 2D cross section through these conjugate margins illustrate well the structural domains of magma-poor rifted margins previously defined (Fig. III-2, Sutra et al., 2013). The characterization of those domains all along the margins is necessary to model the 3D evolution of the system. These margins are divided from south to north into 3 segments (Alves et al., 2009; Welford et al., 2010b), the southern Newfoundland Basin–Tagus Abyssal Plain segment, the Iberia Abyssal Plain–northern Newfoundland Basin segment and the Flemish Cap–Galicia Bank segment. The two northern segments have been drilled whereas the distal part of the southern segment have not been drilled and necking and breakup ages remain only approximated by stratigraphic studies (Alves et al., 2009). Tithonian and Berriasian sediments from the Iberia Abyssal Plain indicate deep marine environments whereas sediments

| Rift system/Basin                          | Events  | Input of the model |
|--|---|--------------------|
| <b>Central Atlantic</b>                    | Onset of rifting 240 <sup>1</sup> , 230 <sup>2,3</sup> , 203 <sup>4</sup> Ma                                  | yes                |
|  | Onset of seafloor spreading 200 <sup>3</sup> , *190 <sup>2,4</sup> Ma   | yes                |
|  | Undisputed magnetic anomaly CM25 154 <sup>5</sup> Ma  | yes                |
| <b>Tagus Abyssal Plain- S Newfoundland</b> | Triassic to Middle-Jurassic rifting 200-161 <sup>6</sup> Ma   | yes                |
|  | Gabro in host peridotite 143 <sup>7</sup> Ma onset of exhumation?   | yes                |
|  | Onset of seafloor spreading 150 <sup>8,9</sup> , 133 <sup>10</sup> , 112 <sup>11</sup> Ma                     | no                 |
|  | Undisputed magnetic anomaly C34 83 <sup>12</sup> Ma   | yes                |
| <b>Iberia Abyssal Plain- Newfoundland</b>  | Triassic to Middle -Jurassic rifting 200-161 <sup>6,13</sup> Ma   | yes                |
|  | Necking and continental def. 150-133 <sup>14</sup> Ma   | yes                |
|  | Onset of mantle exhumation 133 <sup>14,15</sup> Ma  | yes                |
|  | Onset of seafloor spreading 145 <sup>9</sup> , 132 <sup>2</sup> , 120 <sup>16,17</sup> , 112 <sup>11</sup> Ma | no                 |
| <b>Galicia-Flemish Cap</b>                 | Triassic to Late -Jurassic rifting 200-145 <sup>13</sup> Ma   | yes                |
|  | Necking and continental def. 150-133 <sup>14</sup> Ma   | yes                |
|  | Onset of mantle exhumation 122 <sup>18,7,14</sup> Ma  | yes                |
|  | Onset of seafloor spreading 121 <sup>19</sup> , 112 <sup>11,16</sup> Ma                                       | no                 |
| <b>Orphan Basin</b>                        | Extension in two main phase Jurassic and Early-Cretaceous 20,21   | no                 |
|  | No necking age available and no mantle exhumation   | no                 |
| <b>Bay of Biscay</b>                       | Onset of rifting 156 <sup>23</sup> , 145 <sup>24</sup> Ma   | no                 |
|  | Exhumation 125 <sup>24,25</sup> Ma  | no                 |
|  | Onset of seafloor spreading 124 <sup>23</sup> , 112 <sup>25,26</sup> Ma                                       | no                 |
|  | End of seafloor spreading 83 <sup>22</sup> Ma   | yes                |
| <b>Parentis</b>                            | Onset of rifting 130 <sup>27</sup> Ma   | yes                |
|  | End of extension 106 <sup>27</sup> Ma   | yes                |
| <b>Pyrenean rift systems</b>               | Transtensional motion <sup>35</sup>   |                    |
|  | Onset of rifting late Jurassic <sup>34</sup>  |                    |
|  | Hyper-extension starts in Albien <sup>27</sup>  | yes                |
|  | Onset of convergence 83 <sup>28</sup> Ma  |                    |
| <b>Central Iberian rift system</b>         | Onset of rifting 155 <sup>29</sup> Ma   | no                 |
|  | End of extension 106 <sup>29</sup> Ma   | no                 |
| <b>Porcupine Basin</b>                     | Extension from Permian to Early Cretaceous <sup>30</sup>  | no                 |
|  | Main rift phase 161-145 <sup>30</sup> Ma  | no                 |
| <b>Rockall Basin</b>                       | Late Jurassic and Early Cretaceous extension <sup>31</sup>  | Partially          |
| <b>NE Newfoundland-Irish margin</b>        | Onset of rifting 130 <sup>32</sup> Ma   | no                 |
|  | Onset of exhumation 112 <sup>32</sup> Ma  | no                 |
|  | Onset of seafloor spreading   | no                 |
|  | First magnetic anomaly C34 83 <sup>5</sup> Ma   |                    |
| <b>Labrador Sea</b>                        | First magnetic anomaly C27 61 <sup>33</sup> Ma  | no                 |
|  | End of seafloor spreading 33 <sup>33</sup> Ma   | no                 |

of the same age on the Galicia Bank are shallow water carbonates. This observation has been interpreted as a younging of the crustal necking northward (Mohn et al., 2015). The sedimentary record from ODP campaigns indicate that necking had to occur in Tithonian-Berriasian time in the Iberia Abyssal Plain and Valanginian time in the Galicia margin. Exhumed serpentized mantle has been sampled in the two northern segments at ODP Sites 637, 897, 898, 1068, and 1070. Seismic refraction data also suggest exhumed mantle on the Gorringer Bank in the Tagus Abyssal Plain (Sallarès et al., 2013). Gabbro zircons included in serpentized peridotites have been dated at 137.5 Ma on the Gorringer Bank (Schärer et al., 2000) and  $^{40}\text{Ar}/^{39}\text{Ar}$  dating of hornblende in a gabbro gave  $145 \pm 1$  Ma (Féraud et al., 1986). In the Iberia Abyssal Plain cooling ages of plagioclase from continental crust amphibolites below 200 to 150°C yield plateau ages at  $136.4 \pm 0.3$  Ma at ODP Site 900 (Féraud et al., 1996)  $133.1 \pm 0.1$  Ma at ODP Site 1068 and  $141.8 \pm 0.4$  Ma at ODP Site 1067 (Jagoutz et al., 2007), which indicate that lower crustal rocks had to be already exhumed to shallow levels at that time. Exhumation of mantle had to occur during Valanginian to Hauterivian time. At ODP Site 637 at the Galicia margin, a diorite dyke has been dated by Ar/Ar on amphiboles at  $122 \pm 0.6$  Ma (Féraud et al., 1996). Zircons from meta-gabbros in the exhumed domain dredged at GAL-32-07 yield an emplacement age of  $121 \pm 0.4$  Ma (Schärer et al., 2000). Mantle exhumation at the seafloor did not start synchronously along the Iberia-Newfoundland margins, initiating in Valanginian time at the Gorringer Bank and in Aptian time further north. A major sedimentary unconformity at the Aptian-Albian boundary has been interpreted as marking the complete separation of the lithosphere and the onset of stable oceanic accretion (Tucholke et al., 2007a).

## 4.2 Orphan Basin

The Orphan Basin is located north-east of the Newfoundland island and is surrounded by the Flemish Cap to the southeast, the Grand Banks to the south, the north-eastern Newfoundland margin to the west and to the north by the Atlantic Ocean. The crustal structure of this basin is

**Table III-1:** Table presenting the major inputs of the modeling. References 1(Kneller et al., 2012), 2(Schettino and Turco, 2009), 3(Sahabi et al., 2004), 4(Labails et al., 2010), 5(Klitgord and Schouten, 1986), 6 (Rasmussen et al., 1998), 7(Féraud et al., 1986), 8 (Mauffret et al., 1989), 9 (Srivastava et al., 2000), 10 (Pinheiro et al., 1992), 11 (Tucholke et al., 2007), 12 (Srivastava and Roest, 1989), 13 (Murillas et al., 1990), 14 (Mohn et al., 2015), 15 (Jagoutz et al., 2007), 16 (Bronner et al., 2011), 17(Olivet, 1996), 18 (Schärer et al., 2000), 19 (Vissers and Meijer, 2012), 20 (Enachescu, 2006), 21 (Dafoe et al., 2015), 22 (Sibuet and Collette, 1991), 23 (Sibuet et al., 2004), 24 (Tugend et al., 2014), 25 (Thinon, 2002), 26 (Montadert et al., 1979), 27 (Tugend et al., 2015), 28 (Capote et al., 2002), 29 (Salas and Casas, 1993), 30 (Tate et al., 1993), 31 (Naylor and Shannon, 2005), 32 (De Graciansky et al., 1985) ; 33 (Oakey and Chalmers, 2012) ; 34( Desegaulx and Brunet, 1990) ; 35 (Olivet, 1996)

divided in two sub-basins, locally overlying less than 15 km thick crust (Watremez et al., 2015) in the East and West Orphan basins, which are separated by a structural high. This high extends northward to the Orphan Knoll. The age of the crustal extension and necking in these basins is not well constrained but stratigraphic studies and well calibration provide some insight (Dafoe et al., 2015; Gouiza et al., 2016). Two main phases of extensions have been proposed. The first one, during the Jurassic which is supposed to mainly affect the eastern sub-basin, whereas the second phase, during Early Cretaceous, was likely more intense in the western sub-basin (Dafoe et al., 2015; Enachescu, 2006; Gouiza et al., 2016). Seismic refraction studies do not present evidence for large areas of exhumed mantle in any of the two sub-basins (Chian et al., 2001; Watremez et al., 2015)).

### **4.3 Bay of Biscay**

The Bay of Biscay is a V-shaped oceanic basin limited to the north-east by the Western Approaches and the Armorican margins and to the south by the North Iberian (or Cantabrian) margin. The Bay of Biscay is open to the west and the southern North Atlantic, terminates to the east in the Parentis Basin and several sedimentary basins in the Pyrenean realm that may be linked kinematically to the opening of the Bay of Biscay (Roca et al., 2011; Tugend et al., 2015a). Marine magnetic anomaly C34 is present in the oceanic basin and highlights the presence of a triple point between the Biscay oceanic ridge and the mid Atlantic ridge. Seafloor spreading ceased in the Bay of Biscay between anomalies C34 and C33 (83 to 79 Ma; Sibuet and Collette, 1991). The northern Iberian margin experienced compression from Late Cretaceous to Oligocene, whereas the Western Approach and Armorican margins are better preserved (Thinon et al., 2003). The main rifting phase occurred from latest Jurassic to Early Cretaceous (Berriasian to Barremian) related to the necking and extreme thinning of the crust (Montadert et al., 1979; Tugend et al., 2014). Mantle exhumation is inferred to occur during the Aptian (Thinon, 2002; Tugend et al., 2014) prior to the beginning of oceanic accretion in latest Aptian-earliest Albian (Montadert et al., 1979; Thinon et al., 2003). These ages are, however, only constrained by correlations from the few drill holes located on the Western Approaches margin (e.g. DSDP Leg 48; Montadert and Roberts, 1979).

### **4.4 Pyrenees, Parentis, Basque-Cantabrian and Central Iberian rift systems**

The Pyrenean mountain belt (*sensus lato*) represents the remnant of a former transient plate boundary between Eurasia and Iberia (Canérot, 2008). This plate boundary initiated by distributed strike slip and transtensional motion from at least Late Jurassic to Aptian (Canérot, 2008; Jammes et al., 2009; Olivet, 1996; Tugend et al., 2015a) associated with a complex

partitioning of the deformation between several oblique rift systems (Central Iberian, Bay of Biscay-Parentis and Pyrenean-Basque-Cantabrian rift systems) separated by relatively stronger crustal blocks (Landes High and Ebro block) interpreted as continental ribbons (Tugend et al., 2015a). The Central Iberian rift is assumed to be Late Jurassic to Albian (Salas and Casas, 1993). Basins from the Pyrenean domain (Basque-Cantabrian, Arzacq-Mauléon) are highly segmented (Tugend et al 2015) and evolved from Late Jurassic to probably the Cenomanian/Turonian with mantle exhumation starting at Albian time (Jammes et al., 2009; Lagabrielle and Bodinier, 2008; Masini et al., 2014). The NNE-SSW segmentation of the Pyrenean-Basque-Cantabrian rift system is still observable at a crustal scale (e.g. Pamplona and Toulouse transfer fault) and may constrain the first-order direction of extension from late Aptian (Chevrot et al., 2015; Jammes, 2009). The cessation of rift activity coincide with the onset of convergence in the Pyrenean domain in Santonian to Campanian time (Capote et al., 2002), whereas in the Central Iberian rift system the main convergence seems to occur during the Eocene (Salas and Casas, 1993). The convergence is related to the northward motion of Africa and lead to the final collision stage of the Pyrenees in Oligocene (Capote et al., 2002).

#### **4.5 Porcupine Basin, Rockall Through and Hatton Basin**

The Porcupine basin is a north trending V-shape deep sedimentary basin located on the Irish shelf, north of the Goban Spur, bounded eastward by the Irish mainland platform and westward by a continental ribbon, referred to as the Porcupine Bank. The basin is narrow (<200 km wide) but presents a very strong crustal thinning, which may have resulted in mantle serpentinization and local mantle exhumation (O'Reilly et al., 2006; Reston et al., 2004). Rifting occurred in several phases during Permo-Triassic, Jurassic and earliest Cretaceous times (Tate et al., 1993) with a major thinning phase during Mid-Late Jurassic.

The Rockall Basin is located between the Irish mainland platform and the Porcupine Bank to the east, by the Rockall Bank to the west and by the Charlie Gibbs fracture zone to the south. The basin is 1100 km long and narrows from south to north. The crust outside the basin is about 30 km thick. The southern Rockall Basin is up to 200 km wide and formed with a thinnest crust of about 10 to 8 km thick (O'Reilly et al., 1996). There are different suggestions concerning the nature of the basement that floors the Rockall basin: oceanic crust, serpentinized mantle or hyper-extended continental crust. Permo-Triassic, Late Jurassic and Early Cretaceous extension have been proposed (Naylor and Shannon, 2005), however the precise age of rifting remains unconstrained.

The Hatton Basin is oriented NE-SW and separated the Rockall Bank on its eastern side and the Hatton Bank on its western side. The basin stratigraphy is poorly understood because of

the lack of well data and the numerous magmatic additions, however, the main extension seems to be related to the breakup of the North Atlantic in Paleocene time (Hitchen, 2004).

#### **4.6 North-eastern Newfoundland margin and Irish shelf**

The third oceanic segment of the southern North Atlantic is located between the Irish shelf to the northeast and the northeastern Newfoundland margin to the southwest. These conjugate margins are complex because they cut obliquely highly thinned continental crust and basins as well as undeformed continental crust. The Irish shelf margin is oriented NW-SE and goes from the Goban Spur at the northern termination of the Western-Approach margin to the southwest of the Rockall Bank. It follows the edge of the Porcupine Basin, the Porcupine Bank and the Rockall Through. The north-eastern Newfoundland margin is composed of the north-eastern Flemish Cap margin and the northern edge of the eastern and western Orphan basins until the Charlie Gibbs fracture zone. Only a few studies are available on this area and most of the data are from the Flemish Cap and Goban Spur conjugate margins. These margins are highly asymmetric (Gerlings et al., 2012). The Goban Spur presents a neck architecture, which thins the crust from ~20 km to ~6 km over ~40 km wide and a 70 km wide zone of exhumed mantle (Bullock and Minshull, 2005). In contrast the Flemish Cap margin presents a sharp neck, which thins the continental crust from 32 km to less than 10 km in only 30 km (Gerlings et al., 2011), a thin continental crust extending over 100 km oceanward and only an approximately 20 km wide domain of exhumed mantle (Welford et al., 2010a). This structure is partly related to several NW-SE transfer zones affecting the margin during Late Jurassic-Early Cretaceous synchronously to the extension of the Orphan basin prior to the NE-SW extension between Ireland and Newfoundland. A small amount of Permo-Triassic extension could have affected Goban Spur, however, the oldest syn-rift strata recovered at DSDP Site 549 on the Goban Spur is lower Barremian (De Graciansky et al., 1985). The unconformity between syn- and post-rift sediments in continental half grabens is dated at the Aptian-Albian boundary (De Graciansky et al., 1985). However, this timing is only valid for the southernmost part of this area (Flemish cap-Goban Spur rifted margins).

#### **4.7 Labrador Sea and Baffin Bay**

The Labrador Sea and Baffin Bay are two oceanic basins separating Greenland from North-America. This domain is beyond the scope of this study but the position of Greenland has to be constrained to determine the position of Eurasia relative to North America. The oceanic evolution of this domain starts in Maastrichtian or Paleocene time prior to Chron C27 (61 Ma) and ends at the Eocene-Oligocene boundary (33Ma) (Oakey and Chalmers, 2012). The

Labrador and SW Greenland margins experienced an important magma-poor rifting leading to the exhumation of lithospheric mantle (Chian et al., 1995). The tectono-stratigraphy on the proximal domain of the Labrador margin (Dickie et al., 2011) suggests two phases of rifting, the first one from Valanginian to Albian focused on the proximal domain, whereas the second one from Cenomanian to Maastrichtian time is better recorded in more distal domains. As the lateral extension related to the formation of the distal domain is likely more important than for the proximal domain, most of the motion of Greenland can be attributed to have occurred during the second rifting phase and oceanic spreading. We used previous palinspastic models (Hosseinpour et al., 2013) to locate the initial position at 200Ma of Greenland relative to North-America.

## **5. TECTONIC EVOLUTION OF THE SOUTHERN NORTH ATLANTIC RIFT DOMAINS**

As highlighted in the previous section, data sets and knowledge on each rift of the southern North Atlantic are very different. In some domains the necking phase, exhumation phase and onset of seafloor spreading are constrained by stratigraphy, geochronology or magnetic anomalies, while in others only one or none of these constraints is known. Therefore our restoration methodology is to implement the kinematic evolution of the well-known domains (Fig. III-6) and to see how the less constrained areas evolve. Hence, the input data of the model is limited to areas from which data are reliable (Table III-1). We consider as “robust data” drill hole data sampling parts of the sedimentary section and the basement. Using this data and the methods explained above, a new plate kinematic model of the southern North Atlantic was developed to visualize the tectonic evolution of the hyper-extended rift systems. The kinematic model is composed of a set of finite rotation poles (Table III-2). This solution is none unique and is used as a visualization tool to discuss the processes of rift propagation. North-America (NAM) is kept fixed whereas the other plates are included in a plate circuit (Fig. III-5), which highlight the interaction between each plate through time.

### **5.1 Constrained positions: Campanian (83 Ma) and full-fit (200 Ma)**

The Mesozoic evolution of the southern North Atlantic is highly debated, however there is a general agreement on the plate configuration at the full-fit and at the first magnetic anomaly after the Cretaceous normal polarity super-chron C34 which is Campanian in age (83Ma) (Vissers and Meijer, 2012b).



### **5.1.1 Campanian position: first constrained oceanic magnetic anomaly (C34)**

The post C34 evolution of the Iberia plate has been recently modified (Vissers and Meijer, 2012b) to unify different studies with a consistent timescale, but most of the rotation poles are from previous studies (Gaina et al., 2002; Srivastava and Roest, 1989; Srivastava and Tapscott, 1986). Hence continents are confidently positioned (Fig. III-6a) after C34. The rift propagates north of the Charlie-Gibbs fracture zone between the northeastern Newfoundland margin and the southwest Rockall Bank margin and northward through the Labrador Sea, which experienced rift deformation until Maastrichtian time (Dickie et al., 2011). The Charlie Gibbs fracture zone laterally offset the mid Atlantic ridge and the Labrador rift system by 200 km. South of the Charlie Gibbs fracture zone the domain map shows that the extensional processes are related to oceanic spreading. The Pyrenean system is composed of thinned continental crust and local exhumed mantle. The maximal width of the Pyrenean extensional system is between 100 and 130 km depending on the size of the Ebro block. These values are in agreement with the expected subduction of 50km plus the crustal shortening of 90km (Mouthereau et al., 2014; Wang et al., 2016), which occurred from Campanian to Late Oligocene (Vergés et al., 2002). The other margins are thermally subsiding.

### **5.1.2 Trias-Jurassic boundary (200Ma): the full fit**

Full-fit restorations are performed since the beginning of the plate tectonic theory (Wegener, 1915) and are based on the coast line, an isobaths or a reconstructed boundary. However most of the models (Jammes et al., 2009; Olivet, 1996; Sibuet, 2004; Vissers and Meijer, 2012b) agree on the closure of hyper-extended domains and on the initial Triassic setting of the southern North Atlantic. Strictly the Triassic-Jurassic boundary does not correspond to the onset of extensional deformation because Triassic rift basins are wide-spread over the Central and North Atlantic domain (e.g. Jeanne d'Arc Basin, Celtic Sea, Lusitanian Basin; see Leleu and Hartley, 2010; Rasmussen et al., 1998; Stolfova and Shannon, 2009; Tankard et al., 1989). Indeed the Triassic extension phase was important and created wide basins but the overall crustal extension, inferred from the basin architecture, remains little constrained (Leleu et al., 2016).

A visual fitting of the polygons limited by the LRCC, which corresponds to the minimum size of the pre-deformation plate was performed. The objective is to reduce to a maximum the continental overlaps, as polygons have the minimum pre-deformation size. The position of NW Africa and Greenland relative to North America (Fig. III-7c) are extracted from previous palinspastic restorations (Barnett-Moore et al., 2016b; Heine et al., 2013; Hosseinpour et al., 2013), but the position of Eurasia and Iberia is not constrained by such studies or by

**Total reconstruction poles**

| Age                 | Lat    | Lon     | Angle  | Fix plate | Ref | Age                                  | Lat   | Lon    | Angle  | Fix plate |  |
|---------------------|--------|---------|--------|-----------|-----|--------------------------------------|-------|--------|--------|-----------|--|
| <b>Eurasia</b>      |        |         |        |           |     | <b>Ebro bloc</b>                     |       |        |        |           |  |
| 200.0               | 70.07  | 153.56  | -23.37 | NAM       |     | 200.0                                | 51.59 | 2.80   | -30.22 | EUR       |  |
| 112.0               | 68.34  | 155.87  | -21.22 | NAM       |     | 160.0                                | 51.59 | 2.80   | -30.22 | EUR       |  |
| 92.0                | 66.67  | 150.26  | -20.37 | NAM       | *   | 150.0                                | 51.69 | 2.68   | -28.85 | EUR       |  |
| 83.0                | 66.54  | 148.91  | -19.70 | NAM       | *   | 140.0                                | 51.93 | 2.76   | -26.58 | EUR       |  |
| <b>Iberia</b>       |        |         |        |           |     | <b>Landes High</b>                   |       |        |        |           |  |
| 200.0               | 50.43  | 1.53    | -37.52 | EUR       |     | 200.0                                | 48.17 | 1.09   | -37.19 | EUR       |  |
| 161.0               | 50.95  | 1.91    | -37.60 | EUR       |     | 160.0                                | 48.17 | 1.09   | -37.19 | EUR       |  |
| 140.0               | 51.64  | 2.59    | -35.62 | EUR       |     | 145.0                                | 47.36 | 0.53   | -36.23 | EUR       |  |
| 120.0               | -50.06 | -177.68 | 22.83  | EUR       |     | 120.0                                | 44.19 | -1.11  | -31.56 | EUR       |  |
| 112.0               | -46.62 | 178.49  | 22.92  | EUR       |     | 105.0                                | 43.99 | -1.75  | -6.53  | EUR       |  |
| 105.0               | -44.99 | 176.89  | 19.01  | EUR       |     | 86.0                                 | 0.00  | 0.00   | 0.00   | EUR       |  |
| 86.0                | -40.18 | 170.57  | 10.07  | EUR       |     | <b>Porcupine Bank</b>                |       |        |        |           |  |
| 83.0                | -39.36 | 170.34  | 9.08   | EUR       | **  | 200.0                                | 52.87 | -10.80 | 19.18  | EUR       |  |
| <b>Greenland</b>    |        |         |        |           |     | <b>Rockal Bank</b>                   |       |        |        |           |  |
| 112.0               | 62.09  | -127.99 | -10.63 | NAM       | *** | 200.0                                | 52.69 | 124.54 | -13.56 | GRN       |  |
| 112.0               | 49.34  | 125.70  | 13.18  | EUR       |     | 112.0                                | 52.69 | 124.54 | -13.56 | GRN       |  |
| 75.0                | 49.34  | 125.70  | 13.18  | EUR       |     | 112.0                                | 60.43 | -18.53 | -0.88  | EUR       |  |
| 75.0                | 61.01  | -129.28 | -6.86  | NAM       |     | 106.0                                | 0.00  | 0.00   | 0.00   | EUR       |  |
| 63.0                | 27.80  | -150.00 | -3.75  | NAM       | #   | <b>* Srivastava and Roest, 1989</b>  |       |        |        |           |  |
| <b>Flemish Cap</b>  |        |         |        |           |     | <b>** Vissers and Meijers, 2012a</b> |       |        |        |           |  |
| 200.0               | 63.94  | -2.84   | 69.15  | IB        |     | <b>*** Hoseinpour et al., 2013</b>   |       |        |        |           |  |
| 160.0               | 63.94  | -2.84   | 69.15  | IB        |     | <b># Oakey and Chalmers, 2012</b>    |       |        |        |           |  |
| 160.0               | 44.34  | -53.79  | 18.95  | NAM       |     |                                      |       |        |        |           |  |
| 140.0               | 44.97  | -52.66  | 20.55  | NAM       |     |                                      |       |        |        |           |  |
| 112.0               | 0.00   | 0.00    | 0.00   | NAM       |     |                                      |       |        |        |           |  |
| <b>Orphan Knoll</b> |        |         |        |           |     |                                      |       |        |        |           |  |
| 200.0               | 42.38  | -54.00  | 12.56  | NAM       |     |                                      |       |        |        |           |  |
| 140.0               | 42.38  | -54.00  | 12.56  | NAM       |     |                                      |       |        |        |           |  |
| 130.0               | 44.97  | -52.57  | 13.20  | NAM       |     |                                      |       |        |        |           |  |
| 112.0               | 0.00   | 0.00    | 0.00   | NAM       |     |                                      |       |        |        |           |  |

Table III-2: Reconstruction poles used in this study

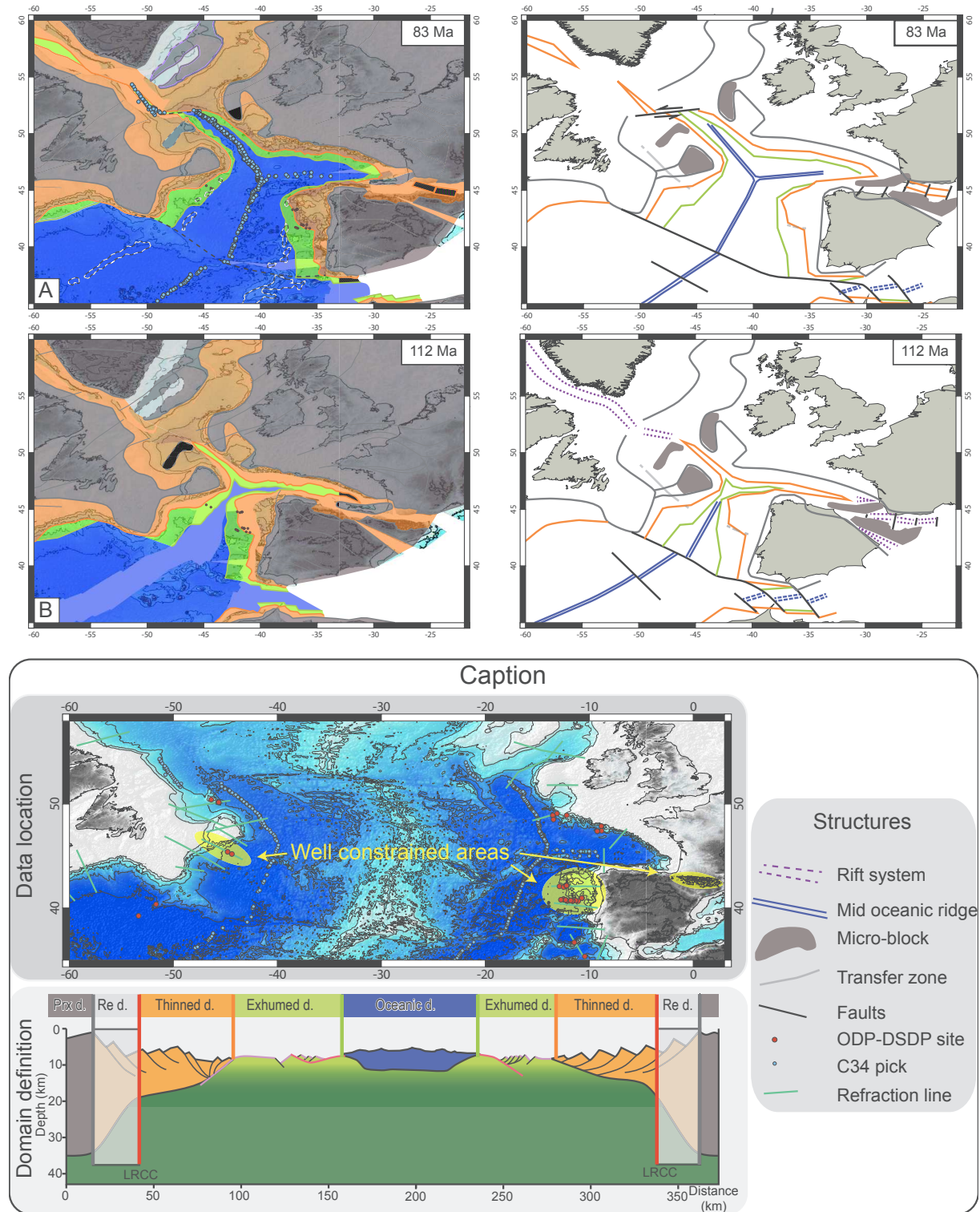


**Fig. III-6:** Restoration of the southern North Atlantic, with North-America fixed on present day coordinates. Left column present the restoration of the rifted domains and the right column shows the plate restoration with the interpreted rift structures at each stage. Re d., reconstructed domain.

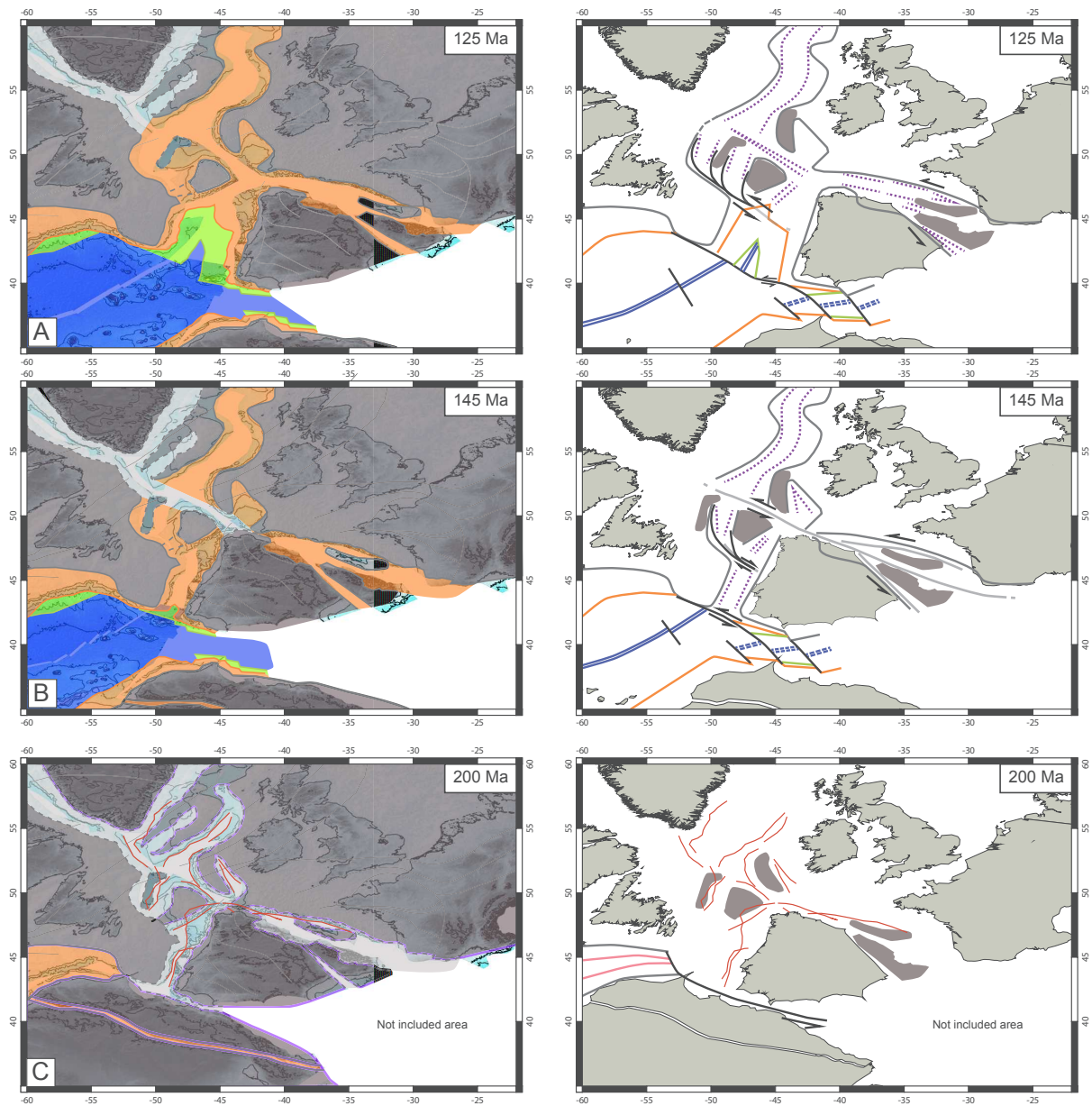


Fig. III-7: see FigIII-6

magnetic anomalies prior to C34 (Nirrengarten et al. 2016b). The western and southern margin of the Iberia plate are first fitted with respect to North-America and Africa plates by closing of the Orphan Basin with the Flemish-Cap. We restored the Porcupine Basin, Hatton Basin and Rockall Through and fitted Eurasia with the other plates from southeastern Greenland to the north Galician margin. The full-fit position is very similar to previous restorations (Barnett-Moore et al., 2016b; Rowley and Lottes, 1988). The gap in the future Bay of Biscay is limited by the Ebro Block and Landes High (Tugend et al., 2015a). Avalonian and Caledonian sutures present good correlation through the proto-Atlantic (Welford et al., 2012), even if the offshore continuation is approximated (Fig. III-8). Variscan domains are showing a similar bending structure between western Europe and Iberia, the correlation is still valid even if Iberia is located westward compared to previous restorations (Balleve et al., 2014; Martínez Catalán, 2011; Matte, 2001).

### ***5.2 Jurassic time (200-145 Ma): distributed deformation and intra continental rifts***

Seafloor spreading in the Central Atlantic began at about 190 Ma (Labails et al., 2010), the eastward motion of NW Africa is accommodated by strike slip motion south of the Iberia plate. During Middle-Jurassic an oblique rifting is observed on the onshore Algarve Basin (Ramos et al., 2015) and related to the motion of Iberia relative to NW Africa. Mantle exhumation and formation of an oceanic crust in the Gulf of Cadiz are suggested to bridge the Alpine and Atlantic oceanic domains south of the Iberia plate (Frizon de Lamotte et al., 2011; Martínez-Loriente et al., 2014; Sallarès et al., 2011). The model suggests a maximum width of 300km between south Iberia and North Africa at 145Ma.

The Triassic extension phase is followed by a similar Early Jurassic rifting, which is recorded in several sedimentary basins located over the Newfoundland Grand Banks, the Iberian Peninsula and on the Eurasia continent (e.g. Lusitanian, Jeanne d'Arc, Porto, Horseshoe, Whale Basins, Porcupine, Rockall) (Rasmussen et al., 1998; Shannon, 1991; Tankard et al., 1989). These sedimentary basins are typically grabens and asymmetric half grabens filled by continental to shallow marine sediments (Murillas et al., 1990; Pereira and Alves, 2011). These basins are mostly oriented NNE-SSW following the trend of the Central Atlantic mid-oceanic ridge. In details, the Jurassic extension might have occurred through several tectonic pulses leading to the formation of several basins, however, it is implemented in the model by a slow eastward motion (<0.2 cm/y) of Eurasia and Iberia relative to North America from 200 Ma to 161 Ma. This motion is located between Iberia and the Grand Banks, in the East Orphan Basin and in the Rockall Through (Skogseid, 2010). The Porcupine Basin is obliquely oriented compared to the Iberia-Newfoundland system and its main rift event is proposed to be Middle

to Late Jurassic (Shannon, 1991; Tate et al., 1993), which creates a sinistral transfer zone on the northeastern margin of Flemish Cap. The formation of the Porcupine basin is modeled by a V-shape opening; however, it causes compression between the Porcupine Bank and the Irish Shelf. Therefore we suggest that the Porcupine basin may be highly segmented, enabling a differential extension without a rotation of the Porcupine Bank.

The second extension phase between Iberia and Newfoundland starts in Late Jurassic, but while the Early Jurassic and Triassic rifting is synchronous over this system, the second event is diachronous starting to the south in the Alentejo Basin at Callovian-Oxfordian time and in Berriasian time at the Galicia Margin (Alves et al., 2009). This phase accelerated the eastward motion of Iberia relative to Eurasia and initiated the motion of the Ebro Block and Landes High, leading to extensional and strike structures in the Bay of Biscay-Pyrenean corridor (Tavani and Muñoz, 2012; Tugend et al., 2015a) as well as in the Central Iberian rift system (Salas and Casas, 1993). However, there is no indication of acceleration between Eurasia and North-America. The Rockall Through deformed at low strain rate, which is consistent with the well known large thinned crustal domain (O'Reilly et al., 1995).

### **5.3 Tithonian to Barremian (145-125Ma): Necking, hyper-extension, exhumation**

This period followed a Late-Jurassic rift event, which initiated the differential motion between Iberia and Eurasia. The snapshot (Fig. III-7b) at the Jurassic-Cretaceous boundary (145 Ma) presents an important change in the kinematics with the cessation of seafloor spreading between Iberia and North Africa (Schettino and Turco, 2011). Interestingly, it also corresponds to the time when the mid Atlantic ridge passed across the south Newfoundland transform margin. North of the future Azores-Gibraltar Fracture Zone the Jurassic-Cretaceous boundary is an important snapshot to understand the partitioning of rift deformation.

At 145 Ma the Iberia-Newfoundland rift system is still intra-continental. During Early-Cretaceous the N-S segmentation of the deformation in the Iberia-Newfoundland rift system is well developed (Alves et al., 2009; Welford et al., 2010b). This is best observed within the sedimentary record between the Galicia-Flemish Cap system and the Iberia Abyssal Plain. In the first system, necking is dated from Valanginian to Hauterivian (140-130 Ma) whereas further south it is dated from Tithonian to Berriasian (150-140 Ma) (Mohn et al., 2015). This delay in the necking phase is interpreted in a differential extension, accommodated by the opening of the East Orphan Basin (Enachescu, 2006) along a transfer zone located in the Flemish Pass Basin and south of the Galicia Bank. On the same two segments, the phase of continental crust hyper-extension is also delayed northward (Mohn et al., 2015). In the model, extension in the East Orphan Basin stopped at 130 Ma whereas it accelerated in West Orphan.

However, the structural and time relations between those two sub-basins remain unclear due to the lack of public drill hole data. Mantle exhumation initiates at the southernmost part of the Iberia-Newfoundland system around 140 Ma, which corresponds to the crystallisation age of gabbros in host peridotites on the Gorrige Bank (145Ma to 137.5Ma) (Féraud et al., 1986; Schärer et al., 2000). In our model mantle exhumation is quasi synchronous at 140 Ma from the NAGFZ to the latitude 45.5°. Exhumation is delayed northward to 120 Ma because the rotation and extrusion of the Flemish Cap out of Orphan and the extension in East and West Orphan compensate the extension south of the Flemish Cap. Seafloor spreading initiated at 130 Ma north of the NAGFZ and propagated northward in a V-shape style. The Bay of Biscay-Pyrenean domain encompassed a strike-slip regime and accommodated the 1.6 cm/yr of left lateral movement relative to Eurasia. Extension between North-America and Eurasia is similar to the Late Jurassic phase and located mostly in the Rockall Through. Seismic interpretations of the north-eastern Flemish Cap margin suggest transfer fault structures (Welford et al., 2010a), which are explained by strike-slip motion between the Flemish Cap and the Porcupine Bank. The two Orphan sub-basins are aligned with the Rockall Through and the Orphan Knoll is suggested to merge with the Rockall Bank.

#### **5.4 Aptian (125-112 Ma): Seafloor spreading propagation**

The Aptian evolution (Fig. III-7A,6B) is marked by the northward propagation of seafloor spreading in the Iberia-Newfoundland conjugate system. At 112 Ma the tip of the propagator reached Galicia Bank.

Indeed this means that the early seafloor spreading on the southern part of the system is compensated by hyper-extension in the West Orphan Basin and mantle exhumation in the Flemish Cap-Galicia Bank system. The left lateral motion of Iberia is accommodated in the Bay of Biscay by the transtensional development of an exhumed domain. The Parentis Basin and the Central Iberian rift are developing at this stage (Salas and Casas, 1993; Tugend et al., 2015a), which inhibit extension between Eurasia and the Ebro Block in the Pyrenean domain. The partitioning of the deformation between each rift zone and between lateral and orthogonal movements is necessary to fit the observations reported from the Iberia-Eurasia plate boundary (Tugend et al., 2014). The Goban Spur rifted away from the North Galicia margin and experienced strike slip motion with the extrusion of the Flemish Cap. This motion is coherent with the highly asymmetric conjugate margin between Goban Spur and Flemish Cap (Gerlings et al., 2012). Rifting continued in the Rockall Through until Aptian, but also between Newfoundland and Ireland where extension was first accommodated by crustal oblique deformation and later by mantle exhumation.

## **5.5 Albian- Santonian (112 Ma- 83 Ma): Northward propagation and Pyrenean hyper-extension**

This stage (Fig. III-6b) presents the propagation of seafloor spreading in the Bay of Biscay and between Newfoundland and Ireland. It also shows the stable simultaneous accretion of three oceanic ridges, in the Bay of Biscay, between Iberia and Newfoundland and between Ireland and Newfoundland (Roest and Srivastava, 1991). Our model represents thanks to the individualisation of the Ebro Block, the extension in the Pyrenees, which could explain the exhumation of mantle rocks during Albian-Cenomanian (Jammes et al., 2009; Lagabrielle et al., 2010; Lagabrielle and Bodinier, 2008; Masini et al., 2014). This period coincides with the start of movement along the Charlie-Gibbs fracture zone, which separates the oceanic domain between Orphan and Porcupine Bank and the ongoing rift system between the north-eastern Newfoundland margin and the Rockall Bank. This fracture zone created a narrow margin between south Rockall Through and the West Orphan Basin with significant magmatism present on both sides (Keen et al., 2014). The Labrador rift system began its activity and accommodated the slow extension between Eurasia, North America and Greenland, which was during this stage part of Eurasia. This is coherent with the cessation of extension and the thermal subsidence of the hyper-extended basins along the future North Atlantic margin (Gabrielsen et al., 1999).

## **6. DISCUSSION**

### **6.1 Method and limitations**

In this paper we propose a kinematic model to describe the rift evolution of the southern North Atlantic from Triassic time (full fit) to the first undisputed oceanic magnetic anomaly C34 (83Ma, Campanian/Santonian Fig. III-6A). Performing a quantitative restoration of rift systems with the same accuracy as for oceanic domains is unrealistic, however, the integration of critical data from rifted margins in a kinematic model can provide spatial and time constraints on the kinematics of the pre-breakup stage of the future margins. Our method is based on a relatively accurate knowledge of small, calibrated areas and their integration in a much larger kinematic system including different tectonic plates and micro-blocks. Therefore the first limitation is the variable quality and resolution of the input data that can be obtained from the southern North Atlantic. As a consequence, the model is not everywhere constrained by data, which is a problem encountered in many geological models. Thus, while the model needs to fit the constrained areas, it can be used as a predictive tool for the unconstrained areas and the model predictions may be tested by future scientific work or proprietary industry data. Other issues are



related to the use of “ages” or the termination and definition of shapes and limits of polygons.

When using “ages” it is important to note the difference between the stratigraphic timescale (Gradstein et al., 2004) and the geomagnetic polarity timescale (Gee and Kent, 2007). The stratigraphic age and magnetic inversions correspond to time intervals, which are not correlated. As the southern North Atlantic does not have well-defined oceanic magnetic anomalies prior to C34 (Nirrengarten et al., 2016b) and as most of the time constraints used are from stratigraphy, we choose to follow the stratigraphic time chart of Gradstein et al. (2004). Moreover, the integration of geochronological data is not straightforward because it corresponds either to the time of crystallisation or the cooling of a mineral, and therefore the correct interpretation of these ages has important implications on the kinematic model. Hence, the ages and the way they are interpreted and correlated remain sensible to the geological interpretation.

The determination of the shape and size of the polygons depends from the areal balancing of the crustal thickness calculated from 3D gravity inversion. In this study we chose consciously a rather high initial thickness of 37.5 km (Fig. III-2). This inversion is calibrated and is highly influenced by the accuracy of the sediments thickness grid. As 37.5 km is the maximum crustal thickness of the proximal domain determined by refraction studies (Lau et al., 2006), the polygon size determined in our work has the tendency to be underestimated and imposes to minimize the overlap during the visual fitting. With an initial crustal thickness of 30 km, which is the thinnest estimation for non-rifted continental crust, the distance between the NL and the LRCC would have increased of 20%. The domain mapping can further induce a bias in the determination of polygon shapes. Indeed, the necking line has to coincide with the Moho slope break otherwise a part of the thinning is omitted or added. Crustal thickness maps and profile extractions from these maps highlight clearly the location of this structural marker. Even if most of the extension and thinning occur between the two conjugate necking lines, the southern North Atlantic experienced extensional deformation since Late Carboniferous-Permian time (Stolfova and Shannon, 2009), which may have extended the polygons prior to their individualization. However, we consider that this extension that is difficult to quantify in detail is minor and within the error bars/uncertainties of our model. In contrast to the necking line, the ECC is more difficult to determine with gravity inversion methods (Cowie et al., 2015) and complementary seismic sections are needed. This makes that the interpretation of the location of the ECC depends on the access to good quality reflection seismic data imaging deeper than 10sec. However, a miss-location of the ECC has a minor impact on the determination of the LRCC, due to the fact that the continental crust is very thin and as a consequence the calculated initial volume/surface of the initial crust is small. For instance a miss-location by 50 km of the

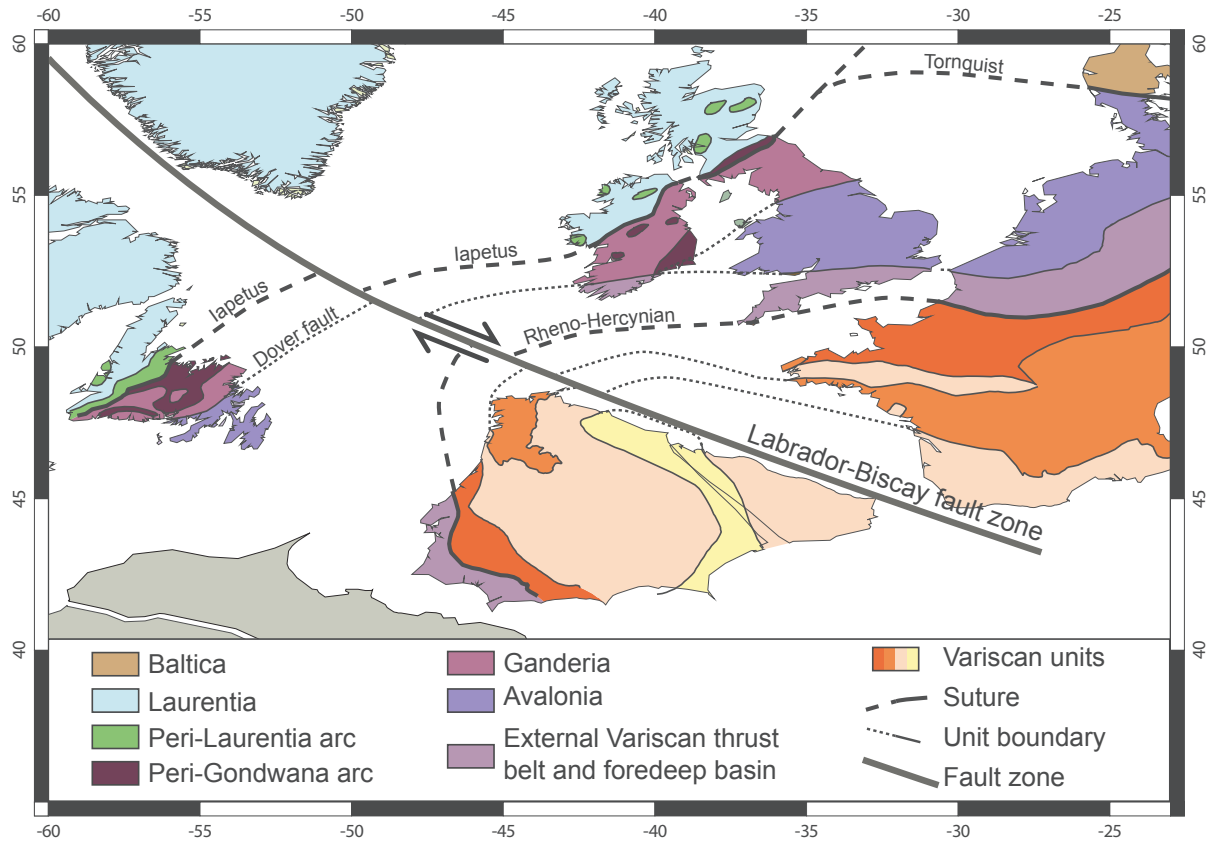


**Fig. III-8:** Synthetic map of the different crustal domains restored at 200 Ma (Pollock et al., 2011; Ballevre et al., 2014). Note that the offshore continuation of the suture is an interpretation based on the width of each terrane NE and SW of the Labrador-Biscay fault zone

location of the ECC only modifies the position of the LRCC by 8 km assuming an average 6 km thick crust. The LRCC position is relatively insensitive to the orientation of extracted profiles along flow lines (Williams et al., 2011) unless the flow lines are completely oblique (Barnett-Moore et al., 2016b). To avoid this problem we extracted “pseudo flow lines” perpendicular to the necking line and not from a previous plate modelling.

## 6.2 Implications for the southern North Atlantic

### 6.2.1 The partitioning of the deformation along the Iberia-Eurasia plate boundary

Previous kinematic models using the magnetic anomaly M0 (Sibuet, 2004; Srivastava et al., 2000; Vissers and Meijer, 2012a) are unable to explain the well-constrained Albian extension in the Pyrenean domain (Jammes et al., 2009; Lagabrielle and Bodinier, 2008; Vacherat et al., 2016) and instead propose an oceanic subduction. Moreover, paleomagnetic data, which support a counter-clockwise rotation of Iberia of 35° (Gong et al., 2008; Van der Voo, 1969) present inconsistencies with the global apparent polar wander path (Neres et al., 2013). Olivet (1996) proposed a restoration of the Iberia plate without using the M0 (J) anomaly

as he already pointed out the weakness of the interpretation of the J-anomaly between Iberia and Newfoundland. However recent studies in the Pyrenees (Jammes et al., 2009; Masini et al., 2014; Tugend et al., 2014) highlight that transfer faults are directed SSW-NNE almost perpendicular to the strike-slip motion, which means that some N-S extension has to be integrated in kinematic models (Jammes et al., 2009). A recent review of kinematic models of the Mesozoic evolution of the Iberia plate by Barnett-Moore et al. (2016a) concludes that none of these models could fit the available geological and geophysical data. In this paper the geological evolution of the Pyrenean rift system is an input and the J-anomaly has not been used for that restoration. Nirrengarten et al., (2016b) were able to demonstrate that the J-magnetic anomaly is polygenic and does not correspond to an isochron, which disqualifies this anomaly as a kinematic indicator. The model implies a partitioning of the left-lateral and orthogonal motion of Iberia relative to Eurasia with two micro-blocks (Ebro Block and Landes High Tugend et al., 2015a). The eastward oriented motion of Iberia relative to the European plate, due to the Atlantic extension, is partly compensated in the Central Iberian rift system and partly in the Pyrenean system creating transtensional corridors prior to Aptian time (Tugend et al., 2015a). During Aptian (Fig. III-7A) the Central Iberian rift potentially reached its maximum extension (~75 km), which was able to compensate the opening of the Bay of Biscay and to keep a constant narrow opening in the Pyrenean system (Lagabrielle and Bodinier, 2008). From Albian to Santonian (Fig. III-6A,B), the Central Iberian rift experienced strike slip motion (Capote et al., 2002) and the Pyrenean system a transtensional rift opening. Although the flow-lines (Fig. III-9) indicate that there is more strike slip motion, locally our model can produce the perpendicular N-S extension interpreted from field observations in the Pyrenean realm (Jammes et al., 2009). The space in the Pyrenean system is constant at 100 km from west to east, which is coherent with the presence of exhumed mantle (Tugend et al., 2015a) and the similar amount of shortening (Mouthereau et al., 2014) over all the length of the Pyrenees. Further studies are needed to better constrain location and kinematics along the boundaries of the Ebro Block in order to refine its initial position and quantity the strike-slip motion predicted by our model.

### ***6.2.2 Partitioning of the deformation in the southern North Atlantic rift systems***

The relatively well-constrained data from the Iberia Abyssal Plain, the Deep Galicia and the northern Newfoundland margins are used as inputs in our model. To compensate the time lag of extension observed between the Deep Galicia margin and the Iberia Abyssal Plain (Mohn et al., 2015), we transfer extension from the southern Iberia-Newfoundland rift system in the Orphan system (Fig. III-7A,B). Extension first localizes in the East and later in the West Orphan basins (Enachescu, 2006), leading to the extraction of the Flemish Cap out of the Grand

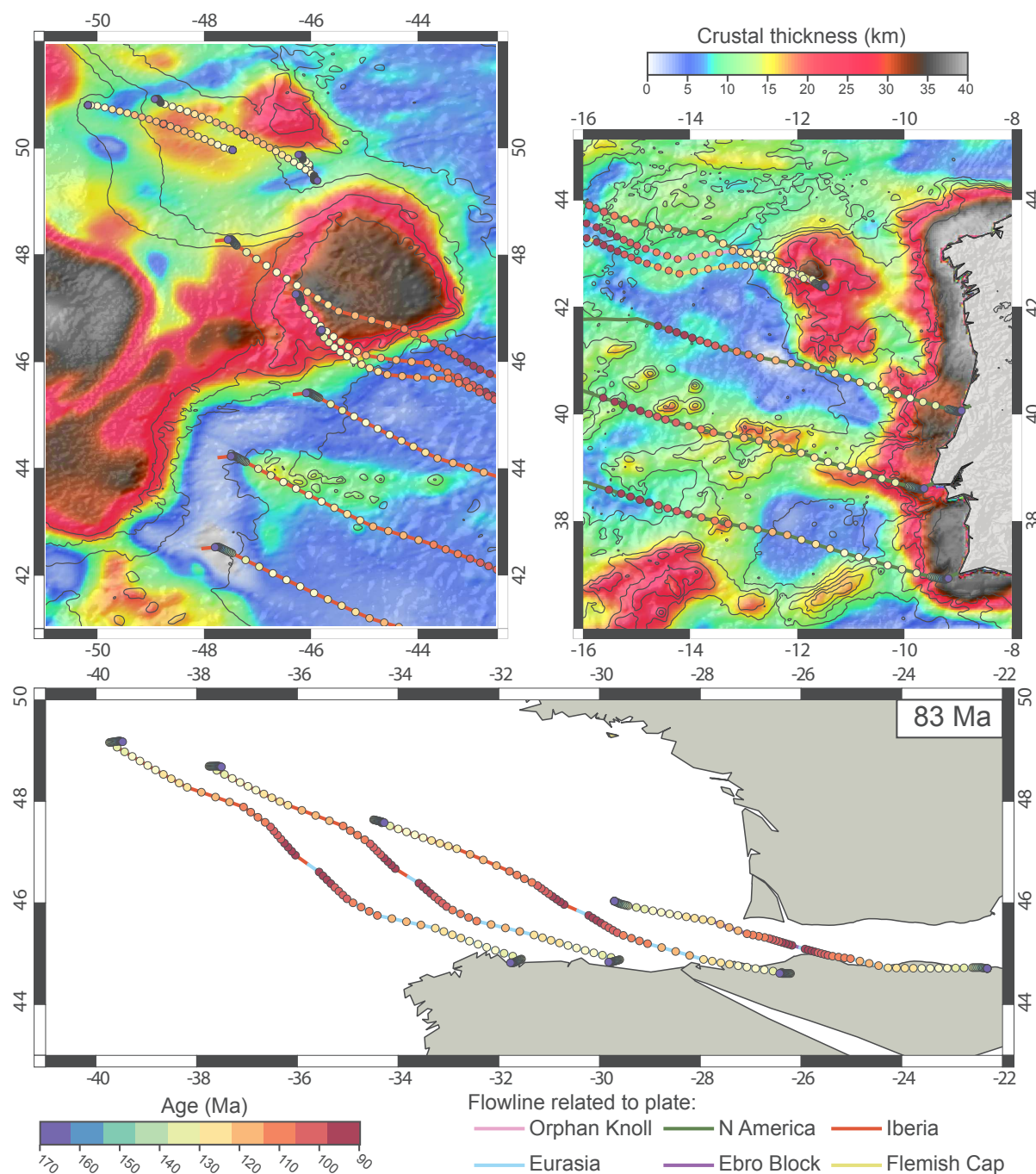


**Fig. III-9:** Age-coded flowline on crustal thickness basemap for the Iberia, Newfoundland and Orphan rifted domains. And age coded flowline of the Eurasia-Iberia system restored at 83Ma

Banks (Sibuet et al., 2007b) (Fig. III-7A,B). This extraction induces strike slip motion between Goban-Spur and the Flemish-Cap as suggested by seismic interpretation (Welford et al., 2010a). This Late-Jurassic-Early-Cretaceous deformation is suggested to be accommodated also in the Rockall Basin, which is at that time located to the north of the Orphan basins. The Porcupine Basin evolution is more difficult to constrain within our model. Its orientation is concordant with the Galicia-Flemish Cap system during Early-Cretaceous (Fig. III-7B) despite the fact that stratigraphic studies suggest a Jurassic age for the thinning in this basin. Extension between

North-America and Eurasia locates after the Aptian-Albian boundary (112 Ma) in the Labrador rift system. This new localisation is concomitant with the cessation of rift activity in the Orphan and Rockall basins.

### ***6.2.3 The Aptian-Albian stratigraphic surface, relation with a triple ridge junction***

The Aptian-Albian boundary (Fig. III-6B) is recorded in the Iberia Newfoundland conjugate margins by a prominent regional unconformity (Soares et al., 2012). This unconformity is well documented in the exhumed domain by tilted Aptian strata passively onlapped by Albian sediments (for an example see continentward side of the high drilled at ODP Site 1277; Tucholke and Sibuet, 2006). Aptian sediments include mass flows and are related to the formation of topographic highs (Péron-Pinvidic et al., 2007) while the Albian sediments are locally absent and mainly formed by turbidites interleaved with hemipelagic sediments (Soares et al., 2012). An alkaline magmatic vein drilled at ODP Site 1277 yield an age of  $113.2 \pm 2.1$  Ma (Jagoutz et al., 2007) and was interpreted to be related to an excess magmatic event (Bronner et al. 2011). In light of those data, the Aptian unconformity was interpreted either as the lithospheric breakup and the formation of a steady state oceanic crust (Bronner et al., 2011; Tucholke et al., 2007b) or as a widespread delocalization of the deformation associated with alkaline magmatism with an already created oceanic crust (Péron-Pinvidic et al., 2007). This unconformity and magmatic activity is, however, not limited to the Iberia-Newfoundland conjugate margins. Further evidence for this event is found in the Bay of Biscay (Montadert et al., 1979), Gobban Spur margin (De Graciansky et al., 1985), Orphan Basin (Dafoe et al., 2015; Gouiza et al., 2016) and Porcupine Basin (Calvès et al., 2012). Moreover, onshore thermochronological data indicate a general uplift of the Galicia margin at that time (Grobe et al., 2014). Our modelling with the mapped COB suggests the onset of the Biscay mid oceanic ridge and the creation of a triple ridge junction at the Aptian-Albian boundary. The relation between this event and the unconformity is not understood, but we propose that uplift and magmatism can be triggered by the onset of a triple ridge junction. Examples for the link between regional uplift, magmatic activity and triple junctions are numerous (Burke and Dewey, 1973). It is commonly thought that triple junctions initiate due to plume proximity. In this work, we suggest that the uplift and magmatism are induced by the formation of a triple junction. A top-down control is suggested as for the propagation of lithospheric breakup in magma rich context (Franke, 2013).

### ***6.2.4 Oceanic magnetic anomalies in the southern Iberia-Newfoundland system***

The integration of our mapped COB in the plate modelling shows that seafloor spreading starts in the southern North Atlantic around 129 Ma at the NAGFZ. Hence, the first

magnetic reversal recorded by the oceanic crustal rocks corresponds to chron M9 (128.93Ma) (Gee and Kent, 2007). However the identification of the magnetic M sequence is based on the interpretation of the J-anomaly as being the M0 isochron. A review of the existing data reveals, however, that the J-anomaly is polygenic and polyphased (Nirrengarten et al. 2016) and therefore cannot be used for plate kinematic restorations. Future magnetic studies will be necessary to carefully interpret, without a-priori on the M0 position, the nature of the so called “M-magnetic anomalies” in the southern North Atlantic.

### ***6.2.5 Initial position of the continents and role of inheritance***

A full-fit position of the continents is proposed for earliest Jurassic time, however, it is interesting to discuss this position in the light of the late and post-orogenic inheritance. The continental lithosphere prior to onset of the North Atlantic rifting results from the amalgamation of Laurentia, Baltica, Avalonian and several Gondwana derived crustal blocks during the Caledonian and Variscan orogenies (e.g. Matte, 2001). The orogenic phase lasted until end of Carboniferous and resulted in the formation of the Pangea supercontinent. The post-orogenic phase is characterized by dextral strike-slip movements located on NW-SE oriented fracture zones (Arthaud and Matte, 1977; Lefort and Miller, 1999). The Labrador-Biscay wrench fault zone is a dextral post-orogenic structure that was preferentially used during rifting in the Bay of Biscay and Labrador Sea during Mesozoic time, even if the orientation is not collinear to the main stress regime (Lefort, 1973). The initiation of the oceanic Charlie Gibbs fracture zone offshore Newfoundland can tentatively be correlated to the Dover Fault onshore Newfoundland corresponding to the suture zone between Laurentia and Avalonia (Pollock et al., 2012; Welford et al., 2012). This suture is also observed in Ireland and its offshore prolongation on the Irish shelf can similarly be correlated to the Charlie Gibbs fracture zone. Moreover, the segmentation of the Iberia margin (Alves et al., 2009) can be related to the different Variscan domains affinity of the Iberia Peninsula (Ballevre et al., 2014). However, contrarily to the Charlie Gibbs fracture zone this segmentation is not observed in the oceanic domain. Therefore, in the southern North Atlantic the importance of inheritance is manifested by the use of old suture zones as transfer zones whereas post-orogenic strike-slip structures were used to localize rifting. However this interpretation is probably due to the orientation of the structures relative to the main extension, because the North Atlantic opened mainly along the Caledonian suture and only partly used the Variscan suture zones (Chenin et al., 2015). Indeed, the impact of inheritance is important, but details remain ill-constrained (Manatschal et al., 2014).

The second structural inheritance is related to the Permian and Triassic extensional basins which are widespread in the southern North Atlantic (Leleu et al., 2016; Stolfova and

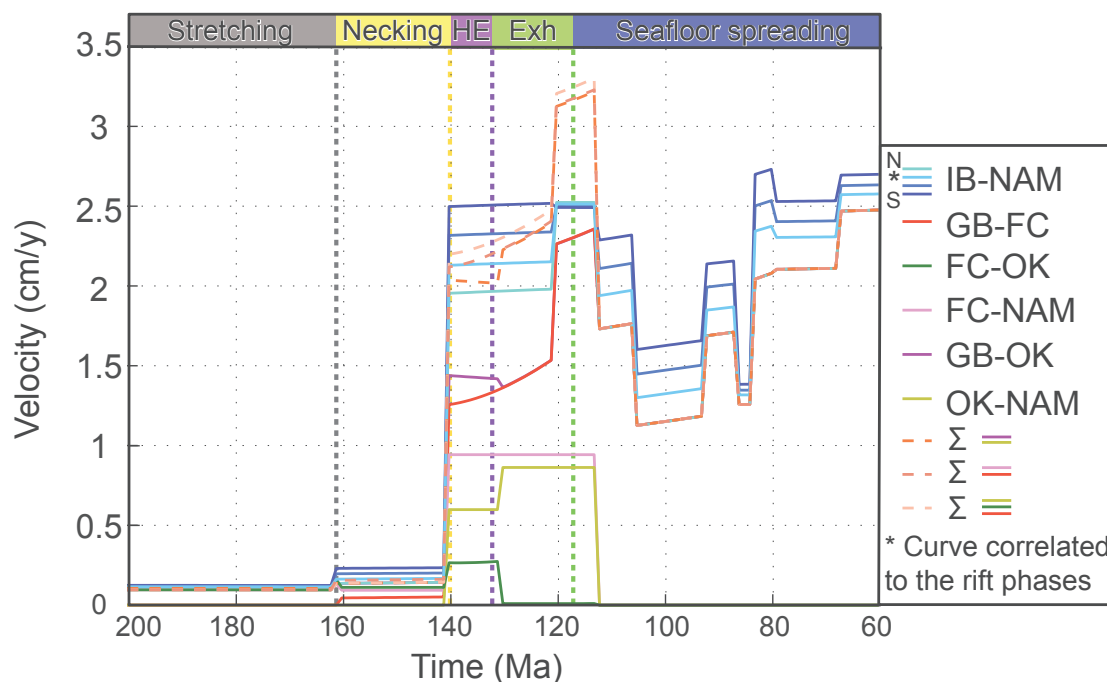


**Fig. III-10:** Extensional velocity of several micro-blocks and plates relative to different fixed plate (moving plate-fixed plate) the abbreviation are the same that in Fig. III-5 The different timing of the different rifting phase is taken from the Central Iberia Abyssal Plain and the northern Newfoundland Basin which are the conjugate margins drilled by ODP campaigns. The correlation between rifting phase and velocity can only be made on the second lighter blue line annotated with the star.

Shannon, 2009). This extensional deformation continues during Jurassic and Cretaceous in some basins but others like the Celtic Sea do not show this later overprint. How far these older rift systems are controlling the later, more localised Late Jurassic and Early Cretaceous rift systems remains, however, one of the intriguing questions.

### 6.3 Propagation and distribution of deformation modes

Our modelling of the opening of the southern North Atlantic enables us to discuss the propagation mode of each rift domain, the role of segmentation and the associated velocities. In the following paragraph we describe the velocities (full rate) of each deformation phase using the timing of the Iberia Abyssal Plain and its conjugate northern Newfoundland margin. The correlation with velocities is only possible for the blue line annotated with the star shown in Fig. III-10.

#### 6.3.1 Distributed rift deformation

During the stretching phase extension is not localised and the deformation is characterized by a wide rift mode (Buck, 1991) in which several half graben basins formed simultaneously (Fig. III-11cI). In the modelling the velocity of this phase is about 1.8 mm/y.

The proximal basins are mostly oriented perpendicularly to the main extension (e.g. Jeanne d'Arc Basin, Lusitanian Basin...). However crustal inheritances can influence the orientation and location of these basins (e.g. Kivu basin in the East African rift (Smets et al., 2016)). With the resolution of our model, it is too ambitious to discuss the influence of inheritance for the stretching phase.

### ***6.3.2 Necking and hyper-extension of the continental crust***

The necking process corresponds to the thinning of the continental crust and the excision of the ductile levels (Mohn et al., 2012). It also corresponds to the localisation of the deformation on a narrower zone (H-block Lavier and Manatschal, 2006), which will be later deformed during the hyper-extension phase. Therefore the volume of rocks between the two conjugate necking lines greatly impacts the final width of the thinned continental domain (necking domain and hyper-extended continental crust). During this deformation phase, extension appears to accelerate weakly to 3 mm/y. The duration of the necking phase is related to the strain rate and the thickness of the ductile levels in the crust (Sutra et al. 2012). Seismic and stratigraphic studies clearly present a northward younging of the onset of necking (Alves et al., 2009; Mohn et al., 2015) within several segments (Welford et al., 2010b). However, rigid plate kinematic modelling cannot well picture this propagation and segmentation as there is a unique rotation pole for Iberia. Each segment is limited by transfer faults, which seem to locate preferentially on Variscan terrane boundaries. The only difference in the velocities of Iberia relative to North America is the northward decreasing velocity, which is caused by the distance to the rotation pole. Nevertheless it should be noted that during this phase, deformation is not only accommodated on a single straight rift system (Fig. III-11cII). The deformation south of the Galicia Bank is accommodated to the north in two different rift systems (Orphan Basin and the Flemish Cap-Galicia Bank rift Fig. III-7A,B), which caused a major transfer zone south of the Flemish Cap potentially link to an inherited structure (Fig. III-8).

The transition from the necking to the hyper-extension phase is a change from a decoupled ductile plus brittle to a fully brittle/coupled deformation at the scale of the crust (Pérez-Gussinyé and Reston, 2001; Sutra and Manatschal, 2012). As a consequence, the main parameters controlling the crustal deformation during final rifting will be the frictional properties of the hyper-extended crust (Nirrengarten et al., 2016a). This event occurred around Berriasian time in the Iberia Abyssal plain and corresponds in our kinematic model to the major acceleration to 2.2 cm/y, which is within the range of slow spreading oceanic crust. This acceleration seems simultaneous along the entire margin based on the velocity extracted from the kinematic model (Fig. III-10). However, as highlighted by subsidence analysis (Mohn et



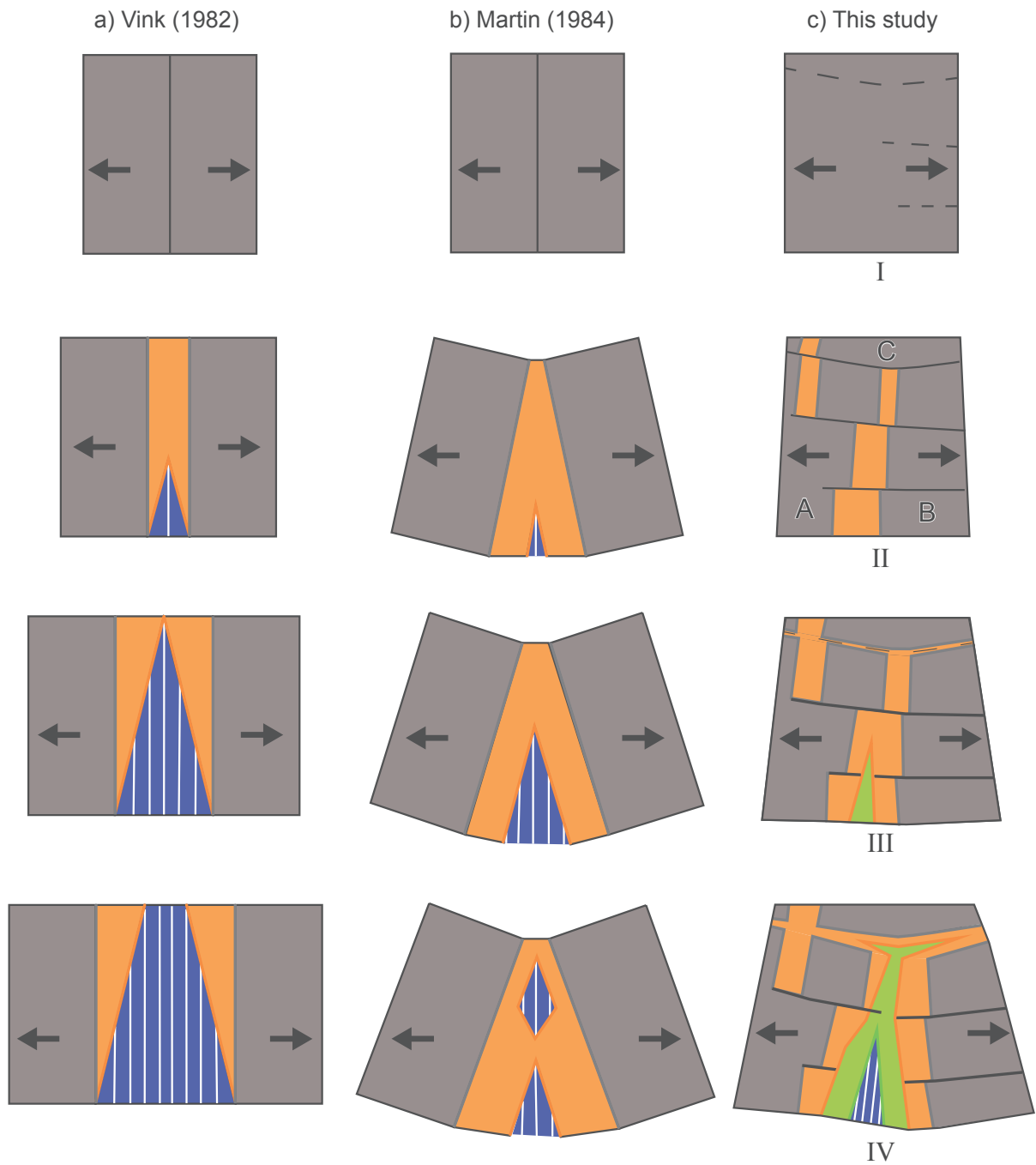


**Fig. III-11:** Propagation model of rift and seafloor spreading from a) Vink, (1982) b) Martin, (1984) c) proposed in this study with a three plates system. Note that the rotation of plate A and B does not imply compression at the tip of the propagation.

al., 2015), hyper-extension is not simultaneous and the simultaneous step in the velocity graph is due to the unique rotation pole for the Iberia plate. The acceleration is meaningful; observed on many rift systems and proposed to be related to the decay of the strength of the lithosphere approaching breakup (Brune et al., 2016). In other words, this acceleration and the transition to hyper-extension coincide with the mechanic and/or thermal/magmatic weakening of the lithosphere leading to lithospheric breakup. This acceleration is also present in the Orphan Basin, which is in our model kinematically linked to the extension in the Iberia-Newfoundland system.

### ***6.3.3 Mantle exhumation***

Onset of mantle exhumation (Fig. III-7A) corresponds to the creation of new basement surface and a change in the mode of extension, controlled mainly by exhumation faults associated with serpentinization. In our model, mantle exhumation is not linked to a change in the extension velocities. South of the Flemish Cap and Galicia Bank the exhumed mantle propagates northward in a very narrow V-shaped domain (the separation, is almost simultaneous from the NAGFZ to south of the Flemish Cap/ Galicia Bank), whereas a much wider V-shape exists between Galicia and Flemish Cap. This V-shape opening (Fig. III-11cIII) is compensated by extension in the Bay of Biscay and between the Irish Shelf and the northeastern Newfoundland margin, which also experiment a V-shape exhumation during Aptian and Early Albian time. The non-segmented propagation may indicate that inherited structures do not influence anymore the partitioning of the deformation. The exhumed material is homogenous and in the brittle field, therefore the deformation is only related to physical properties (frictional properties of exhuming material), the tectonic regime and magmatic additions. The transfer zone south of the Flemish Cap is still active during mantle exhumation, possibly due to the fact that extension is still partitioned between the Iberian-Newfoundland and Orphan systems.

### ***6.3.4 Oceanic seafloor spreading***

The initiation of the steady state seafloor spreading is related to onset of a stable localized spreading ridge (Gillard et al., 2016). Indeed, onset of seafloor spreading is associated with an increase of the magmatic budget, however velocities do not change. Seafloor spreading is propagating northward in a V-shape (Fig. III-7A, III-11cIV) with a velocity of 3.8 cm/y of the propagation tip. This V-shaped propagation occurred later in the Bay of Biscay and between the Irish and the northeast Newfoundland margin creating a triple ridge junction. If well-defined magnetic anomalies could be observed (note that this propagation occurs during a magnetic superchron) they might have been oblique to the COBs as observed in the Southern Atlantic

(Rabinowitz and LaBrecque, 1979) or the South China Sea (Barckhausen et al., 2014). Oceanic propagation does not always correspond to a V-shape and can also be segmented following oceanic transfer zone (e.g. Gulf of Aden Fournier et al., (2010), Woodlark Basin Taylor et al., (2009), South China Sea (Sibuet et al., 2016))

### ***6.3.5 Propagation model***

Onset of seafloor spreading is not instantaneous over a whole rift system and creates V-shape oceanic basins (e.g. South-Atlantic, Gulf of Aden, Red Sea, South-China Sea), hence the propagation modes have to be investigated. Some models propose a differential extension of the continental crust where rifted margins are wider toward the tip of the propagator (Vink, 1982 Fig. III-11a). However, it seems that the variation of the width of the margin is not systematic (Eagles et al., 2015). Another model proposes a V-shape propagation of rifts and breakup (Martin, 1984 Fig. III-11b), which implies a constant width of the margins along strike and compression at the tip of propagation. This compression is, however, not recorded. We modify the V-shape propagation model based on observations and kinematic modelling of the southern North Atlantic (Fig. III-11c). The initial rift phase is best described by a segmented propagation. Each segment has its own timing and is linked by transfer faults to its neighbour (Fig. III-11c). This segmentation may be related to crustal or lithospheric inheritance often reactivated in extensional settings (e.g. Sutra and Manatschal 2012; Tugend et al. 2014). The motion and the area formed during the necking phase are almost insignificant relative to large rigid plate kinematics (Brune et al., 2016), hence the relative differential extension along the propagation can be accommodated by intra-continental transfer zones. The exhumed mantle and seafloor spreading propagates in a V-shape style in the rifted domain implying a rotation of the two surrounding plates. However to avoid compression in front of the propagator obliquely oriented system are extending in transtensional mode .

## **7. CONCLUSION**

We re-evaluate the kinematic evolution of the southern North Atlantic by incorporating data and knowledge from hyper-extended rift systems. This study presents an innovative approach merging local constrains with large scale plate kinematic modelling, which is therefore less well constrained than restorations focused on oceanic magnetic anomalies only. The model presented corresponds to one possible solution aiming to conciliate the discrepancies raised on the kinematics of the Iberia plate (Barnett-Moore et al., 2016a). The present model is the first coherent model at the scale of the southern north Atlantic that reconciles the data available from the northern Iberia-Newfoundland margins and the field analysis of the Pyrenean system.

Beyond the study of the kinematic of the southern North Atlantic, this study addresses issues on the rift evolution and breakup propagation. This paper suggests that:

1) The partitioning of the deformation between several small rift systems can explain the Albo-Cenomanian extension in the Pyrenees.

2) The propagation of rift deformation during the necking phase is observable but accommodated within several segments bounded by transfer zones (e.g. Iberia-Newfoundland and Orphan rift systems).

3) Inherited sutures and transfer zones preferentially localise rift segments and transfer zones.

4) Mantle exhumation and seafloor spreading propagates in the southern North Atlantic in a V-shape style, but propagates with several segments in other areas (e.g. Gulf of Aden, Woodlark Basin).

5) The V-shape propagation implies rotation of the adjacent plate and compression behind the rotation pole. Here the compression is inhibited by transtensional opening of rift systems obliquely oriented to the spreading ridge in front of the propagation tip.

6) The initiation of a triple ridge junction at Aptian/Albian boundary could induce a regional magmatic activity and uplift..

## **ACKNOWLEDGEMENTS**

This project is financially supported by the MM4 consortium (BP, Conoco Phillips, Statoil, Petrobras, Total, Shell, BHP-Billiton, and BG). We acknowledge the constructive discussions during the consortium meetings. We thank the developers of the free software Gplates and QGis.

**SUPPLEMENTARY MATERIAL**

|                                       | A       | B     | C      | D      |
|---------------------------------------|---------|-------|--------|--------|
| Critical thinning factor ( $\gamma$ ) | 0.7     | 0.5   | 0.7    | 0.7    |
| Reference crustal thickness           | 37.5 km | 35 km | 35 km  | 40 km  |
| Breakup age                           | 112 Ma  | 54 Ma | 112 Ma | 112 Ma |
| Volcanic additions                    | 7 km    | 10 km | 7 km   | 7 km   |

**Table III-3:** Table of parameters used in the gravity inversion to perform the maps of Fig. III-3





---

## *CHAPITRE IV*

---



# ***DISCUSSION GÉNÉRALE***

Ce travail de thèse s'inscrit dans la thématique très vaste de l'analyse des processus de déformation des systèmes de rift. La déformation des systèmes de rift hyper-étirés est caractérisée par une évolution polyphasée due à des modifications physico-chimiques des roches déformées (Brune et al., 2014; Lavier and Manatschal, 2006). Cependant les processus physiques contrôlant chaque phase de déformation et particulièrement l'hyper-extension ne sont que partiellement compris. De plus l'évolution de ces différents modes de déformation n'a jamais été intégrée à un modèle cinématique permettant une visualisation dans le temps et dans l'espace. Ainsi ce travail de thèse contient deux objectifs distincts, le premier est de caractériser physiquement la phase d'hyper-extension afin d'expliquer la similarité des structures observées, le second est d'analyser le partitionnement et la propagation des modes de déformation dans le temps et dans l'espace.

Ces deux grandes questions scientifiques ont été abordées grâce aux exemples de marges hyper-étirées du sud de l'Atlantique Nord. Ces systèmes font partis des mieux imagés (Afilhado et al., 2008; Bullock and Minshull, 2005; Davy et al., 2016; Dean et al., 2015; Hopper et al., 2004), contiennent les reliques des marges pyrénéennes exposées à l'affleurement (Jammes et al., 2009; Lagabrielle and Bodinier, 2008) et possèdent des forages profonds (Sawyer, 1994; Tucholke and Sibuet, 2006). Ceci permet d'obtenir des observations représentatives et de créer des cartes de domaines précises (Fig. IV-1). Cependant l'évolution cinématique du sud de l'Atlantique Nord au Crétacé est controversée ce qui ne permet pas d'y intégrer la déformation de rift. Ainsi l'analyse des problèmes cinématiques a été une étape essentielle pour mener ce projet.

Ce dernier chapitre synthétise les résultats majeurs, répond aux questions à l'origine de ce travail et discute l'influence du mode de déformation sur l'architecture et l'évolution cinématique des marges hyper-étirées.

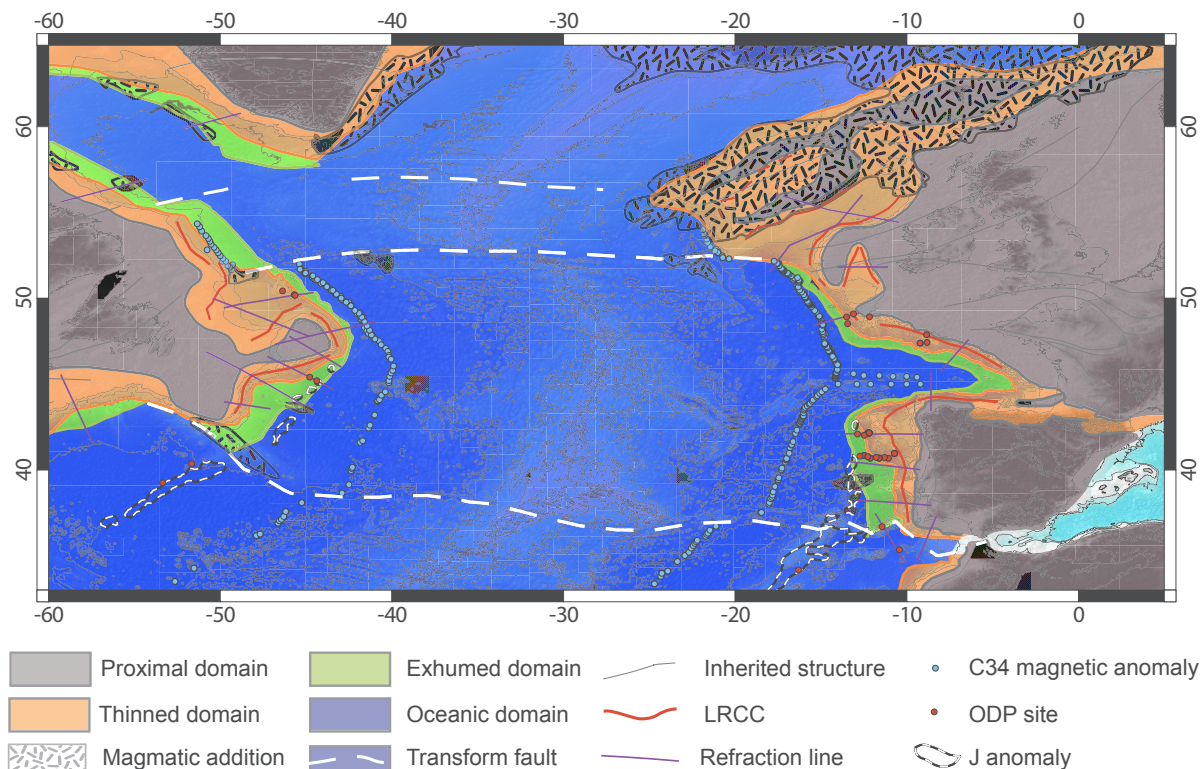


**Fig. IV-1:** Carte des domaines de rift du sud de l'Atlantique Nord

**Fig. IV-1:** Rift domains map of the southern North Atlantic

### 1. Quelle est la relation entre l'architecture de la terminaison continentale et son mode de déformation ? (Chap. I)

Les avancées techniques de la sismique réflexion et réfraction ont permis d'imager très nettement des structures crustales profondes, ainsi plusieurs transitions continent-océan du sud de l'Atlantique Nord ont été déterminées (e.g. Reston et al., 1996; Shillington et al., 2006; Sutra and Manatschal, 2012; Zelt et al., 2003). Ces données ont permis de distinguer les différents domaines des marges hyper-étirées en fonction de critères structuraux et compositionnels (Peron-Pinvidic et al., 2013; Sutra et al., 2013; Tugend et al., 2015b). De plus, alors que les domaines proximaux et d'étranglement présentent une certaine variabilité architecturale, le domaine de croûte hyper-étirée, qui constitue la terminaison crustale (ou prisme continental hyper-étiré) présente de grandes similitudes entre les différents exemples de marge. Ainsi Sutra et Manatschal (2012) observent un angle d'ouverture du prisme hyper-étiré constant d'environ  $11^\circ$  (Fig. 15). Cette observation implique un mode de déformation et des paramètres physiques communs à tous les systèmes hyper-étirés. Les observations de terrain et les forages profonds montrent que les roches de la croûte continentale hyper-étirée sont faillées, ont été altérées et contiennent des phylosilicates néoformés (Manatschal, 1999). La terminaison continentale des marges hyper-étirées est caractérisée par une forme prismatique. De plus la structure de ce prisme est dominée par des failles à faible pendage (Manatschal, 1999; Reston et al., 2007). Ces

observations indiquent un style structural cassant et un mécanisme de déformation frictionnel durant la dernière phase de déformation de la croûte continentale hyper-étirée. Seule la dernière phase de déformation crustale est uniquement cassante, les niveaux crustaux initialement ductiles deviennent fragiles durant l'amincissement à cause de l'hydratation et du refroidissement (Pérez-Gussinyé and Reston, 2001). Cette hydratation affecte également le matériel mantélique sous-jacent formant des minéraux de serpentine à faible friction permettant le glissement de la croûte continentale à l'interface manteau-croûte (Manatschal et al., 2006; Reston et al., 2007). Il est important de noter que le plus fort amincissement, qui est induit par la phase d'étranglement précédant l'hyper-extension est accommodé par des styles structuraux plus complexes mêlant des niveaux cassants et ductiles qui provoquent le boudinage de certaines couches rigides (Duretz et al., subm). La limite spatiale entre une déformation ductile plus cassante et une déformation uniquement cassante est la ligne de couplage (Sutra and Manatschal, 2012). Cette ligne définie grâce à des critères structuraux (Nirrengarten et al., 2016a; Sutra and Manatschal, 2012) correspond à la bordure du prisme continental hyper-étiré (côté continent). Le point d'exhumation forme la pointe distale du prisme et correspond à un changement de nature du toit du socle.

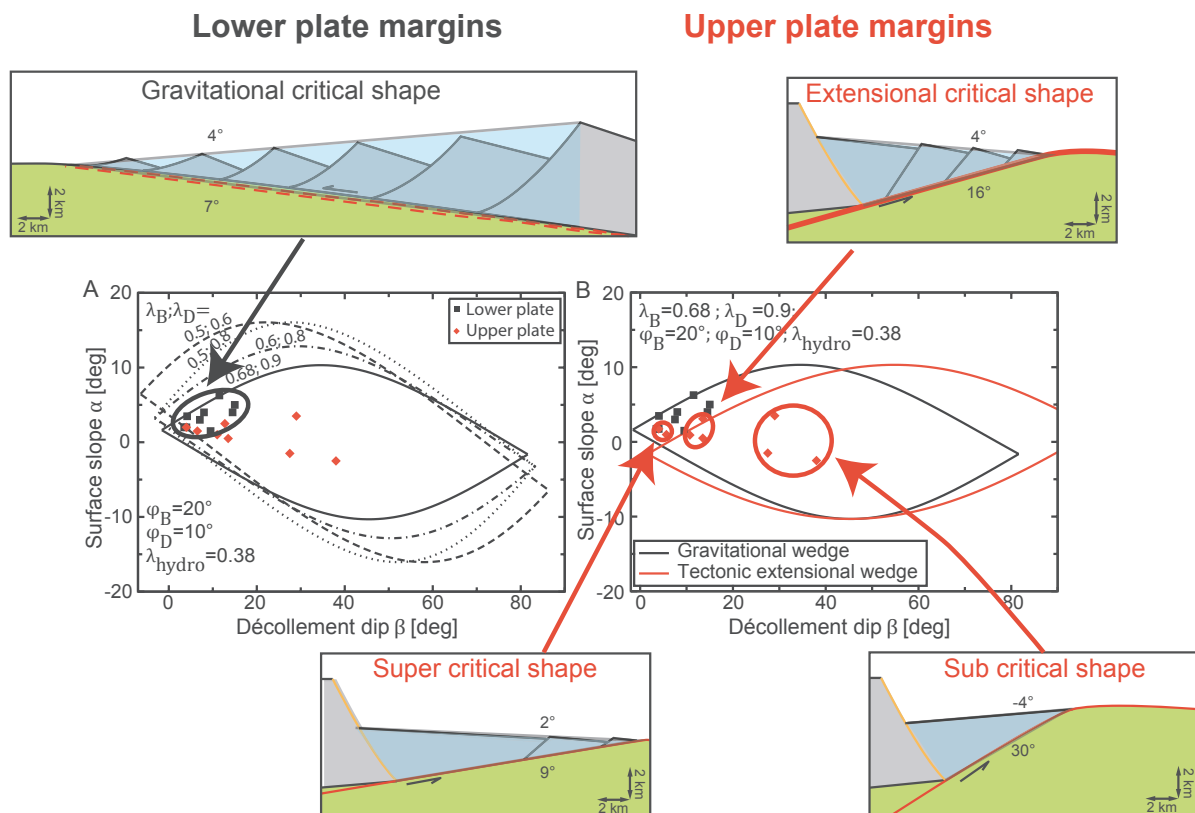


**Fig. IV-2:** Enveloppes de stabilité des prismes critiques de Coulomb gravitaire et tectonique extensionnel. Représentation schématique des architectures crustales théoriques des différents prismes continentaux hyper-étirés.

**Fig. IV-2:** Stability envelopes of gravitational and tectonic extensional critical Coulomb wedge. Cartoon of the theoretic crustal architectures of the different hyper-extended continental wedges.

Le prisme continental hyper-étiré ainsi défini possède les trois aspects fondamentaux de la théorie du prisme critique de Coulomb. La théorie du prisme critique de Coulomb est définie pour des prismes frictionnels glissant sur un décollement basal (Dahlen et al., 1984; Davis et al., 1983) et est particulièrement utilisée pour l'analyse des prismes d'accrétion et des chaînes d'avant-pays. Lister et al. (1986) propose un modèle de séparation crustale basé sur une faille de détachement séparant une marge « upper-plate » dans le toit du détachement et une marge de « lower-plate » dans le mur du détachement (Fig I-3A). Ceci implique des directions de mouvement opposées induisant la formation d'un prisme de Coulomb tectonique extensionnel (upper-plate) et un prisme gravitaire (lower-plate). La comparaison des angles de surface et basaux des prismes continentaux hyper-étirés avec la théorie du prisme de Coulomb paramétrée avec des frictions de phyllosilicate et des pressions de fluide typique de bassin sédimentaire, présente une très bonne corrélation. Les mesures des prismes de « lower-plate » se regroupent sur la limite supérieure du prisme gravitaire indiquant une forme critique. Alors que les mesures des prismes de « upper-plate » sont au-dessus, en-dessous ou au niveau de la limite critique (Fig . IV-2). Ces variations sont expliquées par l'évolution de la séparation continentale via la faille de détachement. Le décollement basal sous le prisme de lower plate est une zone de décollement et non un détachement tectonique ainsi la seule contrainte sur le prisme après la séparation continentale est gravitaire. La marge conjuguée est quant à elle délimitée du manteau par un détachement actif si le prisme au-dessus de ce détachement est dans les limites de stabilité au moment de la séparation continentale, ce prisme gardera cette architecture et ne sera pas déformé. Si le prisme est au-dessus de la limite de stabilité il sera déformé et réduira son angle d'ouverture jusqu'à atteindre la stabilité, ou si le détachement se délocalise dans le manteau exhumé (Gillard et al., 2016a) le prisme restera au-dessus des limites de stabilité. Cependant tous les prismes sont dans les limites de stabilité du prisme de Coulomb gravitaire (Fig. IV-2).

L'aspect particulièrement intéressant de l'application du prisme de Coulomb pour les marges hyper-étirées est la prédictibilité des structures et des architectures sédimentaires associées. En effet le domaine hyper-étiré est en premier lieu étiré et aminci par des failles en séquences migrantes vers le côté « upper-plate » (Ranero and Pérez-Gussinyé, 2010) et implique la formation d'éventail sédimentaire (Masini et al., 2011). Puis la déformation se localise sur une faille de détachement qui s'aplatit et induit des bassins à fort beta (Wilson et al., 2001) accompagnés de sédiments downlap sur la faille exhumée (Masini et al., 2011). Cette faille permet la séparation des deux prismes continentaux, le prisme de « lower-plate » se rééquilibre gravitairement alors que le prisme « upper-plate » est toujours actif. En effet le prisme « upper plate » se déforme via des failles en séquence orientées vers le continent qui

peuvent extraire des allochtones de croûte continentale (Fig. I-7). L'évolution de la séparation continentale et l'architecture des marges hyper-étirées peut être analysée grâce à la théorie du prisme de Coulomb qui permet d'être assez prédictive pour lier des observations sismiques ou de terrain dans un modèle cohérent. Cependant cette théorie ne s'applique que pour une phase très limitée du rift et ne permet pas de modéliser l'architecture globale de la marge qui induit des déformations ductiles.

## **2. Quelle est la nature de l'anomalie magnétique J ? Est-elle utilisable pour des restaurations cinématiques ? (Chap. II)**

Un des objectifs de cette thèse est d'analyser l'évolution 3D cinématique (de manière spatiale et temporelle) des systèmes de rift hyper-étiré du sud de l'Atlantique Nord. Ceci implique la connaissance de la position des continents avant et à la fin de la phase de rifting. Même si un consensus existe sur la position pré-rift et après l'anomalie C34 (~83Ma), la cinématique de la plaque ibérique reste très débattue en partie à cause de l'interprétation de l'anomalie J et de son intégration dans les modèles cinématiques. L'anomalie magnétique J au nord de la zone de fracture de Terre-Neuve Açores Gibraltar (ZFTAG) a été interprétée comme enregistrant un inversement de polarité du champ géomagnétique et représentant un isochrone (Rabinowitz et al., 1978) ou comme un excès magmatique survenu au moment de la rupture lithosphérique et étant ou non, un isochrone (Bronner et al., 2011). Cependant dans les deux cas des problèmes cinématiques subsistent, liés à une subduction pyrénéenne à l'Albien ou à une accélération brutale de la vitesse d'accrétion de la ride medio Atlantique (Bronner et al., 2012; Tucholke and Sibuet, 2012). La compilation de données sismiques montre que l'anomalie J n'est pas localisée tout au long de la marge à la transition croûte océanique manteau exhumé. Du sud au nord, l'anomalie J se situe sur de la croûte océanique, au niveau de la première croûte océanique et dans le domaine de manteau exhumé. De plus les données géochronologiques récoltées au niveau de l'anomalie J présentent une grande variété d'âges (Fig. IV-3). Ainsi il semblerait que l'anomalie J n'ait pas la même nature tout le long de la marge et que le magmatisme post et syn-rift contribue majoritairement au signal magnétique. Ceci implique que l'anomalie J n'est pas un isochrone, ni une limite de domaine continu le long de la marge elle résulte donc de processus polygéniques et polyphasés et ne peut pas servir dans les restaurations cinématiques. La linéarité et la symétrie de cette anomalie sont néanmoins surprenantes et pourraient potentiellement être potentiellement liées à une structure mantéllique héritée du rift qui canalise les additions magmatiques ou à des variations lithologiques ou minéralogiques pouvant affecter sa fertilité.

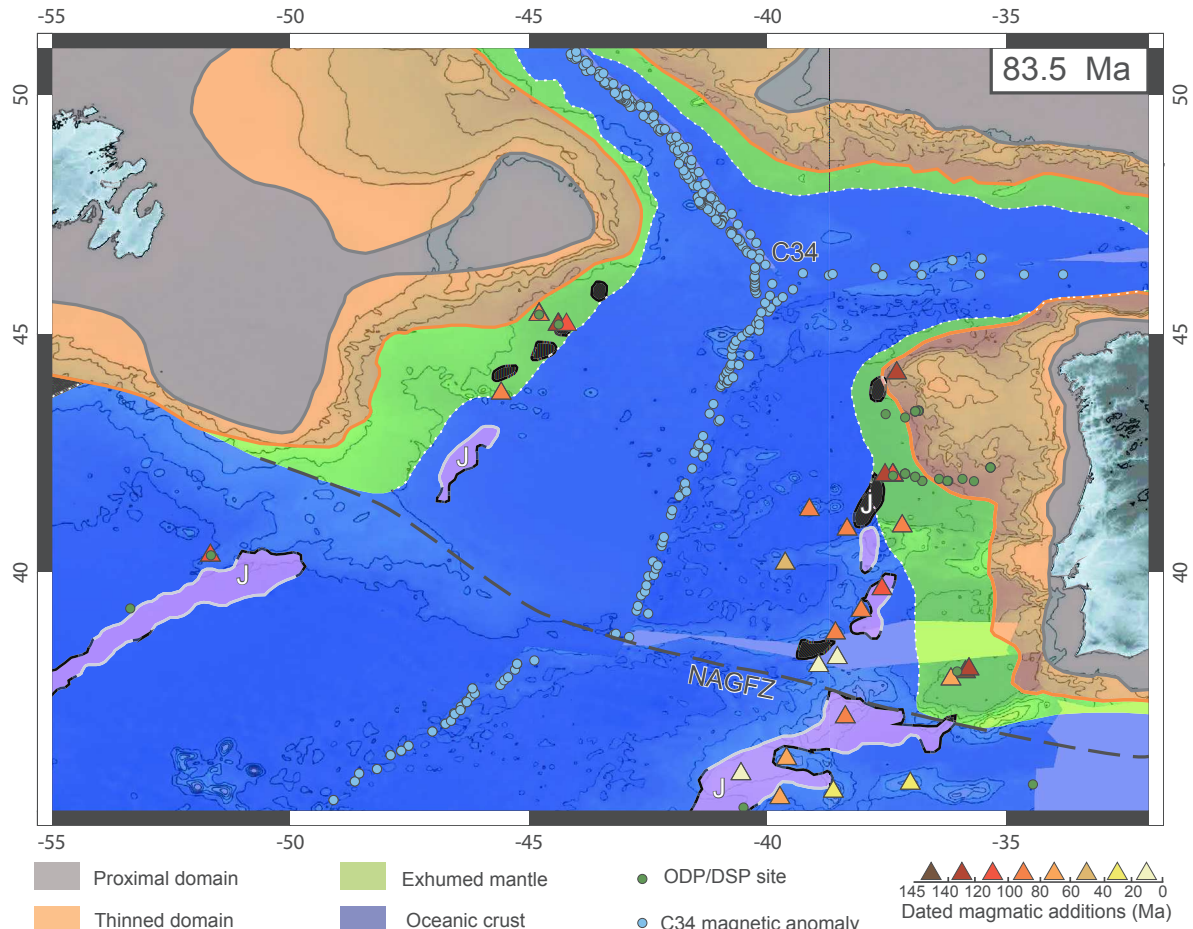


**Fig. IV-3:** Carte des domaines de rift restauré à l'isochrone C34 (83.5 Ma) présentant la partie positive de l'anomalie J ainsi qu'une compilation de données géochronologiques.

**Fig. IV-3:** Rift domains map restored at isochron C34 (83.5 Ma) showing the positive part of the J-anomaly and a compilation of geochronological data

Les anomalies magnétiques océaniques (Heirtzler et al., 1968) sont le pilier principal des études cinématiques sur les derniers 200 Ma (Seton et al., 2012). Cette technique est dans la plupart des cas très performante car les processus d'accrétion de la croûte océanique sont continus et se localisent uniquement au niveau de la dorsale. Cependant l'exemple de l'anomalie J montre qu'au niveau des zones de transition entre un océan et un continent ou sur des domaines océaniques affectés par du magmatisme hors axe le signal magnétique peut-être différent et ne pas être utilisable comme isochrone. Il faut déterminer le ou les processus tectono-magmatiques créant l'anomalie, en effet des événements magmatiques polyphasés et une déformation tectonique non localisée (Gillard et al., 2015) ne permettent pas un enregistrement continu et symétrique des inversions du champ géomagnétique. L'anomalie J dans le sud de l'Atlantique Nord n'est pas le seul exemple d'anomalie de forte amplitude situé à la transition continent-océan. En effet ce type d'anomalie est présent en Atlantique Centrale (ECMA) (Schettino and Turco, 2009), en Atlantique Sud (LMA/ anomalie G) (Moulin et al., 2010; Rabinowitz and LaBrecque, 1979) et sur les marges conjuguées australienne et antarctique (Tikku and

Cande, 1999). L'utilisation de ces anomalies magnétiques pour effectuer des restaurations cinématiques est dangereuse tant que deux points de blocage ne sont pas levés :1) comment déterminer si une anomalie magnétique n'est issue que d'une seule source, autrement dit est-ce que l'anomalie est formée par un seul processus et au même moment? Et 2) comment évolue tectono-magmatiquement le domaine transitionnel ? Coupler une analyse physique du signal magnétique avec des modèles tectoniques de mise en place du domaine transitionnel sur les deux marges conjuguées semble être une approche nécessaire avant l'utilisation des anomalies magnétiques pour des reconstructions cinématiques.

### **3. Comment se propage et est partitionnée la déformation dans un système de rift hyper-étiré ? (Chap. III)**

Le sud de l'Atlantique Nord (Fig. IV-1) a été choisi pour cette étude car il est bordé par de nombreuses marges hyper-étirées peu magmatiques qui sont parmi les mieux étudiées mondialement. Cependant l'évolution de ces domaines qui ont enregistré une extension de plus de 100 km, n'est que rarement prise en compte dans les restaurations cinématiques. Ainsi la majorité des reconstructions de plaques proposait une position au moment de la fermeture totale du système et une seconde à la première anomalie magnétique (Rowley and Lottes, 1988; Sibuet, 2004; Vissers and Meijer, 2012) cependant l'évolution des systèmes de rift est un processus polyphasé complexe qui se propage dans une lithosphère continentale. L'intégration des données des marges hyper-étirées dans les modèles cinématiques est ainsi nécessaire pour contraindre l'évolution cinématique des plaques voisines mais aussi pour analyser les interactions et la propagation de la déformation entre les différents systèmes des rifts.

La méthode développée (chap III) a permis de montrer les différents processus de propagation des systèmes de rift hyper-étirés du sud de l'Atlantique Nord. Ainsi la propagation du rift du sud de l'Atlantique Nord ne correspond ni au modèle d'extension continentale différentielle suivi d'une propagation océanique en V (Vink, 1982) ni à une propagation en V du système de rift et de l'océanisation (Martin, 1984) (Fig. IV-4 a,b). En effet la déformation de rift débute par la formation de bassins de rifts orientés perpendiculairement au sens d'extension et couvrant un large domaine, cependant ce système de rift (« wide rift » Buck, 1991) ne permet pas l'accommodation de grande quantité d'extension. L'étranglement localise la déformation sur des segments (Mohn et al., 2015) qui se connectent via des failles de transfert. Dans l'exemple du sud de l'Atlantique Nord la déformation se localise en premier dans le segment sud et se propage vers le nord segment par segment (Alves et al., 2009; Mohn et al., 2015). La répartition des zones de transfert peut être en partie liée à des héritages structuraux cependant leur relation est complexe et pas systématique. La phase d'hyper-extension marque dans les

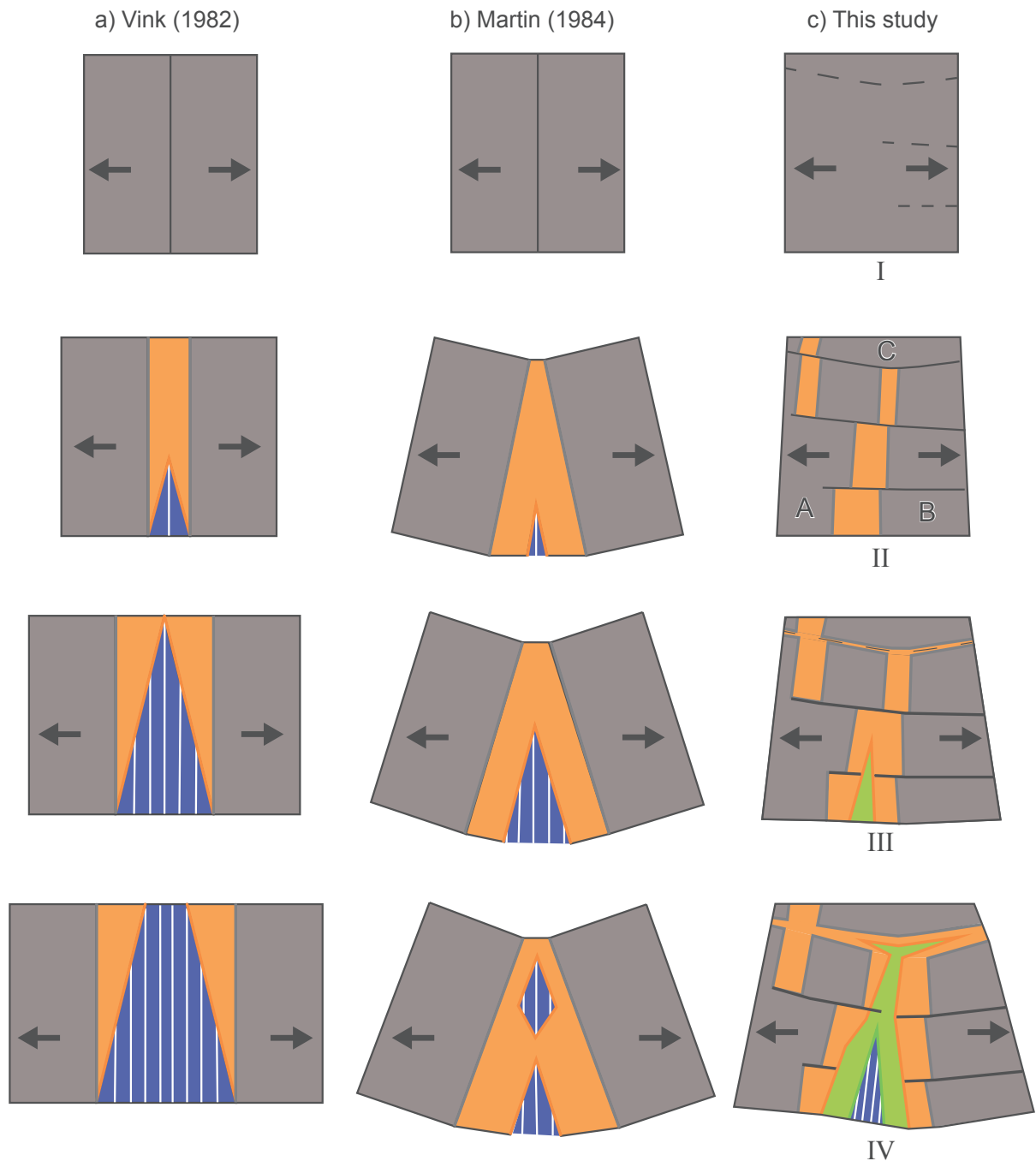


**Fig. IV-4:** Modèle de propagation de rift classique (Martin, 1984; Vink, 1982) et modèle de propagation proposé pour l'évolution du Sud de l'Atlantique Nord

**Fig. IV-4:** Classical rift propagation models (Martin, 1984; Vink, 1982) and the propagation model proposed for the evolution of the southern North Atlantic

modèles cinématiques une accélération de la déformation (Brune et al., 2016), cette phase de déformation suit à priori la segmentation formée durant la phase d'étranglement. Cette extension latérale est accommodée le long d'une grande faille de transfert en amont du segment le plus jeune, et permet l'extension lithosphérique sans rotation des blocs qui s'écartent. L'exhumation mantéllique et l'océanisation se propagent du sud vers le nord en forme de V et recoupent les segments, cette propagation implique une rotation des blocs et de la compression en amont du



propagateur (Martin, 1984). Cette compression est accommodée dans le cas du sud de l'Atlantique par de l'extension oblique au système principal, localisée dans le Golfe de Gascogne et entre les marges irlandaises et NE de Terre-Neuve (Fig. IV-4c). Ce système de propagation est adapté à une zone géographique précise en revanche la segmentation des zones d'étranglement est également observée sur les marges de Nouvelle-Ecosse et marocaines avec des inversions « upper-lower plate » à chaque segment (Louden et al., 2012) similaires aux observations de la marge armoricaine (Tugend et al., 2014). La propagation en V de la croûte océanique est dans d'autres systèmes beaucoup plus segmentée (e.g. Golfe d'Aden, Atlantique Sud, Bassin de Woodlark Autin et al., 2013; Benes et al., 1994; Stica et al., 2014) mais existe également similairement au sud de l'Atlantique Nord sans ces segments (e.g. Mer Rouge Augustin et al., 2014). L'océanisation en forme de V simple ou en V segmenté est potentiellement due à l'obliquité du système, de plus l'obliquité du rift semble favoriser l'ouverture océanique (Heine and Brune, 2014). Les zones de transfert sont un élément essentiel dans l'évolution d'un système de rift, ces failles peuvent être héritées ou néoformées et continuer à se développer durant le rift et l'expansion océanique ou stopper leur mouvement à n'importe quel stade (Bellahsen et al., 2013) ou alors les zones transformantes océaniques sont néoformées et n'ont pas d'héritage (Taylor et al., 2009). Ces zones partitionnent la propagation de la déformation et du magmatisme (Franke et al., 2007; Koopmann et al., 2014) et structurent l'extension entre deux plaques rigides, ce qui nécessite une attention particulière.

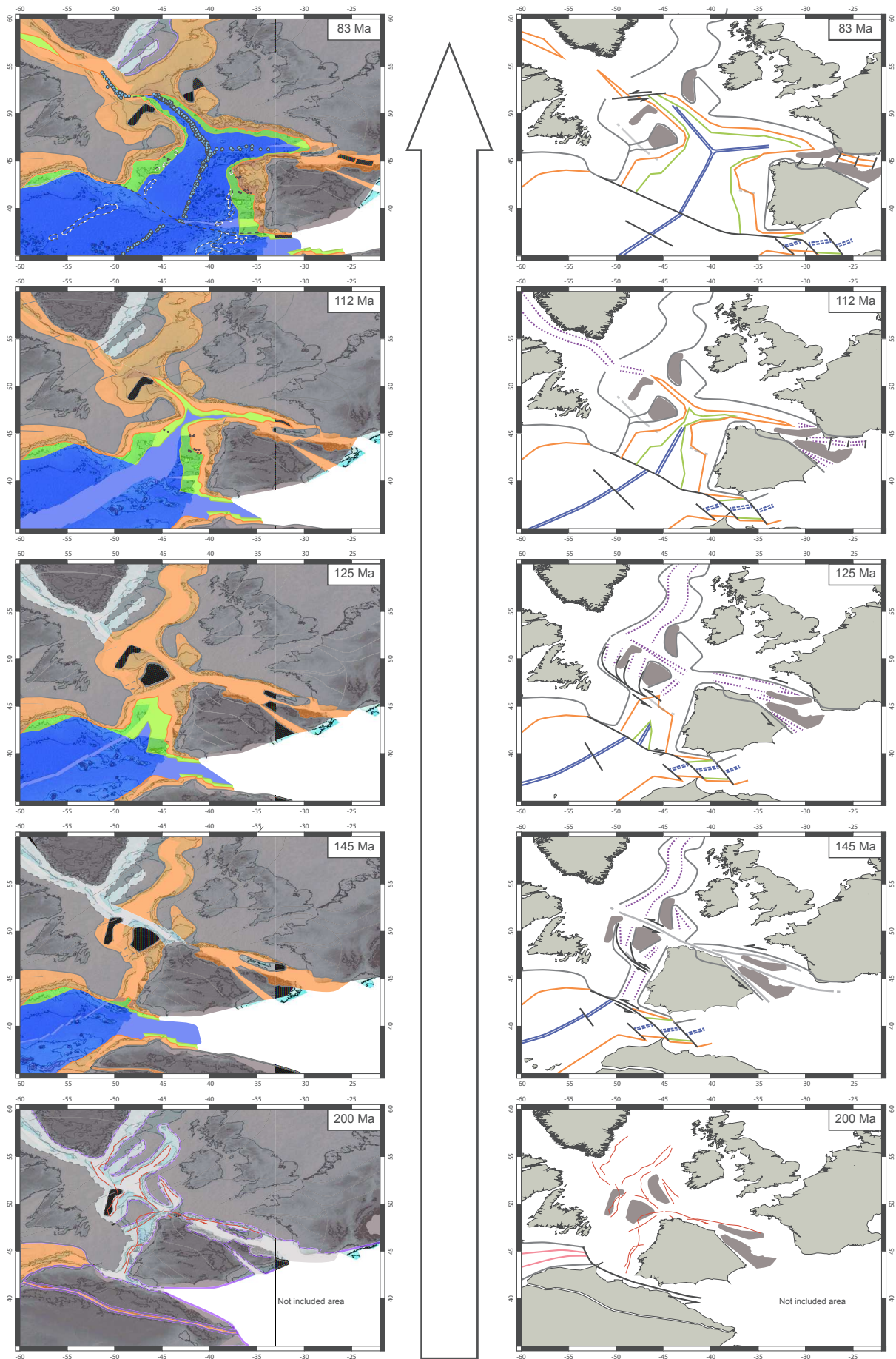
#### **4. Quelles sont les implications des rifts hyper-étirés sur l'évolution du sud de l'Atlantique Nord ? (Chap. III)**

Le sud de l'Atlantique Nord et particulièrement les mouvements de la plaque ibérique sont très contestés entre la communauté des cinématiciens et celle des géologues pyrénéens. L'anomalie J n'est ni un isochrone ni une limite de domaine et ne peut plus être utilisée dans les reconstructions cinématiques, ainsi seules les informations des rifts hyper-étirés contraignent le modèle. Le modèle proposé (Fig. IV-5) n'est sûrement pas le seul à concilier les informations disponibles, cependant il devra être éprouvé par l'acquisition de nouvelles données. Les implications de ce modèle sont grandes et demanderaient une investigation plus poussée, cependant il est possible de mettre en avant l'influence du partitionnement de la déformation parmi les différents systèmes de rift et de l'implication de la propagation océanique.

Ce modèle utilise le concept de partitionnement de la déformation entre la plaque eurasienne et ibérique via des micro-blocs continentaux rigides, développé par Tugend et al. (2015). L'intégration de ce concept dans un modèle cinématique quantitatif a permis de représenter l'extension Albienne des Pyrénées en compensant en partie l'extension de la ride

médio-atlantique par des mouvements latéraux sénestres entre le bloc d'Ebre et l'Ibérie. Ce partitionnement via des micro-blocs permet la formation de bassins de rift orientés obliquement aux contraintes tectoniques grande échelle. Cependant la déformation peut être également partitionnée en plusieurs systèmes concomitants alignés, séparés par un bloc rigide et orientés perpendiculairement à l'extension principale, ce qui est le cas entre les bassins d'Orphan et de Galice. L'évolution cinématique du sud de l'Atlantique Nord est contrôlée par le partitionnement de la déformation en plusieurs systèmes de rift hyper-étirés concomitants qui permettent d'expliquer des mouvements locaux différents de l'orientation de l'extension principale (e.g. les Pyrénées, le bassin de Porcupine). Le partitionnement de l'extension en plusieurs systèmes de rift séparés par des blocs rigides est un processus souvent lié à un héritage crustal ou lithosphérique (e.g. Mer de Barentsz, Mer de Chine du sud (Ding and Li, 2015; Gernigon et al., 2014). Cette observation est également valable pour le sud de l'Atlantique Nord, l'influence des structures variques, tardi-varisques et calédoniennes sont majeures. Par exemple la zone de fracture de Charlie Gibbs suit la suture de l'océan Iapetus (Buitter and Torsvik, 2014; Welford et al., 2012). De plus, les limites des domaines crustaux varisques (Balleve et al., 2014) semblent corrélés avec les zones de transfert segmentant les marges riftées d'Ibérie et de Terre-Neuve. Certains grands décrochements continentaux dextre tardi et post Varisque (Arthaud and Matte, 1977) sont également réutilisés en décrochement et dans le cas du Golfe de Gascogne facilite l'ouverture océanique. Cependant la quantité de mouvement accommodée par ces grands décrochements post-orogéniques est difficilement déterminable ainsi la position de l'Eurasie et du Groenland par rapport à l'Amérique du Nord au moment de l'initiation du rifting (Trias) est peu contrainte du fait de la zonale Biscaye-Labrador (Lefort, 1973).

Le modèle cinématique proposé apporte également une nouvelle interprétation de la surface stratigraphique Aptien/Albien qui est partiellement une discordance liée à la surrection du domaine (Soares et al., 2012; Tucholke et al., 2007). Cette surface et cette surrection sont observées sur toutes les marges du sud de l'Atlantique Nord ainsi qu'au niveau des continents (e.g. thermo-chronologie en Galice Grobe et al., 2014) et sont accompagnées de magmatisme alcalin (Jagoutz et al., 2007; Peron-Pinvidic et al., 2010). Cette discordance majeure a été interprétée comme la séparation de la lithosphère sous-continentale et la formation d'une croûte océanique normale entre Ibérie et Terre-Neuve (Tucholke et al., 2007). Cependant afin de conserver un faible écartement et un mouvement décrochant limité dans le domaine Pyrénéen l'initiation de l'accrétion océanique doit être antérieure. Le modèle présente néanmoins une structure particulière à la limite Aptien-Albien, en effet ce moment correspond à l'initialisation d'un point triple entre trois rides océaniques à l'extrême ouest du Golfe de Gascogne. La relation entre les points triples et les plumes mantélliques a été mise en évidence (Burke and Dewey,



1973), cependant il semblerait que l'activité mantéllique créant le bombement lithosphérique et le magmatisme alcalin délocalisé soit induite par la formation de ce point triple. Les processus et interactions entre les différents types de points triples au moment de la propagation océanique et l'activité magmatique de point chaud restent peu contraints (Franke, 2013; Koopmann et al., 2014). De plus les relations entre le magmatisme, l'évolution topographique et les processus géodynamiques de rupture lithosphérique et de point triple sont encore mal compris et demandent de nouvelles études.

**Fig. IV-5:** *Modèle cinématique de l'ouverture du sud de l'Atlantique Nord. La colonne de gauche présente l'évolution des domaines et celles de droite l'évolution des structures tectoniques associées. La légende est identique que dans la figure Fig. III-6*

**Fig. IV-5:** *Plate modeling of the opening of the southern North Atlantic. The left column presents the evolution of the domain and the right column the evolution of the associated tectonic structures. The Legend is the same as in figure Fig. III-6*



---

# ***CONCLUSION***

---



Ce travail de thèse met en évidence grâce aux exemples de marges hyper-étirées pauvre en magma du sud de l'Atlantique Nord l'évolution des processus de rifting dans le temps et dans l'espace. Cette étude s'est focalisée sur trois aspects majeurs 1) la déformation de la croûte continentale hyper-étirée, 2) la nature et les implications cinématiques de l'anomalie magnétique J et 3) la propagation et le partitionnement de la déformation des systèmes de rift hyper-étirés.

### **Comparaison entre la théorie du prisme critique de Coulomb et la terminaison de la croûte continentale**

- Les observations majeures à propos du domaine de croûte hyper-étirée sont : 1) ce domaine forme un prisme 2) limité à sa base par un niveau de décollement et 3) les déformations observées sont cassantes dues à l'hydratation et au refroidissement de la croûte continentale pendant l'amincissement. Ces trois observations sont les pré-requis pour appliquer la théorie du prisme critique de Coulomb.

- Les prismes continentaux hyper-étirés ont été comparés à un prisme critique de Coulomb. Le prisme situé dans le toit du détachement principal (« prisme d'upper plate ») est un prisme tectonique extensionnel car le cisaillement basal est orienté vers le continent. Alors que le prisme continental situé dans le mur du détachement (« prisme de lower plate ») est un prisme gravitaire car le cisaillement basal est orienté vers la pointe du prisme

- Les mesures des angles de surface et basaux d'un échantillon de prismes continentaux hyper-étirés et leur comparaison avec la théorie du prisme critique de Coulomb, paramétré avec des frictions de phyllosilicate et de serpentine et des pressions de fluides typiques de bassin sédimentaire, présentent une bonne corrélation. En effet, les mesures de prisme de lower plate s'alignent selon la limite supérieure de l'enveloppe de stabilité du prisme gravitaire indiquant une forme critique. Alors que le prisme de upper plate sont au-dessus, en-dessous et sur la limite de stabilité d'un prisme tectonique extensionnel, ce qui induit une évolution plus complexe liée à l'évolution du détachement sous-jacent.

- Cette théorie permet d'expliquer les failles orientées vers les continents sur le prisme d'upper plate ainsi que la formation des blocs allochtones. De plus cette théorie est prédictive et peut aider l'interprétation tectono-stratigraphique des domaines distaux en sismique et sur le terrain.



### **Nature et implications cinématiques de l'anomalie J**

- Le passage de la déformation en 2D à la déformation en 3D nécessite un modèle cinématique fiable ce qui n'est pas le cas du sud de l'Atlantique Nord, en raison de l'anomalie magnétique J qui est interprétée comme un isochrone ou comme une limite du domaine de croûte océanique.
- La compilation de données magnétiques, sismiques et géochronologiques montre que cette anomalie résulte d'évènements magmatiques polygéniques et polyphasés. Ainsi l'anomalie J n'est ni un isochrone ni une limite de domaine et ne peut être utilisée pour des reconstructions cinématiques.
- La détermination de la nature des premières anomalies magnétiques est une question récurrente dans les systèmes de marge pauvre en magma (e.g. Australie-Antartique, l'Atlantique Sud, Atlantique Central)

### **Evolution cinématique des systèmes hyper-étirés**

- Un nouveau modèle cinématique du sud de l'Atlantique Nord intégrant la déformation des rifts hyper-étirés est proposé. Cependant ce modèle n'est pas le but de l'étude mais un moyen de discuter les modes de propagation et des implications cinématiques des systèmes de rift hyper-étirés.
- La méthode utilisée pour reconstruire le sud de l'Atlantique Nord se base sur des observations locales très précises pour contraindre spatialement, via la taille pré-déformation des polygones continentaux, des zones moins étudiées.
- Le partitionnement et la segmentation des zones de rift semblent être un processus majeur au moment de la localisation de la déformation. Durant cette phase d'étranglement la déformation se propage via des segments, séparés des zones de transfert. Ainsi chaque segment a sa propre évolution.
- L'héritage lithosphérique est un paramètre important de la localisation des segments de rift. Ainsi les zones de transfert semblent se situer préférentiellement au niveau d'anciennes sutures orogéniques. De plus des anciens systèmes de décrochement post-orogénique sont réutilisés durant le rifting.
- La propagation de l'exhumation mantellique et de la croûte océanique semble beaucoup moins segmentée et forme un V se propageant du sud vers le nord. L'influence de l'héritage semble moins importante dans ces domaines.
- L'exemple du sud de l'Atlantique Nord permet de proposer un modèle de propagation où l'ouverture en forme de V entre Ibérie et Terre-Neuve n'induit pas de compression

à l'avant du propagateur car elle est compensée par de l'extension oblique dans le Golfe de Gascogne et entre les marges irlandaises et NE de Terre-Neuve.

- Cependant ces modes de propagation ne sont pas directement applicables de manière générale ainsi chaque système de rift doit être étudié spécifiquement.
- Ce modèle intègre l'extension (Aptien-Cenomanienne) du domaine Pyrénéen grâce à un partitionnement complexe de la déformation avec des blocs rigides séparés par des zones de rift.
- La discordance Aptien-Albien présente sur tout le sud de l'Atlantique Nord ne correspond pas à la rupture du manteau lithosphérique et à la création d'une croûte océanique, mais est potentiellement induite par la jonction de trois rides océaniques qui peuvent former un bombement et un magmatisme hors-axe généralisé.

Cette étude propose à partir de l'observation des marges hyper-étirées pauvres en magma du sud de l'Atlantique Nord, des modèles évolutifs 2D et 3D de la déformation de rift. Ces modèles ont un message général sur le mode de déformation de la croûte continentale hyper-étirée, sur la mise en place des anomalies magnétiques dans des domaines transitionnels, sur le partitionnement de la déformation de rift et sur la propagation de la rupture continentale dans des systèmes pauvres en magma. Cependant d'autres études seront nécessaires pour comprendre l'influence de chaque paramètre physique sur l'évolution du rift et notamment les paramètres liés à l'héritage crustal et mantéllique qui peuvent contrôler l'évolution rhéologique ainsi que la localisation et la quantité de magma. Les additions magmatiques dans les domaines transitionnels sont particulièrement importantes car elles créent des anomalies magnétiques pouvant être confondues avec des anomalies magnétiques océaniques, cependant leur mode de mise en place est différent. Ainsi la compréhension de l'évolution tectono-sédimentaire des domaines hyper-étirés et exhumés est particulièrement importante pour les reconstructions cinématiques. De plus les modèles de partitionnement et de propagation doivent être comparés à des contextes géologiques et à des contraintes aux limites différentes pour déterminer si ces modèles sont uniquement locaux ou généraux.



---

# *PERSPECTIVES*

---



Deux questions principales ont guidé ce travail. La première était de comprendre la relation entre l'architecture de la terminaison d'une marge et son mode de déformation. La seconde était de déterminer grâce aux exemples du sud de l'Atlantique Nord le partitionnement et la propagation de la déformation d'un système hyper-étiré dans le temps et dans l'espace. Des éléments de réponse ont été apportés à ces questions, grâce à la théorie du prisme critique de Coulomb et à une nouvelle méthode de reconstruction cinématique. En revanche ces avancées mènent vers de nouvelles questions: Comme par exemples comment mieux caractériser les propriétés physiques des marges hyper-étirées ? et comment évolue la déformation au cours du temps ? Ou comment modifier la méthode de restauration cinématique pour intégrer des domaines de rift repris en compression ?

### **1 Comment contraindre les paramètres physiques des marges hyper-étirées ? Comment évolue la déformation liée au prisme critique de Coulomb au cours du temps ?**

La forme finale du prisme continental hyper-étiré est comparable à la théorie du prisme critique de Coulomb. Cependant l'étude présentée utilise des paramètres de friction standards de minéraux phyllosilicatés et de serpentine. Ces deux paramètres pourraient être mieux contraints par l'analyse physique spécifique des roches du Leg ODP 103 (Boillot et al., 1988) échantillonnant la marge de Galice. De plus, de nouvelles données de sismique 3D (Bayrakci et al., 2016) permettront de mieux contraindre l'architecture de cette terminaison crustale. Ainsi cette marge semble un lieu de prédilection pour analyser en détail l'architecture crustale et approximer les pressions de fluides rencontrés dans ces domaines distaux. Ces pressions de fluides sont également importantes pour les circulations hydrothermales et les relations physico-chimiques associées. Une seconde perspective serait d'effectuer un modèle évolutif de la rupture continentale modéliser grâce à la version séquentielle de l'analyse limite (Yuan, 2016) afin de modéliser l'évolution de la rupture continentale en faisant varier les angles du détachement basal.

### **2 Comment modifier la méthode de restauration cinématique pour intégrer des domaines de rift repris en compression ? L'exemple de la Téthys Alpine**

L'évolution de la Téthys Alpine est liée à l'ouest à l'ouverture de l'Atlantique Central et Nord ainsi qu'à l'est à la fermeture de la Paléo-Téthys (Keppie, 2015). Ce système a été entièrement repris en compression à partir du Crétacé Inférieur (Frisch, 1981) mais la reconnaissance de différents types d'ophiolites a permis de mettre en évidence la présence de bassin océanique Jurassique et Crétacé Inférieur (Picazo et al., in press). Grâce au modèle

du sud de l'Atlantique Nord la position de l'Eurasie, de l'Ibérie et de l'Afrique du Nord sont contraintes, ainsi l'espace disponible entre la limite nord et sud est définie. Cependant des verrous scientifiques et techniques majeurs empêchent la création d'un modèle cinématique consensuel (Handy et al., 2010; Stampfli and Hochard, 2009; Vissers et al., 2013). Un des problèmes est la définition des blocs continentaux et leurs tailles au moment de l'ouverture du système, même si à l'heure actuelle les connaissances et la cartographie des unités paléogéographiques alpines sont plus ou moins définies (Schmid et al., 2004) elles ont subi un raccourcissement, ont été chevauchées et charriées par l'orogénèse alpine. Ainsi la taille et la forme pré-orogénique ne peuvent être estimées plus ou moins précisément. De plus l'ouverture des domaines océaniques a été proposée en utilisant la position du bloc adriatique fixe par rapport à l'Afrique (Vissers et al., 2013) cependant ce modèle utilise l'anomalie J comme l'isochrone M0. Une autre méthode serait de compiler les âges des gabbros ophiolitiques des Alpes et d'appliquer une vitesse d'extension de ride océanique lente (2cm/an) pour déterminer une quantité d'ouverture sans modèle cinématique (Beltrando pers. com.). Ces problèmes techniques sont cependant tout aussi intéressants que les problèmes cinématiques de la Téthys Alpine. Ainsi la détermination de la taille des blocs et l'extension maximum des domaines océaniques donnent des contraintes spatiales temporelles qui couplées avec des données stratigraphiques, géochronologiques et paléomagnétiques peuvent apporter de nouvelles idées sur le partitionnement de la déformation, les zones de transfert, la connexion des bassins océaniques et la relation entre l'ouverture à l'ouest et la fermeture à l'est de domaines océaniques.







---

# *RÉFÉRENCES*

---



- Afilhado, A., Matias, L., Shiobara, H., Hirn, A., Mendes-Victor, L., Shimamura, H., 2008. From unthinned continent to ocean: The deep structure of the West Iberia passive continental margin at 38°N. *Tectonophysics* 458, 9–50. doi:10.1016/j.tecto.2008.03.002
- Alves, T.M., Moita, C., Cunha, T., Ullnaess, M., Myklebust, R., Monteiro, J.H., Manuppella, G., 2009. Diachronous evolution of late jurassic-cretaceous continental rifting in the northeast atlantic (west iberian margin). *Tectonics* 28, n/a-n/a. doi:10.1029/2008TC002337
- Amante, C., Eakins, B.W., 2009. ETOPO1 1 Arc-Minute Global Relief Model: Procedures, Data Sources and Analysis. NOAA Tech. Memo. NESDIS NGDC-24. Natl. Geophys. Data Center, NOAA. doi:10.7289/V5C8276M
- Arthaud, F., Matte, P., 1977. Late Palaeozoic strike-slip faulting in Southern Europe and Northern Africa: Results of a right-lateral shear zone between the Appalachians and Urals. *Geol. Soc. Am. Bull.* 88, 1305–1320.
- Ask, M.V.S., 2001. Mechanical tests on claystone from Ocean Drilling Program Hole 1070A (Leg 173) - Implications for elevated pore-fluid pressure in sediments within the ocean-continent transition zone, West Iberia. *Mar. Geol.* 177, 395–410. doi:10.1016/S0025-3227(01)00173-6
- Aslanian, D., Moulin, M., 2012. Palaeogeographic consequences of conservative models in the South Atlantic Ocean. *Geol. Soc. London, Spec. Publ.* 369, 75–90. doi:10.1144/SP369.5
- Augustin, N., Devey, C.W., van der Zwan, F.M., Feldens, P., Tominaga, M., Bantan, R.A., Kwasnitschka, T., 2014. The rifting to spreading transition in the Red Sea. *Earth Planet. Sci. Lett.* 395, 217–230. doi:10.1016/j.epsl.2014.03.047
- Autin, J., Bellahsen, N., Husson, L., Beslier, M.-O., Leroy, S., D’Acremont, E., 2010a. Analog models of oblique rifting in a cold lithosphere. *Tectonics* 29, n/a-n/a. doi:10.1029/2010TC002671
- Autin, J., Bellahsen, N., Leroy, S., Husson, L., Beslier, M.-O., d’Acremont, E., 2013. The role of structural inheritance in oblique rifting: Insights from analogue models and application to the Gulf of Aden. *Tectonophysics* 607, 51–64. doi:10.1016/j.tecto.2013.05.041
- Autin, J., Leroy, S., Beslier, M.-O., d’Acremont, E., Razin, P., Ribodetti, A., Bellahsen, N., Robin, C., Al Toubi, K., 2010b. Continental break-up history of a deep magma-poor margin based on seismic reflection data (northeastern Gulf of Aden margin, offshore Oman). *Geophys. J. Int.* 180, 501–519. doi:10.1111/j.1365-246X.2009.04424.x
- Ballevre, M., Martinez Catalan, J.R., Lopez-Carmona, a., Pitra, P., Abati, J., Fernandez, R.D., Ducassou, C., Arenas, R., Bosse, V., Castineiras, P., Fernandez-Suarez, J., Gomez Barreiro, J., Paquette, J.-L., Peucat, J.-J., Poujol, M., Ruffet, G., Sanchez Martinez, S., 2014. Correlation of the nappe stack in the Ibero-Armorican arc across the Bay of Biscay: a joint French-Spanish project. *Geol. Soc. London, Spec. Publ.* 77–113. doi:10.1144/SP405.13
- Barckhausen, U., Engels, M., Franke, D., Ladage, S., Pubellier, M., 2014. Evolution of the South China Sea: Revised ages for breakup and seafloor spreading. *Mar. Pet. Geol.* 58, 599–611. doi:10.1016/j.marpetgeo.2014.02.022
- Barnett-Moore, N., Hosseinpour, M., Maus, S., 2016a. Assessing discrepancies between previous plate kinematic models of Mesozoic Iberia and their constraints. *Tectonics*. doi:10.1002/2015TC004019
- Barnett-Moore, N., Müller, R.D., Williams, S., Skogseid, J., Seton, M., 2016b. A reconstruction of the North Atlantic since the earliest Jurassic. *Basin Res.* doi:10.1111/br.12214
- Beard, J.S., Fullagar, P.D., Sinha, K., 2002. Gabbroic pegmatite intrusions, Iberia Abyssal Plain, ODP Leg 173, Site 1070: Magmatism during a transition from non-volcanic rifting to sea-floor spreading. *J. Petrol.* 43, 885–905. doi:10.1093/petrology/43.5.885
- Bellahsen, N., Leroy, S., Autin, J., Razin, P., d’Acremont, E., Sloan, H., Pik, R., Ahmed, a., Khanbari, K., 2013. Pre-existing oblique transfer zones and transfer/transform relationships in continental margins: New insights from the southeastern Gulf of Aden, Socotra Island, Yemen. *Tectonophysics* 607, 32–50. doi:10.1016/j.tecto.2013.07.036
- Beltrando, M., Stockli, D.F., Decarlis, A., Manatschal, G., 2015. A crustal-scale view at rift localization along the fossil Adriatic margin of the Alpine Tethys preserved in NW Italy. *Tectonics* n/a-n/a. doi:10.1002/2015TC003973
- Benes, V., Scott, S.D., Binns, R.A., 1994. Tectonics of rift propagation into a continental margin: Western Woodlark Basin, Papua New Guinea. *J. Geophys. Res.* 99, 4439. doi:10.1029/93JB02878
- Beslier, M.-O., Cornen, G. and Girardeau, J., 1996. Tectono-metamorphic evolution of peridotites from the ocean/continent transition of the Iberia Abyssal Plain margin. In: *Proceedings of the Ocean Drilling Program, 149 Scientific Results Ocean Drilling Program*, p. 397–412.

- Boillot, G., Grimaud, S., Mauffret, A., Mougénou, D., Kornprobst, J., Mergoïl-Daniel, J., Torrent, G., 1980. Ocean-continent boundary off the Iberian margin: A serpentinite diapir west of the Galicia Bank. *Earth Planet. Sci. Lett.* 48, 23–34. doi:10.1016/0012-821X(80)90166-1
- Boillot, G., Recq, M., Winterer, E.L., Meyer, A.W., Applegate, J., Baltuck, M., Bergen, J.A., Comas, M.C., Davies, T.A., Dunham, K., Evans, C.A., Girardeau, J., Goldberg, G., Haggerty, J., Jansa, L.F., Johnson, J.A., Kasahara, J., Loreau, J.P., Luna-Sierra, E., Moullade, M., Ogg, J., Sarti, M., Thuro, J., Williamson, M., 1987. Tectonic denudation of the upper mantle along passive margins: a model based on drilling results (ODP leg 103, western Galicia margin, Spain). *Tectonophysics* 132, 335–342. doi:10.1016/0040-1951(87)90352-0
- Boillot, G., Winterer, E.L., Al., E., 1988. Proceedings of the Ocean Drilling Program, 103 Scientific Results, Proceedings of the Ocean Drilling Program. Ocean Drilling Program. doi:10.2973/odp.proc.sr.103.1988
- Bonatti, E., Seyler, M., 1987. Crustal underplating and evolution in the Red Sea Rift: Uplifted gabbro/gneiss crustal complexes on Zabargad and Brothers Islands. *J. Geophys. Res.* 92, 12803. doi:10.1029/JB092iB12p12803
- Bond, C.E., Lunn, R.J., Shipton, Z.K., Lunn, A.D., 2012. What makes an expert effective at interpreting seismic images? *Geology* 40, 75–78. doi:10.1130/G32375.1
- Boyden, J.A., Müller, R.D., Gurnis, M., Torsvik, T.H., Clark, J.A., Turner, M., Ivey-Law, H., Watson, R.J., Cannon, J.J., 2011. Next-generation plate-tectonic reconstructions using GPlates 95–114. doi:10.1017/CBO9780511976308.008
- Bronner, A., Sauter, D., Manatschal, G., Péron-Pinvidic, G., Munschy, M., 2012. Reply to “Problematic plate reconstruction.” *Nat. Geosci.* 5, 677–677. doi:10.1038/ngeo1597
- Bronner, A., Sauter, D., Manatschal, G., Péron-Pinvidic, G., Munschy, M., 2011. Magmatic breakup as an explanation for magnetic anomalies at magma-poor rifted margins. *Nat. Geosci.* 4, 549–553. doi:10.1038/ngeo1201
- Brun, J.P., Beslier, M.O., 1996. Mantle exhumation at passive margins. *Earth Planet. Sci. Lett.* 142, 161–173. doi:10.1016/0012-821X(96)00080-5
- Brune, S., Heine, C., Pérez-Gussinyé, M., Sobolev, S. V., 2014. Rift migration explains continental margin asymmetry and crustal hyper-extension. *Nat. Commun.* 5, 4014. doi:10.1038/ncomms5014
- Brune, S., Williams, S.E., Butterworth, N.P., Müller, R.D., 2016. Abrupt plate accelerations shape rifted continental margins. *Nature* 1–4. doi:10.1038/nature18319
- Buck, W.R., 1991. Modes of continental lithospheric extension. *J. Geophys. Res.* 96, 20161. doi:10.1029/91JB01485
- Buck, W.R., 1988. Flexural Rotation of Normal Faults. *Tectonics* 7, 959. doi:10.1029/TC007i005p00959
- Buiter, S.J.H., Torsvik, T.H., 2014. A review of Wilson Cycle plate margins: A role for mantle plumes in continental break-up along sutures? *Gondwana Res.* 26, 627–653. doi:10.1016/j.gr.2014.02.007
- Bullard, E., Everett, J.E., Smith, a. G., 1965. The Fit of the Continents around the Atlantic. *Philos. Trans. R. Soc. A Math. Phys. Eng. Sci.* 258, 41–51. doi:10.1098/rsta.1965.0020
- Bullard, E., Masson, R., 1963. The magnetic field over the ocean, in: Hill, M.N. (Ed.), *The Sea*. New-York, pp. 175–217.
- Bullock, A.D., Minshull, T. a., 2005. From continental extension to seafloor spreading: crustal structure of the Goban Spur rifted margin, southwest of the UK. *Geophys. J. Int.* 163, 527–546. doi:10.1111/j.1365-246X.2005.02726.x
- Burke, K., Dewey, J.F., 1973. Plume-Generated Triple Junctions : Key Indicators in Applying Plate Tectonics to Old Rocks. *J. Geol.* 81, 406–433.
- Calvès, G., Torvela, T., Huuse, M., Dinkelman, M.G., 2012. New evidence for the origin of the Porcupine Median Volcanic Ridge: Early Cretaceous volcanism in the Porcupine Basin, Atlantic margin of Ireland. *Geochemistry, Geophys. Geosystems* 13, n/a-n/a. doi:10.1029/2011GC003852
- Canérot, J., 2008. Les Pyrénées: histoire géologique et itinéraires de découvertes.
- Cannat, M., 1996. How thick is the magmatic crust at slow spreading oceanic ridges ? Melt Migration in the Axial Lithosphere of Slow Spreading Ridges : Constraints from Ultramafic and Gabbroic Samples 101, 2847–2857.
- Cannat, M., Sauter, D., Mendel, V., Ruellan, E., Okino, K., Escartin, J., Combier, V., Baala, M., 2006. Modes of seafloor generation at a melt-poor ultraslow-spreading ridge. *Geology* 34, 605–608. doi:10.1130/G22486.1
- Capote, R., Muñoz, J.A., Simón, J.L., Arlegui, 2002. Alpine tectonics I: The Alpine system north of the Betic Cordillera, in: *The Geology of Spain*. Gibbons, W., and Moreno, M. T, pp. 367–400.
- Chappell, a. R., Kusznir, N.J., 2008. Three-dimensional gravity inversion for Moho depth at rifted

- continental margins incorporating a lithosphere thermal gravity anomaly correction. *Geophys. J. Int.* 174, 1–13. doi:10.1111/j.1365-246X.2008.03803.x
- Chenin, P., Manatschal, G., Lavier, L.L., Erratt, D., 2015. Assessing the impact of orogenic inheritance on the architecture, timing and magmatic budget of the North Atlantic rift system: a mapping approach. *J. Geol. Soc. London.* XXX, 2014–139. doi:10.1144/jgs2014-139
- Chevrot, S., Sylvander, M., Diaz, J., Ruiz, M., Paul, A., 2015. The Pyrenean architecture as revealed by teleseismic P-to-S converted waves recorded along two dense transects. *Geophys. J. Int.* 200, 1094–1105. doi:10.1093/gji/ggu400
- Chevrot, S., Villaseñor, A., Sylvander, M., Benahmed, S., Beucler, E., Cougoulat, G., Delmas, P., De Saint Blanquat, M., Díaz, J., Gallart, J., Grimaud, F., Lagabrielle, Y., Manatschal, G., Mocquet, A., Pauchet, H., Paul, A., Péquegnat, C., Quillard, O., Roussel, S., Ruiz, M., Wolyniec, D., 2014. High-resolution imaging of the Pyrenees and Massif Central from the data of the PYROPE and IBERARRAY portable array deployments. *J. Geophys. Res. Solid Earth* 119, 6399–6420. doi:10.1002/2014JB010953
- Chian, D., Louden, K.E., Reid, I., 1995. Crustal structure of the Labrador Sea conjugate margin and implications for the formation of nonvolcanic continental margins. *J. Geophys. Res.* 100, 24239. doi:10.1029/95JB02162
- Chian, D., Reid, I.D., Jackson, H.R., 2001. Crustal structure beneath Orphan Basin and implications for nonvolcanic continental rifting. *J. Geophys. Res.* 106, 10923. doi:10.1029/2000JB900422
- Choukroune, P., Le Pichon, X., Seguret, M., Sibuet, J., 1973. Bay of Biscay and Pyrennes. *Earth Planet. Sci. Lett.* 32, 109–118.
- Clark, S. a., Sawyer, D.S., Austin, J. a., Christeson, G.L., Nakamura, Y., 2007. Characterizing the Galicia Bank-Southern Iberia Abyssal Plain rifted margin segment boundary using multichannel seismic and ocean bottom seismometer data. *J. Geophys. Res. Solid Earth* 112, B03408. doi:10.1029/2006JB004581
- Clerc, C., Jolivet, L., Ringenbach, J.-C., 2015. Ductile extensional shear zones in the lower crust of a passive margin. *Earth Planet. Sci. Lett.* 431, 1–7. doi:10.1016/j.epsl.2015.08.038
- Clerc, C., Lagabrielle, Y., 2014. Thermal control on the modes of crustal thinning leading to mantle exhumation: Insights from the Cretaceous Pyrenean hot paleomargins. *Tectonics* 33, 1340–1359. doi:10.1002/2013TC003471
- Colletini, C., 2011. The mechanical paradox of low-angle normal faults: Current understanding and open questions. *Tectonophysics* 510, 253–268. doi:10.1016/j.tecto.2011.07.015
- Contrucci, I., Klingelhöfer, F., Perrot, J., Bartolome, R., Gutscher, M. -a., Sahabi, M., Malod, J., Rehault, J.-P., 2004. The crustal structure of the NW Moroccan continental margin from wide-angle and reflection seismic data. *Geophys. J. Int.* 159, 117–128. doi:10.1111/j.1365-246X.2004.02391.x
- Contrucci, I., Matias, L., Moulin, M., Géli, L., Klingelhofer, F., Nouzé, H., Aslanian, D., Olivet, J.-L., Réhault, J.-P., Sibuet, J.-C., 2004. Deep structure of the West African continental margin (Congo, Zaïre, Angola), between 5°S and 8°S, from reflection/refraction seismics and gravity data. *Geophys. J. Int.* 158, 529–553. doi:10.1111/j.1365-246X.2004.02303.x
- Cowie, L., Kuszniir, N., Manatschal, G., 2015. Determining the COB location along the Iberian margin and Galicia Bank from gravity anomaly inversion, residual depth anomaly and subsidence analysis. *Geophys. J. Int.* 203, 1355–1372. doi:10.1093/gji/ggv367
- Dafoe, L.T., Keen, C.E., Dickie, K., Williams, G.L., 2015. Regional stratigraphy and subsidence of Orphan Basin near the time of breakup and implications for rifting processes. *Basin Res.* n/a-n/a. doi:10.1111/bre.12147
- Dahlen, F.A., 1984. Noncohesive critical Coulomb wedges: An exact solution. *J. Geophys. Res.* 89, 10125. doi:10.1029/JB089iB12p10125
- Dahlen, F. a., Suppe, J., Davis, D., 1984. Mechanics of fold-and-thrust belts and accretionary wedges: Cohesive Coulomb Theory. *J. Geophys. Res.* 89, 10087. doi:10.1029/JB089iB12p10087
- Davis, M. and Kuszniir, N., 2002. Are buoyancy forces important during the formation of rifted margins? *Geophysical Journal International*, 149, p. 524–533, doi: 10.1046/j.1365-246X.2002.01666.x.
- Davis, D., Suppe, J., Dahlen, F.A., 1983. Mechanics of fold-and-thrust belts and accretionary wedges. *J. Geophys. Res.* 88, 1153. doi:10.1029/JB088iB02p01153
- Davy, R.G., Minshull, T.A., Bayrakci, G., Bull, J.M., Klaeschen, D., Papenberg, C., Reston, T.J., Sawyer, D.S., Zelt, C.A., 2016. Continental hyperextension, mantle exhumation and thin oceanic crust at the continent-ocean transition, West Iberia: new insights from wide-angle seismic. *J. Geophys. Res. Solid Earth.* doi:10.1002/2016JB012825
- De Graciansky, P.C., Poag, C.W., Cunningham, R., Loubere, P., Masson D.G., Mazzulo, J.M., Montadert, L.,

- Muller, C., Otsuka, K., Reynolds, L.A., Sigal, J., Snyder, S.W., Townsend, H.A., Vaos, S.P., Waples, D., 1985. The Goban Spur transect: Geologic evolution of a sediment-starved passive continental margin. *Geol. Soc. Am. Bull.* 96, 58. doi:10.1130/0016-7606(1985)96<58:TGSTGE>2.0.CO;2
- Dean, S.L., Sawyer, D.S., Morgan, J.K., 2015. Galicia Bank ocean–continent transition zone: New seismic reflection constraints. *Earth Planet. Sci. Lett.* 413, 197–207. doi:10.1016/j.epsl.2014.12.045
- Dean, S.M., Minshull, T.A., Whitmarsh, R.B., Louden, K.E., 2000. Deep structure of the ocean-continent transition in the southern Iberia Abyssal Plain from seismic refraction profiles: The IAM-9 transect at 40°20'N. *J. Geophys. Res.* 105, 5859. doi:10.1029/1999JB900301
- Desegaulx, P., Brunet, M.F., 1990. Tectonic subsidence of the Aquitaine Basin since Cretaceous times. *Bull. la Soc. Geol. Fr.* VI, 295–306. doi:10.2113/gssgfbull.VI.2.295
- Dick, H.J.B., Lin, J., Schouten, H., 2003. An ultraslow-spreading class of ocean ridge. *Nature* 426, 405–412. doi:10.1038/nature02128
- Dickie, K., Keen, C.E., Williams, G.L., Dehler, S.A., 2011. Tectonostratigraphic evolution of the Labrador margin, Atlantic Canada. *Mar. Pet. Geol.* 28, 1663–1675. doi:10.1016/j.marpetgeo.2011.05.009
- Ding, W., Li, J., 2015. Propagated rifting in the Southwest Sub-basin, South China Sea: Insights from analogue modelling. *J. Geodyn.* doi:10.1016/j.jog.2016.02.004
- Direen, N.G., Stagg, H.M.J., Symonds, P.A., Norton, I.O., 2013. Variations in rift symmetry: cautionary examples from the Southern Rift System (Australia–Antarctica). *Geol. Soc. London, Spec. Publ.* 369, 453–475. doi:10.1144/SP369.4
- Divins, D.L., 2003. Total Sediment Thickness of the World's Oceans & Marginal Seas.
- Driscoll, N.W., Karner, G.D., 1998. Lower crustal extension across the Northern Carnarvon basin, Australia: Evidence for an eastward dipping detachment. *J. Geophys. Res.* 103, 4975. doi:10.1029/97JB03295
- Duarte, J.C., Rosas, F.M., Terrinha, P., Schellart, W.P., Boutelier, D., Gutscher, M.A., Ribeiro, A., 2013. Are subduction zones invading the Atlantic? Evidence from the southwest Iberia margin. *Geology* 41, 839–842. doi:10.1130/G34100.1
- Duretz, T., Petri, B., Mohn, G., Schmalholz, S.M., Schenker, F.L., Müntener, O. subm Structural softening controls the evolution and architecture of passive margins
- Eagles, G., Pérez-Díaz, L., Scarselli, N., 2015. Getting over Continent Ocean boundaries. *Earth Sci. Rev.* 1–56. doi:10.1016/j.earscirev.2015.10.009
- Eldholm, O., Thiede, J., Taylor, E., 1989. Evolution of the Vøring Volcanic Margin, in: *Proceedings of the Ocean Drilling Program, 104 Scientific Results. Ocean Drilling Program.* doi:10.2973/odp.proc.sr.104.191.1989
- Enachescu, M.E., 2006. Structural Setting and Petroleum Potential of the Orphan Basin, offshore Newfoundland and Labrador. *Can. Soc. Explor. Geophys. Rec.* 31, 5–13.
- Epin, M.E., Manatschal, G., Amman, M., subm. What controls the reactivation or preservation of Ocean-Continent Transitions in orogens: Err-Platta nappes, SE Switzerland.
- Evans, C.A., Baltuck, M., 1988. Low-Temperature Alteration of Peridotite, Hole 637A, in: *Proceedings of the Ocean Drilling Program, 103 Scientific Results. Ocean Drilling Program,* pp. 235–239. doi:10.2973/odp.proc.sr.103.139.1988
- Evans, D. a D., Pisarevsky, S. a, 2008. Plate tectonics on early Earth ? Weighing the paleomagnetic evidence Plate tectonics on early Earth ? Weighing the paleomagnetic evidence. *Geol. Soc. Am.* 440, 249–263. doi:10.1130/2008.2440(12).
- Féraud, G., Beslier, M.-O., Cornen, G., 1996. <sup>40</sup>Ar/<sup>39</sup>Ar dating of gabbros from the ocean/continent transition of the western Iberia Margin: preliminary results, in: *Proceedings of the Ocean Drilling Program, 149 Scientific Results. Ocean Drilling Program.* doi:10.2973/odp.proc.sr.149.224.1996
- Féraud, G., York, D., Mével, C., Cornen, G., Hall, C.M., Auzende, J.-M., 1986. Additional <sup>40</sup>Ar-<sup>39</sup>Ar dating of the basement and the alkaline volcanism of Gorrige Bank (Atlantic Ocean). *Earth Planet. Sci. Lett.* 79, 255–269. doi:10.1016/0012-821X(86)90184-6
- Florineth, D., Froitzheim, N., 1994. Transition from continental to oceanic basement in the evidence for Early Cretaceous opening of the Valais ocean. *Schweiz. Miner. petrogr.* 74, 437–448.
- Fossen, H., 2010. *Structural Geology.* Cambridge University Press, Cambridge. doi:10.1017/CBO9780511777806
- Fournier, M., Chamot-Rooke, N., Petit, C., Huchon, P., Al-Kathiri, A., Audin, L., Beslier, M.O., D'Acremont, E., Fabbri, O., Fleury, J.M., Khanbari, K., Lepvrier, C., Leroy, S., Maillot, B., Merkouriev, S., 2010. Arabia-Somalia plate kinematics, evolution of the Aden-Owen Carlsberg triple junction, and opening of the Gulf of Aden. *J. Geophys. Res. Solid Earth* 115, 1–24. doi:10.1029/2008JB006257
- Franke, D., 2013. Rifting, lithosphere breakup and volcanism: Comparison of magma-poor and volcanic

- rifted margins. *Mar. Pet. Geol.* 43, 63–87. doi:10.1016/j.marpetgeo.2012.11.003
- Franke, D., Neben, S., Ladage, S., Schreckenberger, B., Hinz, K., 2007. Margin segmentation and volcano-tectonic architecture along the volcanic margin off Argentina/Uruguay, South Atlantic. *Mar. Geol.* 244, 46–67. doi:10.1016/j.marpetgeo.2007.06.009
- Franke, D., Savva, D., Pubellier, M., Steuer, S., Mouly, B., Auxietre, J.-L., Meresse, F., Chamot-Rooke, N., 2014. The final rifting evolution in the South China Sea. *Mar. Pet. Geol.* 58, 704–720. doi:10.1016/j.marpetgeo.2013.11.020
- Frizon de Lamotte, D., Raulin, C., Mouchot, N., Wrobel-Daveau, J.-C., Blanpied, C., Ringenbach, J.-C., 2011. The southernmost margin of the Tethys realm during the Mesozoic and Cenozoic: Initial geometry and timing of the inversion processes. *Tectonics* 30, 1–22. doi:10.1029/2010TC002691
- Froitzheim, N., Rubatto, D., 1998. Continental breakup by detachment faulting: field evidence and geochronological constraints (Tasna nappe, Switzerland). *Terra Nov.* 10, 171–176. doi:10.1046/j.1365-3121.1998.00187.x
- Funk, T., 2004. Crustal structure of the northern Nova Scotia rifted continental margin (eastern Canada). *J. Geophys. Res.* 109, B09102. doi:10.1029/2004JB003008
- Funk, T., Hopper, J.R., Larsen, H.C., Loudon, K.E., Tucholke, B.E., Holbrook, W.S., 2003. Crustal structure of the ocean-continent transition at Flemish Cap: Seismic refraction results. *J. Geophys. Res.* 108, 2531. doi:10.1029/2003JB002434
- Gabrielsen, R., Odinsen, T., Grunnaleite, I., 1999. Structuring of the Northern Viking Graben and the Møre Basin; the influence of basement structural grain, and the particular role of the Møre-Trøndelag Fault Complex. *Mar. Pet. Geol.* 16, 443–465. doi:10.1016/S0264-8172(99)00006-9
- Gaina, C., Roest, W.R., Müller, R.D., 2002. Late Cretaceous Cenozoic deformation of northeast Asia. *Earth Planet. Sci. Lett.* 197, 273–286.
- Gee, J.S., Kent, D.V., 2007. Source of Oceanic Magnetic Anomalies and the Geomagnetic Polarity Timescale. *Treatise Geophys.* 5, 455–507.
- Geoffroy, L., 2005. Volcanic passive margins. *Comptes Rendus Geosci.* 337, 1395–1408. doi:10.1016/j.crte.2005.10.006
- Gerlings, J., Loudon, K.E., Jackson, H.R., 2011. Crustal structure of the Flemish Cap Continental Margin (eastern Canada): an analysis of a seismic refraction profile. *Geophys. J. Int.* 185, 30–48. doi:10.1111/j.1365-246X.2011.04931.x
- Gerlings, J., Loudon, K.E., Minshull, T. a., Nedimović, M.R., 2012. Flemish Cap-Goban Spur conjugate margins: New evidence of asymmetry. *Geology* 40, 1107–1110. doi:10.1130/G33263.1
- Gernigon, L., Brönnner, M., Roberts, D., Olesen, O., Nasuti, a., Yamasaki, T., 2014. Crustal and basin evolution of the southwestern Barents Sea: From Caledonian orogeny to continental breakup. *Tectonics* 33, 347–373. doi:10.1002/2013TC003439
- Gillard, M., Autin, J., Manatschal, G., 2016a. Fault systems at hyper-extended rifted margins and embryonic oceanic crust: Structural style, evolution and relation to magma. *Mar. Pet. Geol.* doi:10.1016/j.marpetgeo.2016.05.013
- Gillard, M., Autin, J., Manatschal, G., 2015. Crustal structure and tectono-magmatic evolution of the final stages of rifting along the deep conjugate Australian-Antarctic margins: constraints from seismic observations. *Tectonics* 753–783. doi:10.1002/2015TC003850
- Gillard, M., Manatschal, G., Autin, J., 2016b. How can asymmetric detachment faults generate symmetric Ocean Continent Transitions? *Terra Nov.* 28, 27–34. doi:10.1111/ter.12183
- Gong, Z., Langereis, C.G., Mullender, T.A.T., 2008. The rotation of Iberia during the Aptian and the opening of the Bay of Biscay. *Earth Planet. Sci. Lett.* 273, 80–93. doi:10.1016/j.epsl.2008.06.016
- Gouiza, M., Hall, J., Welford, J.K., 2016. Tectono-stratigraphic evolution and crustal architecture of the Orphan Basin during North Atlantic rifting. *Int. J. Earth Sci.* doi:10.1007/s00531-016-1341-0
- Gradstein, F.M., Ogg, J.G., Smith, A., 2004. *A Geologic Time Scale 2004*, Cambridge. ed.
- Grobe, R.W., Alvarez-Marrón, J., Glasmacher, U.A., Stuart, F.M., 2014. Mesozoic exhumation history and palaeolandscape of the Iberian Massif in eastern Galicia from apatite fission-track and (U+Th)/He data. *Int. J. Earth Sci.* 103, 539–561. doi:10.1007/s00531-013-0976-3
- Handy, M.R., Schmid, S., Bousquet, R., Kissling, E., Bernoulli, D., 2010. Reconciling plate-tectonic reconstructions of Alpine Tethys with the geological-geophysical record of spreading and subduction in the Alps. *Earth-Science Rev.* 102, 121–158. doi:10.1016/j.earscirev.2010.06.002
- Hart, S.R., Blusztajn, J., 2006. Age and geochemistry of the mafic sills, ODP site 1276, Newfoundland margin. *Chem. Geol.* 235, 222–237. doi:10.1016/j.chemgeo.2006.07.001
- Hauptert, I., Manatschal, G., Decarlis, A., Unternehr, P., 2016. Upper-plate magma-poor rifted margins: Stratigraphic architecture and structural evolution. *Mar. Pet. Geol.* 69, 241–261. doi:10.1016/j.



- marpetgeo.2015.10.020
- Heine, C., Brune, S., 2014. Oblique rifting of the Equatorial Atlantic: Why there is no Saharan Atlantic Ocean. *Geology* 42, 211–214. doi:10.1130/G35082.1
- Heine, C., Zoethout, J., Müller, R.D., 2013. Kinematics of the South Atlantic rift. *Solid Earth* 4, 215–253. doi:10.5194/se-4-215-2013
- Heirtzler, J.R., Dickson, G.D., Herron, E.M., Pitman III, W.C., Le Pichon, X., 1968. Marine magnetic anomalies, geomagnetic field reversals, and motion of the ocean floor and continents. *J. Geophys. Res.* 73.
- Henning, A.T., Sawyer, D.S., Templeton, D.C., 2004. Exhumed upper mantle within the ocean-continent transition on the northern West Iberia margin: Evidence from prestack depth migration and total tectonic subsidence analyses. *J. Geophys. Res. Solid Earth* 109, B05103. doi:10.1029/2003JB002526
- Hitchen, K., 2004. The geology of the UK Hatton-Rockall margin. *Mar. Pet. Geol.* 21, 993–1012. doi:10.1016/j.marpetgeo.2004.05.004
- Hopper, J.R., Funck, T., Tucholke, B.E., 2007. Structure of the Flemish Cap margin, Newfoundland: insights into mantle and crustal processes during continental breakup. *Geol. Soc. London, Spec. Publ.* 282, 47–61. doi:10.1144/SP282.3
- Hopper, J.R., Funck, T., Tucholke, B.E., Larsen, H.C., Holbrook, W.S., Loudon, K.E., Shillington, D., Lau, H., 2004. Continental break-up and the onset of ultraslow seafloor spreading off Flemish Cap on the Newfoundland rifted margin. *Geology* 32, 93–96. doi:10.1130/G19694.1
- Hosseinpour, M., Müller, R.D., Williams, S.E., Whittaker, J.M., 2013. Full-fit reconstruction of the Labrador Sea and Baffin Bay. *Solid Earth Discuss.* 5, 917–962. doi:10.5194/sed-5-917-2013
- Huisman, R., Beaumont, C., 2011. Depth-dependent extension, two-stage breakup and cratonic underplating at rifted margins. *Nature* 473, 74–8. doi:10.1038/nature09988
- Huisman, R.S., 2003. Symmetric and asymmetric lithospheric extension: Relative effects of frictional-plastic and viscous strain softening. *J. Geophys. Res.* 108, 2496. doi:10.1029/2002JB002026
- Huisman, R.S., Beaumont, C., 2014. Rifted continental margins: The case for depth-dependent extension. *Earth Planet. Sci. Lett.* 407, 148–162. doi:10.1016/j.epsl.2014.09.032
- Huisman, R.S., Beaumont, C., 2008. Complex rifted continental margins explained by dynamical models of depth-dependent lithospheric extension. *Geology* 36, 163. doi:10.1130/G24231A.1
- Jagoutz, O., Müntener, O., Manatschal, G., Rubatto, D., Péron-Pinvidic, G., Turrin, B.D., Villa, I.M., 2007. The rift-to-drift transition in the North Atlantic: A stuttering start of the MORB machine? *Geology* 35, 1087–1090. doi:10.1130/G23613A.1
- Jammes, S., 2009. Processus d'amincissement crustal en contexte transtensif: L'exemple du Golfe de Gascogne et des Pyrénées. Université de Strasbourg.
- Jammes, S., Manatschal, G., Lavier, L., Masini, E., 2009. Tectonosedimentary evolution related to extreme crustal thinning ahead of a propagating ocean: Example of the western Pyrenees. *Tectonics* 28. doi:10.1029/2008TC002406
- Jolivet, L., Gorini, C., Smit, J., Leroy, S., 2015. Continental breakup and the dynamics of rifting in back-arc basins: The Gulf of Lion margin. *Tectonics* 34, 662–679. doi:10.1002/2014TC003570
- Karig, D.E., 1996. Uniaxial reconsolidation tests on porous sediments: mudstones from Site 897, in: Whitmarsh, R.B., Sawyer, D.S., Klaus A., M.D.G. (Ed.), *Proceedings of ODP Science Results*. pp. 363–373.
- Keen, C.E., Dafoe, L.T., Dickie, K., 2014. A volcanic province near the western termination of the Charlie-Gibbs Fracture Zone at the rifted margin, offshore northeast Newfoundland. *Tectonics* 33, 1133–1153. doi:10.1002/2014TC003547
- Kimbell, G.S., Ritchie, J.D., Henderson, a. F., 2010. Three-dimensional gravity and magnetic modeling of the Irish sector of the NE Atlantic margin. *Tectonophysics* 486, 36–54. doi:10.1016/j.tecto.2010.02.007
- Klitgord, K.D., Schouten, H., 1986. Plate kinematics of the central Atlantic. *Geol. North Am.* 1000, 351–378.
- Kneller, E. a., Johnson, C. a., Karner, G.D., Einhorn, J., Queffelec, T. a., 2012. Inverse methods for modeling non-rigid plate kinematics: Application to mesozoic plate reconstructions of the Central Atlantic. *Comput. Geosci.* 49, 217–230. doi:10.1016/j.cageo.2012.06.019
- Koopmann, H., Brune, S., Franke, D., Breuer, S., 2014. Linking rift propagation barriers to excess magmatism at volcanic rifted margins. *Geology*. doi:10.1130/G36085.1
- Kusznir, N.J., Hunsdale, R., Roberts, A.M., 2004. Timing of depth-dependent lithosphere stretching on the S. Lofoten rifted margin offshore mid-Norway: Pre-breakup or post-breakup? *Basin Res.* 16, 279–296. doi:10.1111/j.1365-2117.2004.00233.x

- Labails, C., Olivet, J.-L., Aslanian, D., Roest, W.R., 2010. An alternative early opening scenario for the Central Atlantic Ocean. *Earth Planet. Sci. Lett.* 297, 355–368. doi:10.1016/j.epsl.2010.06.024
- Lagabrielle, Y., Bodinier, J.-L., 2008. Submarine reworking of exhumed subcontinental mantle rocks: field evidence from the Lherz peridotites, French Pyrenees. *Terra Nov.* 20, 11–21. doi:10.1111/j.1365-3121.2007.00781.x
- Lagabrielle, Y., Labaume, P., de Saint Blanquat, M., 2010. Mantle exhumation, crustal denudation, and gravity tectonics during Cretaceous rifting in the Pyrenean realm (SW Europe): Insights from the geological setting of the lherzolite bodies. *Tectonics* 29, n/a-n/a. doi:10.1029/2009TC002588
- Lau, K.W.H., Loudon, K.E., Deemer, S., Hall, J., Hopper, J.R., Tucholke, B.E., Holbrook, W.S., Christian Larsen, H., 2006a. Crustal structure across the Grand Banks-Newfoundland Basin Continental Margin - II. Results from a seismic reflection profile. *Geophys. J. Int.* 167, 157–170. doi:10.1111/j.1365-246X.2006.02989.x
- Lau, K.W.H., Loudon, K.E., Funck, T., Tucholke, B.E., Holbrook, W.S., Hopper, J.R., Christian Larsen, H., 2006b. Crustal structure across the Grand Banks-Newfoundland Basin Continental Margin - I. Results from a seismic refraction profile. *Geophys. J. Int.* 167, 127–156. doi:10.1111/j.1365-246X.2006.02988.x
- Lavier, L.L., Manatschal, G., 2006. A mechanism to thin the continental lithosphere at magma-poor margins. *Nature* 440, 324–8. doi:10.1038/nature04608
- Le Pichon, X., 1968. Sea-Floor Spreading and Continental Drift: 73, p. 3661–3697.
- Le Pichon, X., Bonnin, J., Sibuet, J.-C., 1970. La faille nord-pyrénéenne: faille transformante liée à l'ouverture du Golfe de Gascogne. *Comptes Rendus l' Acad. des Sci. Paris* 1944, 1941–1944.
- Le Pichon, X., Sibuet, J.-C., 1971. Western extension of boundary between European and Iberians plates during the Pyrenean orogeny. *Earth Planet. Sci. Lett.* 12, 83–88.
- Le Pichon, X., Sibuet, J.-C., Francheteau, J., 1977. The fit of the continents around the North Atlantic Ocean. *Tectonophysics* 38, 169–209. doi:10.1016/0040-1951(77)90210-4
- Lefort, J.P., 1973. La “zonale” Biscaye-Labrador: mise en évidence de cisaillements dextres antérieurs à l'ouverture de l'Atlantique Nord. *Mar. Geol.* 23, 491–495.
- Lefort, J.P., Miller, H.G., 1999. NW-oriented features on both sides of the Atlantic Ocean: Evidence for a Paleozoic collision that formed the Labrador-Biscay wrench fault zone? *Atl. Geol.* 35, 203–213.
- Leleu, S., Hartley, A.J., van Oosterhout, C., Kennan, L., Ruckwied, K., Gerdes, K., 2016. Structural, stratigraphic and sedimentological characterisation of a wide rift system: The Triassic rift system of the Central Atlantic Domain. *Earth-Science Rev.* 158, 89–124. doi:10.1016/j.earsci-rev.2016.03.008
- Leleu, S., Hartley, a. J., 2010. Controls on the stratigraphic development of the Triassic Fundy Basin, Nova Scotia: implications for the tectonostratigraphic evolution of Triassic Atlantic rift basins. *J. Geol. Soc. London.* 167, 437–454. doi:10.1144/0016-76492009-092
- Lister, G.S., Etheridge, M.A., Symonds, P.A., 1986. Detachment faulting and the evolution of passive continental margins Detachment faulting and the evolution of passive continental margins. *Geology* 14, 246–250. doi:10.1130/0091-7613
- Loudon, K., Wu, Y., Tari, G., 2012. Systematic variations in basement morphology and rifting geometry along the Nova Scotia and Morocco conjugate margins. *Geol. Soc. London, Spec. Publ.* 267–287. doi:10.1144/SP369.9
- Manatschal, G., 2004. New models for evolution of magma-poor rifted margins based on a review of data and concepts from West Iberia and the Alps. *Int. J. Earth Sci.* 93, 432–466. doi:10.1007/s00531-004-0394-7
- Manatschal, G., 1999. Fluid- and reaction-assisted low-angle normal faulting: evidence from rift-related brittle fault rocks in the Alps (Err Nappe, eastern Switzerland). *J. Struct. Geol.* 21, 777–793. doi:10.1016/S0191-8141(99)00069-3
- Manatschal, G., Bernoulli, D., 1999. Architecture and tectonic evolution of nonvolcanic margins: Present-day Galicia and ancient Adria. *Tectonics* 18, 1099–1119. doi:10.1029/1999TC900041
- Manatschal, G., Engström, A., Desmurs, L., Schaltegger, U., Cosca, M., Müntener, O., Bernoulli, D., 2006. What is the tectono-metamorphic evolution of continental break-up: The example of the Tasna Ocean–Continent Transition. *J. Struct. Geol.* 28, 1849–1869. doi:10.1016/j.jsg.2006.07.014
- Manatschal, G., Froitzheim, N., Rubenach, M., Turrin, B.D., 2001. The role of detachment faulting in the formation of an ocean-continent transition: insights from the Iberia Abyssal Plain. *Geol. Soc. London, Spec. Publ.* 187, 405–428. doi:10.1144/GSL.SP.2001.187.01.20
- Manatschal, G., Lavier, L., Chenin, P., 2014. The role of inheritance in structuring hyperextended rift systems: Some considerations based on observations and numerical modeling. *Gondwana Res.*

- doi:10.1016/j.gr.2014.08.006
- Manatschal, G., Nievergelt, P., 1997. A continent-ocean transition recorded in the Err and Platta nappes (Eastern Switzerland). *Eclogae Geol. Helv.* doi:10.5169/seals-168142
- Manatschal, G., Sauter, D., Karpoff, A.M., Masini, E., Mohn, G., Lagabrielle, Y., 2011. The Chenaillet Ophiolite in the French/Italian Alps: An ancient analogue for an Oceanic Core Complex? *Lithos* 124, 169–184. doi:10.1016/j.lithos.2010.10.017
- Martin, a. K., 1984. Propagating rifts: Crustal extension during continental rifting. *Tectonics* 3, 611–617. doi:10.1029/TC003i006p00611
- Martínez Catalán, J.R., 2011. Are the oroclines of the Variscan belt related to late Variscan strike-slip tectonics? *Terra Nov.* 23, 241–247. doi:10.1111/j.1365-3121.2011.01005.x
- Martínez-Loriente, S., Sallarès, V., Gràcia, E., Bartolome, R., Dañobeitia, J.J., Zitellini, N., 2014. Seismic and gravity constraints on the nature of the basement in the Africa-Eurasia plate boundary: New insights for the geodynamic evolution of the SW Iberian margin. *J. Geophys. Res. Solid Earth* 119, 127–149. doi:10.1002/2013JB010476
- Masini, E., Manatschal, G., Mohn, G., 2013. The Alpine Tethys rifted margins: Reconciling old and new ideas to understand the stratigraphic architecture of magma-poor rifted margins. *Sedimentology* 60, 174–196. doi:10.1111/sed.12017
- Masini, E., Manatschal, G., Mohn, G., Ghienne, J.F., Lafont, F., 2011. The tectono-sedimentary evolution of a supra-detachment rift basin at a deep-water magma-poor rifted margin: The example of the Samedan Basin preserved in the Err nappe in SE Switzerland. *Basin Res.* 23, 652–677. doi:10.1111/j.1365-2117.2011.00509.x
- Masini, E., Manatschal, G., Tugend, J., Mohn, G., Flament, J.-M., 2014. The tectono-sedimentary evolution of a hyper-extended rift basin: the example of the Arzacq–Mauléon rift system (Western Pyrenees, SW France). *Int. J. Earth Sci.* 103, 1569–1596. doi:10.1007/s00531-014-1023-8
- Matte, P., 2001. The Variscan collage and orogeny (480–290 Ma) and the tectonic definition of the Armorica microplate: A review. *Terra Nov.* 13, 122–128. doi:10.1046/j.1365-3121.2001.00327.x
- Matte, P., 1986. Tectonics and plate tectonics model for the Variscan belt of Europe. *Tectonophysics* 126, 329–374. doi:10.1016/0040-1951(86)90237-4
- Mauffret, A., Mougénot, D., Miles, P.R., Malod, J.A., 1989. Cenozoic deformation and Mesozoic abandoned spreading centre in the Tagus Abyssal Plain (west of Portugal): results of a multichannel seismic survey. *Can. J. Earth Sci.* 26, 1101–1123. doi:10.1139/e89-095
- Maus, S., Sazonova, T., Hemant, K., Fairhead, J.D., Ravat, D., 2007. National geophysical data center candidate for the world digital magnetic anomaly map. *Geochemistry, Geophys. Geosystems* 8, 1–10. doi:10.1029/2007GC001643
- McDermott, K., Belligham, P., Pindell, J., Graham, R., Horn, B., 2014. Some Insights into Rifted Margin Development and the Structure of the Continent-Ocean Transition Using a Global Deep Seismic Reflection Database, in: 4th Atlantic Conjugate Margins Conference, St John's 2014.
- McDermott, K., Reston, T., 2015. To see, or not to see? Rifted margin extension. *Geology* 43, G36982.1. doi:10.1130/G36982.1
- McKenzie, D., 1978. Some remarks on the development of sedimentary basins. *Earth Planet. Sci. Lett.* doi:10.1016/0012-821X(78)90071-7
- Medvedev, S., 2002. Mechanics of viscous wedges: Modeling by analytical and numerical approaches. *J. Geophys. Res.* 107, 2123. doi:10.1029/2001JB000145
- Merle, R., Jourdan, F., Marzoli, a., Renne, P.R., Grange, M., Girardeau, J., 2009. Evidence of multi-phase Cretaceous to Quaternary alkaline magmatism on Tore-Madeira Rise and neighbouring seamounts from <sup>40</sup>Ar/<sup>39</sup>Ar ages. *J. Geol. Soc. London.* 166, 879–894. doi:10.1144/0016-76492008-060
- Meyer, B., Saltus, R., Chulliat, A., 2016. EMAG2: Earth Magnetic Anomaly Grid (2-arc-minute resolution) Version 3.
- Miles, P., Bouysse, P., De Souza, K., 2012. Structural Map of the Atlantic Ocean.
- Minshull, T.A., Dean, S.M., Whitmarsh, R.B., 2014. The peridotite ridge province in the southern Iberia Abyssal Plain: Seismic constraints revisited. *J. Geophys. Res. Solid Earth* 119, 1580–1598. doi:10.1002/2014JB011011
- Mohn, G., Karner, G., Manatschal, G., Johnson, C., 2015. Structural and stratigraphic evolution of the Iberia-Newfoundland margin : A quantitative modeling approach. *Geol. Soc. London, Spec. Publ.* 15, 13810. doi:10.1144/SP413.9
- Mohn, G., Manatschal, G., Beltrando, M., Masini, E., Kusznir, N., 2012. Necking of continental crust in magma-poor rifted margins: Evidence from the fossil Alpine Tethys margins. *Tectonics* 31.

- doi:10.1029/2011TC002961
- Mohn, G., Manatschal, G., Müntener, O., Beltrando, M., Masini, E., 2010. Unravelling the interaction between tectonic and sedimentary processes during lithospheric thinning in the Alpine Tethys margins. *Int. J. Earth Sci.* 99, 75–101. doi:10.1007/s00531-010-0566-6
- Montadert, L., Roberts, D.G., 1979. Initial Reports of the Deep Sea Drilling Project, 48, Initial Reports of the Deep Sea Drilling Project. U.S. Government Printing Office. doi:10.2973/dsdp.proc.48.1979
- Montadert, L., Roberts, D.G., De Charpal, O., Guennoc, P., 1979. Rifting and subsidence of the northern continental margin of the Bay of Biscay. *Initial Reports Deep Sea Drill. Proj. Leg 48*, 1025–1060.
- Moore, D.E., Lockner, D. a., Tanaka, H., Iwata, K., 2004. The Coefficient of Friction of Chrysotile Gouge at Seismogenic Depths. *Int. Geol. Rev.* 46, 385–398. doi:10.2747/0020-6814.46.5.385
- Morgan, W.J., 1968. Rises, trenches, great faults, and crustal blocks: *Journal of Geophysical Research*, 73, p. 1959–1982, doi: 10.1029/JB073i006p01959.
- Moulin, M., Aslanian, D., Unternehr, P., 2010. A new starting point for the South and Equatorial Atlantic Ocean. *Earth-Science Rev.* 98, 1–37. doi:10.1016/j.earscirev.2009.08.001
- Mourgues, R., Lacoste, A., Garibaldi, C., 2014. The Coulomb critical taper theory applied to gravitational instabilities. *J. Geophys. Res. Solid Earth* 119, 754–765. doi:10.1002/2013JB010359
- Mouthereau, F., Filleaudeau, P., Vacherat, A., Pik, R., Lacombe, O., Fellin, M.G., Castelltort, S., Christophoul, F., Masini, E., 2014. Placing limits to shortening evolution in the Pyrenees: Role of margin architecture and implications for the Iberia/Europe convergence. *Tectonics* 33, 2283–2314. doi:10.1002/2014TC003663
- Müller, R.D., Roest, W.R., 1992. Fracture zones in the North Atlantic from combined Geosat and Seasat data. *J. Geophys. Res.* 97, 3337. doi:10.1029/91JB02605
- Müller, R.D., Roest, W.R., Royer, J.-Y., Gahagan, L.M., Sclater, J.G., 1997. Digital isochrons of the world's ocean floor. *J. Geophys. Res.* doi:10.1029/96JB01781
- Müller, R.D., Royer, J.Y., Lawver, L.A., 1993. Revised plate motions relative to the hotspots from combined Atlantic and Indian Ocean hotspot tracks. *Geology* 21, 275–278. doi:10.1130/0091-7613(1993)021<0275:RPMRTT>2.3.CO;2
- Müller, R.D., Sdrolias, M., Gaina, C., Roest, W.R., 2008. Age, spreading rates, and spreading asymmetry of the world's ocean crust. *Geochemistry, Geophys. Geosystems* 9, 1–19. doi:10.1029/2007GC001743
- Murillas, J., Mougénot, D., Boulot, G., Comas, M., Banda, E., Mauffret, a, 1990. Structure and evolution of the Galicia Interior Basin (Atlantic western Iberian continental margin). *Tectonophysics* 184, 297–319. doi:10.1016/0040-1951(90)90445-E
- Nagel, T.J., Buck, W.R., 2004. Symmetric alternative to asymmetric rifting models. *Geology* 32, 937–940. doi:10.1130/G20785.1
- Naylor, D., Shannon, P.M., 2005. The structural framework of the Irish Atlantic Margin, in: *Petroleum Geology: North-West Europe and Global Perspectives – Proceedings of the 6th Petroleum Geology Conference*. Geological Society of London, pp. 1009–1021. doi:10.1144/0061009
- Nemcok, M., Sinha, S.T., Stuart, C.J., Welker, C., Choudhuri, M., Sharma, S.P., Misra, a. a., Sinha, N., Venkatraman, S., 2012. East Indian margin evolution and crustal architecture: integration of deep reflection seismic interpretation and gravity modelling. *Geol. Soc. London, Spec. Publ.* 369, 477–496. doi:10.1144/SP369.6
- Neres, M., Font, E., Miranda, J.M., Camps, P., Terrinha, P., Mirão, J., 2012. Reconciling Cretaceous paleomagnetic and marine magnetic data for Iberia: New Iberian paleomagnetic poles. *J. Geophys. Res.* 117, B06102. doi:10.1029/2011JB009067
- Neres, M., Miranda, J.M., Font, E., 2013. Testing Iberian kinematics at Jurassic-Cretaceous times. *Tectonics* 32, 1312–1319. doi:10.1002/tect.20074
- Nirrengarten, M., Gernigon, L., Manatschal, G., 2014. Lower crustal bodies in the Møre volcanic rifted margin: Geophysical determination and geological implications. *Tectonophysics* 636, 143–157. doi:10.1016/j.tecto.2014.08.004
- Nirrengarten, M., Manatschal, G., Yuan, X.P., Kuszniir, N.J., Maillot, B., 2016. Application of the critical Coulomb wedge theory to hyper-extended, magma-poor rifted margins. *Earth Planet. Sci. Lett.* 442, 121–132. doi:10.1016/j.epsl.2016.03.004
- O'Reilly, B.M., Hauser, F., Jacob, A.W.B., Shannon, P.M., 1996. The lithosphere below the Rockall Trough: wide-angle seismic evidence for extensive serpentinisation. *Tectonophysics* 255, 1–23. doi:10.1016/0040-1951(95)00149-2
- O'Reilly, B.M., Hauser, F., Jacob, a. W.B., Shannon, P.M., Makris, J., Vogt, U., 1995. The transition between the Erris and the Rockall basins: new evidence from wide-angle seismic data. *Tectono-*

- physics 241, 143–163. doi:10.1016/0040-1951(94)00166-7
- O'Reilly, B.M., Hauser, F., Ravaut, C., Shannon, P.M., Readman, P.W., 2006. Crustal thinning, mantle exhumation and serpentinitization in the Porcupine Basin, offshore Ireland: evidence from wide-angle seismic data. *J. Geol. Soc. London*. 163, 775–787. doi:10.1144/0016-76492005-079
- Oakey, G.N., Chalmers, J. a, 2012. A new model for the Paleogene motion of Greenland relative to North America : Plate reconstructions of the Davis Strait and Nares Strait regions between Canada and Greenland. *J. Geophys. Res.* 117, 1–28. doi:10.1029/2011JB008942
- Olivet, J., 1996. La cinématique de la plaque Ibérique. *Bull. des Centres Rech. Explor. Elf-Aquitaine*, 20, 131–195.
- Osmundsen, P.T., Redfield, T.F., 2011b. Crustal taper and topography at passive continental margins. *Terra Nov.* 23, 349–361. doi:10.1111/j.1365-3121.2011.01014.x
- Pastor-Galan, D., Groenewegen, T., Brouwer, D., Krijgsman, W., Dekkers, M.J., 2015. One or two oroclines in the Variscan orogen of Iberia? Implications for Pangea amalgamation. *Geology* 527–530. doi:10.1130/G36701.1
- Pe-Piper, G., Meredyk, S., Zhang, Y., Piper, D.J.W., Edinger, E., 2013. Petrology and tectonic significance of seamounts within transitional crust east of Orphan Knoll, offshore eastern Canada. *Geo-Marine Lett.* 33, 433–447. doi:10.1007/s00367-013-0342-2
- Pereira, R., Alves, T.M., 2011. Margin segmentation prior to continental break-up: A seismic-stratigraphic record of multiphased rifting in the North Atlantic (Southwest Iberia). *Tectonophysics* 505, 17–34. doi:10.1016/j.tecto.2011.03.011
- Pérez-Gussinyé, M., Reston, T.J., 2001. Rheological evolution during extension at nonvolcanic rifted margins: Onset of serpentinitization and development of detachments leading to continental break-up. *J. Geophys. Res.* 106, 3961. doi:10.1029/2000JB900325
- Peron-Pinvidic, G., Manatschal, G., 2010. From microcontinents to extensional allochthons: witnesses of how continents rift and break apart? *Pet. Geosci.* 16, 189–197. doi:10.1144/1354-079309-903
- Péron-Pinvidic, G., Manatschal, G., 2009. The final rifting evolution at deep magma-poor passive margins from Iberia-Newfoundland: A new point of view. *Int. J. Earth Sci.* 98, 1581–1597. doi:10.1007/s00531-008-0337-9
- Péron-Pinvidic, G., Manatschal, G., Minshull, T. a., Sawyer, D.S., 2007. Tectonosedimentary evolution of the deep Iberia-Newfoundland margins: Evidence for a complex breakup history. *Tectonics* 26, n/a-n/a. doi:10.1029/2006TC001970
- Peron-Pinvidic, G., Manatschal, G., Osmundsen, P.T., 2013. Structural comparison of archetypal Atlantic rifted margins: A review of observations and concepts. *Mar. Pet. Geol.* 43, 21–47. doi:10.1016/j.marpetgeo.2013.02.002
- Peron-Pinvidic, G., Osmundsen, P.T., 2016. Architecture of the distal and outer domains of the mid-Norwegian rifted margin: Insights from the Rån-Gjallar ridges system. *Mar. Pet. Geol.* 77, 280–299. doi:10.1016/j.marpetgeo.2016.06.014
- Peron-Pinvidic, G., Osmundsen, P.T., Ebbing, J., 2016. Mismatch of geophysical datasets in distal rifted margin studies. *Terra Nov.* doi:10.1111/ter.12226
- Peron-Pinvidic, G., Shillington, D.J., Tucholke, B.E., 2010. Characterization of sills associated with the U reflection on the Newfoundland margin: Evidence for widespread early post-rift magmatism on a magma-poor rifted margin. *Geophys. J. Int.* 182, 113–136. doi:10.1111/j.1365-246X.2010.04635.x
- Petri, B., 2014. Formation et exhumation des granulites permiennees.
- Pinheiro, L.M., Whitmarsh, R.B., Miles, P.R., 1992. The ocean-continent boundary off the western continental margin of Iberia - II. Crustal structure in the Tagus Abyssal Plain, *Geophysical Journal International*. doi:10.1111/j.1365-246X.1990.tb01788.x
- Pinto, V.H.G., Manatschal, G., Karpoff, A.M., Viana, A., 2015. Tracing mantle-reacted fluids in magma-poor rifted margins: The example of Alpine Tethyan rifted margins. *Geochemistry, Geophys. Geosystems* 16, 3271–3308. doi:10.1002/2015GC005830
- Pitman, W.C., Talwani, M., 1972. Sea-Floor Spreading in the North Atlantic. *Geol. Soc. Am. Bull.* 83, 619.
- Pollock, J.C., Hibbard, J.P., Staal, C.R. Van, 2012. A paleogeographical review of the peri-Gondwanan realm of the Appalachian orogen. *Can. J. Earth Sci.* 49, 259–288. doi:10.1139/E11-049
- Rabinowitz, P.D., Cande, S.C., Hayes, D.E., 1979. The J-Anomaly in the Central North Atlantic Ocean, in: *Initial Reports of the Deep Sea Drilling Project*, 43. U.S. Government Printing Office, pp. 879–885. doi:10.2973/dsdp.proc.43.145.1979
- Rabinowitz, P.D., Cande, S.C., Hayes, D.E., 1978. Grand Banks and J-Anomaly Ridge. *Science* (80-. ).

- 202, 71–73.
- Rabinowitz, P.D., LaBrecque, J., 1979. The Mesozoic South Atlantic Ocean and Evolution of Its Continental Margins. *J. Geophys. Res.* 84, 5973–6002. doi:10.1029/JB084iB11p05973
- Ramos, A., Fernández, O., Terrinha, P., Muñoz, J.A., 2015. Extension and inversion structures in the Tethys–Atlantic linkage zone, Algarve Basin, Portugal. *Int. J. Earth Sci.* 1–17. doi:10.1007/s00531-015-1280-1
- Ranero, C.R., Pérez-Gussinyé, M., 2010. Sequential faulting explains the asymmetry and extension discrepancy of conjugate margins. *Nature* 468, 294–299. doi:10.1038/nature09520
- Rasmussen, E.S., Lomholt, S., Andersen, C., Vejbæk, O. V., 1998. Aspects of the structural evolution of the Lusitanian Basin in Portugal and the shelf and slope area offshore Portugal. *Tectonophysics* 300, 199–225. doi:10.1016/S0040-1951(98)00241-8
- Reinen, L.A., Weeks, J.D., Tullis, T.E., 1994. The frictional behavior of lizardite and antigorite serpentinites: Experiments, constitutive models, and implications for natural faults. *Pure Appl. Geophys. PAGEOPH* 143, 317–358. doi:10.1007/BF00874334
- Reston, T., 2007. Extension discrepancy at North Atlantic nonvolcanic rifted margins: Depth-dependent stretching or unrecognized faulting? *Geology* 35, 367. doi:10.1130/G23213A.1
- Reston, T.J., 2009. The structure, evolution and symmetry of the magma-poor rifted margins of the North and Central Atlantic: A synthesis. *Tectonophysics* 468, 6–27. doi:10.1016/j.tecto.2008.09.002
- Reston, T.J., Gaw, V., Pennell, J., Klaeschen, D., Stubenrauch, A., Walker, I., 2004. Extreme crustal thinning in the south Porcupine Basin and the nature of the Porcupine Median High: implications for the formation of non-volcanic rifted margins. *J. Geol. Soc. London.* 161, 783–798. doi:10.1144/0016-764903-036
- Reston, T.J., Krawczyk, C.M., Klaeschen, D., 1996. The S reflector west of Galicia (Spain): Evidence from prestack depth migration for detachment faulting during continental breakup. *J. Geophys. Res. Solid Earth* 101, 8075–8091. doi:10.1029/95JB03466
- Reston, T.J., Leythaeuser, T., Booth-Rea, G., Sawyer, D., Klaeschen, D., Long, C., 2007. Movement along a low-angle normal fault: The S reflector west of Spain. *Geochemistry, Geophys. Geosystems* 8, n/a-n/a. doi:10.1029/2006GC001437
- Reston, T.J., McDermott, K.G., 2011. Successive detachment faults and mantle unroofing at magma-poor rifted margins. *Geology* 39, 1071–1074. doi:10.1130/G32428.1
- Reston, T.J., Morgan, J.P., 2004. Continental geotherm and the evolution of rifted margins. *Geology* 32, 133–136. doi:10.1130/g19999.1
- Roberts, A.M., Yielding, G., Kusznir, N.J., Walker, I., Dorn-Lopez, D., 1993. Mesozoic extension in the North Sea: constraints from flexural backstripping, forward modelling and fault populations, in: *Petroleum Geology of Northwest Europe: Proceedings of the 4th Conference.* Geological Society of London, pp. 1123–1136. doi:10.1144/0041123
- Roberts, a. M., Kusznir, N.J., Yielding, G., Styles, P., 1998. 2D flexural backstripping of extensional basins; the need for a sideways glance. *Pet. Geosci.* 4, 327–338. doi:10.1144/petgeo.4.4.327
- Robertson, A.H.F., 2007. Evidence of continental breakup from the Newfoundland rifted margin (Ocean drilling program LEG 210): lower Cretaceous seafloor formed by exhumation of subcontinental mantle lithosphere and the transition to seafloor spreading. *Proc. Ocean Drill. Program, Sci. Results* 210, 1–69. doi:10.2973/odp.proc.sr.210.104.2007
- Roca, E., Muñoz, J.A., Ferrer, O., Ellouz, N., 2011. The role of the Bay of Biscay Mesozoic extensional structure in the configuration of the Pyrenean orogen: Constraints from the MARCONI deep seismic reflection survey. *Tectonics* 30. doi:10.1029/2010TC002735
- Roest, W.R., Srivastava, S.P., 1991. Kinematics of the plate boundaries between Eurasia, Iberia, and Africa in the North Atlantic from the Late Cretaceous to the present. *Geology* 19, 613. doi:10.1130/0091-7613(1991)019<0613:KOTPB>2.3.CO;2
- Rosenbaum, G., Lister, G.S., Duboz, C., 2002. Relative motions of Africa, Iberia and Europe during Alpine orogeny. *Tectonophysics* 359, 117–129. doi:10.1016/S0040-1951(02)00442-0
- Rowley, D.B., Lottes, A.L., 1988. Plate-kinematic reconstructions of the North Atlantic and Arctic: Late Jurassic to Present. *Tectonophysics* 155, 73–120. doi:10.1016/0040-1951(88)90261-2
- Russell, S.M., Whitmarsh, R.B., 2003. Magmatism at the west Iberia non-volcanic rifted continental margin: Evidence from analyses of magnetic anomalies. *Geophys. J. Int.* 154, 706–730.
- Saffer, D.M., Marone, C., 2003. Comparison of smectite- and illite-rich gouge frictional properties: Application to the updip limit of the seismogenic zone along subduction megathrusts. *Earth Planet. Sci. Lett.* 215, 219–235. doi:10.1016/S0012-821X(03)00424-2
- Sahabi, M., Aslanian, D., Olivet, J.L., 2004. Un nouveau point de départ pour l’histoire de l’Atlantique

- central. *Comptes Rendus - Geosci.* 336, 1041–1052. doi:10.1016/j.crte.2004.03.017
- Salas, R., Casas, A., 1993. Mesozoic extensional tectonics, stratigraphy and crustal evolution during the Alpine cycle of the eastern Iberian basin. *Tectonophysics* 228, 33–55. doi:10.1016/0040-1951(93)90213-4
- Sallarès, V., Gailler, A., Gutscher, M.-A., Graindorge, D., Bartolomé, R., Gràcia, E., Díaz, J., Daño-beitia, J.J., Zitellini, N., 2011. Seismic evidence for the presence of Jurassic oceanic crust in the central Gulf of Cadiz (SW Iberian margin). *Earth Planet. Sci. Lett.* 311, 112–123. doi:10.1016/j.epsl.2011.09.003
- Sallarès, V., Martínez-Loriente, S., Prada, M., Gràcia, E., Ranero, C., Gutscher, M.A., Bartolome, R., Gailler, A., Daño-beitia, J.J., Zitellini, N., 2013. Seismic evidence of exhumed mantle rock basement at the Goringe Bank and the adjacent Horseshoe and Tagus abyssal plains (SW Iberia). *Earth Planet. Sci. Lett.* 365, 120–131. doi:10.1016/j.epsl.2013.01.021
- Sandwell, D.T., Muller, R.D., Smith, W.H.F., Garcia, E., Francis, R., 2014. New global marine gravity model from CryoSat-2 and Jason-1 reveals buried tectonic structure. *Science (80-. )*. 346, 65–67. doi:10.1126/science.1258213
- Sandwell, D.T., Smith, W.H.F., 2009. Global marine gravity from retracked Geosat and ERS-1 altimetry: Ridge segmentation versus spreading rate. *J. Geophys. Res.* 114, B01411. doi:10.1029/2008JB006008
- Sauter, D., Cannat, M., Rouméjon, S., Andreani, M., Birot, D., Bronner, A., Brunelli, D., Carlut, J., Delacour, A., Guyader, V., MacLeod, C.J., Manatschal, G., Mendel, V., Ménez, B., Pasini, V., Ruellan, E., Searle, R., 2013. Continuous exhumation of mantle-derived rocks at the Southwest Indian Ridge for 11 million years. *Nat. Geosci.* 6, 314–320. doi:10.1038/ngeo1771
- Savva, D., Pubellier, M., Franke, D., Chamot-Rooke, N., Meresse, F., Steuer, S., Auxietre, J.L., 2014. Different expressions of rifting on the South China Sea margins. *Mar. Pet. Geol.* 58, 579–598. doi:10.1016/j.marpetgeo.2014.05.023
- Sawyer, D.S., 1994. Proceedings of the Ocean Drilling Program, 149 Initial Reports, Proceedings of the Ocean Drilling Program. *Ocean Drilling Program*. doi:10.2973/odp.proc.ir.149.1994
- Sawyer, D. S.; Clark, S.; Morgan, J.K.K.M., 2005. Large scale mass wasting as a possible mechanism of formation of highly thinned continental crust and the S reflector on the Galicia rifted margin. In: *American Geophysical Union*.
- Schärer, U., Girardeau, J., Cornen, G., Boillot, G., 2000. 138-121 Ma asthenospheric magmatism prior to continental break-up in the North Atlantic and geodynamic implications. *Earth Planet. Sci. Lett.* 181, 555–572. doi:10.1016/S0012-821X(00)00220-X
- Schettino, A., Turco, E., 2009. Breakup of Pangaea and plate kinematics of the central Atlantic and Atlas regions. *Geophys. J. Int.* 178, 1078–1097. doi:10.1111/j.1365-246X.2009.04186.x
- Schettino, a., Turco, E., 2011. Tectonic history of the western Tethys since the Late Triassic. *Geol. Soc. Am. Bull.* 123, 89–105. doi:10.1130/B30064.1
- Seton, M., Müller, R.D., Zahirovic, S., Gaina, C., Torsvik, T., Shephard, G., Talsma, a., Gurnis, M., Turner, M., Maus, S., Chandler, M., 2012. Global continental and ocean basin reconstructions since 200Ma. *Earth-Science Rev.* 113, 212–270. doi:10.1016/j.earscirev.2012.03.002
- Seton, M., Whittaker, J.M., Wessel, P., Müller, R.D., DeMets, C., Merkouriev, S., Cande, S., Gaina, C., Eagles, G., Granot, R., Stock, J., Wright, N., Williams, S.E., 2014. Community infrastructure and repository for marine magnetic identifications. *Geochemistry, Geophys. Geosystems* 15, 1629–1641. doi:10.1002/2013GC005176
- Shannon, P.M., 2009. Permo-Triassic development from Ireland to Norway : basin architecture and regional controls *TOLFOVA* 676, 652–676. doi:10.1002/gj
- Shannon, P.M., 1991. The development of Irish offshore sedimentary basins. *J. Geol. Soc. London.* 1, 181–189.
- Shillington, D.J., Holbrook, W.S., Van Avendonk, H.J.A., Tucholke, B.E., Hopper, J.R., Louden, K.E., Larsen, H.C., Nunes, G.T., 2006a. Evidence for asymmetric nonvolcanic rifting and slow incipient oceanic accretion from seismic reflection data of the Newfoundland margin. *J. Geophys. Res. Solid Earth* 111. doi:10.1029/2005JB003981
- Sibson, R.H., 1977. Fault rocks and fault mechanisms. *J. Geol. Soc. London.* 133, 191–213. doi:10.1144/gsjgs.133.3.0191
- Sibuet, J.-C., 2004. Pyrenean orogeny and plate kinematics. *J. Geophys. Res.* 109, B08104. doi:10.1029/2003JB002514
- Sibuet, J.-C., 1992. New constraints on the formation of the non-volcanic continental Galicia-Flemish Cap conjugate margins. *J. Geol. Soc. London.* 149, 829–840. doi:10.1144/gsjgs.149.5.0829

- Sibuet, J.-C., Collette, B.J., 1991. Triple junctions of Bay of Biscay and North Atlantic: New constraints on the kinematic evolution. *Geology* 19, 522. doi:10.1130/0091-7613(1991)019<0522:TJOBBO>2.3.CO;2
- Sibuet, J.-C., Dymant, J., Bois, C., Pinet, B., Ondreas, H., 1990. Crustal structure of the Celtic Sea and western approaches from gravity data and deep seismic profiles: Constraints on the formation of continental basins. *J. Geophys. Res.* 95, 10999. doi:10.1029/JB095iB07p10999
- Sibuet, J.-C., Rouzo, S., Srivastava, S., Dehler, S., Deptuck, M., Karim, A., 2012. Plate tectonic reconstructions and paleogeographic maps of the central and North Atlantic oceans. *Can. J. Earth Sci.* 49, 1395–1415. doi:10.1139/e2012-071
- Sibuet, J.-C., Srivastava, S., Manatschal, G., 2007a. Exhumed mantle-forming transitional crust in the Newfoundland-Iberia rift and associated magnetic anomalies. *J. Geophys. Res.* 112, B06105. doi:10.1029/2005JB003856
- Sibuet, J.-C., Srivastava, S., Spakman, W., 2004. Pyrenean orogeny and plate kinematics. *J. Geophys. Res.* 109, B08104. doi:10.1029/2003JB002514
- Sibuet, J.-C., Srivastava, S.P., Enachescu, M., Karner, G.D., 2007b. Early Cretaceous motion of Flemish Cap with respect to North America: implications on the formation of Orphan Basin and SE Flemish Cap Galicia Bank conjugate margins. *Geol. Soc. London, Spec. Publ.* 282, 63–76. doi:10.1144/SP282.4
- Sibuet, J.-C., Yeh, Y.-C., Lee, C.-S., 2016. Geodynamics of the South China Sea. *Tectonophysics*. doi:10.1016/j.tecto.2016.02.022
- Skogseid, J., 2010. The Orphan Basin – a key to understanding the kinematic linkage between North and NE Atlantic Mesozoic rifting. II Cent. North Atl. Conjug. Margins Conf. II, 13–23.
- Skogseid, J., Planke, S., Faleide, J.I., Pedersen, T., Eldholm, O., Neverdal, F., 2000. NE Atlantic continental rifting and volcanic margin formation, Geological Society, London, Special Publications. doi:10.1144/GSL.SP.2000.167.01.12
- Smets, B., Delvaux, D., Ross, K.A., Poppe, S., Kervyn, M., D’Oreye, N., Kervyn, F., 2016. The role of inherited crustal structures and magmatism in the development of rift segments: Insights from the Kivu basin, western branch of the East African Rift. *Tectonophysics* 683, 62–76. doi:10.1016/j.tecto.2016.06.022
- Smith, W.H., Sandwell, D., 1997. Global Sea Floor Topography from Satellite Altimetry and Ship Depth Soundings. *Science* (80-. ). 277, 1956–1962. doi:10.1126/science.277.5334.1956
- Soares, D.M., Alves, T.M., Terrinha, P., 2012. The breakup sequence and associated lithospheric breakup surface: Their significance in the context of rifted continental margins (West Iberia and Newfoundland margins, North Atlantic). *Earth Planet. Sci. Lett.* 355–356, 311–326. doi:10.1016/j.epsl.2012.08.036
- Srivastava, S.P., Roest, W., Kovacs, L., Oakey, G., Lévesque, S., Verhoef, J., Macnab, R., 1990. Motion of Iberia since the Late Jurassic: Results from detailed aeromagnetic measurements in the Newfoundland Basin. *Tectonophysics* 184, 229–260.
- Srivastava, S.P., Roest, W.R., 1989. Seafloor spreading history II–IV, in: Bell, J.S. (Ed.), . Atlantic Geoscience Centre, Geologic Survey of Canada, Map sheets L17-2–L17-6.
- Srivastava, S.P., Sibuet, J.C., Cande, S., Roest, W.R., Reid, I.D., 2000. Magnetic evidence for slow seafloor spreading during the formation of the Newfoundland and Iberian margins. *Earth Planet. Sci. Lett.* 182, 61–76.
- Srivastava, S.P., Tapscott, C.R., 1986. Plate kinematics of the North Atlantic, in: Vogt, R.R., Tucholke, B.E. (Eds. . (Ed.), *The Geology of North America*. Geological Soc. Am, pp. 379–404.
- Stampfli, G.M., Hochard, C., 2009. Plate tectonics of the Alpine realm. *Geol. Soc. London, Spec. Publ.* 327, 89–111. doi:10.1144/SP327.6
- Stampfli, G.M., Hochard, C., Vérard, C., Wilhem, C., vonRaumer, J., 2013. The formation of Pangea. *Tectonophysics* 593, 1–19. doi:10.1016/j.tecto.2013.02.037
- Stanton, N., Manatschal, G., Autin, J., Sauter, D., Maia, M., Viana, A., 2016. Geophysical fingerprints of hyper-extended, exhumed and embryonic oceanic domains: the example from the Iberia–Newfoundland rifted margins. *Mar. Geophys. Res.* doi:10.1007/s11001-016-9277-0
- Stica, J.M., Zalán, P.V., Ferrari, A.L., 2014. The evolution of rifting on the volcanic margin of the Pelotas Basin and the contextualization of the Paraná–Etendeka LIP in the separation of Gondwana in the South Atlantic. *Mar. Pet. Geol.* 50, 1–21. doi:10.1016/j.marpetgeo.2013.10.015
- Stolfova, K., Shannon, P.M., 2009. Permo-Triassic development from Ireland to Norway: Basin architecture and regional controls. *Geol. J.* 44, 652–676. doi:10.1002/gj.1187
- Sullivan, K.D., Keen, C., 1977. Newfoundland Seamounts—petrology and geochemistry, in: Baragar,



- W.R.A., Coleman, L.C., Hall, J.M. (Eds.), Volcanic Regimes of Canada. pp. 461–476.
- Sutra, E., Manatschal, G., 2012. How does the continental crust thin in a hyperextended rifted margin? Insights from the Iberia margin. *Geology* 40, 139–142. doi:10.1130/G32786.1
- Sutra, E., Manatschal, G., Mohn, G., Unternehr, P., 2013. Quantification and restoration of extensional deformation along the Western Iberia and Newfoundland rifted margins. *Geochemistry, Geophys. Geosystems* 14, 2575–2597. doi:10.1002/ggge.20135
- Tankard, A.J., Welsink, H., Jenkins, M.W.A., 1989. Structural Styles and Stratigraphy of the Jeanne d'Arc Basin, Grand Banks of Newfoundland, in: Tankard, A.J. and Balkwill, H.R. (Eds.), *Extensional Tectonics and Stratigraphy of the North Atlantic Margins*. AAPG Mem., pp. 265–282.
- Tate, M., White, N., Conroy, J.-J., 1993. Lithospheric extension and magmatism in the Porcupine Basin west of Ireland. *J. Geophys. Res.* 98, 13905. doi:10.1029/93JB00890
- Tavani, S., Muñoz, J.A., 2012. Mesozoic rifting in the Basque-Cantabrian Basin (Spain): Inherited faults, transversal structures and stress perturbation. *Terra Nov.* 24, 70–76. doi:10.1111/j.1365-3121.2011.01040.x
- Taylor, B., Goodliffe, A., Martinez, F., 2009. Initiation of transform faults at rifted continental margins. *Comptes Rendus Geosci.* 341, 428–438. doi:10.1016/j.crte.2008.08.010
- Thinon, I., 2002. The syn-rift sedimentary cover of the North Biscay Margin (bay of Biscay): from new reflection seismic data. *Bull. la Société géologique Fr.* 173, 515–522. doi:10.2113/173.6.515
- Thinon, I., Matias, L., Rehault, J.P., Hirn, A., Fidalgo-Gonzalez, L., Avedik, F., 2003. Deep structure of the Armorican Basin (Bay of Biscay): a review of Norgasis seismic reflection and refraction data. *J. Geol. Soc. London.* 160, 99–116. doi:10.1144/0016-764901-103
- Tikku, A. a., Cande, S.C., 1999. The oldest magnetic anomalies in the Australian-Antarctic Basin: Are they isochrons? *J. Geophys. Res.* 104, 661. doi:10.1029/1998JB900034
- Torsvik, T.H., Müller, R.D., Van der Voo, R., Steinberger, B., Gaina, C., 2008. Global plate motion frames: Toward a unified model. *Rev. Geophys.* 46, RG3004. doi:10.1029/2007RG000227
- Torsvik, T.H., Rehnström, E.F., 2003. The Tornquist Sea and Baltica-Avalonia docking. *Tectonophysics* 362, 67–82. doi:10.1016/S0040-1951(02)00631-5
- Torsvik, T.H., Van der Voo, R., Preeden, U., Niocail, C. Mac, Steinberger, B., Doubrovine, P. V., van Hinsbergen, D.J.J., Domeier, M., Gaina, C., Tohver, E., Meert, J.G., McCausland, P.J.A., Cocks, L.R.M., 2012. Phanerozoic polar wander, palaeogeography and dynamics. *Earth-Science Rev.* 114, 325–368. doi:10.1016/j.earscirev.2012.06.002
- Tucholke, B.E., Austin, J.A., Uchupi, E., 1989. Crustal Structure and Rift-Drift Evolution of the Newfoundland Basin, in: Tankard, A. & Balkwill, H. (Ed.), *Extensional Tectonics and Stratigraphy of the North Atlantic Margins*. pp. 247–264.
- Tucholke, B.E., Ludwig, W.J., 1982. Structure and origin of the J Anomaly Ridge, western North Atlantic Ocean. *J. Geophys. Res.* 87, 9389. doi:10.1029/JB087iB11p09389
- Tucholke, B.E., Sawyer, D.S., Sibuet, J.-C., 2007. Breakup of the Newfoundland Iberia rift. *Geol. Soc. London, Spec. Publ.* 282, 9–46. doi:10.1144/SP282.2
- Tucholke, B.E., Sibuet, J.-C., 2012. Problematic plate reconstruction. *Nat. Geosci.* 5, 676–677. doi:10.1038/ngeo1596
- Tucholke, B.E., Sibuet, J.-C., 2006. Proceedings of the Ocean Drilling Program, 210 Scientific Results, Proceedings of the Ocean Drilling Program. Ocean Drilling Program. doi:10.2973/odp.proc.sr.210.2007
- Tugend, J., Manatschal, G., Kuszniir, N., 2015a. Spatial and temporal evolution of hyperextended rift systems: implication for the nature, kinematics and timing of the Iberian-European plate boundary. *Geology* 43, 15–18. doi:10.1130/G36072.1
- Tugend, J., Manatschal, G., Kuszniir, N.J., Masini, E., 2015b. Characterizing and identifying structural domains at rifted continental margins: application to the Bay of Biscay margins and its Western Pyrenean fossil remnants. *Geol. Soc. London, Spec. Publ.* 413, 171–203. doi:10.1144/SP413.3
- Tugend, J., Manatschal, G., Kuszniir, N.J., Masini, E., Mohn, G., Thinon, I., 2014. Formation and deformation of hyperextended rift systems: Insights from rift domain mapping in the Bay of Biscay-Pyrenees. *Tectonics* 33, 1239–1276. doi:10.1002/2014TC003529
- Unternehr, P., Curie, D., Olivet, J.L., Goslin, J., Beuzart, P., 1988. South Atlantic fits and intraplate boundaries in Africa and South America. *Tectonophysics* 155, 169–179. doi:10.1016/0040-1951(88)90264-8
- Unternehr, P., Peron-Pinvidic, G., Manatschal, G., Sutra, E., 2010. Hyper-extended crust in the South Atlantic: in search of a model. *Pet. Geosci.* 16, 207–215. doi:10.1144/1354-079309-904
- Vacherat, A., Mouthereau, F., Pik, R., Bellahsen, N., Gautheron, C., Bernet, M., Daudet, M., Balansa,

- J., Tibari, B., Pinna Jamme, R., Radal, J., 2016. Rift-to-collision transition recorded by tectono-thermal evolution of the northern Pyrenees. *Tectonics* 35. doi:10.1002/2015TC004016
- VanAvendonk, H.J.A., Holbrook, W.S., Nunes, G.T., Shillington, D.J., Tucholke, B.E., Loudon, K.E., Larsen, H.C., Hopper, J.R., 2006. Seismic velocity structure of the rifted margin of the eastern Grand Banks of Newfoundland, Canada. *J. Geophys. Res.* 111, B11404. doi:10.1029/2005JB004156
- Van der Voo, R., 1969. Paleomagnetic evidence for the rotation of the Iberia peninsula. *Tectonophysics* 7, 5–56.
- van Staal, C.R., Barr, S.M., Murphy, J.B., 2012. Provenance and tectonic evolution of Ganderia: Constraints on the evolution of the Iapetus and Rheic oceans. *Geology* 40, 987–990. doi:10.1130/G33302.1
- Vergés, J., Fernández, M., Martínez, A., 2002. The Pyrenean orogene: pre-, syn-, and post-collisional evolution. *J. Virtual Explor.* 8, 55–74.
- Vine, F.J., Matthews, D.H., 1963. Magnetic Anomalies Over Oceanic Ridges. *Nature* 199, 947–949. doi:10.1038/199947a0
- Vink, G.E., 1982. Continental rifting and the implications for plate tectonic reconstructions. *J. Geophys. Res. Solid Earth* 87, 10677–10688. doi:10.1029/JB087iB13p10677
- Vissers, R.L.M., Meijer, P.T., 2012a. Mesozoic rotation of Iberia: Subduction in the Pyrenees? *Earth-Science Rev.* 110, 93–110. doi:10.1016/j.earscirev.2011.11.001
- Vissers, R.L.M., Meijer, P.T., 2012b. Iberian plate kinematics and Alpine collision in the Pyrenees. *Earth-Science Rev.* 114, 61–83. doi:10.1016/j.earscirev.2012.05.001
- Vissers, R.L.M., van Hinsbergen, D.J.J., van der Meer, D.G., Spakman, W., 2016. Cretaceous slab break-off in the Pyrenees: Iberian plate-kinematics in paleomagnetic and mantle reference frames. *Gondwana Res.* doi:10.1016/j.gr.2016.03.006
- Wang, K., He, J., Hu, Y., 2006. A note on pore fluid pressure ratios in the Coulomb wedge theory. *Geophys. Res. Lett.* 33, 6–8. doi:10.1029/2006GL027233
- Wang, Y., Chevrot, S., Monteiller, V., Komatitsch, D., Mouthereau, F., Manatschal, G., Sylvander, M., Diaz, J., Ruiz, M., Grimaud, F., Benahmed, S., Pauchet, H., Martin, R., 2016. The deep roots of the western Pyrenees revealed by full waveform inversion of teleseismic P waves. *Geology* 44, G37812.1. doi:10.1130/G37812.1
- Watremez, L., Helen Lau, K.W., Nedimović, M.R., Loudon, K.E., 2015. Traveltime tomography of a dense wide-angle profile across Orphan Basin. *Geophysics* 80, B69–B82. doi:10.1190/geo2014-0377.1
- Wegener, A., 1929. *Die Entstehung der Kontinente und Ozeane*, Druck und. ed.
- Wegener, A., 1915. *Die Entstehung der Kontinente und Ozeane*, F. Vieweg. ed. Braunschweig.
- Welford, J.K., Shannon, P.M., O'Reilly, B.M., Hall, J., 2012. Comparison of lithosphere structure across the Orphan Basin-Flemish Cap and Irish Atlantic conjugate continental margins from constrained 3D gravity inversions. *J. Geol. Soc. London.* 169, 405–420. doi:10.1144/0016-76492011-114
- Welford, Hall, J., Sibuet, J.-C., Srivastava, S.P., 2010a. Structure across the northeastern margin of Flemish Cap, offshore Newfoundland from Erable multichannel seismic reflection profiles: evidence for a transtensional rifting environment. *Geophys. J. Int.* 183, 572–586. doi:10.1111/j.1365-246X.2010.04779.x
- Welford, Smith, J. a., Hall, J., Deemer, S., Srivastava, S.P., Sibuet, J.-C., 2010b. Structure and rifting evolution of the northern Newfoundland Basin from Erable multichannel seismic reflection profiles across the southeastern margin of Flemish Cap. *Geophys. J. Int.* 180, 976–998. doi:10.1111/j.1365-246X.2009.04477.x
- Welford, K.J., Shannon, P.M., O'Reilly, B.M., Hall, J., 2010c. Lithospheric density variations and Moho structure of the Irish Atlantic continental margin from constrained 3-D gravity inversion. *Geophys. J. Int.* 183, 79–95. doi:10.1111/j.1365-246X.2010.04735.x
- Wernicke, B., 1985. Uniform-sense normal simple shear of the continental lithosphere. *Can. J. Earth Sci.* 22, 108–125. doi:10.1139/e85-009
- Wessel, P., Kroenke, L.W., 2008. Pacific absolute plate motion since 145 Ma: An assessment of the fixed hot spot hypothesis. *J. Geophys. Res.* 113, B06101. doi:10.1029/2007JB005499
- White, L.T., Gibson, G.M., Lister, G.S., 2013. A reassessment of paleogeographic reconstructions of eastern Gondwana: Bringing geology back into the equation. *Gondwana Res.* 24, 984–998. doi:10.1016/j.gr.2013.06.009
- Whitmarsh, R.B., Beslier, M.-O., Wallace, P.J., 1998. Proceedings of the Ocean Drilling Program, 173 Initial Reports, Proceedings of the Ocean Drilling Program. Ocean Drilling Program. doi:10.2973/odp.proc.ir.173.1998

- Whitmarsh, R.B., Manatschal, G., Minshull, T. a, 2001. Evolution of magma-poor continental margins from rifting to seafloor spreading. *Nature* 413, 150–4. doi:10.1038/35093085
- Whitmarsh, R.B., Miles, P.R., 1995. Models of the development of the West Iberia rifted continental margin at 40°30'N deduced from surface and deep-tow magnetic anomalies. *J. Geophys. Res.* 100, 3789–3806. doi:10.1029/94JB02877
- Whitmarsh, R.B., Wallace, P.J., 2001. Proceedings of the Ocean Drilling Program, 173 Scientific Results, Proceedings of the Ocean Drilling Program. Ocean Drilling Program. doi:10.2973/odp.proc.sr.173.2001
- Williams, S.E., Whittaker, J.M., Müller, R.D., 2011. Full-fit, palinspastic reconstruction of the conjugate Australian-Antarctic margins. *Tectonics* 30. doi:10.1029/2011TC002912
- Wilson, J.T., 1966. Did the Atlantic Close and then Re-Open? *Nature* 211, 676–681. doi:10.1038/211676a0
- Wilson, R.C.L., Manatschal, G., Wise, S., 2001. Rifting along non-volcanic passive margins: stratigraphic and seismic evidence from the Mesozoic successions of the Alps and western Iberia. *Geol. Soc. London, Spec. Publ.* 187, 429–452. doi:10.1144/GSL.SP.2001.187.01.21
- Wu, Y., Louden, K.E., Funck, T., Jackson, H.R., Dehler, S. a., 2006. Crustal structure of the central Nova Scotia margin off Eastern Canada. *Geophys. J. Int.* 166, 878–906. doi:10.1111/j.1365-246X.2006.02991.x
- Xiao, H., Dahlen, F.A., Suppe, J., 1991. Mechanics of extensional wedges. *J. Geophys. Res.* 96, 10301. doi:10.1029/91JB00222
- Yuan, X.P., Leroy, Y.M., Maillot, B., 2015. Tectonic and gravity extensional collapses in overpressured cohesive and frictional wedges. *J. Geophys. Res. Solid Earth* 120, 1833–1854. doi:10.1002/2014JB011612
- Zelt, C. a., Sain, K., Naumenko, J. V., Sawyer, D.S., 2003. Assessment of crustal velocity models using seismic refraction and reflection tomography. *Geophys. J. Int.* 153, 609–626. doi:10.1046/j.1365-246X.2003.01919.x





---

# *ANNEXES*

---

De nombreuses données géologiques et géophysiques sont disponibles le long des marges du sud de l'Atlantique Nord. Une des premières étapes de ce travail de thèse a été de compiler ces données, de comprendre leur nature, leurs limites et enfin de les sélectionner. Le jeu de données est varié et constitué de cartes, de sections 2D et de forages 1D qui donnent des contraintes lithologiques et temporelles. Toutes les données décrites en annexe ne sont pas présentées dans le corps du manuscrit cependant elles ont permis de contraindre la réflexion et de proposer des modèles en accord avec celles-ci.

## A.1 LES DONNÉES DE MÉTHODES POTENTIELLES

Afin d'interpoler des données 2D locales, nous avons utilisé des cartes de méthode potentiel de gravité à l'air libre et des anomalies magnétiques. La carte de gravité à l'air libre provient d'un modèle global fait à partir de mesures satellitaires (Sandwell et al., 2014). Ces données gravimétriques ont également été traitées grâce à différents opérateurs avec le logiciel Geosoft Oasis Montaj. La dérivée verticale du signal gravimétrique permet dans le cas d'une structure limitée (e.g. pluton, bloc crustal, cavité...) de localiser plus précisément l'aplomb de la structure. La dérivée horizontale permet dans le cas d'un contact géologique pseudo-vertical (e.g. faille...) de localiser le maximum de l'anomalie à l'aplomb du contact. Les données magnétiques proviennent de la compilation Emag2v3 (Meyer et al., 2016). La réduction des données n'a pas été effectuée sur tout le domaine car cette méthode nécessite une inclinaison et une déclinaison apparente locale qui varient selon la position. Cependant un test a été effectué sur la marge ibérique (Supplementary material Chap.II Fig. II-7) montrant peu de variation dans la position des anomalies. Le traitement de tilt angle permet de représenter les anomalies fortes et les faibles de la même manière sur une carte ce qui permet des interprétations plus précises.

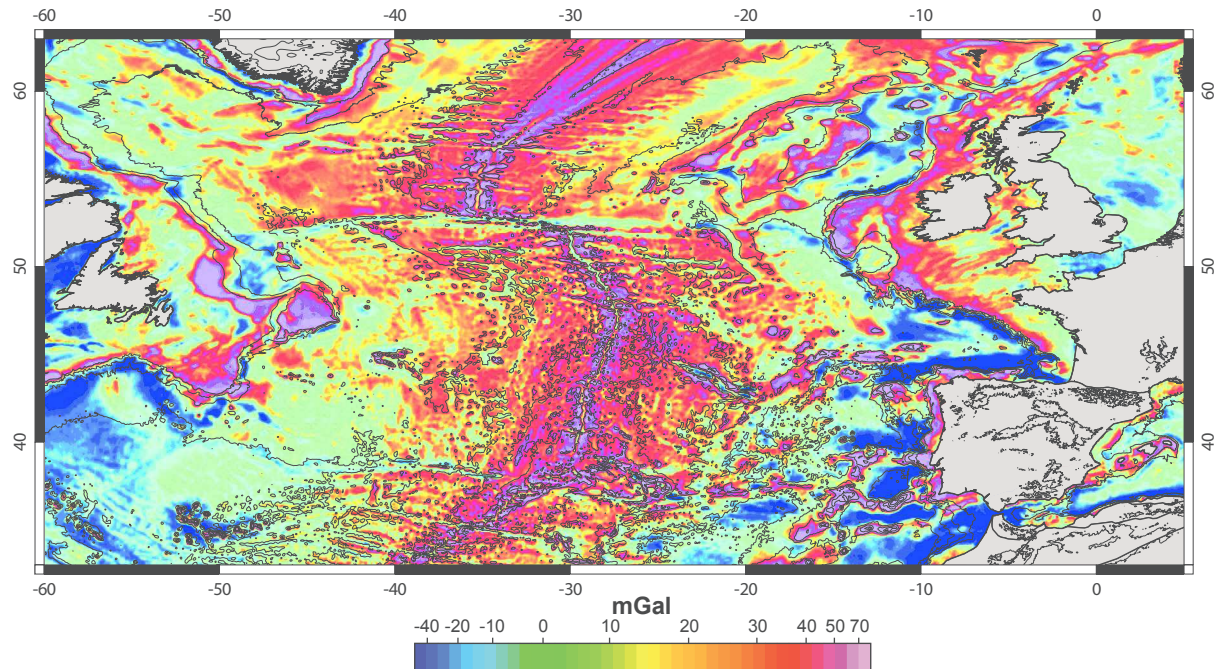


*Fig. A-1: Carte de gravité à l'air libre (Sandwell et al., 2014)*

*Fig. A-1: Free air gravity map (Sandwell et al., 2014)*



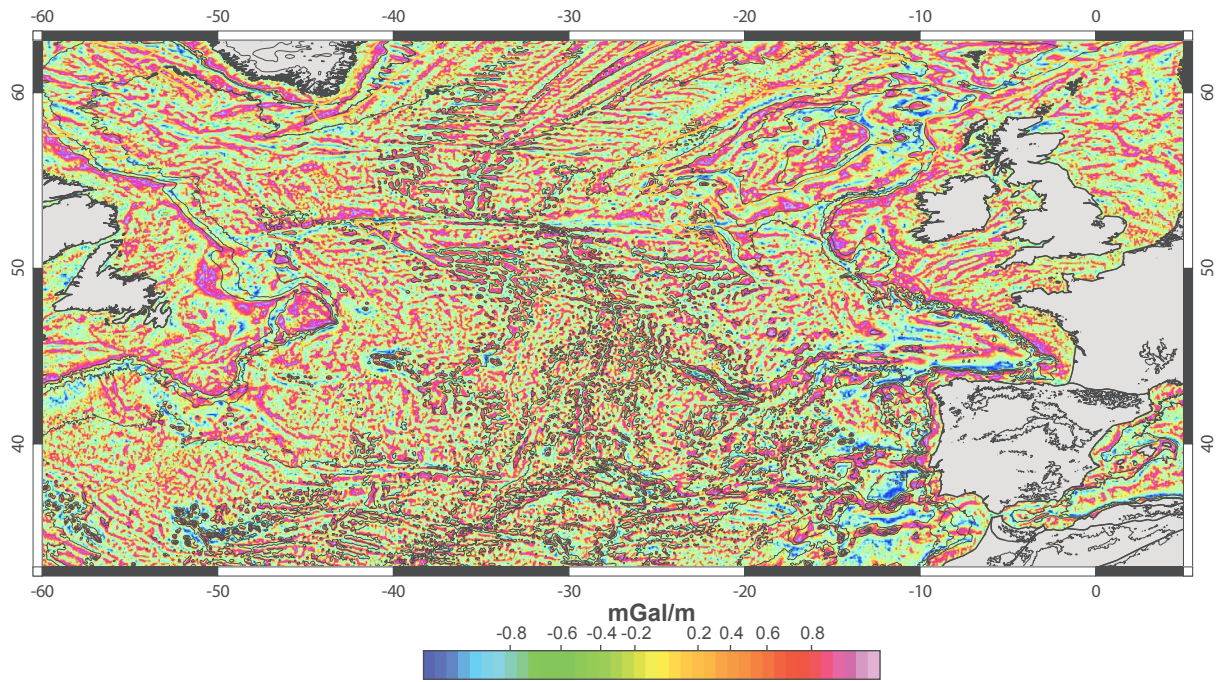


*Fig. A-2: Dérivée verticale de la carte de gravité à l'air libre*

*Fig. A-2: Vertical derivative of the free air gravity map*

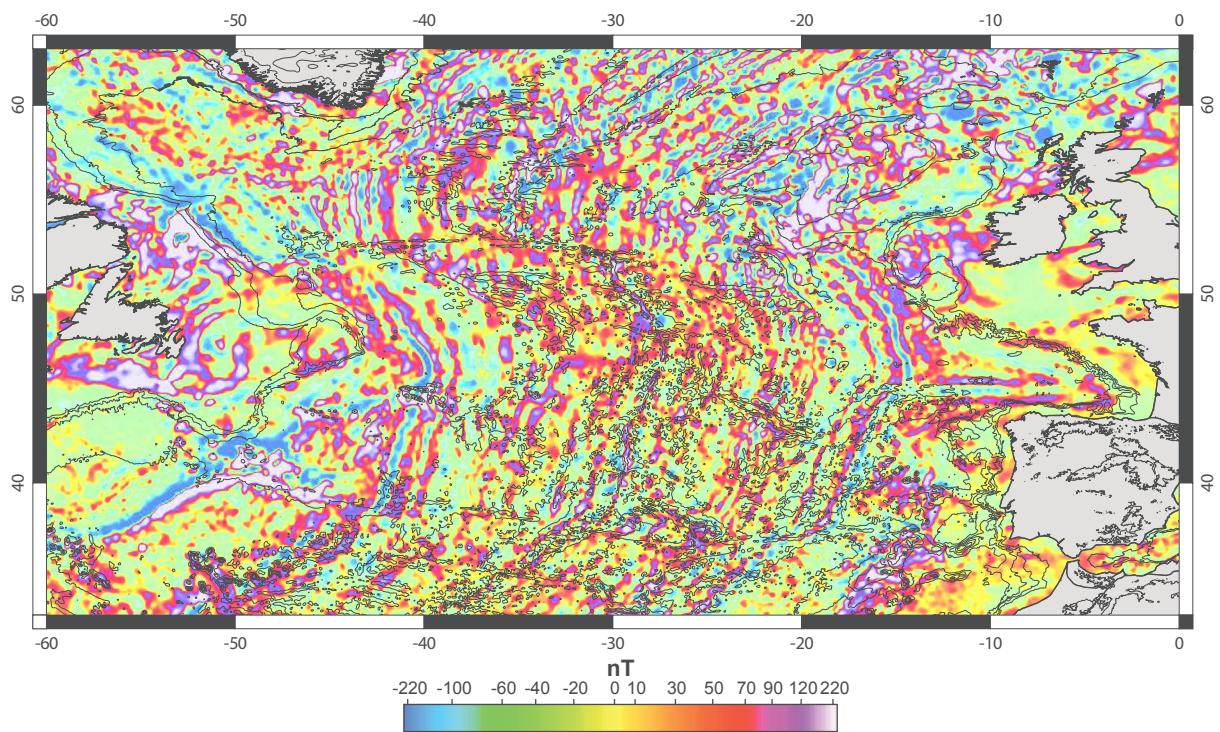


*Fig. A-3: Carte des anomalies magnétique terrestre Emag2v3 (Meyer et al., 2016)*

*Fig. A-3: Global magnetic anomaly map Emag2v3 (Meyer et al., 2016)*

## A.2 LES DONNÉES DE SISMIQUE RÉFRACTION

Les coupes de sismique réfraction sont un outil majeur dans la visualisation de l'architecture crustale grande échelle, ainsi que dans la détermination de la nature du matériel. En effet les lignes de sismique réfraction sont en profondeur et montrent les variations de vitesse dans le sous-sol. Trois sauts de vitesse correspondant à trois limites sont essentiels dans l'analyse de ses données : le fond marin, le toit sur socle et le Moho qui correspond à une vitesse supérieure à 8 km/s. De plus la présence de manteau serpentinisé est caractérisé par un gradient de vitesse augmentant avec la profondeur (Contrucci et al., 2004), et des ratios entre les vitesses d'ondes P et S peuvent aider à contraindre la lithologie du socle. Cette méthode est basée sur une modélisation inverse des ondes sismiques permettant de déterminer la vitesse de propagation des ondes dans la croûte ce qui renseigne sur la nature des roches. Cependant la résolution de ces données est souvent faible et elle n'indique que des vitesses alors que la plupart des roches des domaines hyper-étirés ont des vitesses similaires entre 6 et 7.5 km/s.

Ces données ont été géo-localisées grâce au logiciel QGis et ont permis de déterminer le long de ces sections des domaines de rifts qui ont été reportés sur la carte et extrapolés grâce aux cartes de méthodes potentielles. De plus ces données ont servi aux mesures d'angles du prisme continental hyper-étiré (cf. chapitre 1). La localisation ainsi que les images des modèles de sismique réfraction et leurs auteurs sont référencés ci-dessous.

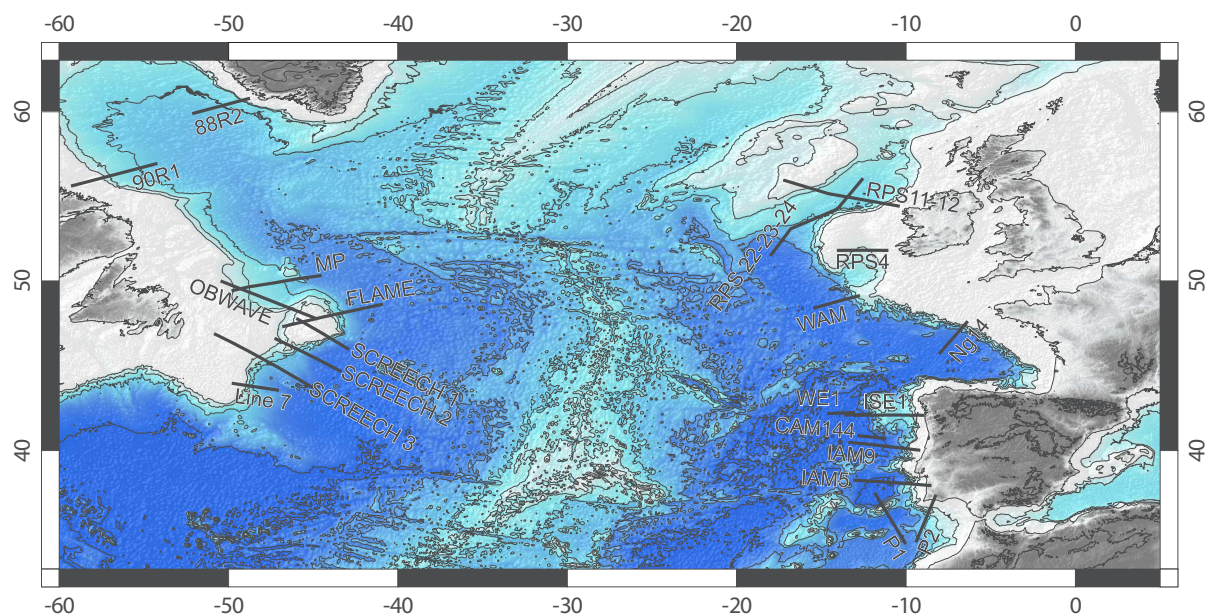
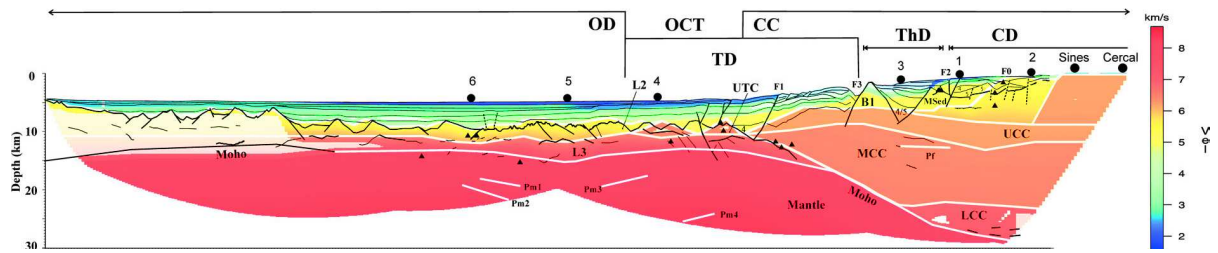
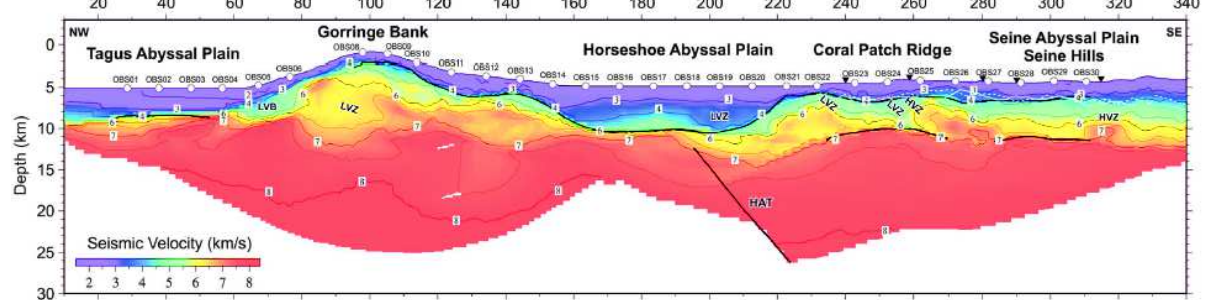


**Fig. A-4:** Localisation des lignes de sismique réfraction

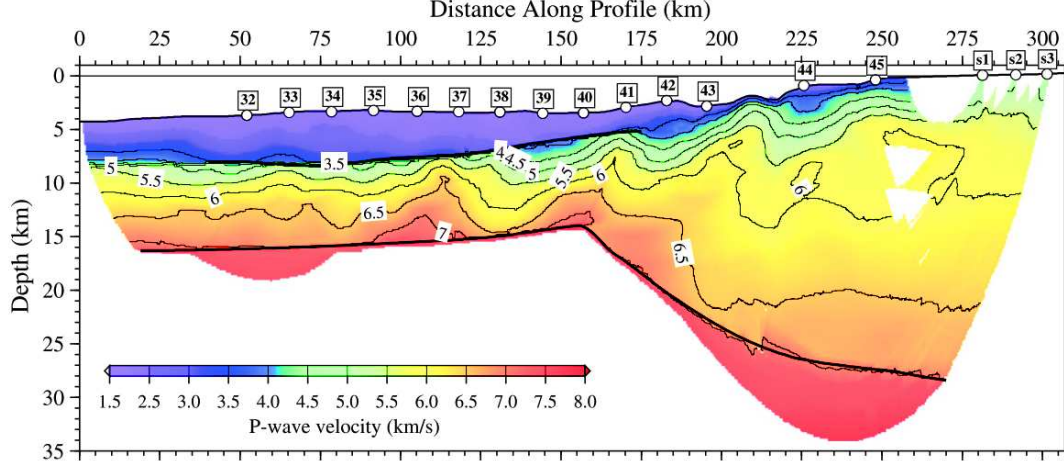
**Fig. A-4:** Localization of refraction seismic lines



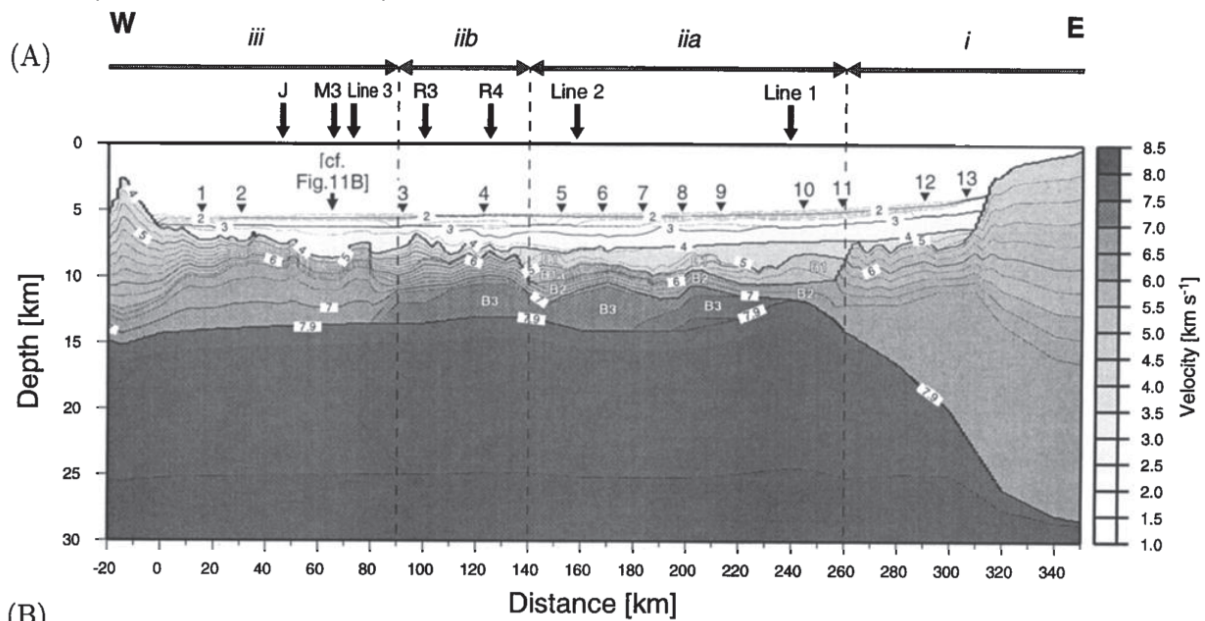
IAM 5, (Afihado et al., 2008)



P1, (Martínez-Lorient et al., 2013)

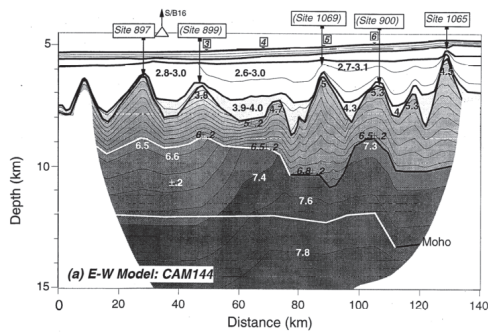


P2, (Sallarès et al., 2011)

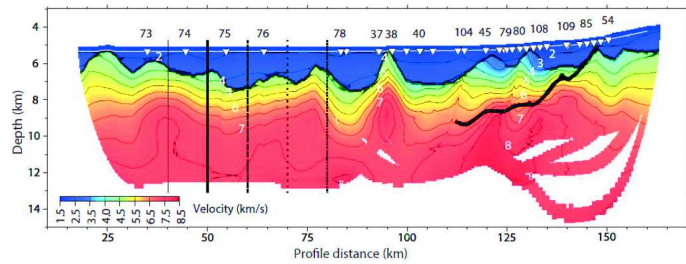


(B)

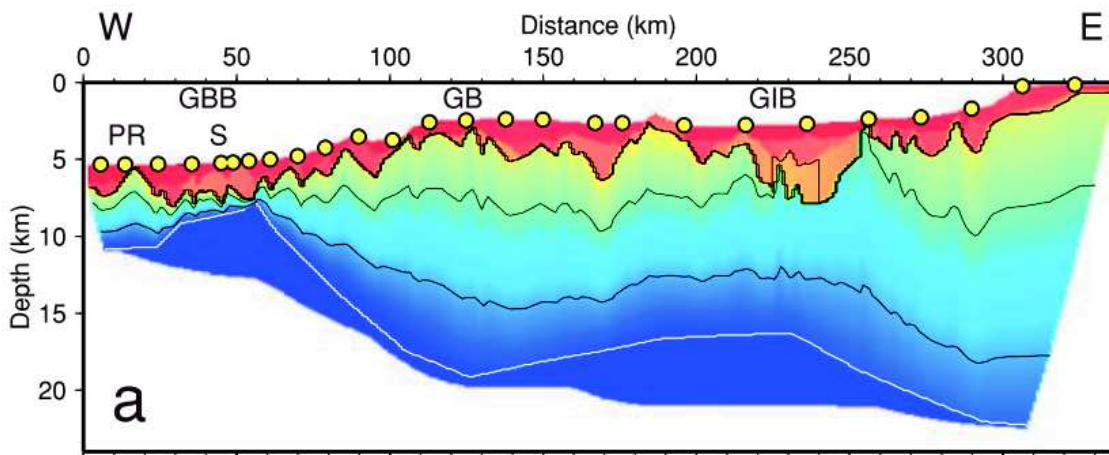
IAM 9 (Dean et al., 2000)



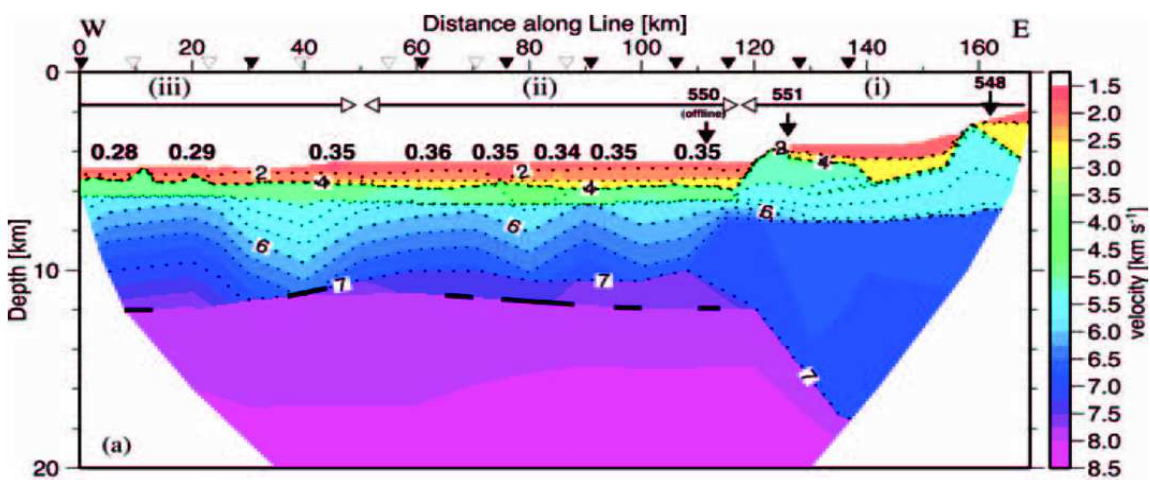
CAM144 (Chian et al., 1999)



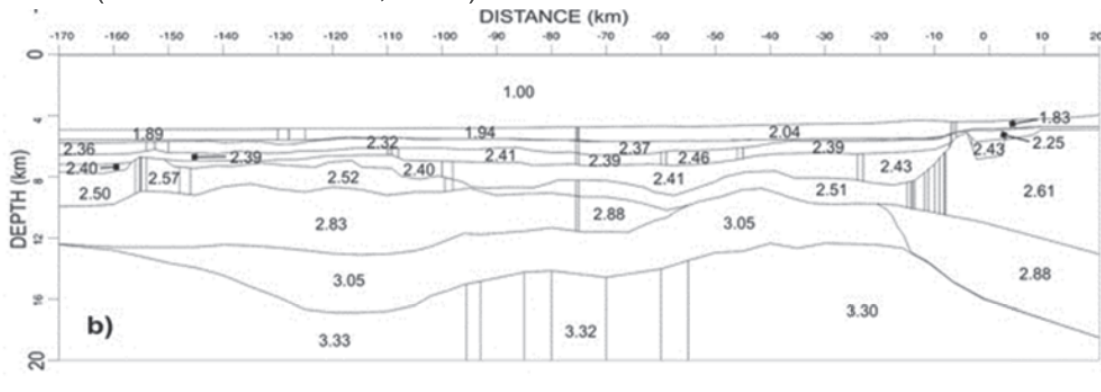
WE1 (Davy et al., 2016)



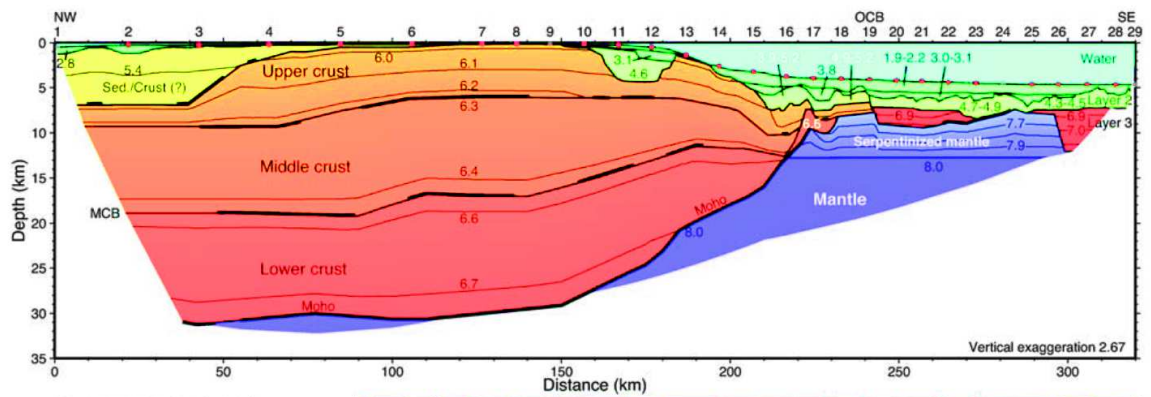
ISE 1 (Zelt et al., 2003)



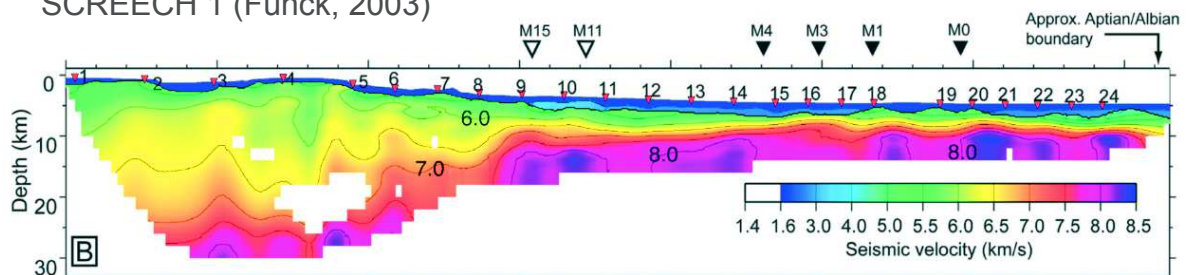
WAM (Bullock and Minsull, 2005)



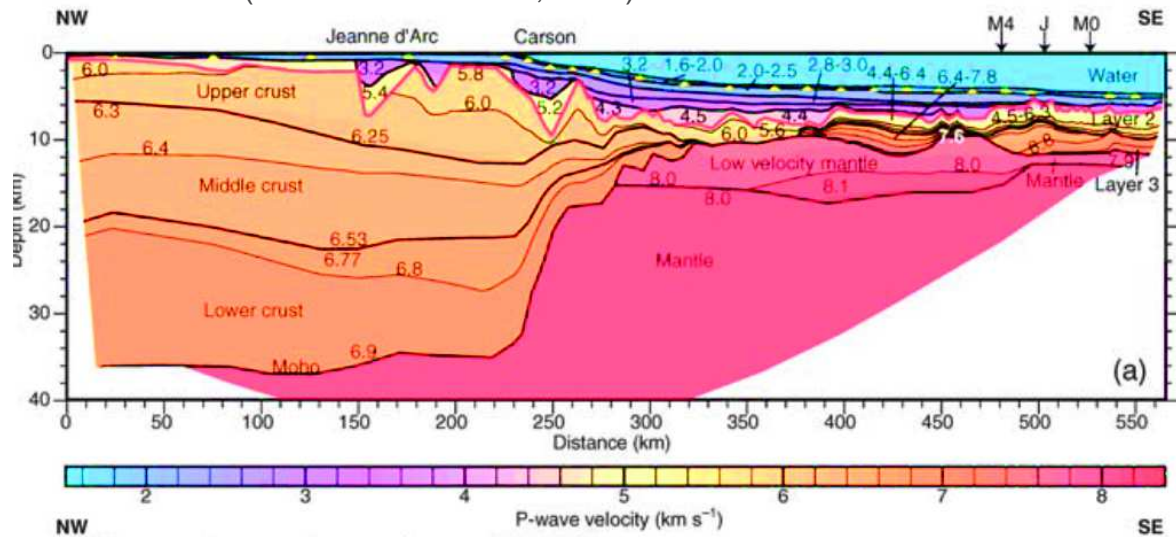
Norgasis 14 (Ng14, Thion et al., 2003)



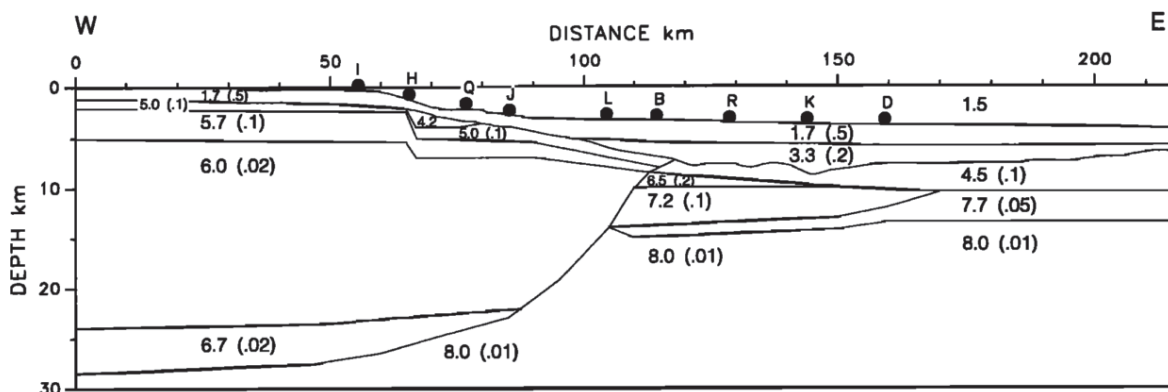
P-wave velocity (km/s)  
SCREECH 1 (Funck, 2003)



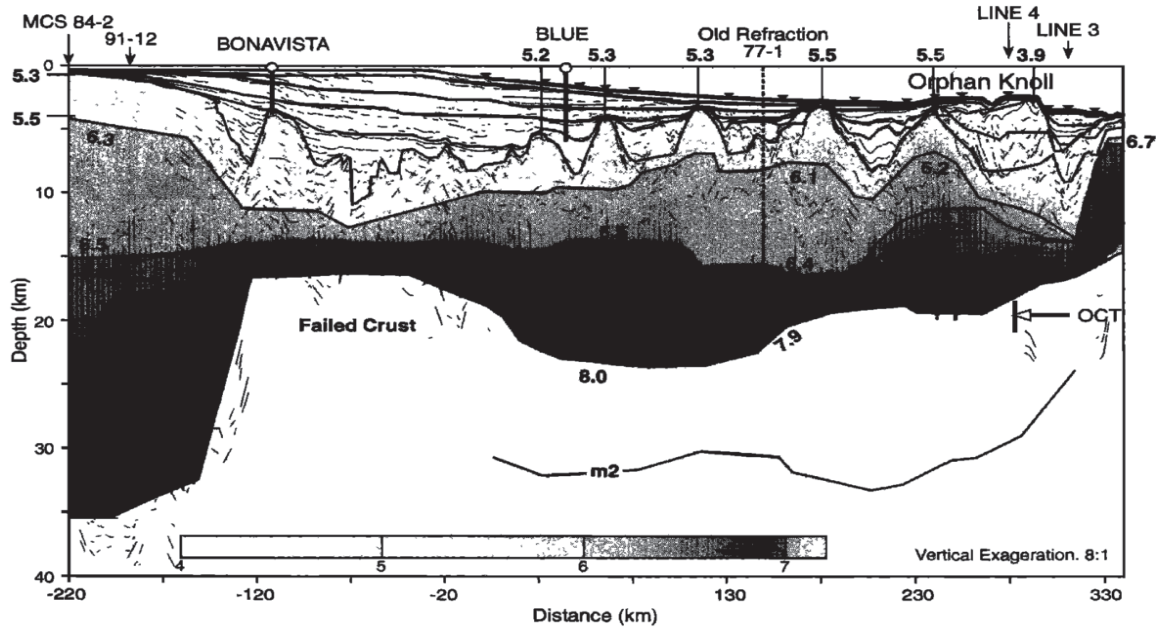
SCREECH 2 (Van Avendonk et al., 2006)



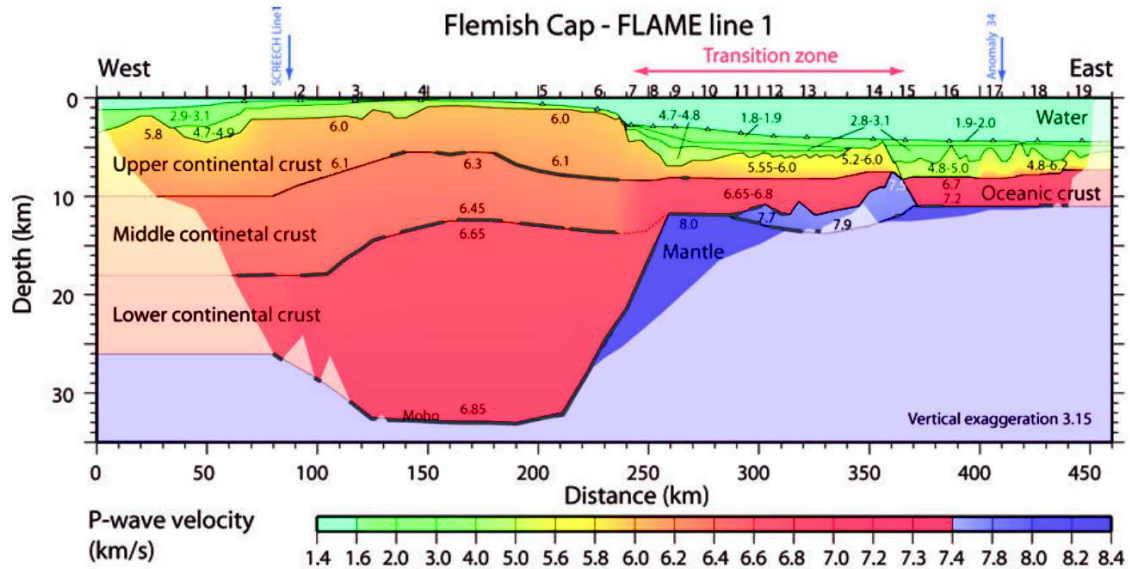
SCREECH 3 (Lau et al., 2006a)



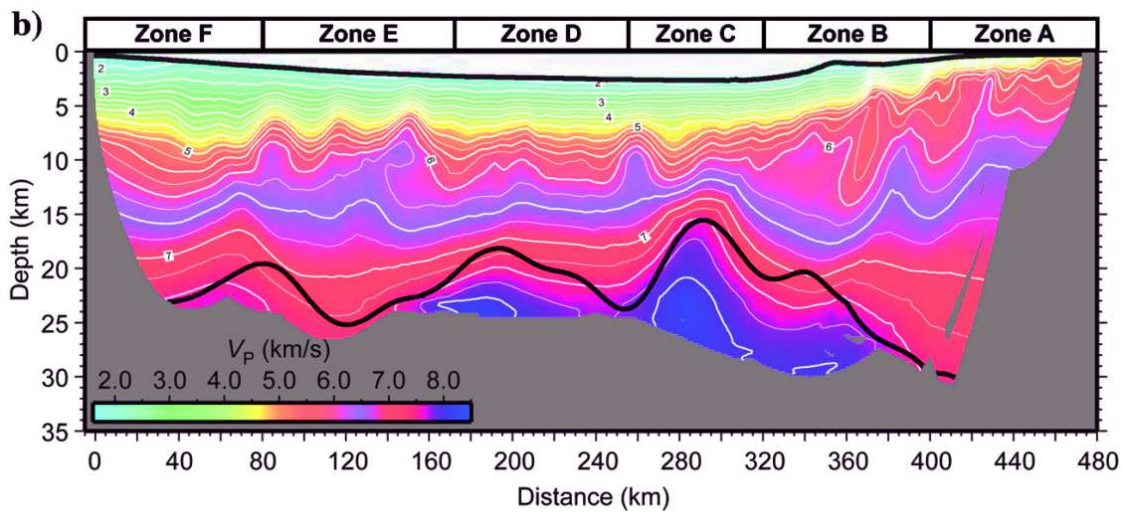
Line 7 (Reid, 1994)



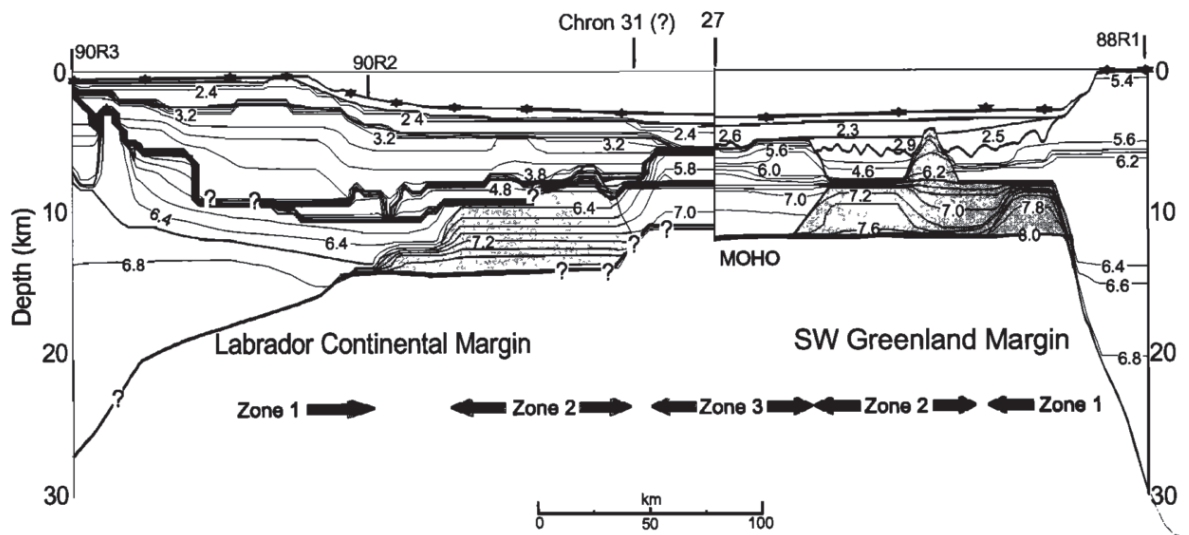
Main Profile (MP, Chian et al., 2001)



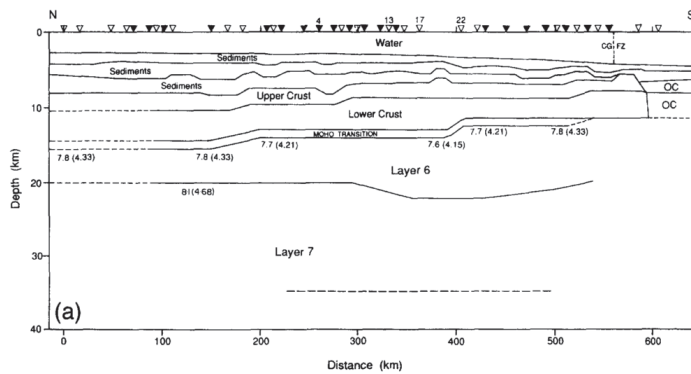
FLAME (Gerlings et al., 2011)



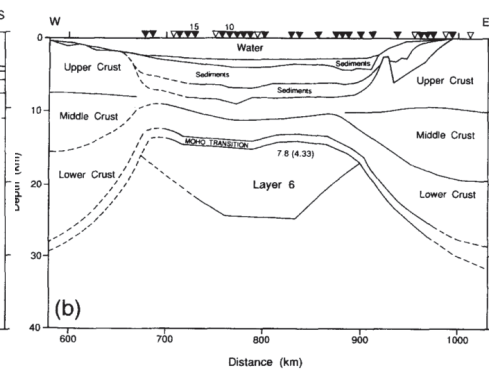
OBWAVE (Watremez et al., 2015)



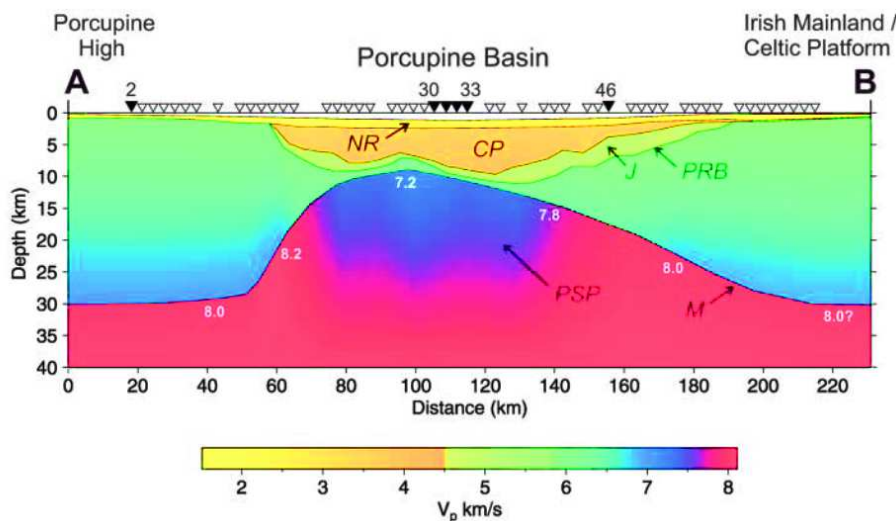
90R1 and 88R2 (Chian et al., 1995)



Rapids 22-23-24 (O'Reilly et al., 1996)



Rapids 11-12 (O'Reilly et al., 1996)



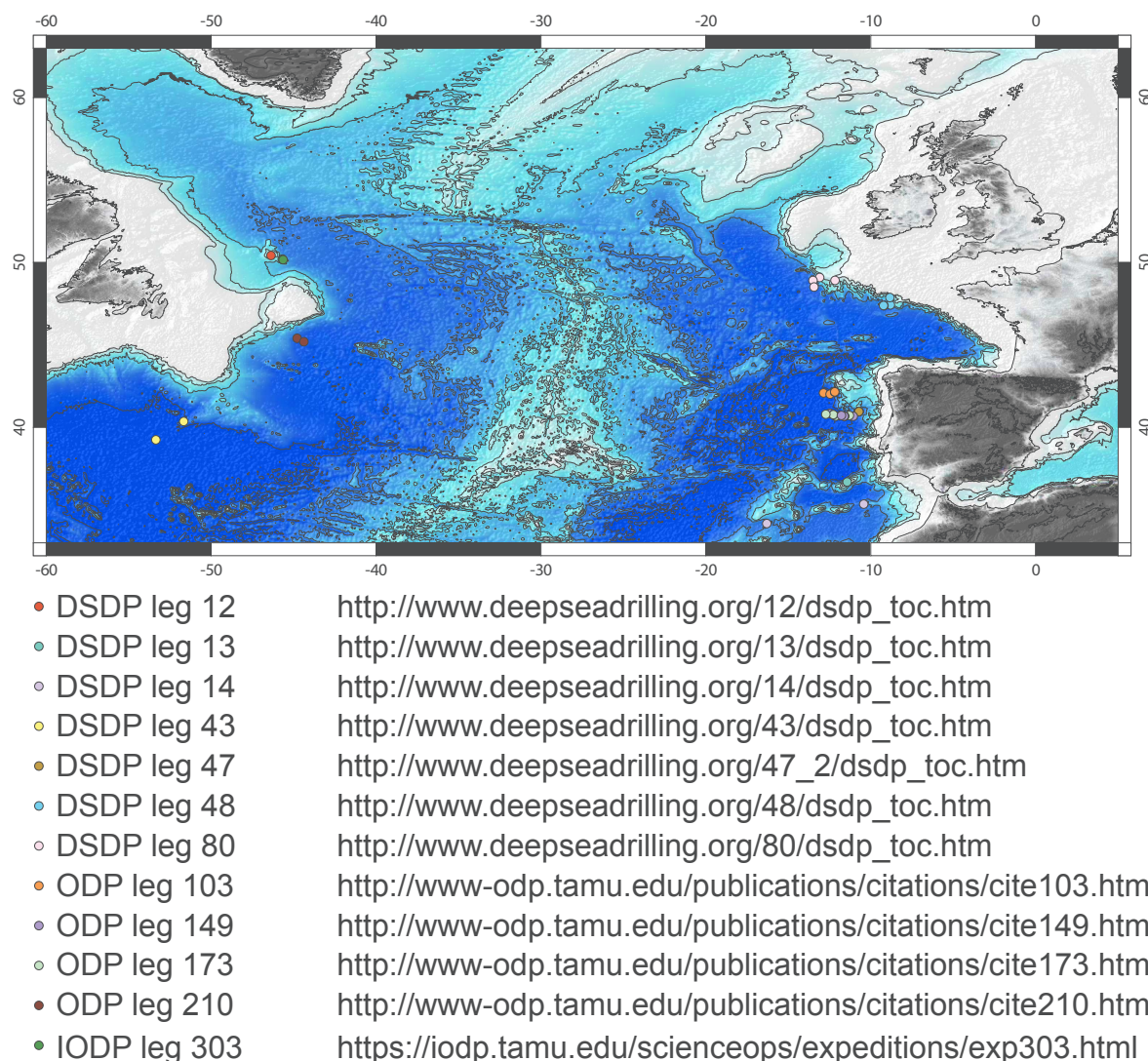
Rapids 4 (O'Reilly et al., 2006)

Fig. A-5: Lignes de sismique réfraction utilisées durant l'étude

Fig. A-5: Refraction seismic lines used in this study

### A.3 LES FORAGES PROFONDS DSDP, OPD, IODP

Les données de forage proviennent pour la plupart des expéditions internationales (DSDP, ODP et IODP). Ces forages profonds échantillonnent une grande partie de la série sédimentaire et dans certains cas le socle pétrologique. Ces données sont importantes pour déterminer la nature, la chimie et l'âge du socle et des sédiments. Ceci permet ainsi de contraindre temporellement l'évolution d'un système de rift hyper-étiré.



**Fig. A-6:** localisation des forages DSDP, ODP et IODP ainsi que les liens internet vers les rapports scientifiques associés

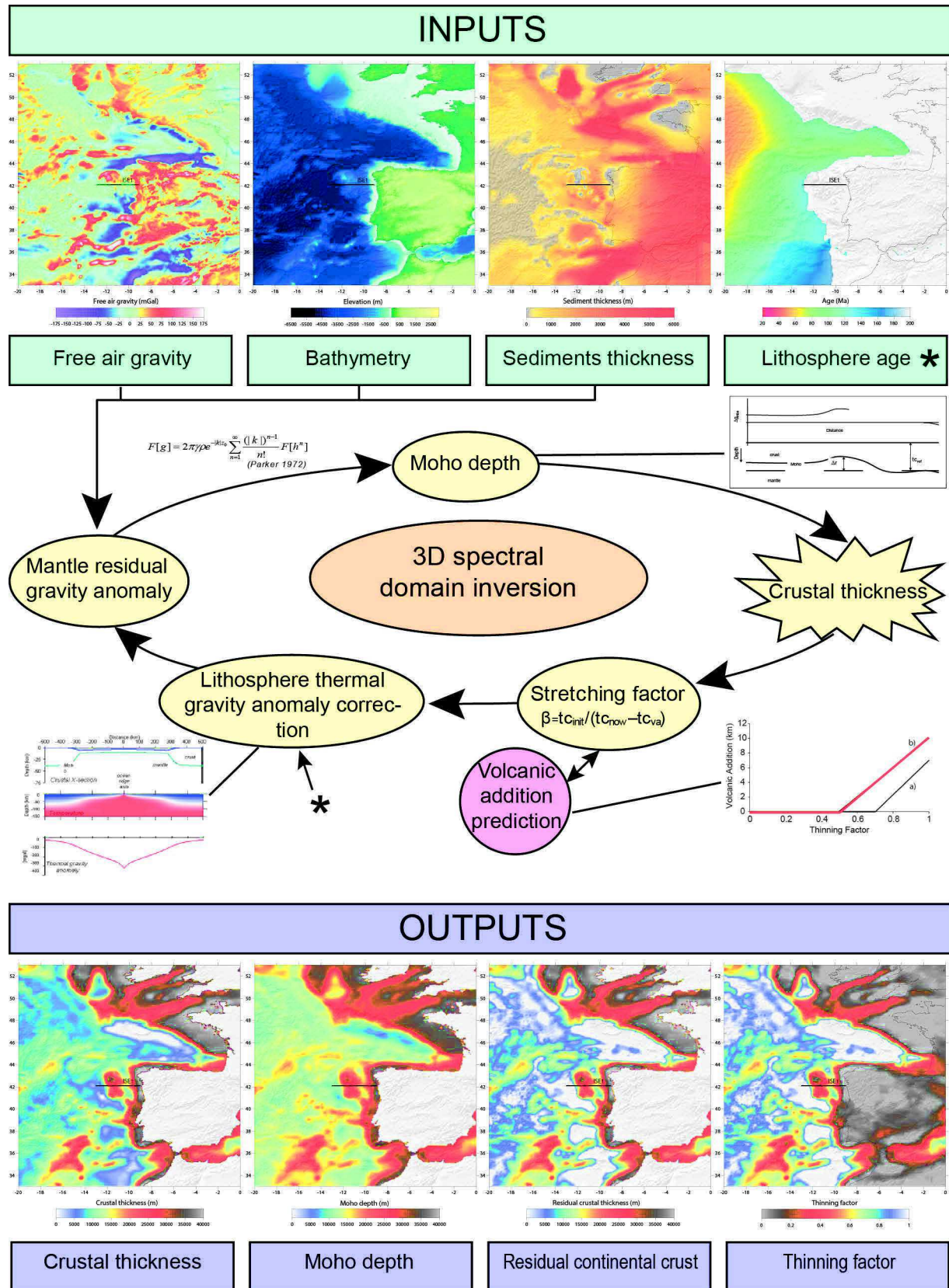
**Fig. A-6:** Localization of DSDP, ODP and IODP drill hole with the associated web link to scientific reports



## **A.4 INVERSION GRAVIMÉTRIQUE**

La méthode d'inversion gravimétrique est une approche itérative qui calcule la profondeur du Moho, l'épaisseur crustale et le facteur d'amincissement de la lithosphère. Cette méthode utilise en entrée des grilles d'anomalies gravimétriques à l'air libre (Sandwell and Smith, 2009), de bathymétrie (ETOPO1, Amante and Eakins, 2009) d'épaisseur de sédiments (NOAA, Divins, 2003) et l'âge de la lithosphère océanique (Müller et al., 1997). Cette méthode inclut une correction de densité due à l'effet de la thermicité, en effet l'expansion thermique (McKenzie, 1978) induit une diminution de la densité (Chappell and Kusznir, 2008). De plus les additions magmatiques sont prises en compte en fonction du taux d'amincissement lithosphérique. La méthode itérative est représentée schématiquement (Fig. A-7). L'inversion est calibrée en fonction de : 1) la quantité de magma observée (riche, normal ou pauvre en magma), 2) l'épaisseur crustale de référence qui est due à l'effet de topographie dynamique ; 3) à l'épaisseur crustale initiale qui détermine le facteur d'amincissement et à 4) l'âge de la première croûte océanique qui correspond à l'anomalie thermique. Certaines de ces valeurs sont connues d'autres sont des paramètres que l'on utilise pour faire correspondre le long d'une ligne de sismique réfraction le Moho sismique et celui déterminé par inversion gravimétrique.

La précision de l'épaisseur de sédiments influe beaucoup sur la résolution de l'inversion gravimétrique (ex ISE1 Fig. A-8 ) cependant pour l'Atlantique Nord il n'existe pas de compilation plus précise que celle de NOAA (Divins, 2003) et l'espacement des données sismiques ne permet pas de faire une grille cohérente.



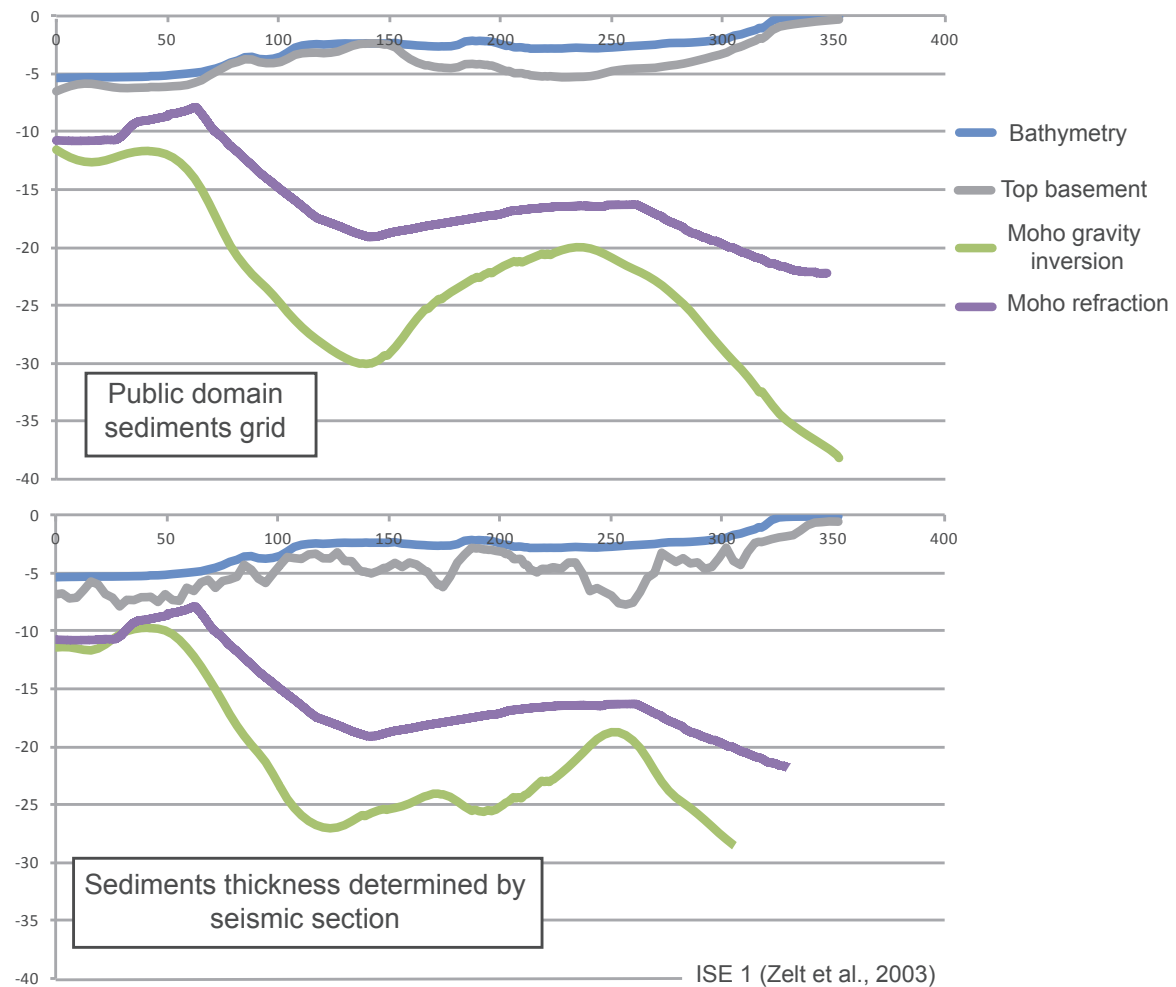


**Fig. A-8:** Comparaison d'inversion gravimétrique le long de la ligne ISE 1 (Zelt et al., 2003) avec des épaisseur de sédiments extraite de la grille global NOAA (Divins, 2003) et mesurée le long de la ligne.

**Fig. A-8:** Comparison of gravity inversion along ISE 1 seismic refraction line (Zelt et al., 2003) using sediments thickness extracted from the global NOAA grid (Divins, 2003) and measured on the seismic line

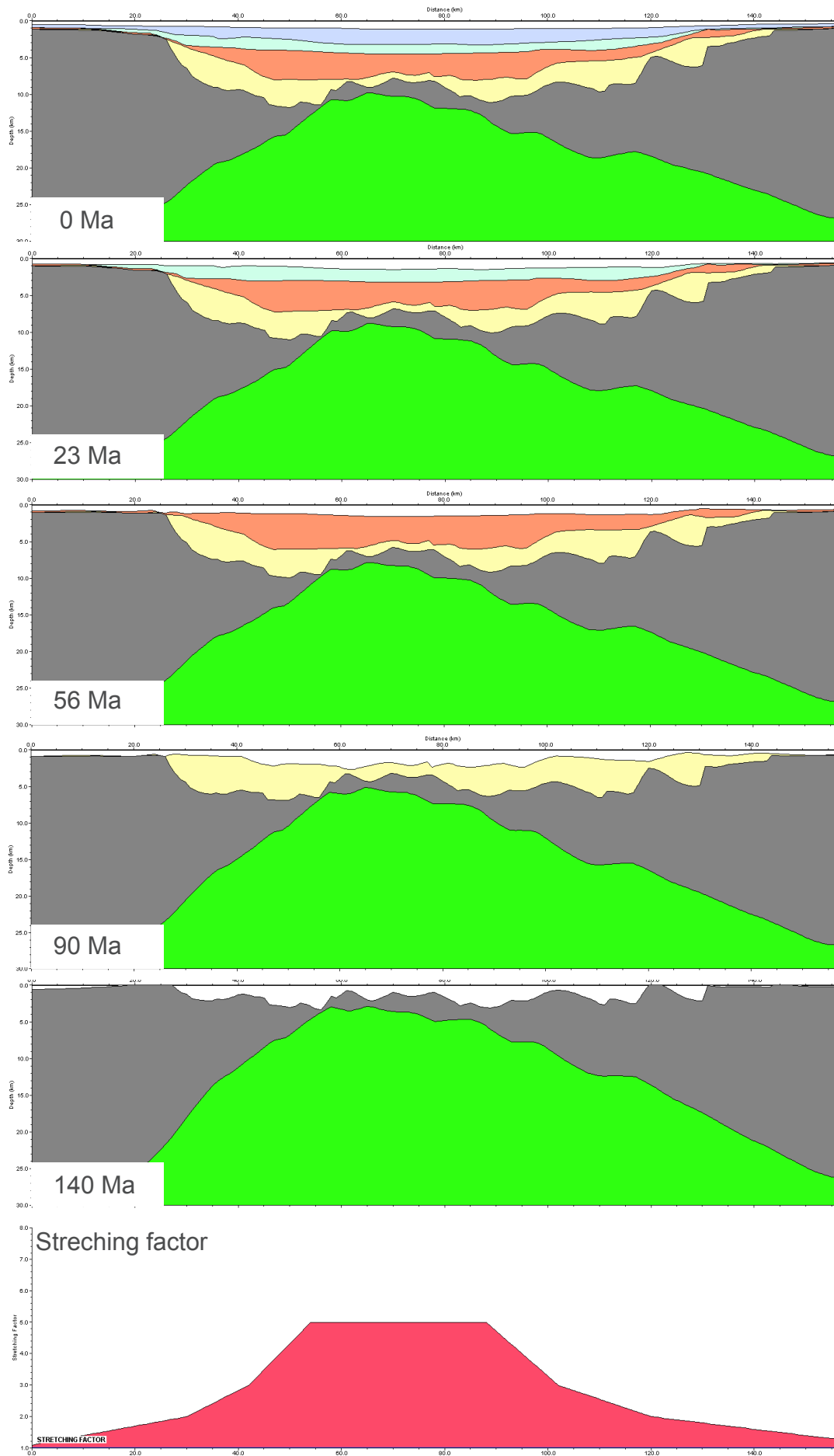
## A.5 FLEXURAL BACKSTRIPPING

Le flexural backstripping est une méthode qui permet à partir d'une ligne sismique actuelle passant à travers des bassins sédimentaires de retirer les couches sédimentaires une par une. Cet exercice permet d'obtenir l'architecture du toit du socle avant le rifting. Cette méthode utilise la flexure isostatique liée à la densité et à la compaction des couches sédimentaires mais corrige également l'effet de la subsidence thermique. Cette procédure incorpore ainsi explicitement la rigidité de la lithosphère et sa réponse isostatique en utilisant le facteur d'amincissement ( $\beta$ ). Le Flexural backstripping est généralement utilisé pour étudier la position des dépoctrans, déterminer la paleo-bathymétrie, l'extension différentielle et les taux de subsidence (e.g. Roberts et al., 1998; Roberts et al., 1993). Cependant le logiciel FlexDecomp a été utilisé pour déterminer les angles du toit du socle et du Moho à la fin du rifting. Le flexural backstripping a été fait sur les 17 exemples de marges du chapitre 1. La détermination des différentes couches sédimentaires était de qualité variable ce qui influe légèrement sur le résultat final. Les figures ci-dessous illustrent le processus suivi pour le bassin de Porcupine.

Je remercie Badleys Geoscience pour la licence étudiante du logiciel FlexDecomp

**Fig. A-9:** *Processus de flexural backstripping pour la ligne imageant le bassin de Porcupine IR 1240 (McDermott et al., 2014)*

**Fig. A-9:** *Flexural backstripping processes for the line crossing the Porcupine basin IR 1240 (McDermott et al., 2014)*



## A.6 MODÈLE CINÉMATIQUE

Le modèle cinématique du chapitre 3 et les images reconstruites du chapitre 2 ont été réalisées grâce au logiciel Gplates (Fig. A-11 Boyden et al., 2011). Ce logiciel libre de droit permet de modéliser le mouvement de plaques rigides sur un globe via une séquence de pôles de rotations organisés de manière hiérarchique. Chaque plaque (polygone) possède un numéro et effectue une rotation autour d'un pôle par rapport à une seconde plaque fixe à un âge donné. Ces informations sont inscrites dans un fichier de rotation (.rot) (Fig. A-10) et intégrées dans le logiciel de visualisation qui est un système d'information géographique (SIG) pouvant remonter dans le temps.

Le logiciel permet de modifier visuellement la position des plaques et d'enregistrer le pôle de rotation dans le fichier de rotation. Cet outil permet également d'intégrer toutes données géolocalisées ainsi les cartes de méthodes potentielles, les cartes d'épaisseur crustale, les limites des domaines de rifts, les forages et les lignes sismiques ont été incorporés à la base de données. Ces données ont permis de définir des polygones et de déterminer les problèmes cinématiques des précédents modèles. Après C34 (83.5 Ma) les anomalies magnétiques permettent des restaurations fiables, cependant l'évolution entre la restauration totale et C34 a été modifiée grâce à l'outil de manipulation directe des pôles par visualisation.

| North America plate ID | Time of rotation | Latitude | Longitude | Angle | Fixed plate ID<br>Northwest Africa | Comments and references           |
|------------------------|------------------|----------|-----------|-------|------------------------------------|-----------------------------------|
| 101                    | 147.7            | 66.54    | -17.98    | 62.08 | 714 !                              | NAM-NWA Mueller et.al 1997        |
| 101                    | 154.3            | 67.15    | -15.98    | 64.75 | 714 !                              | NAM-NWA Mueller et.al 1997        |
| 101                    | 170.0            | 67.09    | -13.86    | 70.55 | 714 !                              | NAM-NWA BSMA Labails et. al. 2010 |

**Fig. A-10:** Exemple de quelques lignes d'un fichier de rotation utilisé par le logiciel Gplates

**Fig. A-10:** Example of a few lines from the rotation file used by the Gplates software

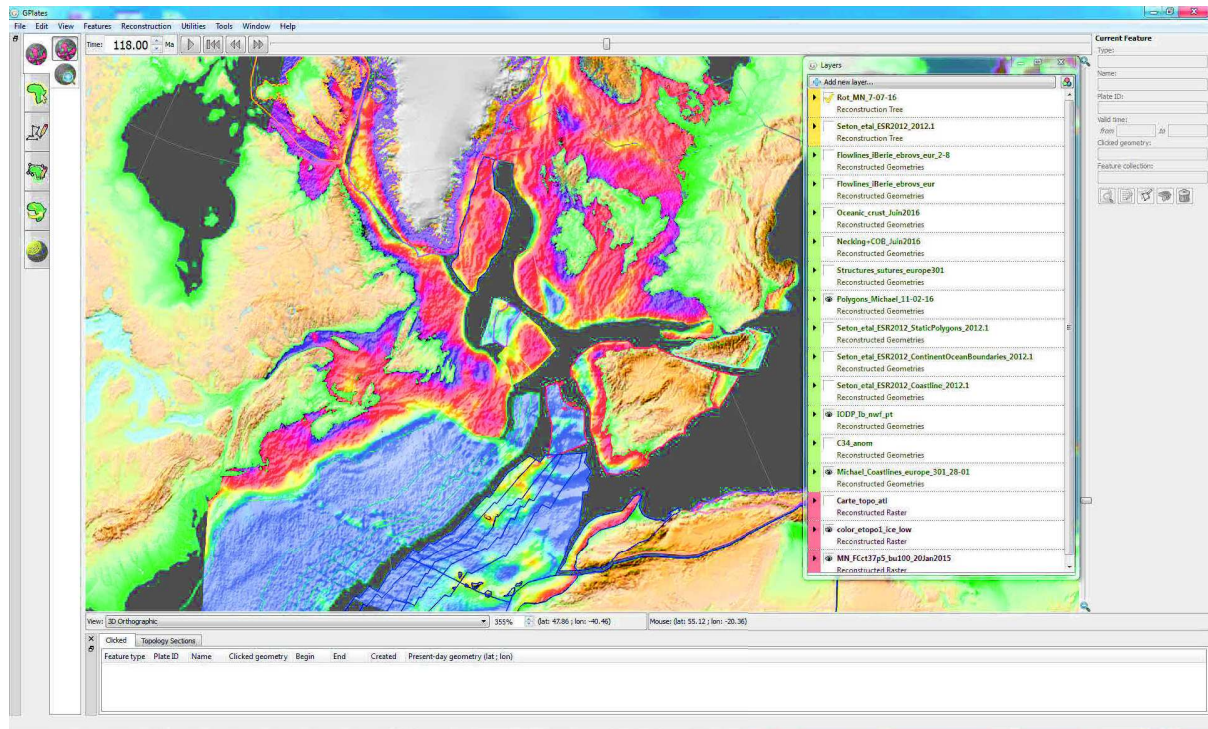
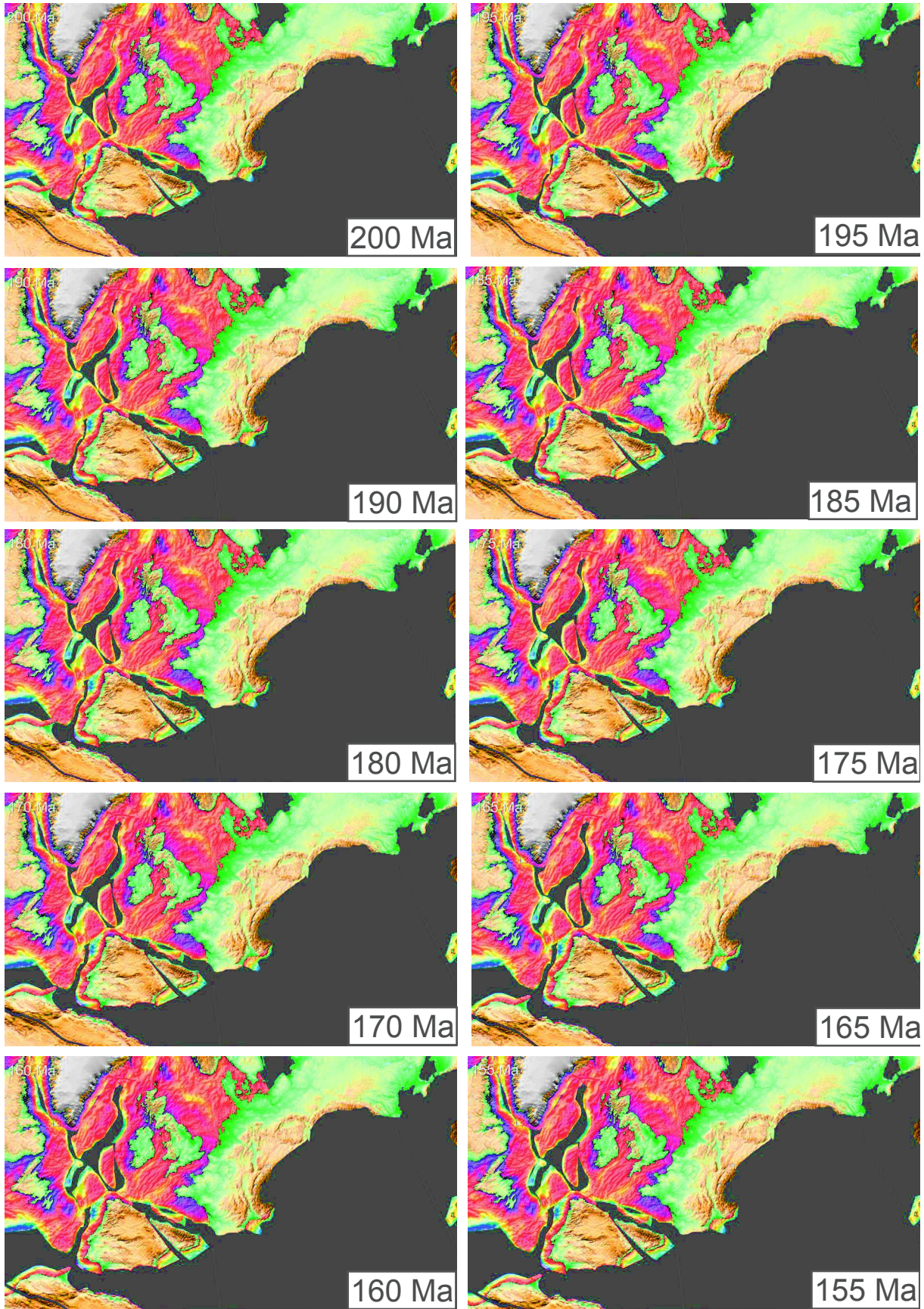


**Fig. A-11:** Capture d'écran du logiciel Gplates montrant les polygones définis. La carte d'épaisseur crustale et la topographie ETOPO 1 sont drapés en fond.

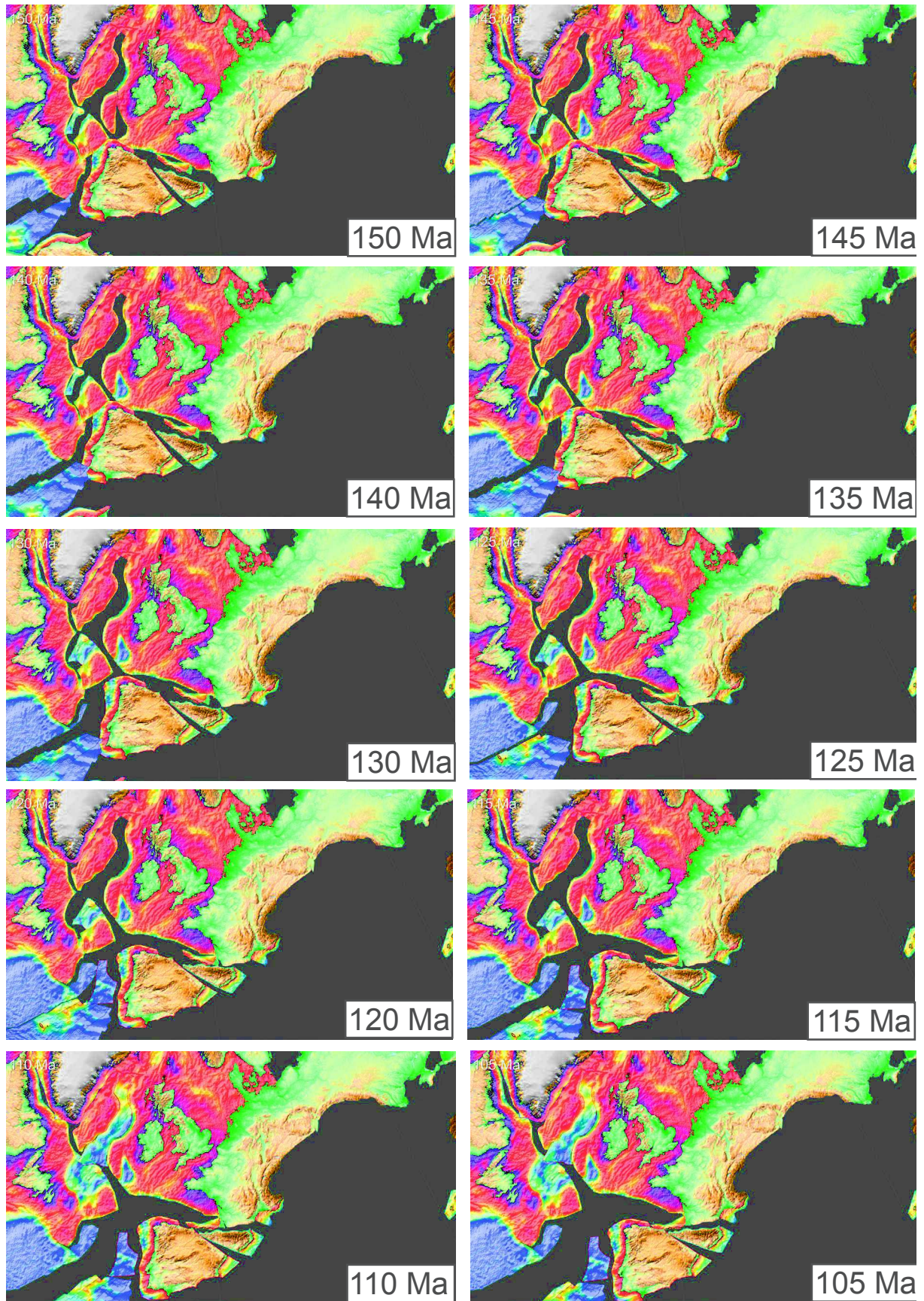
**Fig. A-11:** Screenshot of the Gplates software showing the determined polygons. Crustal thickness map and the elevation ETOPO 1 are used as background images

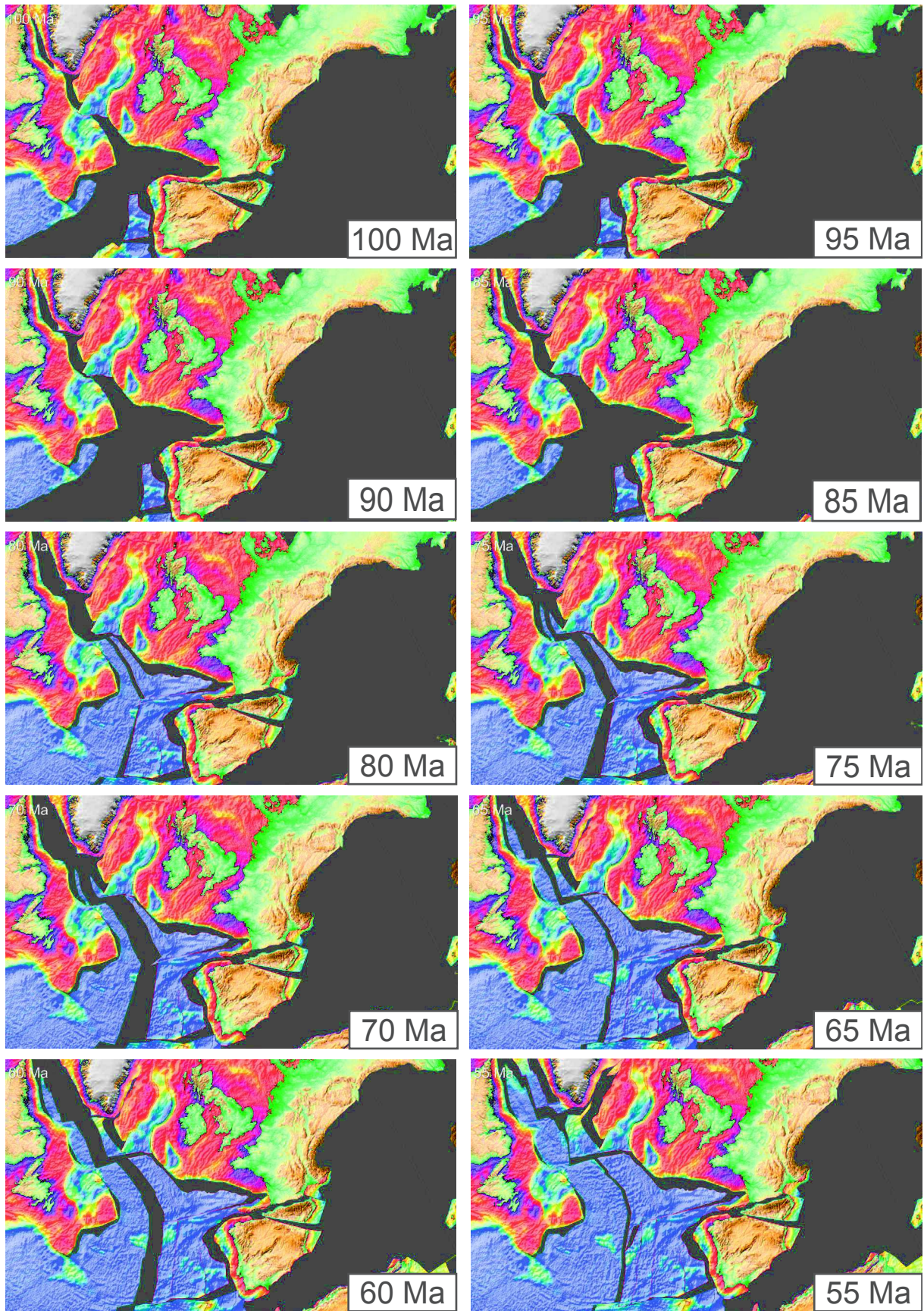
**Fig. A-12:** Evolution du sud de l'Atlantique Nord du Trias à l'actuel. Les images de fond sont l'épaisseur crustale déterminé par inversion gravimétrique ainsi que la topographie pour les zones émergées à l'actuel.

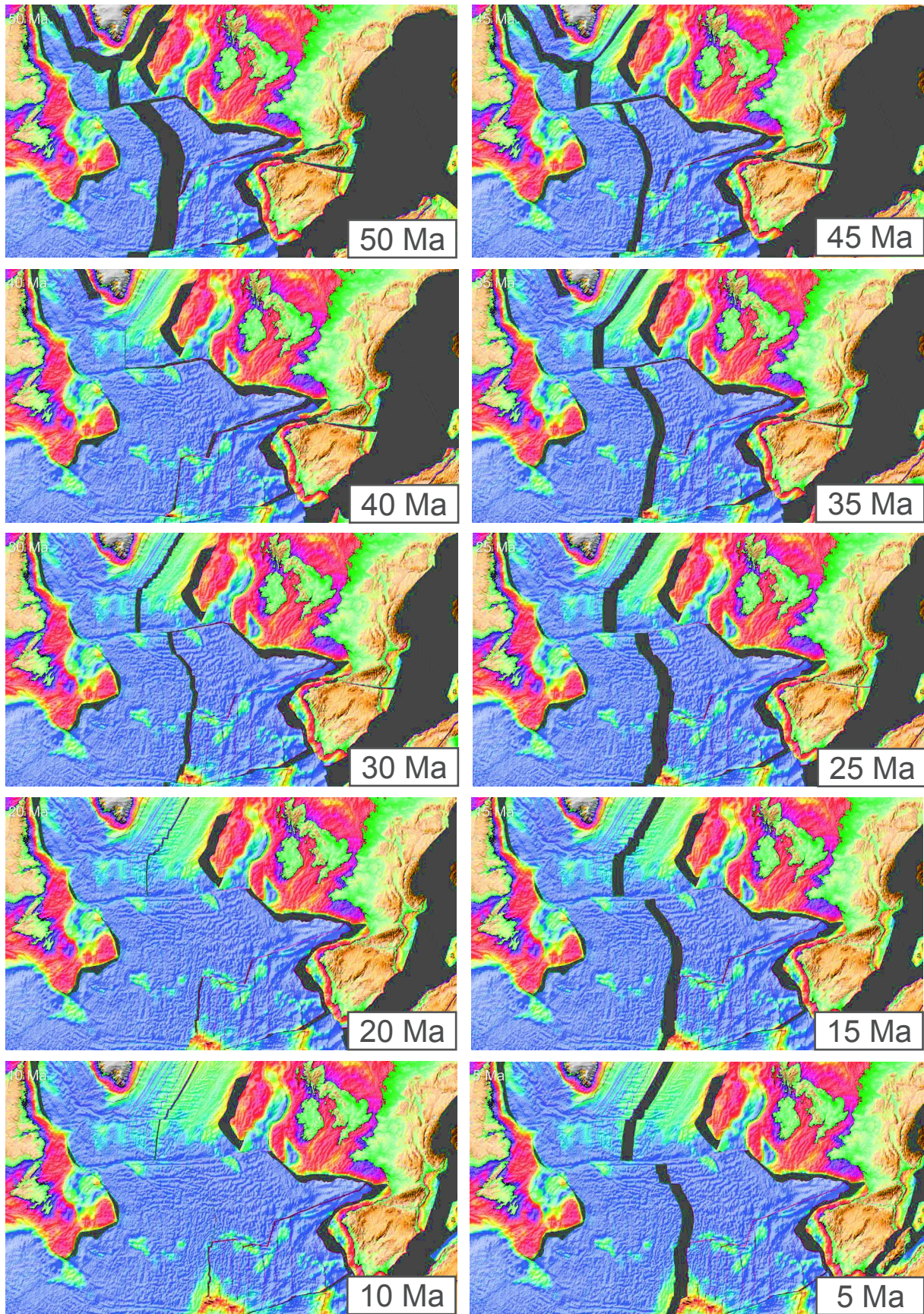
**Fig. A-12:** Evolution of the southern North Atlantic from Trias to present. Background images are the crustal thickness determined by gravity inversion and the elevation for the currently emerged domains.











## **A.7 ANNEXE ÉLECTRONIQUE**

Les fichiers ci-dessous sont disponible sur le CD accompagnant le manuscrit.

### **Video du modèle cinématique (Chap. III):**

Nirrengarten\_phd.mp4

### **Fichier utilisé dans Gplates (Chap. III):**

Nirrengarten\_phd.rot

Coastlines\_Nirrengarten\_phd.gpml

Polygons\_Nirrengarten\_phd.gpml

# ***LISTE DES FIGURES***

## **INTRODUCTION**

|   |    |
|---|----|
| <b>Fig. 1:</b> cisaillement pur et simple   | 28 |
| <b>Fig. 2:</b> Carte des marges passives  | 30 |
| <b>Fig. 3:</b> Coupe des domaines de rift   | 32 |
| <b>Fig. 4:</b> Terminologie des domaines de rifts                                     | 33 |
| <b>Fig. 5:</b> Modèle évolutif d'un système de rift pauvre en magma                   | 35 |
| <b>Fig. 6:</b> Représentation du théorème d'Euler                                     | 36 |
| <b>Fig. 7:</b> Premières tentatives de restauration paléogéographique                 | 37 |
| <b>Fig. 8:</b> Fonctionnement des anomalies magnétiques océaniques                    | 39 |
| <b>Fig. 9:</b> Méthode de restauration palinspatique                                  | 40 |
| <b>Fig. 10:</b> Carte bathymétrique de l'Océan Atlantique                             | 41 |
| <b>Fig. 11:</b> Carte structurale du sud de l'Atlantique Nord                         | 43 |
| <b>Fig. 12:</b> Cartes paléogéographiques de l'Atlantique Nord                        | 45 |
| <b>Fig. 13:</b> Reconstruction cinématique globale du Cambrien au Trias               | 46 |
| <b>Fig. 14:</b> Propositions de restauration de la plaque ibérique                    | 48 |
| <b>Fig. 15:</b> Coupes crustales de la marge ibérique                                 | 50 |
| <b>Fig. 16:</b> Différentes propositions pour l'évolution du sud de l'Atlantique Nord | 51 |
| <b>Fig. 17:</b> Modèle évolutif d'un système de rift hyper-étiré pauvre en magma      | 52 |

## **CHAPITRE I**

|  |    |
|--|----|
| <b>Fig. I-1:</b> Critical Coulomb wedge theory   | 62 |
| <b>Fig. I-2:</b> : EExamples of determination of HECW  | 65 |
| <b>Fig. I-3:</b> Flexural backstripping of the Porcupine basin                                 | 67 |
| <b>Fig. I-4:</b> Hyper-extended rocks  | 69 |
| <b>Fig. I-5:</b> Measured HECW   | 71 |
| <b>Fig. I-6:</b> Stability diagrams for critical Coulomb wedges                                | 74 |
| <b>Fig. I-7:</b> Conceptual evolution of the most distal part of a hyper-extended rift system  | 77 |
| <b>Fig. I-8:</b> Stability envelope of a critical gravitational and tectonic extensional wedge | 82 |
| <b>Fig. I-9:</b> Lower-plate hyper-extended continental wedges                                 | 84 |
| <b>Fig. I-10:</b> Seismic line ION IR 1000 82.   | 86 |
| <b>Fig. I-11:</b> Panoramic picture and interpretation of the Tasna outcrop                    | 87 |

## CHAPITRE II

|  |     |
|--|-----|
| <b>Fig. II-1:</b> Reconstructed magnetic map Emag2v3 at chron C34                      | 95  |
| <b>Fig. II-2:</b> Southern North Atlantic plate reconstruction.                        | 97  |
| <b>Fig. II-3:</b> Reflection and refraction seismic lines from the Iberia margin       | 99  |
| <b>Fig. II-4:</b> Reflection and refraction seismic lines from the Newfoundland margin | 100 |
| <b>Fig. II-5:</b> Rifted domain map reconstructed at chron C34                         | 102 |
| <b>Fig. II-6:</b> Seismic line NB21  | 104 |
| <b>Fig. II-7:</b> Magnetic anomaly map reduced to the pole                             | 104 |

## CHAPITRE III

|   |     |
|---|-----|
| <b>Fig. III-1:</b> Bathymetric maps of the southern North Atlantic              | 113 |
| <b>Fig. III-2:</b> Schematic restoration of conjugate margins                   | 115 |
| <b>Fig. III-3:</b> Crustal thickness maps                                       | 117 |
| <b>Fig. III-4:</b> Map of the rift domains of the southern North Atlantic based | 120 |
| <b>Fig. III-6:</b> Restoration of the southern North Atlantic                   | 130 |
| <b>Fig. III-7:</b> Restoration of the southern North Atlantic                   | 131 |
| <b>Fig. III-8:</b> Map of inherited structures at 200Ma                         | 137 |
| <b>Fig. III-9:</b> Flowlines  | 139 |
| <b>Fig. III-10:</b> Velocity graph  | 142 |
| <b>Fig. III-11:</b> Propagation model   | 144 |

## CHAPTIRE IV

|  |     |
|--|-----|
| <b>Fig. IV-1:</b> Carte des domaines de rift du sud de l'Atlantique Nord         | 153 |
| <b>Fig. IV-2:</b> Les différents types HECW                                      | 154 |
| <b>Fig. IV-3:</b> Carte des domaines de rift restauré à l'isochrone C34.         | 157 |
| <b>Fig. IV-4:</b> Modèles de propagation   | 159 |
| <b>Fig. IV-5:</b> Modèle cinématique de l'ouverture du sud de l'Atlantique Nord. | 163 |

## ANNEXES

|   |     |
|---|-----|
| <b>Fig. A-1:</b> Carte de gravité à l'air libre                         | 199 |
| <b>Fig. A-2:</b> Dérivée verticale de la carte de gravité à l'air libre | 200 |
| <b>Fig. A-3:</b> Carte des anomalies magnétique terrestre Emag2v3       | 200 |
| <b>Fig. A-4:</b> Localisation des lignes de sismique réfraction         | 201 |
| <b>Fig. A-5:</b> Lignes de sismique réfraction utilisées durant l'étude | 206 |

|  |     |
|--|-----|
| <b>Fig. A-6:</b> localisation des forages  | 207 |
| <b>Fig. A-7:</b> Schéma illustrant le processus itératif d'inversion gravimétrique           | 209 |
| <b>Fig. A-8:</b> Comparaison d'inversion gravimétrique le long de la ligne ISE 1             | 210 |
| <b>Fig. A-9:</b> Processus de flexural backstripping   | 211 |
| <b>Fig. A-10:</b> Exemple de lignes d'un fichier de rotation utilisé par le logiciel Gplates | 213 |
| <b>Fig. A-11:</b> Capture d'écran du logiciel Gplates  | 214 |
| <b>Fig. A-12:</b> Modèle évolutif du sud de l'Atlantique Nord                                | 214 |

# ***LISTE DES TABLEAUX***

## **CHAPITRE I**

**Table I-1:** Measurements of  $\alpha$  and  $\beta$  angle of HECW 72

**Table I-2:** References of the sections presented in Fig. I-5 89

## **CHAPITRE II**

**Table II-1:** Poles of rotation used in Fig. II-2 104

**Table II-2:** Recorded magmatic activity in the southern North Atlantic 105

## **CHAPITRE III**

**Table III-1:** Table presenting the major inputs of the modeling 123

**Table III-2:** Reconstruction poles used in this study 129

**Table III-3:** Table of parameters used in the gravity inversion 148







## Modes de déformation et implications cinématiques des marges hyper-étirées: Les exemples du sud de l'Atlantique Nord

Les modes de déformation des systèmes de rift hyper-étirés pauvres en magma évoluent dans le temps et dans l'espace. Ainsi les structures et architectures observées varient le long d'une section en profondeur ainsi que sur une carte. Cette étude vise à caractériser les modes de déformation des systèmes hyper-étirés et leur propagation en utilisant les exemples du sud de l'Atlantique Nord.

L'architecture de la terminaison de la croûte continentale a été comparée à la théorie du prisme critique de Coulomb car sa forme est prismatique, la déformation finale est cassante/frictionnelle et ce prisme glisse sur un décollement basal. Cette théorie met en évidence le comportement distinct des deux marges conjuguées. De plus, elle contraint l'architecture crustale, permet l'intégration des failles contre-régionales et explique la formation des blocs allochtones dans un modèle de failles en séquence.

L'intégration des modes de déformation dans un modèle évolutif 3D impose un contexte cinématique fiable, ce qui n'est pas le cas de l'ouverture océanique du sud de l'Atlantique Nord. Ceci est dû à l'interprétation de l'anomalie J comme un isochrone. L'investigation de cette anomalie indique une formation polygénique et polyphasée incohérente avec un isochrone ou une limite de domaine. Ainsi l'anomalie J est inutilisable pour les reconstructions cinématiques.

L'évolution de la déformation de rift a été analysée grâce à une nouvelle reconstruction cinématique du sud de l'Atlantique Nord. Il apparaît alors que la déformation de la croûte continentale est segmentée alors que la propagation de la croûte océanique forme un V. L'approche développée dans cette thèse pose également de nouvelles questions géodynamiques quant à l'influence de l'héritage et l'effet des points triple.

*Mot clefs:* Marges hyper-étirées, Mode de déformations, Sud de l'Atlantique Nord, Anomalie magnétique J, Reconstruction cinématique, Partitionnement et propagation de la déformation

Deformation modes of magma-poor hyper-extended rift systems evolve through time and space. Hence the observed structures and architectures vary along a depth section as well as on a map. This study aims to characterize the deformation modes of hyper-extended systems and their propagation using the examples of the southern North Atlantic.

The architecture of the continental crust termination has been compared to the critical Coulomb wedge theory because it has a wedge shape, the final deformation is brittle/frictional and this wedge is gliding over a basal detachment. This theory highlights the distinct behavior of the two conjugate margins. Moreover it constrains crustal architecture of the continental crust termination, integrates continentward dipping faults and explain the formation of extensional allochthons in a sequential faulting model.

The integration of deformation modes in an evolving 3D model necessitates a reliable kinematic context, which is not the case for the opening of the southern North Atlantic Ocean. This is linked to the interpretation of the J-magnetic anomaly as an oceanic isochron. Re-investigations of this anomaly revealed its polygenic and polyphased formation, which is inconsistent for an oceanic isochrons or a domain boundary making it unusable for plate reconstruction.

The evolution of rift deformation has been analyzed with a new plate reconstruction of the southern North Atlantic. It appears that the continental crust deformation is segmented whereas oceanic crust propagates in a V-shape. The approach developed in this thesis also asks new geodynamical questions on the influence of inheritance and the effect of triple junction.

*Keywords:* Hyper-extended rifted margins, Deformation modes, Southern North Atlantic, J-magnetic anomaly, Plate modelling, Partitioning and propagation of the deformation